Dissertation

Submitted to the
Combined Faculties for the Natural Sciences and for Mathematics
of the Ruperto-Carola University of Heidelberg, Germany
for the degree of
Doctor of Natural Sciences

Presented by

M.Sc. Hui Wang

Born in: Henan province, P.R.China

Oral-examination: 28th June 2013

Functional and Epidemiological Characterization of Non-Synonymous Single Nucleotide Polymorphisms in IRAK2

Referees: Prof. Dr. med. Hans-Georg Kräusslich

Prof. Dr. Alexander Weber

This thesis was conducted at the German Cancer Research Center (Deutsches Krebs forschungs zentrum, DKFZ) Heidelberg and Department of Immunology of Tübingen University, Germany; both are under the supervision of Prof. Dr. Alexander Weber.

This thesis is the presentation of my original research work and every effort has been taken to specifically indicate the work done in collaboration with others, and is referenced with names for the contributions of collaborators. I hereby declare that the following thesis is my own work and has been written by the undersigned and without any assistance from third parties. Furthermore, I confirm that no sources have been used in the preparation of this thesis other than those indicated.

Heidelberg, 11th April

Acknowledgement

First I would like to thank my Ph.D. supervisor Prof. Dr. Alexander Weber. He provided me the valuable opportunity to do my Ph.D. in his group. During the four-year study, his selfless scientific discussion and guidance support me to accomplish the goal of my Ph.D. project and let me understand the world of molecular biology. Meanwhile, as a foreigner, Alex also helped me a lot in my private life.

I also would like to thank the Chinese Scholarship Council who sponsored me for the four-year study. Without their support, I could not concentrate on my research.

I appreciate the opportunity to work both at the German Cancer Research Centre (DKFZ) in Heidelberg and at the University of Tübingen, both of which provided me an excellent scientific working environment and an opportunity to get to know the other areas of research, as well as cooperation with other colleagues. In particular, I would like to express my thanks to Dr. Markus Feuerer and Dr. David Richard who provided me with many research tools and techniques. Additionally, I am very thankful for the technical help which I obtained from and Dr. Tore Kempf and Gabriella Siszler, who work at the core facility of DKFZ.

I also thank for the help from Tübingen to help us setting up the new lab. Particularly, Dr. Kevin Dannehy and Beate Pömmerl helped me to conquer the technical problems of retroviral transduction. I also highly appreciate the help from my lab mates. Particularly, I would like to express my special gratitude to my “private teacher” -Julie George, who taught me from the basic plasmid extraction to design a small intact experiment and helped me with many trivial things of the lab life. Additionally, Dr. Tica Pichulik also helped me a lot in the end of Ph.D. work and translated the Abstract into German. I also thank our lab technicians Birgit Kaiser and Sabine Dickhöfer, they both helped me a lot in preparing constructs or conducting experiments.

In the end I would like to express my thanks to my parents and Xu who constantly have supported and encouraged me during my Ph.D. time. I also appreciate their understanding and patience for me.

Abstract

Toll-like receptors (TLR) play an essential role in innate immunity, in which they indentify invasive pathogens and initiate the immune responses to eliminate the pathogens. Interleukine-1receptor-associated kinases are key kinases in the TLR signalling pathway where they integrate signals from activated receptor complexes to then induce the activation of downstream transcription factors NF-κB, AP-1 and IRFs. It is known that IRAK4 deficiency in humans is related with recurrent pyogenic bacterial infections which can be lethal without any facilitation of health care and antibiotics. In light of this fact, this study focuses on analysing the general role of IRAK2 on the pathogenesis of certain kinds of diseases.

Known non-synonymous single nucleotide polymorphisms (SNPs) of IRAK2 were selected from the NCBI SNP database, which served as probes to gain insights of the molecular functions of IRAK2. The SNPs of interest were screened by overexpressing the constructs of variants into a human cell line and detecting the activation of NF-κB. IRAK2 R214G and L392V decreased the activation of NF-κB and the production of IL-8. Although R214G and L392V varied the interaction intensity with IRAK2 and IRAK4, these two variants still maintained the interaction with the downstream signalling partner TRAF6. Interestingly, IRAK2 R214G and L392V both reduced the ubiquitination levels of TRAF6. The ubiquitination of TRAF6 is an essential step for the NF-κB activation. Moreover, when stimulating human IRAK2 WT reconstituted murine *Irak2* knockout macrophages with TLR2, 4 and 7 ligands, the TNF-α production was massively enhanced. Meanwhile, phosphorylation of p38, p65, ERK was enhanced as well. Intriguingly, the phosphorylation of Akt was only observed in the IRAK2 WT reconstituted macrophages. Additionally, the R214G and L392V reconstituted macrophages reduced the transcriptional activation of *Il-1β* and *Il-6* in comparison to IRAK2 WT.

The epidemiological analyses revealed that IRAK2 R214G (rs35060588) reduced the survival time of colorectal cancer patients; IRAK2 L392V (rs3855283) significantly reduced the auto clearance of HCV in patients who are then susceptible to become a chronic HCV infection; additionally L392V also increased the possibility of progression from gastritis to gastric cancer. Collectively, this information would be helpful for the future personalized therapy.

Zusammenfassung

Toll-like Rezeptoren (TLR) spielen eine wichtige Rolle in der angeborenen Immunantwort, da sie invasive Pathogene identifizieren und eine Immunantwort initiieren um das Pathogen zu eliminieren. I*nterleukin-1 Rezeptor*-assoziierten *Kinasen* sind wichtige Kinasen in der TLR Signalkaskade, die Signale von verschiedenen aktivierten Rezeptorkomplexen integrieren, was schließlich zur Aktivierung der Transkriptionsfaktoren NF-κB, AP-1 und IRFs führt. Es ist bekannt, dass eine IRAK4 Defizienz im Menschen mit wiederkehrenden pyogenen bakteriellen Infektionen einher geht, welche ohne medizinische Behandlung und die Gabe von Antibiotika tödlich enden können. Angesichts dessen untersucht diese Studie die grundliegende Rolle von IRAK2 in der Pathogenese von verschiedenen Krankheiten.

Bekannte nicht synonyme Einzelnukleotid-Polymorphismen (SNPs) in IRAK2 wurden aus der NCBI SNP Datenbank selektiert und dienten als Mittel, um die molekulare Funktion von IRAK2 zu untersuchen. Die interessanten SNPs wurden überprüft, indem Konstrukte von verschiedenen Varianten in einer humanen Zellenlinie überexprimiert und die Aktivierung von NF-κB gemessen wurde. IRAK2 R214G und L392V zeigten eine verringerte Aktivierung von NF-κB und Produktion von IL-8. Obwohl R214G und L392V unterschiedliche Interaktionsstärken zu IRAK2 und IRAK4 aufweisen, konnten diese beiden Varianten die Interaktion zu ihrem Signalpartner TRAF6 bewahren. Interessanterweise reduzierten IRAK2 R214G und L392V allerdings die *Ubiquitinierung* von TRAF6, ein wichtiger Schritt für die Aktivierung von NF-κB. Außerdem führte die Stimulierung von murinen *Irak2* knockout Makrophagen, die mit wildtype IRAK2 konstituiert wurden, zu einer massiv erhöhten Produktion von TNF-α. Die Stimulierung wurde mit TLR2, 4 und 7 Liganden durchgeführt. Auch die Phosphorylierung von p38, p65 und ERK war in diesen Zellen erhöht. Interessanterweise konnte die Phosphorylierung von Akt nur in den IRAK2 rekonstituierten Makrophagen nachgewiesen werden. Die Makrophagen, die mit R214G und L392V rekonstituiert wurden, wiesen eine reduzierte Transkription von *Il-1β* und *Il-6* im Gegensatz zu wildtyp IRAK2 auf.

Die epidemiologische Analyse hat gezeigt, dass IRAK2 R214G (rs35060588) die Überlebenszeit von Patienten mit Kolorektalkarzinom verringert. IRAK2 L392V (rs3855283) hingegen reduziert die spontane Eliminierung von HCV und begünstigt

einen chronischen Krankheitsverlauf. Zusätzlich erhöht L392V das Risiko, dass sich aus einer Gastritis ein Margenkarzinom entwickelt. Zusammen könnten diese Ergebnisse hilfreich für die zukünftige Entwicklung einer personalisierten Therapie sein.

Table of contents

Figures & Tables iv
List of abbreviation vi
Chapter 1: Introduction 1
1.1 The human immune system 2
1.2 The pattern recognition receptors 4
1.2.1 The Toll- like receptors/interleukin-1 receptor superfamily 6
1.2.2 The RIG-I-like receptors family 13
1.2.3 The Nod-like receptor family 15
1.3 The TIR-domain containing adaptor protein in TLR signalling pathways ... 17
1.3.1 Myd88 dependent signalling pathway 19
1.3.2 The TIRF dependent signalling pathway 22
1.4 The IRAK family 24
1.4.1 IRAK1 25
1.4.2 IRAK2 26
1.4.3 IRAK3 30
1.4.4 IRAK4 31
1.5 The death fold superfamily for homotypic interaction 34
1.5.1 Overview on the death fold superfamily 34
1.5.2 Myddosome structure 35
1.6 Ubiquitination in TLR signalling pathway 36
1.6.1 Overview on ubiquitination 36
1.6.2 Ubiquitination in the MyD88 dependent signalling pathway 37
1.6.3 The ubiquitination communication in the TLR signalling pathway... 38
1.7 The relationship between TLR signalling pathway genetic variants and diseases. 39
1.7.1 The MyD88-IRAK4 deficiency 40
1.7.2 The TLR3-UNC93B1-TRIF-TRAF3 deficiency 41
1.7.3 TLR signalling pathway polymorphisms. 42
1.8 Aim of Ph.D. project 44
Chapter 2: Methods and Materials 45
2.1 Molecular Biological Methods 47
2.1.1 Generation of ds-oligonucleotide sequences. 47
2.1.2 Polymerase chain reaction (PCR) 47
2.1.3 Quantitative real-time polymerase chain reaction 48
2.1.4 Plasmids and DNA purification 49
2.1.5 Agarose gel electrophorsis 50
2.1.6 Restriction digestion 50
2.1.7 Ligation 50
2.1.8 Plasmids transformation 51
2.1.9 Gateway® cloning: LR cloning 51
2.1.10 Plasmid constructs and cloning stragtegies 52
2.1.11 Cultivation and cryo-preservation of transformed bacteria cells..... 55
2.2 Biochemical Methods 56
2.2.1 Protein quantification 56
2.2.2 SDS-polyacrylamid electrophoresis 56

2.2.3 Immunoblot analysis 57
2.2.4 Two-dimensional gel electrophoresis 58
2.3 Cell Biological Assay 59
2.3.1 Cell lines and cultivation 59
2.3.2 Transfection of plasmids to mammalian cell lines 59
2.3.3 Stable transfections of Flp-In™ 293T-REx™ cell lines 61
2.3.4 Gene expression analysis 61
2.3.5 Dual luciferase assay 62
2.3.6 LUMIER 63
2.3.7 ELISA 65
2.3.8 Immunoprecipitation 66
2.3.9 Retroviral transduction 67
2.4 Infection of reconstituted macrophages with Influenza A 68
2.5 Infection of reconstituted macrophages with *Salmonella typhimurium* 69
2.6 Computational methods. 69
2.6.1 Homology modelling of IRAK2 kinase domain. 69
2.6.2 Software tools and web-based browsers 70
2.6.3 Statistic analysis 70
Chapter 3: Results and Discussion 71
3.1 Part I: IRAK2 played a central role in the TLR signalling pathway. 73
3.1.1 Introduction 73
3.1.2 IRAK2 can only induce NF-κB activation in HEK293 cells 73
3.1.3 IRAK2 rescued the pro-inflammatory cytokines production in macrophages 75
3.1.4 IRAK2 enhanced the phosphorylation of p38, p65, ERK and Akt 77
3.1.5 Post-translational modifications in IRAK2 79
3.1.6 Discussion 83
3.2 Part II: IRAK2 plays a central role in the Myddosome formation 92
3.2.1 Introduction 92
3.2.2 Results 92
3.2.3 Discussion 99
3.3 Part III: IRAK2 genetic variants R214G and L392V reduced TLR dependent signalling 104
3.3.1 Introduction 104
3.3.2 Results 107
3.3.3 Discussion 122
3.4 Part IV: Genetic variants in IRAK2 impact on the progress and prognosis of infection-related diseases 127
3.4.1 Introduction 127
3.4.2 Results 127
3.4.3 Discussion 132
Chapter 4: Conclusion 135
4.1 IRAK2 generally plays a central role in TLR-NF-κB signalling pathway 137
4.2 IRAK2 genetic variants are related with the progression or prognosis of certain kinds of diseases. 139
4.3 Could IRAK2 be a therapeutic target? 141
Reference 143
Appendix 153
Appendix A: Reagent and buffers 155
A1: Cloning primers 155

A2: Mutagenesis primers 156
A3: qPCR primers 156
A4: Overview of purchased and gifted plasmids 157
A5: Overview of antibodies list 158
A6: TLR ligands 158
A7: Recipes of buffers 159
A8: Recipes of medium 159
Appendix B1: The signalling properties of defect mutants of IRAK2 160
Appendix B2: The signalling properties of defect mutants of IRAK3 160

Figures & Tables

Chapter 1

Figure 1.1: Major PRRs in human innate immunity……..……5
Figure 1.2: A Plasma membrane located TLRs and their ligands……..…9
Figure 1.2: B Endolysosome membrane located TLRs and their ligands..……10
Figure 1.3: The IL-1/ TLR superfamily …….....……11
Figure 1.4: The cross talk between TLRs/IL-1R signalling pathways…..…….....12
Figure 1.5: Process IL-1receptor family and their ligands……..……13
Figure 1.6: The schematic diagram of RLR family members……..……..13
Figure 1.7: Sensing of viral dsRNA by TLR3 and RLR…….……...15
Figure 1.8: The schematic diagram of NLR family members…….……...16
Figure 1.9: The cross talk among TLRs, IL-1RI and inflammasome…….……17
Figure 1.10: The schematic diagram of five TIR-domain containing adaptors……..18
Figure 1.11: The TIR domain structure of human TLR2……..…….....18
Figure 1.12: The MyD88 dependent signalling pathway……...20
Figure 1.13: The Mal dependent signalling pathway…….22
Figure 1.14: The TRIF dependent signalling pathway……..…….23
Figure 1.15: The schematic diagram of IRAK family members……...……27
Figure 1.16: Schematic diagram of human and murine IRAK2…….30
Figure 1.17: Protein sequence alignments of human and murine IRAK2……....31
Figure 1.18: Tertiary structure of the different death-fold subfamilies……..34
Figure 1.19: DD mediates three interaction types through six interaction patches...35
Figure 1.20: The schematic diagram of Myddosome structure……..36
Figure 1.21: The ubiquitination in MyD88 dependent signalling pathway……....38
Figure 1.22: The ubiquitination communication in TLR signalling pathway……..…39

Table 1.1: Major PRRs and their ligands…….……..6
Table 1.2: The affect of absence of IRAKs on IL-1R/TLR signalling…….....33

Chapter 2

Figure 2.1: The schematic diagram for LR reactions……..52
Figure 2.2: The diagram of generation of Flp-In stable cell line……54
Figure 2.3: The schematic structure of pMXs-IP retroviral vector……55
Figure 2.4: The schematic diagram of the LUMIER procedure……65

Table 2.1: PCR cloning program……48
Table 2.2: Site-directed mutagenesis……...……48
Table 2.3: The calcium phosphate transfection method……..……60
Table 2.4: The lipofectamine2000 transfection method……..……60

Chapter 3

Figure 3.1: IRAK2 overexpression results in NF-κB avtivation, but not MAPK or IRF3 signalling in HEK293T cells……74
Figure 3.2: IRAK2 rescues TNF-α production in IRAK2 KO macrophages stimulated with TLR2, TLR4 and TLR7 ligands……..76

Figure 3.3: IRAK2 is critical for the pro-inflammatory response against *Salmonella typhimurium*……77
Figure 3.4: IRAK2 enhanced the activation of NF-κB and MALP kinases signalling pathways and triggered the phosphorylation of Akt upon TLR stimulation……78
Figure 3.5: Profile of post-translational modifications in IRAK2……81
Figure 3.6: The novel phosphorylation site in IRAK2……82
Figure 3.7: Structure of generating IRAK2 deficient mice……..86
Figure 3.8: Akt pathway control of pro and anti-inflammatory cytokines production……89
Figure 3.9: IRAK1, 2 and 3 FL and DD genes expression……93
Figure 3.10: NF-κB signalling assay of IRAK1, 2 and 3 FL and DD constructs…....94
Figure 3.11: IRAK2DD interacts with all IRAKs DDs……..……..96
Figure 3.12: IRAK2FL interacts with all FL of IRAKs……..……97
Figure 3.13: IRAK2 bridges the interaction between IRAK4 and IRAK1/IRAK3….98
Figure 3.14: The charge and shape complementarity in MyD88-IRAK4-IRAK2 interaction……99
Figure 3.15: IRAK family involved in the TLR signalling pathway……..……101
Figure 3.16: The schematic diagram of sequential assembly and disassembly in Myddosome structure……..……...103
Figure 3.17: SNPs in human IRAK1, 2 and 3……105
Figure 3.18: Gene expression of IRAK mutants……..…..……107
Figure 3.19: NF-κB activation analysis of SNPs in IRAK1, 2 and3……109
Figure 3.20: R214G and L392V reduced IL-8 production……..……110
Figure 3.21: 3D homology model of the IRAK2 kinase domain……..……..111
Figure 3.22: Sequence conservation of R214 and L392……..……..112
Figure 3.23: LUMIER interaction assay for IRAK2 R214G and L392V…..……113
Figure 3.24: R214G and L392V maintain the interaction with TRAF6……114
Figure 3.25: R214G and L392V reduce the ubiquitiantion of TRAF6……116
Figure 3.26: Post-translational modifications profiles of IRAK2 WT, R214G and L392V……...……..117
Figure 3.27: Expression of IRAK2 WT and mutants in reconstituted macrophage..118
Figure 3.28: R214G and L392V do not alter TNF-α production……..…119
Figure 3.29: IRAK2 R214G and L392V reduced the transcriptional induction of *Il-1β* and *Il-6*……..121

Table 3.1: Reported the dependency of IRAK2 in various TLRs……..……84
Table 3.2: The dependency of IRAK2 at early or later time point of NF-κB activation……..……85
Table 3.3: Frequency information of selected non-synonymous SNPs in human IRAK1, 2 and 3……....……106
Table 3.4 Frequencies of IRAK2 rs3844283 and 35060588 with CRC-specific survival……..……128
Table 3.5: Frequencies of IRAK2 rs3844283 and IL-28B rs1297860 and rs8099917 in HCV infection patients……..130
Table 3.6: Association of IRAK2 rs3844283 and IL-28B rs8099917 and the natural course of HCV infection and spontaneous virologic response……..130
Table 3.7: Frequencies of IRAK2 rs3844283 in gastritis and gastric cancer patients……...131

List of abbreviation

AP-1	activating protein-1
ASC	apoptosis-associated speck-like
ATP	adenosine triphosphate
BIR	baculovitus inhibition of apoptosis protein
BSA	bovine serum albumin
Btk	Bruton's tyrosine kinase
CARDs	caspase recruitment domain
cDNA	coding DNA
CIP	calf intertinal phosphatase
CIITA	CARD-containing activation domain of the classII Transactivator
CLR	C-type lectin receptor
CMV	Human cytomegalovrius
Co-IP	Co-immunoprecipitation
CREB	Camp reponse element binding protein
DAMP	damage-associated molecular patterns
DD	death domain
DED	death effector domain
DMEM	Dulbecco's Modified Eagles Medium
DNA	deoxy-ribonucleic acid
dNTP	deoxy-nucleotide-triphosphate
DTT	dithiothreitol
E.coli	*Escherichia coli*
EDA-ID	ectodermal dysphasia with immunodeficiency
EDTA	ethylenediaminetetraacetic acid
EGFP	enhanced green fluorescent protein
ELISA	Enzyme-Linked immunosorbent Assay
EMCV	Encephalomyocarditis Virus
ER	endoplasmatic reticulum
FADD	Fas-assocaited death domain
FL	full length
FRT	Flp recognition target
GST	Glutathion-S-Transferase
HA	hemagglutinin
HCB	Han Chinese in Beijing
HCV	hpatitis C virus
HLA	human leukocyte antigen
HRP	horseradish peroxidase
HSE	Herpes simplex encepalitis
HSV	herpes simplex virus
IEF	isoelectric focusing
IFN	interferon
Ig	Immune-globuline
IKK	IκB kinase

IL	interleukin
IL-1R	interleukin 1 receptor
IP	immunoprecipitation
IRAK	interleukin-1 receptor assocaited kinase
IRF	interferon regulatory transcription factor
JNK	c-Jun N-terminal kinase
KO	knock out
LBP	LPS-binding protein
LPS	lipopolysaccharide
LRR	leucine rich repeats
LUMIER	LUminescence-based Mammalian Interactome mapping
MAL	MyD88-adaptor like
MAP	Mitogen-activated protein
MAPK	Mtiogen-activated protein kinase
MAVS	mitochondrial antiviral signalling protein
MBL	mannose binding protein
MCMV	murine cytomegalovirus
MD	molecular dynamics
MDA5	melanoma differentiation-associated gene 5
MES	2-(N-morpholino) ethane-sulfonic acid
MKK	Map kinase kinase
mRNA	messenger RNA
MSR	macrophage scavenger receptor
MyD88	myloid differentiation factor 88
NACHT	NAIP, CIITA, HET-E and TP1
NCBI	National Center for Biotechnology Information
NEMO	NF-κB essential modulator
NLR	NOD-like receptor
NLRP	NOD-, LRR-and PYD cotaining
NOD	Nucleotide-binding oligomerisation domain
Ns	non-synonymous
OD	optical density
ORF	open reading frame
PAGE	polyacrylamide gel eletrophoresis
PBMC	peripheral blood mononuclear Cell
PBS	phosphate buffered saline
PCR	polymerase chain reaction
PEST	proline-glutamate-serine-theronine motif
pH	potential hydrogen
PI3K	phosphatidyl inositol 3 kinase
PIP2	phosphatidylinositol 4,5-bisphosphate
PKB	protein kinase B
PKC	protein kinase C
PKR	protein kinase R
PTEN	phosphatase and tensin homologue
PYD	pyrin domain
PYHIN	pyrin and HIN domain containing

qPCR	quantitative PCR
RHIM	RIP homotypic interaction motif
RIG-I	retinoic acid inducible gene-I
RIP	receptor interacting protein
RLR	RIG-I like receptor
ROS	reactive oxygen species
SARM	sterileα and armadillo motif containing
SDS	sodium-dodecyl-sulfate
SLE	systemic lupus erythematosus
SNP	single nucletoide polymorphism
SOCS	suppressor of cytokine signalling
SP	surfactant protein
STAT	signal transducers and activators of transcription
TAK	TGF-β activated kinase
TBK1	TANK-binding kinase
TGF	tumour growth factor
TIR	Toll/IL-1 receptor
TIRAP	Toll-interleukin 1 receptor domain containing adaptor
TLR	Toll-like receptor
TNF	tumour necrosis factor
Tpl	tumour progegression locus
TRADD	TNF receptor type-1 associated death domain
TRAF	TNF receptor associated factor
TRIF	TIR-domain-containing adaptor proteininducing IFNβ
UTR	untranslated region
VAVC	Vaccine virus
VSV	Vesicular stomatitis virus
WCL	whole cell lysate
WT	wild type

Chapter 1: Introduction

1.1 The human immune system

The immune system can recognize and eliminate exogenous pathogens which invade and cause infection and diseases in humans. Additionally, it can distinguish and remove endogenous oncogenic cells, cellular debris, and other toxic substances. In general, the tenet of the immune system is keeping the human organism in a stable and healthy condition[1]. However, pathogens can avoid the detection and neutralization of the immune system by quickly evolving and adapting to the surrounding environment. Correspondingly, multiple defence mechanisms have also evolved to identify and eradicate pathogens. Therefore, the immune system can be divided into two parts: the innate immune system and the adaptive immune system. The former serves as the first barrier to protect organisms against pathogens. As we know, even a unicellular organism has a rudimentary immune system that can resist bacteriophage infection by the means of enzymes. Additionally, plants and insects have a basic innate immune system as well, as phagocytosis, antimicrobial peptides called defensins and the complement system [1].

In humans, the innate immune system includes macrophages, dendritic cells, natural killer cells, natural killer T cells, eosinophil, basophils and neutrophils. All of these cells can produce pro-inflammatory cytokines, chemokines or interferon immediately when they recognize exogenous pathogens [2]. One important function of macrophages is the phagocytosis, which can clean aged cells and remove dead cellular debris in the late stage of infection. Another important role of macrophages is antigen presentation which bridges the innate and the adaptive immune system. After ingesting and digesting a pathogen, macrophages can present an antigen of a pathogen to T cells that can induce the adaptive immune system [2]. Other than macrophages, dendritic cells are present in tissues which are in contact with the external environment, such as the skin and the lining of the nose, lungs, stomach and intestines. After being activated by the pathogens, dendritic cells migrate to the lymph node where they present the antigen to T cells or B cells to initiate and shape the adaptive immune response. Meanwhile, certain dendritic cells can produce a high amount of interferon after the recognition of viruses [3]. On the other hand, eosinophils are responsible for fighting against multicellular parasites and certain invertebrates [4]. Along with mast cells and basophils, they also play a role in allergic reactions [4]. Neutrophils, are the most

abundant type of polymorphonuclear cells in mammals. They play an essential role in innate immunity. Because of the high migration ability, they can quickly congregate at the centre of an infection at the early phase of inflammation, especially for those caused by bacterial infection, environmental exposure and some cancers[4]. Moreover, neutrophils can detect chemokines gradients of interleukine-8 (IL-8), and interferon gama (IFN-gama), which lead to neutrophils migration. Additionly, neutrophils can express and release cytokines, which in turn amplify inflammatory reaction. Furthermore, since neutrophils have Fc receptor for opsonin.They can internalize and kill microorganisms and particles that are coated in opsonins via phagocytosis and degradation [4].

The initial response of innate immunity to the pathogen invasion is vital for eliminateing the bacterial conserved pathogen associated molecular pattern (PAMP). However, in the face of the variable and quickly evolving viruses or bacterium, a more efficient adaptive immunity is needed to produce a strong and specific antibody. The adaptive immune system can then induce specific memory to a pathogen to protect our body against secondary invasion [2]. The adaptive immune system only exists in jawed vertebrates, as well as human beings. It is highly adaptable because of the somatic hypermutaion and V (D) J recombination [5]. This feature triggers a small number of genes to generate a vast number of different antigen receptors, which are further uniquely expressed on each individual lymphocyte. Moreover, these irreversible and specific changes are inherited by the progeny cells. Consequently, the memory T cells and memory B cells are generated and become the keys of long lived specific immunity [6]. T cells and B cells are the major types of lymphocytes for adaptive immunity. T cells play a major role in cell- mediated immune response. CD8+ T cells, also known as cytotoxic T cells, identify the specific antigens which are present by MHC-I molecular and majorly produced by viruses and cancer cells. CD4+ T cells, also known as T helper cells, assist other immune response, such as maturation of B cells, into plasma cells and memory B cells [2]. Once they are activated, they begin dividing rapidly and differentiating into several subtypes, such as T_H-1, T_H-2, T_H-3 and T_H-17, which release different cytokines to regulate the immune response [7]. Regulatory T cells are also known as suppressor T cells. The major function of them is to reduce T cell mediated immunity [8]. On the other hand, the main functions of B cells are taking part in the humoral immune response, producing specific antibodies against exogenous antigen

and developing into memory B cells[9].

The human immune system is complicated and includes a lot of sophisticated defence mechanisms. Innate immunity serves as the first fence to eradicate pathogens. Once the infection surpasses a certain threshold, adaptive immunity can be activated by the innate immunity and boost the immune response in unspecific and specific way[2]. Meanwhile, the immune system produces certain types of suppressive cytokines to balance the immune response. Alltogether, innate immunity and adaptive immunity cooperate with each other and keep the homeostasis of the organisms.

1.2 The pattern recognition receptors

One unique feature of the innate immunity is the ability to detect noxious substances and this recognition is mediated by counterparts that one part was encoded in human genome and another part was encoded by the genomes of different species. Interestingly, the selective advantage provided by the recognition of the components of the host, usually implies a selective weakness to the pathogens [10]. CA Janeway pointed out that this conflict directs the evolution of innate immunity toward recognition of invariant molecular constituents of the infectious agents. Conservation of these molecular structures indicates that they are shared by large groups of pathogens. Thus, this work suggested that the innate immune system would detect the presence of infection via recognition of conserved microbial pathogen-associated molecular patterns (PAMPs) by germ-line encoded receptors. Therefore, they were named pattern recognition receptors (PRRs) [6]. Current research indicates that PRRs are also detecting molecular from non-pathogenic molecular (i.e. DAMPs) and responsible for recognizing endogenous molecules which were released from damaged cells, thus termed as damage-associated molecular patterns (DAMP) [11]. It is now becoming clear that innate immunity is not only responsible for the early pathogen invasion and elimination, but also for initiating, shaping and checking adaptive immunity [12]. For example, innate immunity determine the origin of the antigen, the type of infection (pathogen class), the extent and duration of infection, and finally, the requirement for immediate defence or future defence. However, not all PRRs are equal in terms of their ability to trigger adaptive immunity. Thus, this phenomenon encouraged research on the mechanism of each type of PRRs.

PRRs are expressed not only in macrophages and DCs but also in epithelial cells, endothelial cells, and fibroblasts[13]. According to the localization in terms of cellular structure of PRRs, they can be divided into three major groups: extracellular soluble PRRs, transmembrane PRRs and cytoplasmic PRRs (Figure1.1).

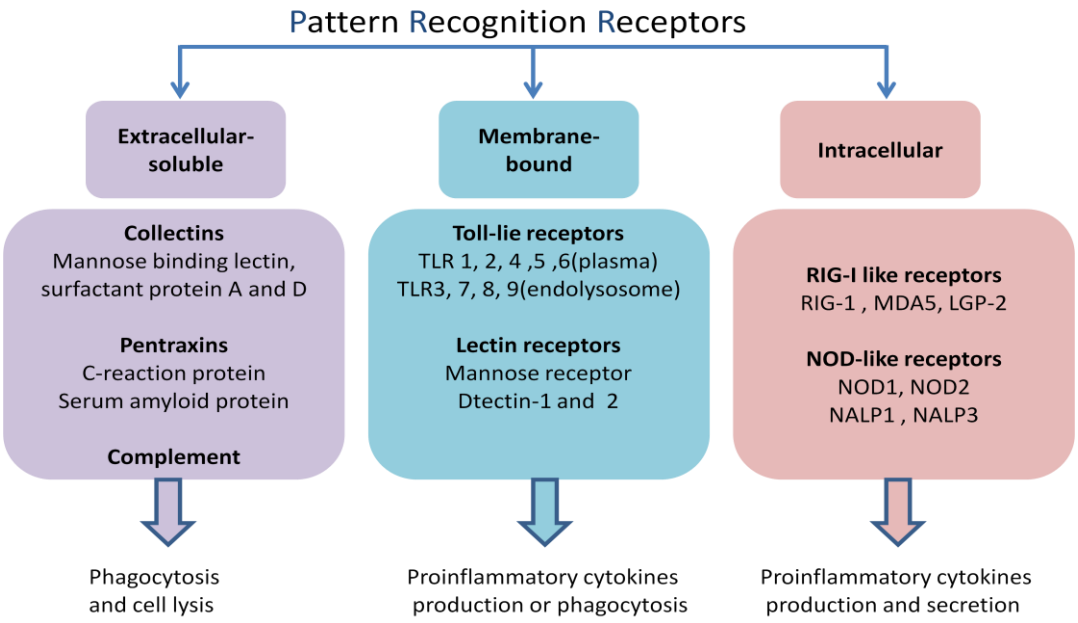

Figure 1.1: Major PRRs in human innate immunity (modified from Ranjan, Bowzard *et al*., 2009)

The major components of soluble PRRs are complement, C-reactive protein, serum amyloid protein and mannose-binding protein. They are mostly synthesised in the liver and kept at a certain concentration in the plasma. When they recognize the pathogen, they can modulate and strengthen innate immunity. The transmembrane PRRs include Toll-like receptors (TLRs) and C-type lectins. Dectin-1 and Dectin-2 are the major members of C-type lectins. They can identify β-glucans from fungal pathogens such as *Candida albians.* The cytosolic PRRs can be separated into two groups based on their mechanism of activation. The first group includes the retinoic acid-inducible gene I (RIG-I)-like helicases receptors (RLRs), and the second group is nucleotide-binding oligomerization domain containing (Nod)-like receptor (NLR) family, it includs Nod1 and Nod2. Both of them directly detect cytosolic PAMPs and activate various signalling pathways[14]. Additionally, the second group contents of NALP3, NLRC4. They are involved in the formation of inflammasomes, which activate caspase-1 and release mature IL-1β. Different from transmembrane PRRs, cytosolic PRRs can distinguish intracellular infections from extracellular infections, cell-intrinsic infections from cell

-extrinsic infection, and pathogenic microorganisms from harmless, commensal microorganisms [12]. Therefore, the following paragraph will describe the Toll-like receptors (TLRs), the retinoic acid inducible gene I (RIG)-like receptors (RLRs) and Nod like receptor in a detailed way.

Table 1.1: Major PRRs and their ligands (modified from Takeuchi and Akira 2010)

PRRs	Localization	Ligands	organisms
Toll-like receptors			
TLR1	Plasam membrane	triacyl lipoprotein	Bacteria
TLR2	Plasam membrane	lipoprotein	Bacteria, viruses, parasites
TLR3	endolysosome	dsRNA	Virus
TLR4	Plasam membrane	LPS	Bacteria
TLR5	Plasam membrane	Flagellin	Bacteria
TLR6	Plasam membrane	Diacyl lipoprotein	Bacteria, Viruses
TLR7/8	endolysosome	ssRNA	Bacteria, Viruses
TLR9	endolysosome	cPG-DNA	Bacteria, Viruses,protozoa
TLR10	endolysosome	unknown	Unknown
C-type lectin receptors			
Dectin-1	cytoplasm	β-Glucan	Fungi
Dectin-2	cytoplasm	β-Glucan	Fungi
RIG-1 like receptors			
RIG-1	cytoplasm	short dsRNA, 5' triphosphate dsRNA	RNA virus, DNA virus
MDA5	cytoplasm	long dsRNA	RNA virus (Picornaviridae)
LGP2	cytoplasm	unknown	RNA virus, DNA virus
NOD-like receptors			
NOD1	cytoplasm	bacterial peptidogylcans	Bacteria
NOD2	cytoplasm	bacterial peptidogylcans	Bacteria
NALP1	cytoplasm	broad ligand specificity	PAMP OR DAMP
NALP3	cytoplasm	broad ligand specificity	PAMP OR DAMP

1.2.1 The Toll- like receptors/interleukin-1 receptor superfamily

1.2.1.1 The Toll-like receptors

The Toll-like receptor family is one of the best researched PRR families. Toll was first found and named by Dr. Christiane Nüsslein-Volhard in *Drosophila* in 1985. It was thought initially vital only for the development of embryonic dorsoventral polarity[15].

However, Dr. Jules A Hoffmann discovered in 1996 that this dorsoventral regulatory gene also plays an essential role in the innate immunity as well. Toll can stimulate NF-κB activation after recognizing fungi [16]. The first human TLR was found in 1994 by Nomura and his colleagues [17], mapped to a chromosome in 1996 [18] and named TLR4. TLR4 was first described as a receptor for LPS in mice [19]. Meanwhile, activation of TLR4 triggers both innate and adaptive immunity [20]. In turn, the other TLRs were investigated sequentially. Till now, 10 TLRs have been identified in humans, out of which 9 TLRs are well characterized (Table 1.1). Particularly, TLR1 to 9 are conserved in both human and mice. As type I integral membrane glycoproteins, TLRs consist of a N-terminal leucine-rich repeat (LRRs) domain, a transmembrane region and a cytoplasmic signalling domain homologous to interleukin 1 receptor (IL-1R), named as Toll/IL-1R homology (TIR) domain [21]. The extracellular LRR domain contains19-25 tandem LRR motifs which includes the motif XLXXLXLXX or conserved amino acid residual XψXXψXXXXFXXLX (ψ=hydrophobic residue) is 24-29 amino acid in length [22]. Each LRR domain is composed of an α helix and a β strand. It was mapped that LRR will form a horseshoe structure [23].

Based on the location and activation of different pro-inflammatory cytokines, TLRs can be divided into two subgroups. TLR 1, 2, 4, 5, 6 are primarily expressed on the plasma membrane, and can recognize PAMPs derived from bacteria, fungi and protozoa. Whereas TLR 3, 7, 8 and 9 are exclusively expressed in the lysosome or endosome membrane and can identify nucleic acid disintegrated from viruses and bacteria, but also from the host [13, 23].

Each TLR identifies certain type of molecular pattern of microorganisms (Figure 1.2.a and b). For instance, TLR2 forms heterodimer with either TLR1 or TLR6 to recognize its ligands. TLR1/TLR2 identifies triacylated lipopeptides, while TLR6/TLR2 recognizes diacylated lipopeptides [13]. The crystal structure of the human TLR1/TLR2 was first described in 2007. It indicates that binding of the triacylated lipopeptides (Pam_3CSK_4) induces the hetrodimerization of TLR1 and TLR2. The ectodomains of TLR1/TLR2 form an “M” shape. The two ester bound lipid chains of Pam_3CSK_4 are submerged into a hydrophobic pocket of TLR2, while the amide –bound lipid chain is inserted into a hydrophobic space in TLR1 [24]. Activation of TLR2 will induce various pro-inflammatory cytokines production, except for type I IFNs.

However, recent research indicates that type I IFNs will be produced after viral infection of TLR2 inflammatory monocytes [25].

The ligand of TLR4 is Lipopolysaccharide (LPS), which is derived from Gram-negative bacteria [19, 20, 26]. However, transfecting TLR4 with myeloid differentiation factor 2 (MD2) can trigger 2-3 folds NF-κB activation than transfecting TLR4 alone into HEK293T cells [27]. Moreover, the crystal structure of TLR4-MD2 indicates that MD-2 binds to TLR4 and generates a hydrophobic space for interaction with LPS [28]. Later, it was proved that two complexes of TLR4-MD2-LPS form a horseshoe shape by homodimerization [29]. TLR4 can recognize viruses via binding to viral envelope proteins [23]. TLR4 has the ability to induce IFN-β production [30].

TLR5 recognizes flagellin [31]. Flagellin is the main component of bacteria flagella, the motility apparatus of many microbial pathogens. The crystal structure of a *Salmonella* flagellin revealed that flagellin domains consists of N- and C- terminal α helix chains(D0), the central α helix chain (D1), and the hypervariable central region with β sheets(D2 and D3). TLR5 specifically recognizes the constant domain D1 in flagellin[32]. TLR5 is mainly expressed on epithelial cells, monocytes, and immature DCs.[23]. Particularly, TLR5 is only expressed on the basolateral of epithelial cells in the intestine. Thus, it can only distinguish the bacteria which have invaded into the epithelial cells and trigger NF-κB and TNF-α activation [31]. Moreover, it was found that TLR5 highly expressed in the lung, which seems to play an important role in cleaning pathogens in the respiratory tract.

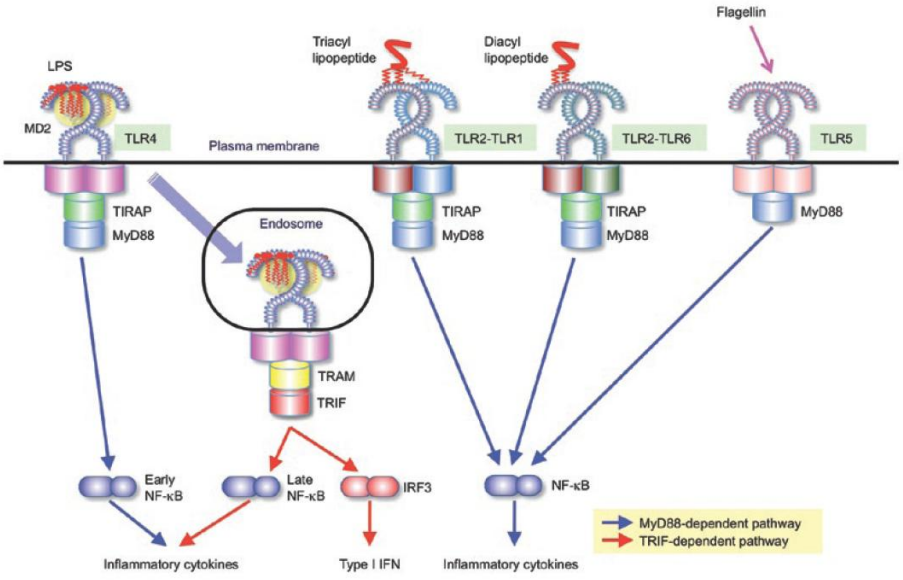

Figure 1.2 A: plasma membrane located TLRs and their ligands (Kawai and Akira 2010)

TLR3 is responsible for double strand RNA which is produced during viral infection, as a replication outcome or a by product of symmetrical transcription in DNA viruses [33]. TLR3 is expressed widely in conventional dendritic cells, epithelial cells, astrocytes and glioblastoma cells in the brain [23]. After binding the ligand, TLR3 can activate NF-κB activation and the production of the type I interferon (IFNs) [33]. A recent study indicates that TLR3 is crucial for the production of IL-12p40 [34]. The crystal structure of TLR3 shows that two ecodomains homodymerized and generated a glycosylation-free face which binds by polyinosinic polycytidylic acid (poly I:C), a synthetic dsRNA analog. Interestingly, it was found that TLR3 deficiency is related with recurrent Herpes simplex encephalitis (HSE) [35].

Human TLR7 is homologous with TLR8, and both of them locate on the X chromosome. TLR7/8 recognizes single strand RNA (ssRNA) as well as small synthetic compounds (imidazoquinolines). TLR7 and TLR8 are expressed on the endosome membrane. Due to the low pH value in the endosomes, it is easy for viruses to release ssRNA. TLR7 can also recognize the RNA derived from bacteria such as Group B Streptococcus [36]. Triggering TLR7/8 has also been shown to have conflicting effects on HIV replication: on the one hand, it suppresses HIV replication in acute *ex vivo*-infected lymphoid tissue; on the other hand, it stimulates the release of HIV virions from latently infected cells. Furthermore, TLR8 mediated NF-κB activation is solely involved in releasing the latent HIV [37]. TLR9 is mainly expressed

on the plasmacytoid dendritic cells (pDC) and identify viral DNA, such as herpes simplex virus 1 (HSV-1) and murine cytomegalovirus (MCMV), both of which contain many of unmethylated CpG motif. It can induce TLR9 activation and produce pro-inflammatory cytokines and type I IFN [38-40]. Furthermore, TLR9 can recognize the pigment hemozoin of malaria [41, 42].

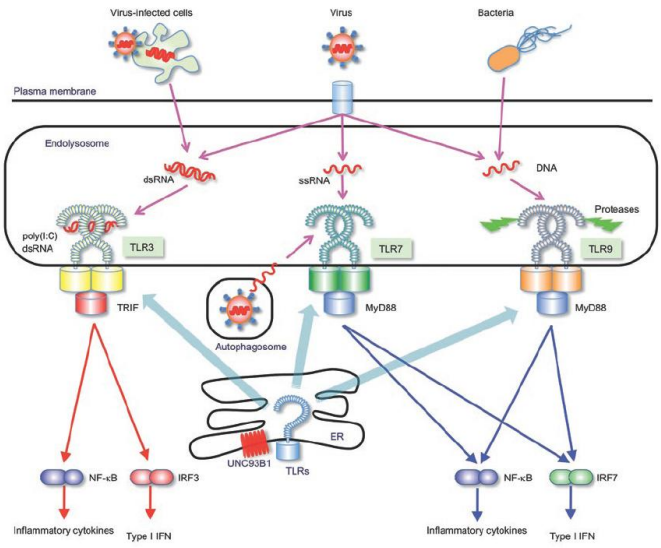

Figure 1.2 B: Endolysosome membrane located TLRs and their ligands (Kawai and Akira 2010)

Current research shows that TLRs are very important for the host defense against the pathogen invasion. The different location and dynamic mobility are key features of TLRs for them to distinguish self and non self ligands [43].

1.2.1.2 The interleukin-1 receptor family

Although interleulin-1 receptor family (IL-1R) is not a PRR, it encompasses the similar conserved TIR domain with TLR family. Hence, the delineation of IL-1R family is presented here. The discovery of interleukin-1 receptor (named as type I IL-1 receptor (IL-1RI) was a critical step to understand the pro-inflammatory cytokines signalling pathway[44]. The IL-1RI has extracellular three immunoglobulin (Ig) domains, but the intracellular domain has not been fully defined at that time. Later discovery revealed that the cytosolic region of IL-1RI had significant homolog to the *Drosophila* protein Toll [45]. This demonstration led to the definition of the IL-1R/Toll-like receptor superfamilly. Due to the homologus cytosolic domain, it was termed as the Toll/IL-1R (TIR) domain in 1998. So far, three subgroups in the

IL-1R/Toll-like receptor superfamily have been identified, which depending on the extracellular region of the protein has homology to the immunoglobulin-like, or to the leucine- rich repeat motif like Toll receptor, or to the adaptor protein(no extracellular domain) (Figure 1.3) [46].

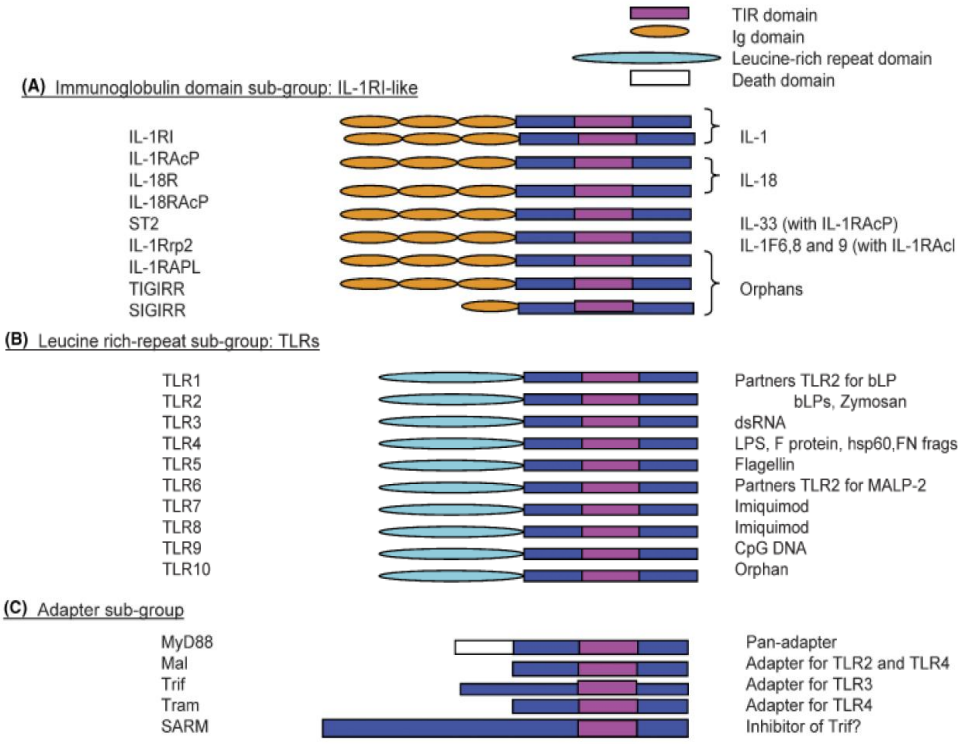

Figure 1.3 The IL-1R/TLR superfamily (Luke A.J. O'Neill, 2008)

The immunoglobulin domain sub-group, which is also named the IL-1RI like group, consists of 9 members. Except for the single immunoglobulin IL-1R-related molecule (SIGIRR), which only has one Ig extracellular domain, all the rest have three Ig domains. IL-1RI and the IL-1 receptor accessory protein (IL-1RAcP) are two components of type I IL-1 receptor complex. The agonists of IL-1RI complex are IL-1α, IL-1β and the naturally occurred antagonist IL-1RA. IL-1RAcP was found by using specific monoclonal antibody (mAb) 4C5 to block IL-1β binding to IL-1RI. However, it binds to IL-1RAcp which is highly homologous to IL-1R [47]. Research revealed that lacking IL-1RAcP cannot induce IL-1 response. However, transfecting IL-1RAcP to the cells can rescue the IL-1 activation and NF-κB activation [48]. IL-1RAcP may be internalised into the cell and interacte with the down steam protein interleukin-1 receptor associated kinase (IRAK) [48, 49]. Analogous to IL-1 receptor complex, the

IL-18 receptor (IL-18R) and IL-18 receptor accessory protein (IL-18AcP, also known as IL-18AcpL) form the IL-18 receptor complex[46], which also requires IRAK to induce NF-κB activation [50]. The agonist of IL-18 receptor complex is IL-18. ST-2 and IL-1RAcp have been identified to be the receptor complex for IL-33[51]. IL-33R activation NF-κB requires TRAF6 to recruit IRAKs for initiating signalling transduction. In general, the IL-1RI family share the intracellular signalling pathway with TLRs-NF-κB starting from MyD88 (see figure1.4). Activation of TLRs produces pro-inflammatory cytokines such as IL-6 and pro-IL-1β. Then the pro-IL-1β can be matured and released to further activate IL-1 receptors.

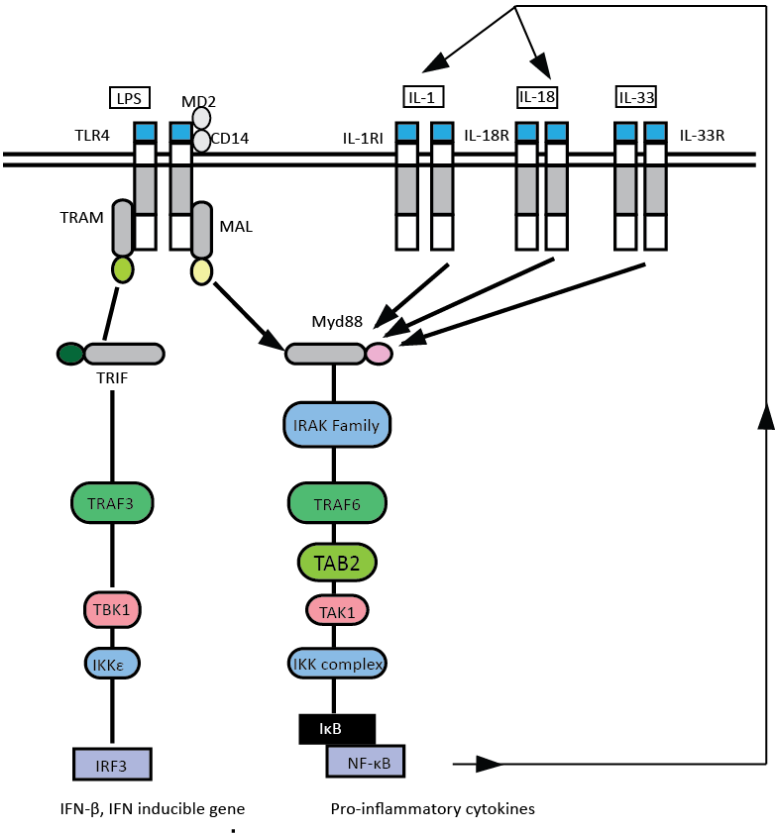

Figure 1.4 The cross talk between TLRs and IL-1R signalling pathways (modified from Dunne and O'Neil, 2003)

Overall, IL-1 family are the general growth factors for T lymphocytes. IL-1 majorly regulates Th17 cells[52], IL-18 promotes Th1cells and IL-33 regulates Th2 cells [46]. (Figure1.5)

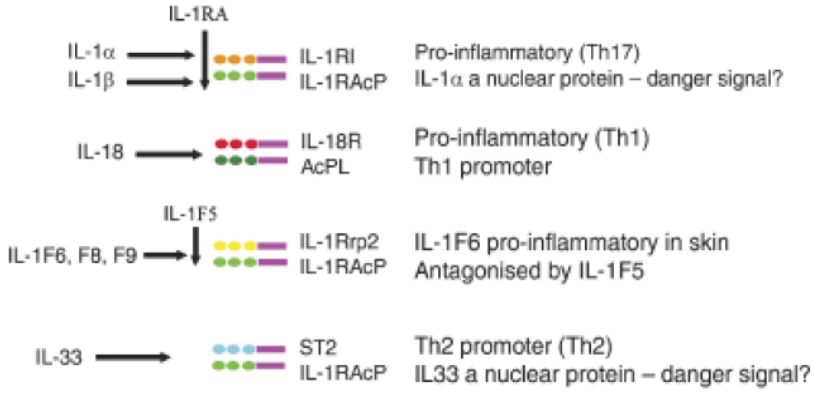

Figure 1.5 Process IL-1 receptor family and their ligands (Luke A.J. O'Neill, 2008)

The other two subgroups are the LRR subgroup (10 members) and adaptor subgroup (5 members). Although the TIR domain is a hallmark for the whole family, little is known about this domain. It seems that it is very important to mediate homotypic interactions with other TIR domain [21]. The activation of TLR/IL-1 superfamily reveals that the receptor TIR domain homo/hetro dimerization is required for downstream activation. TIR domain dimerization is used for recruiting the adaptor proteins which also contain the TIR domain to induce further signalling (see figure1.3). The signalling pathway of each TIR domain containing protein will be described in section 1.3

1.2.2 The RIG-I-like receptors family

The RIG-I-like receptors (RLR) family consists of retinoic-acid-inducible protein I (RIG-I), melanoma differentiation-associated gene 5 (MDA-5), and laboratory of genetics and physiology 2 (LGP-2) [53]. Structural analyses demonstrated that RIG-I and MDA-5 are comprised of two N-terminal caspase recruitment domains (CARDs), a central DEAD box helicase/ATPase domain, and a C-terminal regulatory domain, while LGP-2 does not have CARDs (Figure 1.6)

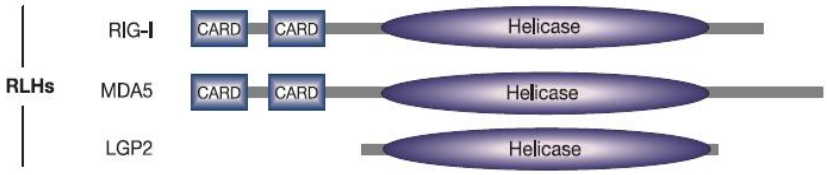

Figure 1.6 The schematic diagram of RLR family members (Meylan, Tschopp *et al*. 2006)

RLRs are located in the cytoplasma. It was verified that they are the receptor to recognize cytoplasmic dsRNA [54]. As aforementioned, TLR3 is also the detector of dsRNA. However, TLR3 cannot recognize the dsRNA when the viruses occur into the cytoplasma. Type I IFN can still be produced even in fibroblasts and cDCs without MyD88 and TRIF [55], indicating that RLR are essential for detecting viruses and compensate for TLR signalling. Similar experiments also confirmed that MDA-5 is a RNA sensor [56]. In contrast to RIG-I and MDA-5, LGP-2 binds to RNA whereas it seems to play a dominant-negative role [57]. Some researches indicats that LGP-2 is dispensable in the RIG-I like receptor signalling pathway. Later researches indicate that the ligands for RIG-I and MDA-5 are different. RIG-I prefers to recognize relatively short dsRNA(<1kb), while MDA-5 can identify long dsRNA [58]. The finding has been confirmed by EMCV (produces long dsRNA during replication) and VSV (generates short dsRNA during replication) which were recognized by MDA-5 and RIG-1 respectively. The presence of a 5' triphosphate at the end of dsRNA greatly enhances RIG-1 induced type I IFN secretion amount. C-terminal domain of RLR is responsible for interacting with dsRNA. Current research shows that RIG-I and LGP-2 have similar RNA binding loops in the C-terminal domain. However, the MDA-5 RNA binding loop looks much flatter due to opened confirmation of loop. It may imply that MDA-5 has weaker interaction with dsRNA [59, 60].

The CARD domains of RLRs are the effect domain to trigger a signalling cascade. The N-terminal of CARDs interacts with IFN-β promoter stimulator 1(IPS-1) (also called VISA, Cardiff and MAVS) [61-64]. IPS-1 contains a N-terminal CARD domain as well. According to the evidence that RIG-1 and MDA-5 are recruited by IPS-1, and IPS-1 can be an adaptor protein of the RLR signalling pathway. By over-expressing IPS-1 into human cells, it can trigger type I IFN and NF-κB activation [23]. Interestingly, the C-terminus of IPS-1 harbours a transmembrane region which targets IPS-1 to the mitochondrial outer membrane. However, when IPS-1 is released from mitochondria to the cytoplasm or is located to endoplasmic reticulum, it can no longer induce IRF and NF-κB activation. It is inferred from the experiments that IPS-1 is cleaved and released by the HCV viral protease NS3/4A [13]. IPS-1 activates TBK1 and IKK-ε then TBK and IKK- ε phophorylate IRF-3 and IRF-7. FADD and RIP1 can also interact with IPS-1 via non-CARD domains to trigger NF-κB activation [23]. Both TLR3 and RIG-I receptors identified dsRNA. However, TLR3 recognize the dsRNA which presents in

endosome and RIG-I receptor identify dsRNA in cytoplasm (See figure 1.7).

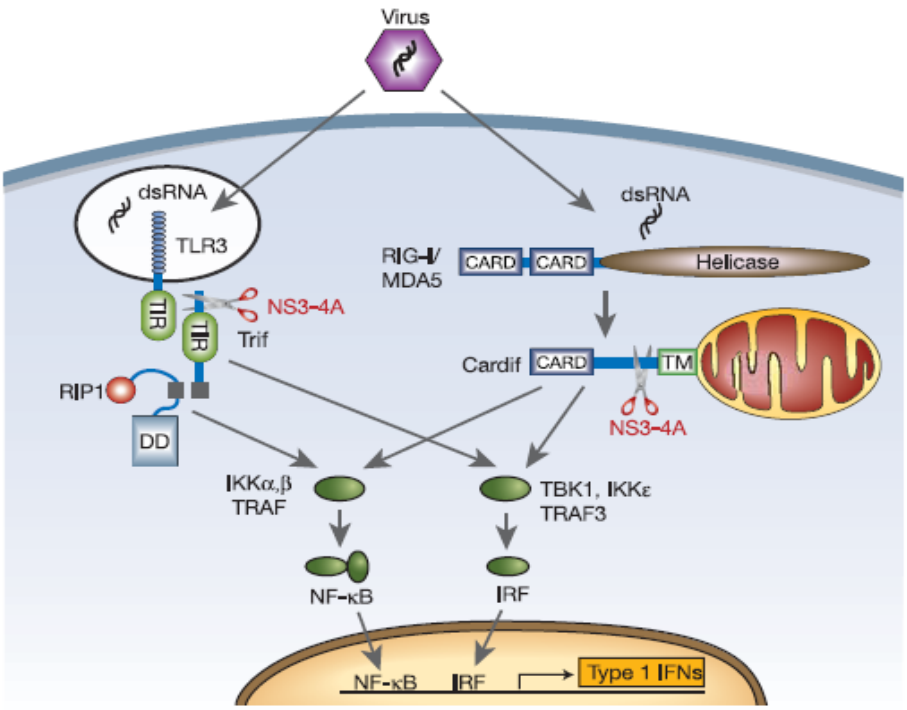

Figure 1.7 Sensing of viral dsRNA by TLR3 and RLR (Meylan, Tschopp *et al*. 2006)

1.2.3 The Nod-like receptor family

The nucleotide binding oligomerization domain (NOD)-like receptor family (also called NLR) is involved into sensing intracellular pathogens and danger associated molecular pattern (PAMPs and DAMPs) [65]. The proteins in this family consist of three domains which have the similar structure with disease resistant R proteins found in plants[66]. The three domains are N-terminal domain, central nucleotide–binding domain and C-terminal LRR domain. The central domain is a nucleotide–binding domain (NBD), which is responsible for self-oligomerization and dNTP activity. The C-terminus of NLRs is a series repeats of the LRR motifs. It is responsible for identifying PAMPs or DAMPs. The LRR folds back and covers the NBD domain in static situation to avoid self-oligomerization. However, when LRR is activated by PAMPs or DAMPs, the NBD domain is exposed and directs the oligomerization [67]. The NBD domain has similar structure with AAA+ domain family, which are apt to form hexamers or heptamers. Thus, NLRs might form structure with this size as well. At the N-terminal, NLRs either have a pyrin domain (PYD), a caspase recruitment

domain (CARD), or a baculovirus inhibitory repeat domain (BIR). An exception is NLRX1, which does not contain the three similar domains. However, it can still fold in a similar way[68]. The N-terminus domain is assumed to conduct homotypic interactions, such as PYD-PYD or CARD-CARD. The function of BIR domain is unclear. There are at least 23 known members of the NLR family, which can be subdivided into 3 subgroups depending on N- terminus structure: NLRC family (contain CARD domain), NLRP (contain pyrin domain), and the rest NLRs including CARD-containing activation domain of the class II transactivator(CIITA), ICE-protease activating factor(IPAF) and NAIP which has the BIR domain (Figure 1.8) [69]. The NLRs with pyrin domain or BIR domain cannot induce transcriptional factor of inflammatory cytokines such as NF-κB. However, they are involved in inflammasome formation and induce caspase-1 activation[13].

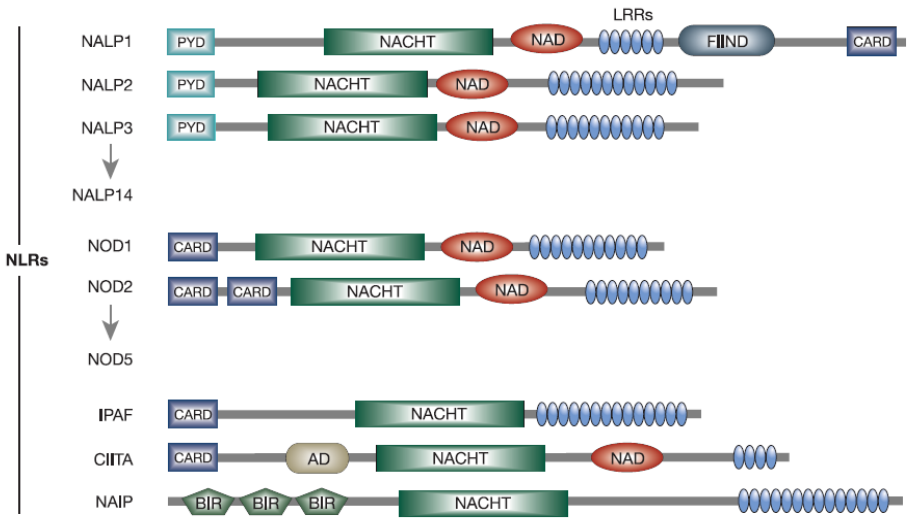

Figure 1.8 The schematic diagram of NLR family members (Meylan, Tschopp *et al*. 2006)

NOD1 and NOD2 are the first reported NLRs members[70]. Both NOD1 and NOD2 recruit serine/theronine kinase receptor-interacting protein (RIP2) which results in the activation of IκB, and finally induces NF-κB activation [71, 72]. However, recent research indicates that the NLRP subfamily plays a key role in forming inflammasome. The common feature of NALP is that they contain N-terminus PYD domain which is used to recruit PYD domain of apoptosis-associated speck like protein (ASC) [73]. Then ASC can recruit caspase-1 through CARD-CARD homophilic interaction. Thus, oligomerization of NLRP is thought to bring the caspases together and generate a

macrocomplex called the inflammasome [74]. Activation of caspase-1 catalyzes the cleavage of pro-IL-1β/IL-18 to mature IL-1β/IL-18 which is released into the extracellular space. In turn, they can activate IL-RI and IL-18R signalling pathways [69]. Regarding the inflammasome induced-maturation of IL-1β and IL-18, early research addresses that pre-priming of TLRs isrequired [75, 76]. In whole, these investigations imply that TLRs, IL-1R and NLRs have tight interaction with each other in terms of orchestrating innate immunity (See figure 1.9)

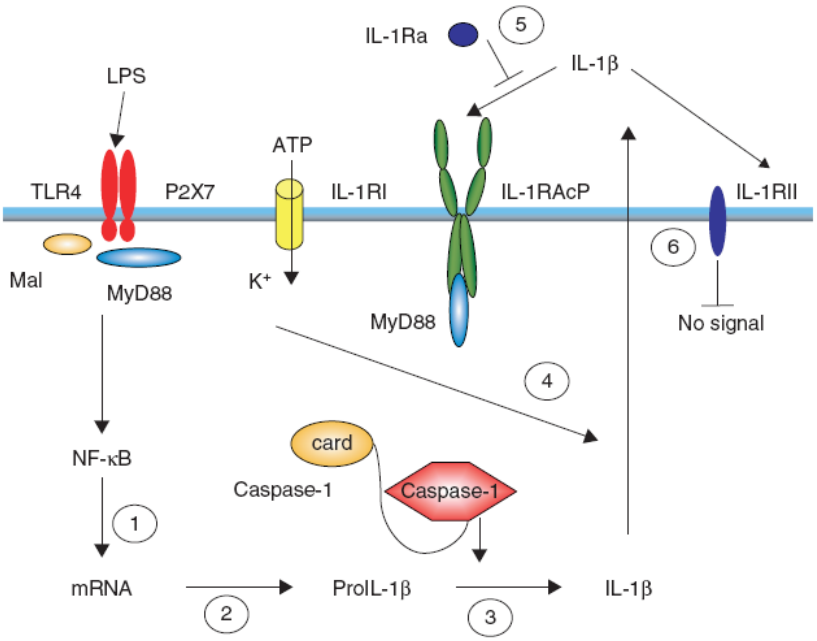

Figure 1.9 The cross talk among TLRs, IL-1RI and inflammasome (Netea and Veerdonk et al, 2008). Several control mechanisms have evolved to modulate the production and activation of IL-1β: ① transcription of IL-1β mRNA when cells were activated by TLR ligands. ② translation to pro-IL-1β. ③ processing of the 31kDa inactive IL-1β precursor into the bioactive 17kDa IL-1β by cleavage of Caspase-1 and 17kDa IL-1β is released to the extracellular space. ④ potassium efflux also triggers the IL-1β maturation and release. ⑤ the extracellular 17kDa IL-1β directly binds to IL-1R and induces the transcription of IL-1β. However, this step is controled by IL-1 receptor antagonist (IL-Ra) and Type II decoy receptors (IL-1RII). ⑥ Blockade of the interaction of bioactive IL-1β with the singnalling type I IL-1R/interleukin 1 receptor accessory protein (IL-1RAcP) complex.

1.3 The TIR-domain containing adaptor protein in TLR signalling pathways

To date, five TIR domain containing adaptor proteins have been found. They are the myeloid differentiation primary response gene 88 (MyD88), MyD88 adaptor-like (MAL), TIR-domain-containing adaptor-inducing interferno-β (TRIF), TRIF-related adaptor molecular (TRAM) and sterile α and HEAT-Armadillo motifs (SARM) [77]. (Figure1.10)

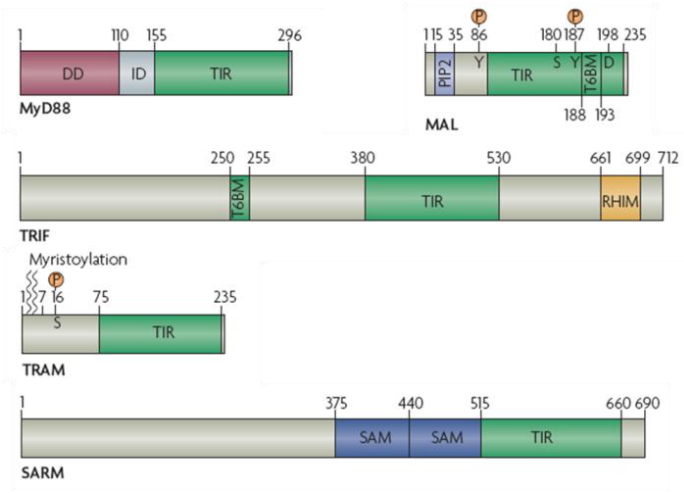

Figure 1.10 The schematic diagram of five TIR-domain containing adaptors (O'Neill, Bowie 2007)

TLRs are activated by their respective ligands. The TIR domain of TLRs then forms homo or heter dimerization and recruits the TIR domain of the adaptor protein to initiate downstream signalling. The TIR domain is a ~160 amino acid motif, and consists of five β-sheets surrounded by five α helices and connected by flexibly loops [78]. Two significant loops are called 'BB loop' and 'DD loop', which are found in each TIR domain [79]. Meanwhile, the TIR domain is divided into three regions, named Box 1, 2, 3. Box1 is the signature of the TIR domain; Box 2 contains the'BB loop' which mostly contains a key proline residue inside; Box 3 is important for signalling [21](see figure1.11).

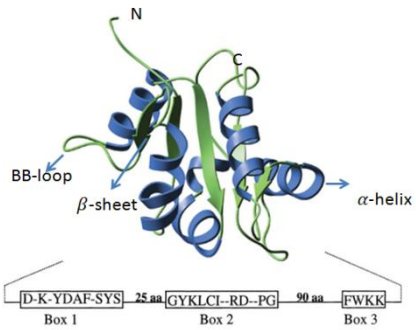

Figure 1.11 The TIR domain structure of human TLR2 (modified from Xu, Tao et el, 2000)

Albeit the backbone structure of TIR domain is conserved, the surface properties can be unique for each TIR-containing-protein, thus they can guide the specific interaction and induce appropriate immune responses [79].

1.3.1 Myd88 dependent signalling pathway

MyD88 was found and named by searching the induced genes in terms of differentiation of M1D+ myeloid precursors in response to IL-6 [80]. It was first found to be involved in the IL-1 receptor signalling pathway [81]. Then it was more widely investigated in TLR signalling pathway [82, 83]. The generation of MyD88 deficient mice demonstrated that MyD88 is essential for TLR2, TL4, TLR5, TLR7 TLR9, IL-1R and IL-18R activation to produce pro-inflammatory cytokines [79]. Therefore, those receptors signalling pathways were named as MyD88-dependent signalling pathway. Only TLR3 and partially TLR4 signalling were not impacted in MyD88 deficient mice. This indicates that there may be another adaptor protein that can induce signalling by a " MyD88-independent signalling pathway" (section1.2.4.2).

It has also been shown that MyD88 is essential for NF-κB, JNK and p38 activation. MyD88 is composed of a C terminus TIR domain, an intermediary domain (ID) and an N-terminal Death domain (DD). The MyD88 TIR domain directly interacts with TLR5, TLR7, TLR8 and TLR9 and its DD domain recruits interleukin-1 receptor associated kinase 4 (IRAK4) via homotypic interaction. The IRAK family consists of four members: IRAK1, IRAK2, IRAK3 (also called IRAK-M) and IRAK4. More detail information will be documented in section 1.4. IRAK4 is the first kinase recruited to MyD88, and autophosphorylates and phosphorylates IRAK1 or IRAK2 [84]. These interactions are all realized via the DD domain homotypic interaction, and form an oligomeric complex named as the Myddosome [85, 86]. IRAK3 plays a negative role that arrests the IRAK1 or IRAK2 and IRAK4 dissociating from Myd88 [87]. Then IRAK1 or IRAK2 interacts with tumour necrosis-factor- receptor-associated factor6 (TRAF6). Recently, the experiments indicated that IRAK2 binding to TRAF6 is essential to trigger the ubiquitination of TRAF6 [88]. Sequentially, TRAF6 recruits transforming-growth-factor-β-activated kinase 1 (TAK1) and TAK 1-binding protein 2/3 (TAB2/3), further leading to TAK1 activation which directs NF-κB and AP-1(ERK1/2 and JNKs)/CREB activation [89]. For NF-κB activation, TAK1 then induces the IκB kinase (IKK) complex which contains two catalytic subunits (IKKα or IKKβ), and one essential regulatory subunit IKKγ (also called NEMO) activation. The complex sequentially phosphorylates the inhibitor subunit IκB [90]. The phosphorylated IκB degrades and releases the p65/p50 to translocate into the nucleus

and activates NF-κB. Similarly, the IKK complex phosphorylates p105 and induces p105 degradation, where the serine/theronine kinase tumour progression locus2 (Tpl2) will be activated [91]. Tpl2 can further induce MKK1/MKK2 to phosphorylate singnal –regulated kinases ERK1 and ERK2. Meanwhile, TAK1 activates MKK4/7, which leads to Jun-N-terminal kinase (JNK) activation. Both JNKs and ERK1/2 direct AP-1 transcription factor activation. Moreover, TAK1 activates MKK3/6, which induces the phosphorylation of p38 [92]. See figure 1.12

MyD88 is also involved in IFN-α production as well. In terms of TLR7, TLR8 and TLR9 activation, the DD of MyD88 interacts with the interferon regulating factor 7 (IRF7), and activates the IFN-α promoter in pDCs. The ubiquitin ligase activity of TRAF6 is required for further IRF7 activation [93]. After this, a complex encompassing IRAK1, IRAK4, MyD88, TRAF6 and IRF7 was detected and IRAK1 was essential for IRF7 phosphorylation [94]. MyD88 also takes part in the IRF1, IRF5 and IFN-γ signalling pathways. IRF1 is required for several genes related to TLRs. IRF5 is vital for the production of pro-inflammatory and type I IFN in response to the activation of all TLRs [95]. Strikingly, IFN-γ is required to induce IRF1 activation.[79].

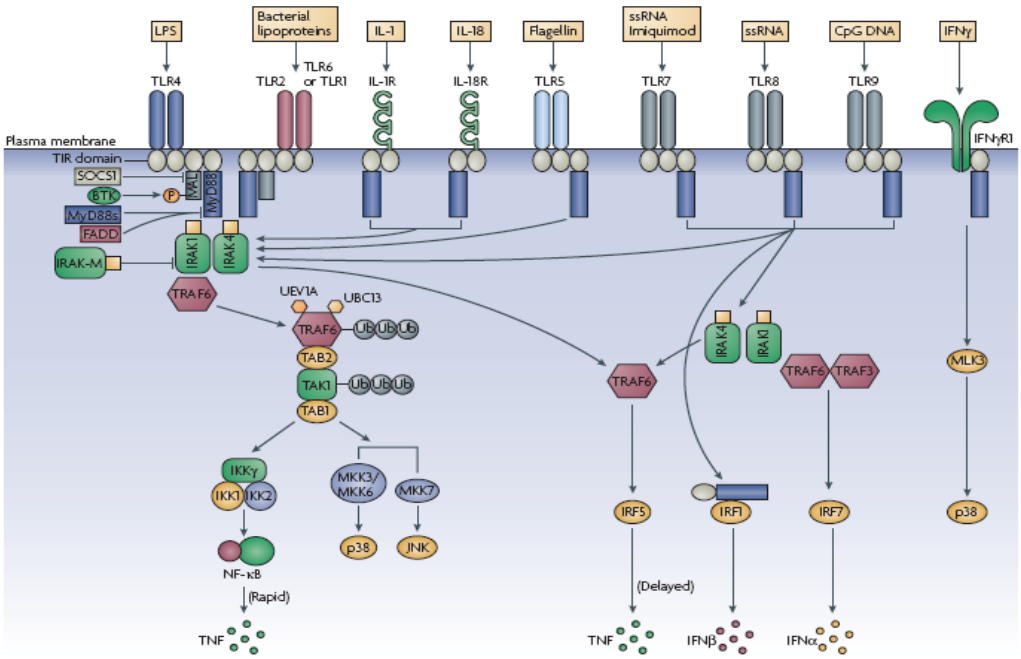

Figure 1.12 The MyD88 dependent signalling pathway (O'Neill and Bowie, 2007)

TLR2 and TLR4 activation also need MyD88. However, this is different from TLR5, 7, 8, 9, which directly interact with MyD88 via the TIR domain. TLR2 and TLR4 need another TIR domain containing adaptor protein called MAL or TIRAP to bridge the interaction between TLR2/4 and MyD88 [96]. Similar to MyD88, no evidence has been found to support that MAL participates in the IRF3 signalling pathway. Then it was thought to be a component in the MyD88 signalling pathway. Except for possessing a TIR domain in the C terminus, MAL encompasses a phosphatidylinositol-4, 5-bisphosphate (PtdIns(4,5)P_2) in the N-terminus which orientates MAL anchoring to the plasma membrane[97]. From the perspective of the protein structure, the electrostatic surface of the TIR domain of MAL is negative, while the TIR domain of MyD88 and TLR4 are positive. Therefore, TLR4 prefers to interact with MAL first [98]. Moreover, MAL has a TRAF6 binding motif, and may be involved directly in the interaction with TRAF6 and further activation of NF-κB and MAPKs [99]. This is the only finding that represents a unique MAL signalling pathway. Additionally, MAL is phosphorylated by Bruton's tyrosine kinase (Btk) and Btk is further involved in TLR2 and TLR4 signalling to activate NF-κB signalling [100]. Meanwhile, the suppressor of cytokine signalling-1 (SOCS-1) recognizes proline (P), glutamine (E), serine(S), threosine (T) rich region, also called PEST domain of MAL, and leads to the degradation of MAL via ubiquitination. Several epidemiological studies indicate that MAL coordinates the immune response of TLR4/2 activation in an appropriate way [101, 102]. Current research finds that MAL was cleaved by caspase-1 which is required for MAL to activate NF-κB [103] (See figure1.13).

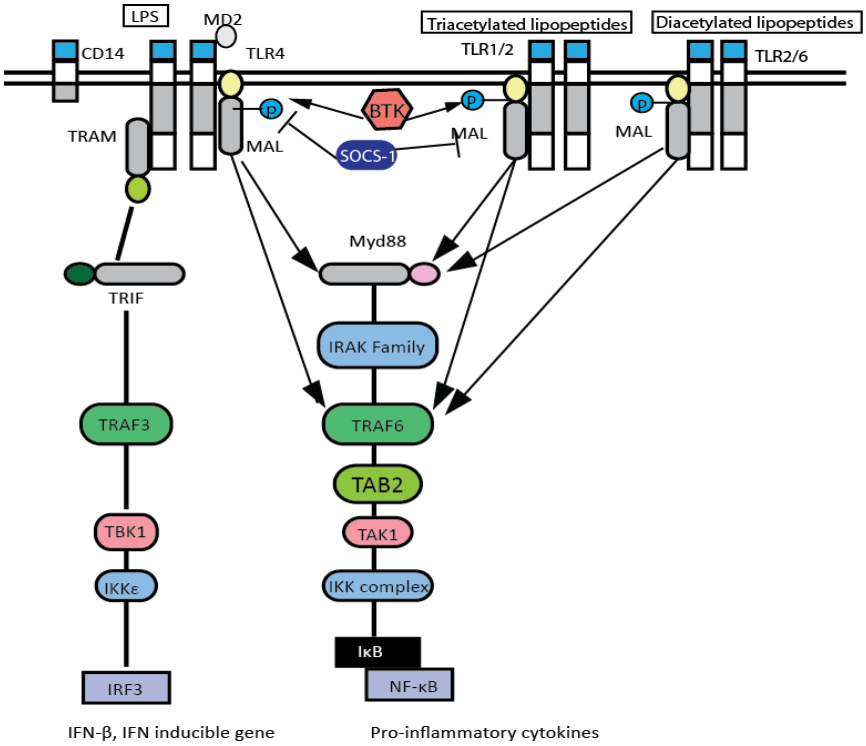

Figure 1.13 The Mal dependent signalling pathway

1.3.2 The TIRF dependent signalling pathway

In view of challenging MyD88/MAL deficient mice with different TLR ligands, only TLR3 and partially TLR4 signalling were not affected. Therefore, there must be another adaptor in charge of this signalling pathway. Hence, TRIF was identified by searching for TIR domain protein in the human genome [104]. One year later, another independent group also found TRIF by a yeast two-hybrid screen with TLR3 [105]. TIRF is very important to activate the IFN-β promoter. Stimulating TRIF-deficient mice demonstrated that IFN-β production and IRF3 activation were reduced, and the pro-inflammatory cytokine production was only reduced in TLR4 signalling pathway. However, no impact on TLR2, TLR7 and TLR9 in macrophage was found [106]. It was confirmed that the activation of NF-κB was abolished when challenging double knock-out MyD88 and TRIF cells with LPS. Furthermore, no genes were induced in double knockout cells which were stimulated with LPS. Therefore, this indicates that Myd88 and TRIF are complementary in terms of theTLR4 signalling pathway [107]. It was known that TRIF has a TIR domain in C terminus, while the TRAF6 binding motif is located in the N-terminus of TRIF. It indicates that TRAF6 can directly interact with TRIF and induce NF-κB. However, more research is needed to confirm this proposal [108, 109]. Moreover, the receptor-interacting protein homotypic interaction motif

(RHIM) was shown in the C-terminus of TRIF, and is involved in NF-κB activation as well [110]. The N-terminus of TRIF was shown to interact with TRAF family member associated NF-B activator (TANK) -binding kinase 1 (TBK1), which is a vital upstream kinase for IRF3 activation.

TLR3 directly interacts with TRIF. However, TLR4 needs another bridge protein called TRAM (also known as TICAM2), which is only involved in the TLR4 signalling pathway. Two biochemical modifications highlight the role of TRAM. Similar to MAL, the N-terminus of TRAM undergoes myristolyation, and thus can anchor TRAM to the plasma membrane [111]. Phosphorylation of TRAM at serine residue in position 16 is essential to activate the downstream signalling to release TRAM-TRIF from the membrane [112].

SARM was the last TIR domain containing adaptor protein found to be involved in TLR signalling pathway. It also participates in TRIF signalling pathway. In contrast to the other four members in TLRs signalling pathway, it interacts directly with TIRF and blocks TRIF signalling with no impact on MyD88-dependent signalling pathway [113] (See figure 1.14).

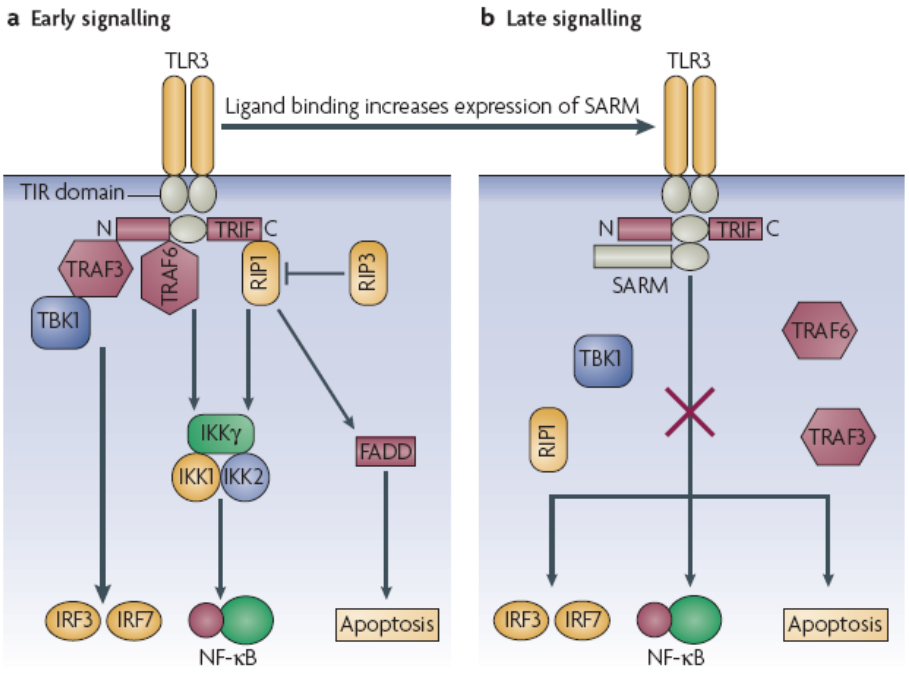

Figure 1.14 The TRIF dependent signalling pathway (O'Neill and Bowie, 2007)

1.4 The IRAK family

Interleukine -1receptor-associated kinases (IRAKs) are a family of serine and theronine kinases which are located intracellularly. The IRAK family consists of four members, IRAK1, IRAK2, IRAK3 (also called IRAK-M) and IRAK4. The IRAK activity was first described in 1994 in T cells responding to IL-1R stimulation [114]. Then the first family member IRAK1 was cloned in 1996. IRAK1 shares high similarity with Pelle a downstream serine/theronine kinase in *Drosophila* which acts in the Toll signalling pathway to induce the activation of *Dorsal* (equivalent to human NF-κB). Therefore, it was assumed that IRAK1 should be the downstream kinase of TLRs to activate of NF-κB [115]. IRAK1, IRAK2 and IRAK4 are expressed ubiquitously, whereas IRAK3 was only found in marcophages and monocytes upon stimulation [116]. All IRAKs share a similar arrangement of their functional domains (Figure1.15). They contain an N-terminal death domain (DD), a ProST domain (proline, serine and threonine rich domain), a conserved kinase domain (KD) and a C-terminal domain (except for IRAK4, which lacks the C-terminal) [117]. The DD interacts with the DD of MyD88 or with the DD of other IRAKs in a multimeric way to induce downstream signalling [118]. First, upon activation, MyD88 recruits IRAK4 via DD domains homotypic interaction. Then IRAK4 recruits IRAK2 by homotypic DD interactions to then form a multimeric complex called the Myddosome [85, 86]. The ProST region is rich in prolines, serines and threonines, and important for post-translation modifications, such as phosphorylation and ubiquitination [119, 120]. The KD of the IRAK family has an activation loop which is important for the kinase activity. Each IRAK encompasses an invariant lysine docked in the ATP binding pocket. Moreover, they also possess a tyrosine gatekeeper residue in the center of the ATP binding site. This tyrosine proves that the IRAK family is an unique serine/threonine kinase family [121, 122]. IRAK1 and IRAK4 contain an aspartate residue at the position 340aa and 311aa respectively. Thus, those two IRAKs are proposed to be active kinases. However, the alignment reveals that IRAK2 encompasses an asparagine residue at position 335aa instead of an aspartate. Moreover, IRAK3 has a serine at position 293 aa. Therefore, initially both of these kinases were thought to be pseudo kinases. The C-terminal domain of IRAKs contains the TRAF6 binding motif which is important to bind TRAF6. There are three TRAF6 binding motifs in IRAK1, two in IRAK2 and one in IRAK3 [123]. The IRAK family members are not only involved into NF-κB activation, but also play a role in

MAP kinase and IRF signalling pathways as described in section 1.2.4.1. The specific function of each IRAK will be presented in the following sections.

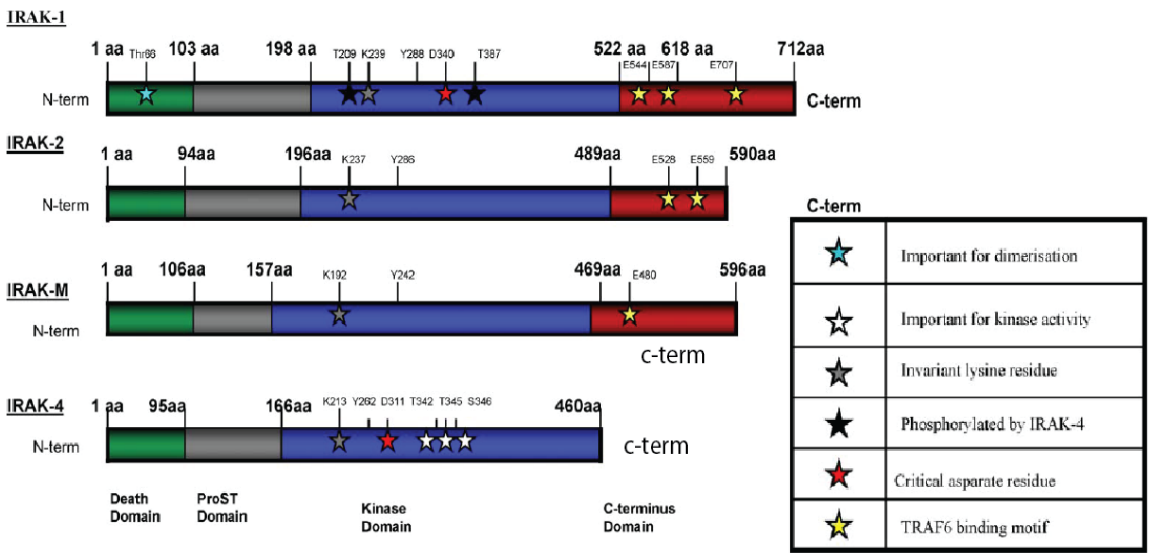

Figure 1.15 The schematic diagram of IRAK family members (Flannery and Bowie, 2010)

1.4.1 IRAK1

IRAK1 was the first IRAK family member to be identified as a downstream kinase in the IL-1R signalling pathway.The IRAK1 gene was mapped to chromosome Xq28, and encodes for a protein with 712 amino acids and a molecular weight of around 80 kDa. It has three splice variants (IRAK1a, b, c) in humans. In this dissertation, IRAK1 refers to IRAK1a (712aa). Except for the general domains that all IRAKs possess, IRAK1 contains a nuclear localization sequence (504-508aa) and a nuclear exit sequence (518-526aa) [124]. It was shown that IRAK1 translocates to the nucleus after the activation of TLRs in an over-expression system [125]. Thr66 in the DD domain of IRAK1 is pivotal to induce NF-κB activation. Although a mutation of this residue still retains the interaction with IRAK2 or IRAK-M, it cannot induce NF-κB activation but several studies argue that IRAK1 can undergo phosphorylation, ubiquitination and sumoylation [119, 126, 127]. Therefore, it is proposed that IRAK1 is tightly regulated and may play various roles in multiple signalling pathways.

IRAK1 undergoes phosphorylation in vitro by several steps. The first phosphorylation occurs at Thr209 which results in a conformational change in the kinase domain, and sequentially induces Thr387 phosphorylation as a secondary phosphorylation, which further leads to full enzymatic activity. Thr387 is also proposed to be the

phosphorylation site for IRAK4 [121]. Sequentially, several autophosphorylations occur in the ProST domain which permit IRAK1 to disassociate from MyD88 and to further trigger NF-κB activation [119]. The auto-phosphorylation may contribute to IRAK1 ubiquitination, which includes both K48-linked polyubiquitination leading to protein degradation [127] and K63-linked polyubiquitination leading to protein interaction and signal transduction [128]. It was assumed that pellino or TRAF6, which both belong to the E3 ligase family, can cause IRAK1 ubiquitination. Intriguingly, it was shown that IRAK1 also undergoes sumoylation through LPS stimulation. The sumoylated IRAK1 translocates into the nucleus and triggers STAT3 avtivation and selected gene expression [129]. Hence, the various modifications of IRAK1 generate more functions of IRAK1.

IRAK1 deficient macrophage cells demonstrate that NF-κB/p38/JNK activation was partially influenced in response to IL-1/LPS stimulation [130, 131]. Recently, it was claimed that IFN-α was totally abolished in response to TLR7/TLR9 ligands activation in IRAK1-deficient plasmacytoid DCs (pDCs). However, the NF-κB/MAP kinase activity was maintained at normal levels. Thus, IRAK1 may play a crucial role in type I IFN production. Strikingly, IRAK1 directly phosphorylates IRF7 [94]. In addition, it was shown that IRAK1 is essential for activation of IRF5 in human and mouse cells [132, 133]. Moreover, IRAK1 can directly interact with TRAF3 which is vital to induce type I IFN [134]. Intriguingly, IRAK1 is also involved in STAT1/STAT3 activation [129, 134, 135]. Conclusively, IRAK1 has diverse role in innate immunity.

1.4.2 IRAK2

IRAK2 was initially found by expressed sequence tag (EST) database search for homologs of IRAK1 in 1997 [136]. It was mapped to chromosome 3 at position 3q25.3-3q24.1. The length of the IRAK2 protein is 625aa and the molecular weight is around ~65 kDa. Compared to IRAK1 or IRAK4, which contain an aspartate in kinase domain, IRAK2 contains an asparagine. Upon over-expression, only full length IRAK2 can activate NF-κB, whereas the DD or central kinase domain plays a dominat-negative role in the signalling pathway. Thus, the integrity of IRAK2 is essential for its function [136]. Interestingly, the residue lysine 237 was thought as an intrinsic kinase of the IRAK2. Reconstitution of K237A into *Irak*2 knockout marocphages dimished the production of TNF-α and IL-6 [137]. Originally, it was assumed that IRAK2 has a

redundant role with IRAK1. The important role of IRAK2 was only discovered by Vaccina Virus (VAVC) induced NF-κB activation. It was shown that A52 (an important component of virus virulence) interacts with IRAK2, not IRAK1, then blocks the activation of NF-κB through TLR2, 3, 4, 5, 7/8, 9. Interestingly, it was claimed that IRAK2 is important for HEK293T which stably expresses TLR3 and is stimulated with polyI:C in terms of NF-κB activation, whereas IRAK1 was not involved in the TLR3 activation [138]. Subsequently, it was shown that over-expression of IRAK2 in HEK293T cells results in the interaction with TRAF6 and induces TRAF6 polyubiquitiantion, whereas over-expression of IRAK1 does not. Moreover, it was shown that IRAK2 triggers TRAF6 ubiquitination in IRAK1 deficient cells. All aforementioned results indicate that IRAK2 possesses a predominant role in NF-κB activation.

It is worth noting that only one isoform of IRAK2 is found in human. However, there are four splice variants in mice (*Irak*2a, *Irak*2b, *Irak*2c and *Irak*2d) [139]. Both of them have 13 exons(Human IRAK2 and *Irak*2a). The sequence identity of IRAK2 between human and mice is around 65%. Figure 1.16 shows the schematic diagram of human IRAK2 and murine *Irak*2.

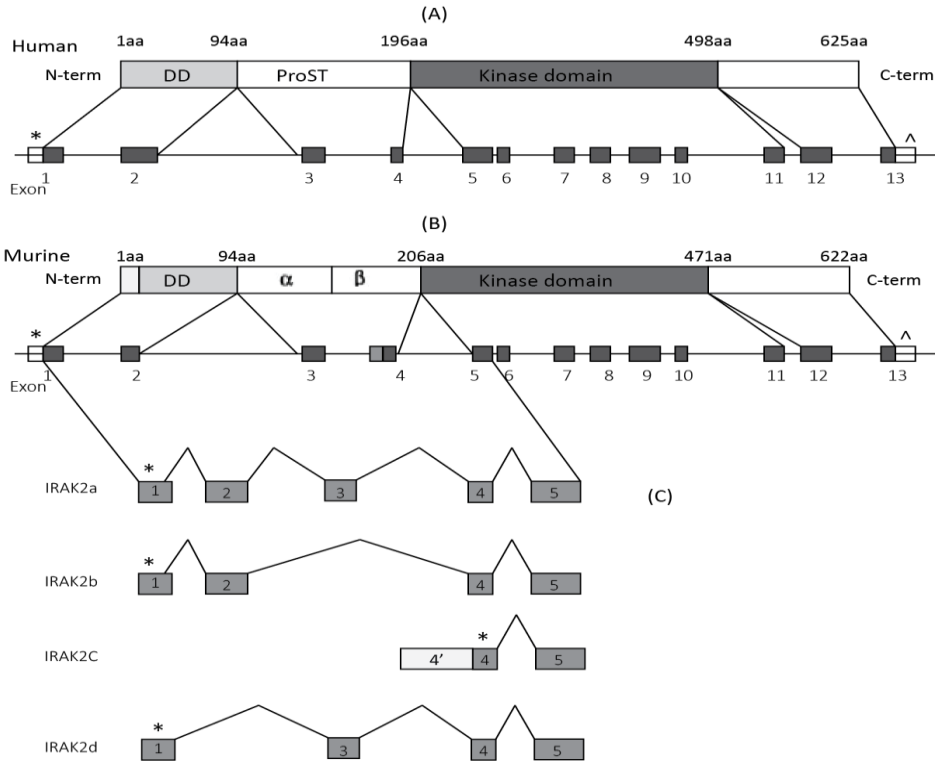

Figure 1.16 Schematic diagram of human and murine IRAK2.(modified from Hardy and O'Neill, 2004) Functional structure of human IRAK2 (a) and murine *Irak*2 (b).Extons(numbered black boxes) are shown on the genomic sequence with start and stop codons marked by asterisks(*) and cartes(^),individually. 5'-UTR and 3'UTR are presented with white box. The human IRAK2 consists of death domain (gray box), the ProST domain, the kinase domain (black box) and the C-terminal domain. Numbers above the bar indicate the amino acid start and stop points of each putative domain. (C) Alternative splicing pattern at the 5'-end of murine IRAK2 leads to the generation of four IRAK2 isoforms. Irak2a compose all exons; Irak2b and Irak2d lack the exon3 and exon 2 respectively. Irak2d misses 10aa in the C-terminal additionally. Irak2c generated by deletion exon1, 2, 3 while it encompass its own 5'-UTR in the exon 4'(intron 3). Start codon used by each isoform are indicated nu asterisks.

*Irak*2a utilizes all exons, which is most similar to human IRAK2. *Irak*2b and *Irak*2d are generated by deleting exon3 and exon2 respectively. Additionally, *Irak*2d lack 10 amino acids in the C-terminus. *Irak*2c is generated by deleting exon 1, 2, 3, while it has its own specific 5'-UTR in exon 4' and its start codon ATG lies in exon 4.

Alignement of human IRAK2 and murine *Irak*2 amino acid (figure 1.17) indicates that they are conserved. Particularly, the death domain and kinase domain are well conserved, whereas the ProST domain and C-terminal display a lower identity. Comparing the whole genomic region of human IRAK2 and murine *Irak*2, it demonstrated that the coding sequences were generally well conserved while there is no identity in non-coding sequence. It indicates that human IRAK2 and murine *Irak*2 might be regulated differently. Thus, caution should be taken when extrapolating date from mice to human in the IRAK2 research.

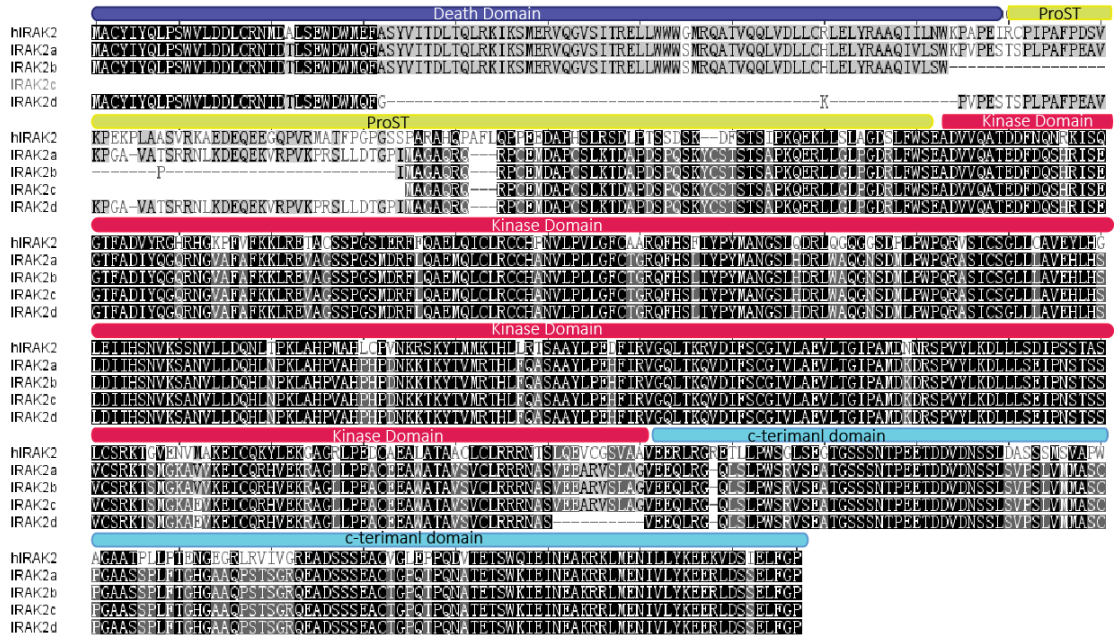

Figure 1.17 Protein sequence alignments of human and murine IRAK2. (Regions of amino acid identity between human IRAK2 and mouse Irak2 are shaded)

*Irak*2 deficient mice were generated in 2008 by Kawagoe, which four splice variants of *Irak*2 were knocked out. In comparison with IRAK1 deficient mice, *Irak*2 deficient mice were highly resistant to LPS and CpG induced septic shock. Moreover, similar to the IRAK1 function in the early time points of a TLR stimulation, IRAK2 is more important in sustaining the NF-κB at later time points and MAPK activation at early time point [137, 140].

As mentioned above, there are four splice variants in mice. *Irak*2a and *Irak*2c are active, whereas *Irak*2c and *Irak*2d are negative in terms of NF-κB activation. Strikingly, one study compared the inbred mice C57BL/6J with wild derived mice strain MOLF/Ei in terms of splice variants of *Irak*2. In classical inbred mice C57BL/6J the *Irak*2c splice variant was expressed highly in early response to TLR stimulation and inhibited the functions of *Irak*2a. Along with the stimulation being longer, *Irak*2c expression levels were found to decrease, whereas the expression of *Irak*2a would become stronger and show positive immune responses. Interestingly, there was a natural mutation in the promoter of *Irak*2c in MOLF/Ei, which resulted in significantly less expression of *Irak*2c to inhibit the isoform of *Irak*2a. Using siRNA to knock down *Irak*2a in the mice, the results show that NF-κB and MAPK activation are abolished, indicating that *Irak*2a is indispensable for NF-κB and MAPK activation. Moreover, it also indicates that wild-derived murine *Irak*2 has many similarities with human IRAK2.

1.4.3 IRAK3

IRAK3 was found by EST search as well. The human IRAK3 gene is mapped to chromosome 12 at position 12q14.1-12q15. It encodes for a protein with 596 amino acids and a molecular weight 68 kDa. Northern blot analysis showed that IRAK3 transcripts are predominantly present in peripheral blood lymphocytes. Human IRAK3 and murine IRAK3 share 71% sequence similarity.

Compared to IRAK1 and 4, which contain aspartate residue in the kinase domain, IRAK3 contains a serine residue. Thus, IRAK3 was thought to be a negative regulator in the TLR signalling pathway. Initial experiments displayed that over-expression of IRAK3 in HEK293T cells induced NF-κB activation. Moreover, IRAK3 can restore NF-κB activation in IRAK1 deficient cells [141]. However, IRAK3 knock out macrophages revealed that NF-κB activation was enhanced in those cells which were stimulated by *Salmonella typhimurium* [87]. The hypothesis is that IRAK3 prevents IRAK1/4 from dissociating from the activated MyD88 complex by building next to the IRAK2 layer of the ternary complex [86].

Phenotypically, IRAK3-/- mice develop severe osteoporosis, which is related to the accelerated differentiation of osteoclasts (increase half-life and activation) [142]. Additional studies reveal that IRAK3 plays a more critical role in alternative NF-κB signalling pathway which depends on the activation of NF-κB inducing kinase (NIK) and subsequent phosphorylation of p100[143]. IRAK3 expression levels are also increased in deactivated macrophages which are incubated with tumour cells, whereas IRAK1 expression decreased [144].

All abovementioned evidences indicate that IRAK3 serves as a negative regulator in the TLR signalling pathway. Strikingly, one recent study showed that IRAK3 was able to interact with MyD88-IRAK4 to form IRAK3 Myddosome and to mediate the MEKK3-dependent TAK1-independent NF-κB activation. This IRAK3 dependent pathway is essential for the second wave of TLR7-induced NF-κB activation in the absence of IRAK1/IRAK2, which is uncoupled from post-translational regulation [145].

1.4.4 IRAK4

IRAK4 is the latest IRAK family member to be identified. Human IRAK4 is the closest homolog to the *Drosophilla Pelle*. It was mapped to the chromosome 12 at position 12p11.22. The IRAK4 protein is composed of 460 amino acids resulting in a molecular weight of 52 kDa. Human IRAK4 shares 87% similarity with murine IRAK4 [146]. Challenging IRAK4-deficient mice with different TLR ligands, showed that NF-κB activation was severely affected. As an IRAK family member, IRAK4 is also involved in the IL-1R signalling pathway. NF-κB, JNK and p38 activation were severely affected by stimulating IRAK4 deficient macrophages with IL-1 [146].

It was shown that the interaction of DD of IRAK4 with DD of MyD88 is vital for downstream activation. This experiment indicates that IRAK4 was the primary kinase that is recruited to MyD88 and that is essential for NF-κB activation [147]. Meanwhile, the Myddosome structure confirmed this as well. 6 DDs of MyD88 assembled as a first layer, then 4 DDs of IRAK4 docked into the Myd88 upper surface and formed the second layer, followed by 4 DDs of IRAK2 sitting on the top of the second layer. This large oligomeric complex was assumed to interact with IRAK1 or IRAK3[86].

However, whether the kinase activity of IRAK4 is vital for NF-κB and MAPK activation is still not fully understood. The *in vivo* assay of the IRAK4 knock in mice revealed that the IRAK4 kinase activity is essential for resistance to TLR-induced shock [148, 149]. However, the macrophages from those mice demonstrate that the kinase activity is dispensable for the activation of NF-κB when challenging the cells with agonists for IL-1, TLR2, TLR4 and TLR7 [150, 151]. It is interesting to note that MAPK activation is more dependent on IRAK4 than NF-κB in IRAK4 inactivity knock-in mice [151].

Intriguingly, human IRAK4 deficient fibroblast cells reconstituted with kinase dead IRAK4 was able to fulfil the NF-κB and JNK activation in response to IL-1 stimulation [152]. Moreover, Capucine Picard et al revealed that IRAK4 deficiency in patients resulted in a recurrent pyogenic bacterial infection in childhood. While no impaired function was found in viral infection[153]. In this context one should be cautious that in applying these results to the human system as there may be differences between human and mouse IRAKs. In conclusion, much effort was done on the mice

experiments. However, there are differences between mouse IRAKs and human IRAKs. In table 1.2, these differences are listed.

Table 1.2 knockout/knockdown studies showing the effect of absence of IRAKs on IL-1/TLR signalling

Name	Species	Phenotype in vivo	Effect on NF-κB activation	Effect on MAPK	Effect on IRF activation
IRAK1	Knockout Mice	Partially resistant to LPS-induced spetic shock	Partial impairment for IL-1/TLR4	Impairment for IL-1/TLR4. No impairment of TLR2 induced ERK and JNK	Effect on TLR7/9 induced IFN
	Human	related to SLE(mutation)	No impatiment of IL-1	N/D	N/D
IRAK2	Knockout Mice	Mice completely resistant to LPS and CpG induced septic shock	Impairment of late TLR2/TLR7 activation. No impairment of TLR4	Impairment of late TLR2 activation	N/D
	Human Silence IRAK2	N/D	Impairment of early TLR4 and TLR7	Reduced phosphorylation of p38	Reduced IRF3 signalling in HEK293-TLR3 cells
IRAK3	Knockout Mice	Reduced survial upon viral infection	Enhanced activation of TLR4 and TLR9	Enhanced activation TLR4 and TLR9. Enhanced TLR2-induced p38. No effect on TLR2-induced ERK and JNK	N/D
	Human	N/D	Enhanced activation of TLR4	N/D	N/D
IRAK4	Knockout Mice	Mice completely resistant to LPS and CpG induced septic shock	Impairment of IL-1 and MyD88-dependent TLR No effect on TLR3	Impairment of TLR4 induced JNK Impairment of IL-1 induced p38	Effect on TLR7/8/9 induced IFN
	Human	Recurrent pyogenic infection, limited to certain kinds of bacteria. IRAK4 deficient patiants	Impairment of TLR2,4,5,7,8,9.No impatiment of IL-1	No effect on TLR3 and TLR4 induced p38 and JNK	Required for TLR7/8/9 induced IFN. No effect on TLR3 and TLR4 induced IRF3

1.5 The death fold superfamily for homotypic interaction

1.5.1 Overview on the death fold superfamily

Signal transduction pathways of inflammation and cell apoptosis depend to a large extent on proteins containing homotypic interaction motifs. Those motifs belong to the death fold family. The well known Death Domain (DD) together with the structurally homologous Death Effector Domains (DEDs), CAspase Recruitment Domains (CARDs) and the PYrin Domains (PYDs) belong to the death domain superfamily. There are 215 proteins in humans that are predicted to have this structure. They are involved in controlling signaling transduction of inflammation, apoptosis or cell death via homotypic interaction. The structural hallmark of the superfamily is the so called death fold which consists of six antiparallel α-helices which arrange into a Greek key topology that folds into two 3-helix bundles. All of the death folds form a hydropobic core. Furthermore, each member encompasses a specific array of homotypic interaction partners that in principle do not cross interaction with another subfamily [154] (See Figure 1.18).

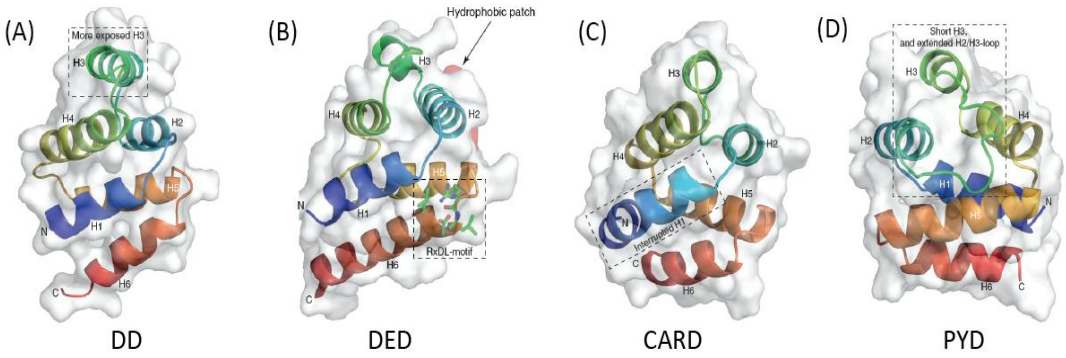

Figure 1.18 Tertiary structures of the different death-fold subfamilies (Kersse and Verspurten et al 2011)

The reason that death folds form oligomeric complexes is that this can generate three distinct types of asymmetric interactions. The type I interaction consists of helices1 and 4 (patch Ia) of one death-fold domain interacting with helices 2 and 3(patch Ib) of another death-fold domain. Type II interaction is formed from helices4 and the loop between helices 4 and 5 (Patch IIa) of one death-fold domain, which interact with the loop between helices 5 and 6 (Patch IIb) of another death fold domain. Type III interaction is formed from helices 3 (Patch IIIa) of one death-fold domain, which interacts with the loop connecting helices 1 and 2 and the loop connecting helices 3 and

4 (Patch IIIb) of another death-fold domain. There is no overlapping between the six patches which are generated by the death fold, suggesting that each patch can interact with the other six patches twice by pairwise interaction [154] (Figure1.19).

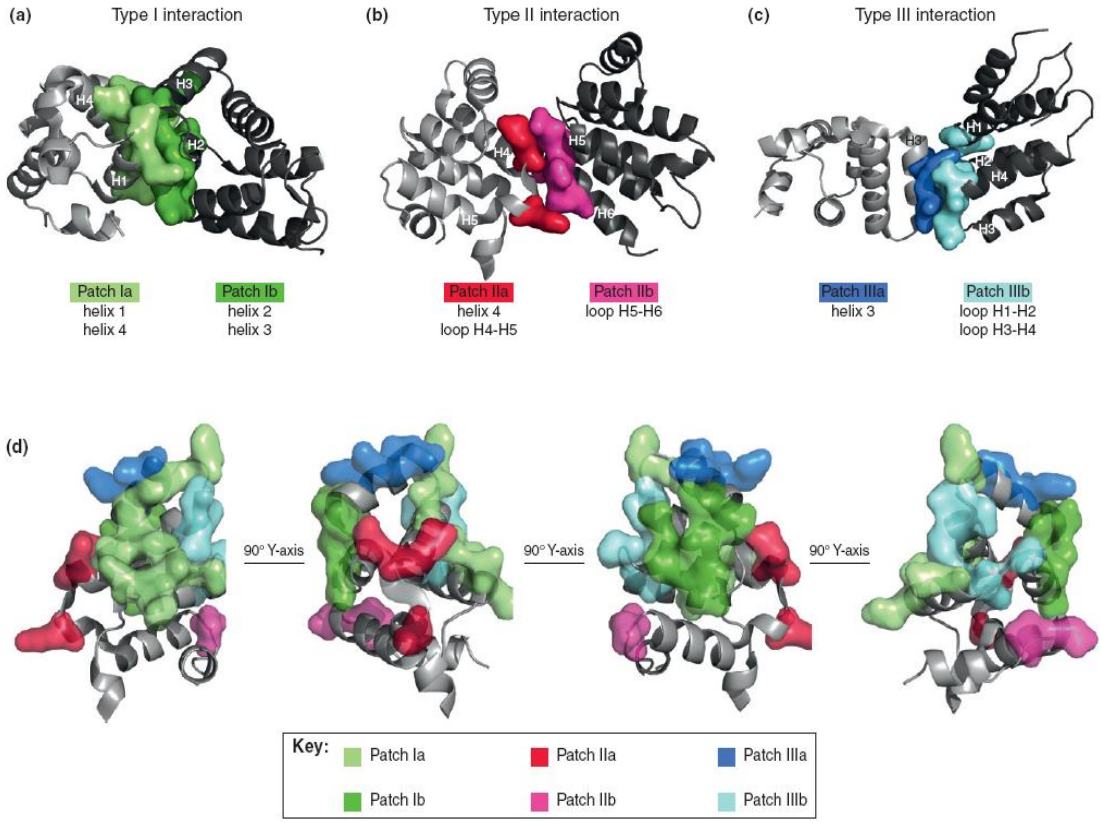

Figure 1.19 DD mediates three interaction types through six interaction patches.(Kersse and Verspurten et al 2011)

1.5.2 Myddosome structure

The Myddosome structure was first proposed by Dr. Precious G. Motshwene in 2009. In his research he displayed a large oligomeric complex which contained 7/8 death domains (DDs) of MyD88 and 4 DDs IRAK4 [85]. In 2010, Su-Chang Lin reported the crystal structure of a Myddsome complex which is consisted of a MyD88-IRAK4-IRAK2 death domain complex. This complex composed of 6 DD MyD88, 4 DD IRAK4 and 4 DD IRAK2, and results in a left-handed helical oligomer [86] (Figure1.20A). The Myddosome structure contains three types of interaction. Type I and II interaction connect the different layers, while type III interaction mediates the connection within one layer.

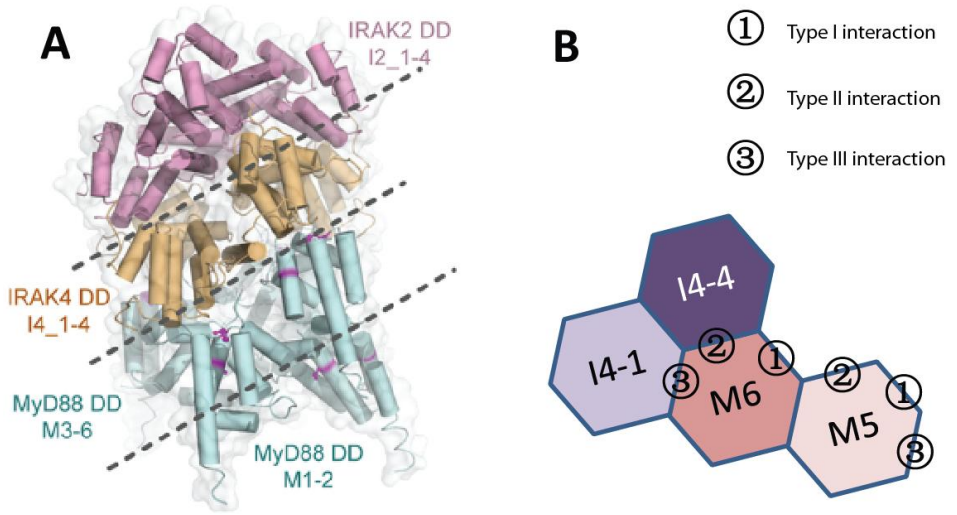

Figure 1.20 The schematic diagram of Myddosome structuer (modified from George, Motshwene *et al*, 2011)

It is worthwhile to notice that the Myddosome structure assembly is tightly controlled. It is a sequential process, since the charge and shape on each layer on bottom and top is different. It determines that the top surface of MyD88 can only recruit IRAK4; sequentially the bottom of IRAK2 can only fit the top surface of IRAK4. This dynamic assembly indicates that IRAK4 is first recruited to MyD88, and can autophosphorylate and phosphorylate IRAK2. Then the phosphorylated IRAK2 is released, and furthermore induces the NF-κB activation. This structural arrangement was also confirmed in vivo by our lab Julie George and her colleagues [155]. Meanwhile, the hypofunctional polymorphisms MyD88 S34Y and R98C provided adequate information for designing therapeutic drugs in the future [154].

1.6 Ubiquitination in TLR signalling pathway

1.6.1 Overview on ubiquitination

Like most signalling pathways, the function of phosphorylation in TLR signalling pathway has been very well described. To date, more and more investigations have been done on ubiquitination, and ubiquitination was found to play an important role in adjusting and regulating in TLR signalling pathway. Ubiquitination is one type of post-translation modifications, in which ubiquitin, a highly conserved polypeptide of 76 amino acids, is covalently attached to other proteins through the enzymes E1, E2 and E3. In principle, ubiquitin binds the target protein via binding motifs. However, the binding affinity is low which provides for more flexible and dynamic regulation in the

cells. A protein can be modified on one lysine residue by a single ubiquitination (monoubiquitination), and it can direct DNA repair, vesicle sorting or receptor internalization [156]. Alternatively, multiple ubiquitination can be added with different K48 or K63 and this named polyubiquitiantion. They are two major non-linear polyubiquitination modifications. The lysine 48 (K48) linked polyubiquitination with at least four ubiquitins, usually guides the targeted protein for degradation via 26S protrasome. The lysine 63(K63)-linked polyubiquitination which is mostly involved in singnal transduction events [157]. In some cases, multiple lysine residues on one protein can be modified by polyubiquitin chain.

1.6.2 Ubiquitination in the MyD88 dependent signalling pathway

Activation of TLRs by pathogens results in the recruitment of IRAK4 to MyD88. Sequentially, IRAK4 interacts with IRAK1 which was shown to undergo lys-63 linked polyubiquitination after IL-1 and LPS stimulation. IRAK1 lys-63 polyubiquitination orientates IRAK1 interaction with NEMO which activates the transcription factor NF-κB. It was assumed that pellino serves as an E3 ubiquitin ligase in assembling polyubiquitin chains on IRAK1 [158]. Interestingly, IRAK1 can phosphorylate pellino and trigger pellino to undergo lys-48 polyubiquitination for degradation [159]. Following IRAK1/IRAK2 activation, TRAF6 a RING-domain ubiquitin E3 ligase is recuited. The interaction of IRAK2 with TRAF6 is hypothesized to turn on TRAF6 lys-63 polyubiquitination via TRAF6 oligomerization. The lys-63 polyubiquitin chain of TRAF6 can be identified by the TAK1 complex which further leads to TAK1 complex activation. Sequentially, MAPK and JNK are activated. Meanwhile, polyubiquitin chain can be recognized by NEMO which can be polyubitquitined at lys-285. It was found that lys-285 polyubiquitination is required for NF-κB activation. Binding of the TRAF6 Lys-63 polyubiquitin chain to TAK1 and IKK complex results in IKKβ phosphorylation, and in turn induces IκB degradation via lys-48 polyubiquitin chain. The IκB degradation releases p65 to enter into the nucleus, and to further activate NF-κB [160] (See figure1.21).

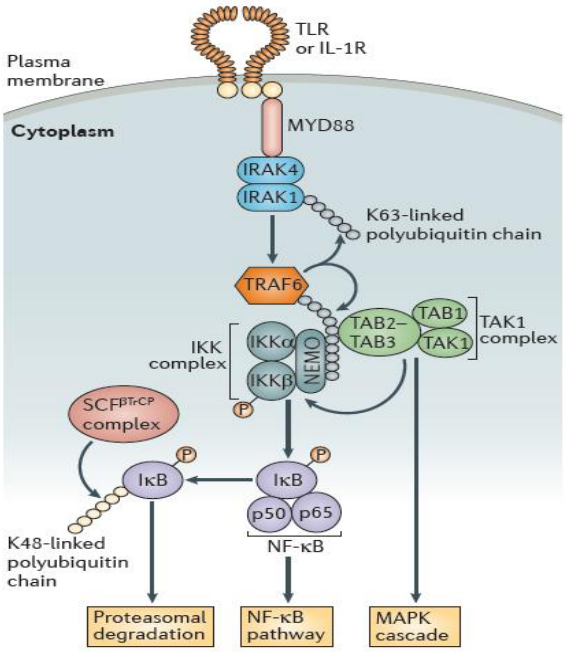

Figure1.21 Ubiquitination in MyD88 dependent signalling pathway (Jiang and Chen 2011)

1.6.3 The ubiquitination communication in the TLR signalling pathway.

Additionally, ubiquitination also occurs in TRIF signalling pathway. Similar to TRAF6, which is an E3 ligase, TRAF3 undergoes lys-63 polyubiquitination after TLR4 has been translocated from the plasma membrane to the endosome. The lys-63 polyubiquitinated TRAF3 directs the activation of TBK1 and IKKε and leads to IRF3 phosphorylation upon stimulation of TLR4. Another protein, the receptor-interacting protein1 (RIP1) is recruited to TRIF and modified on lys-63 polyubiquitin via pellino 1 [161]. Lys-48 and lys-63 polyubiquitinations collaborate with each other. For instance, following the activation of MyD88 triggered by TLR4 ligands, several ubiquitin E3 ligases are recruited together. TRAF6 induced its own lys-63 polyubiquitination and activates cellular inhibitor of apopotosis protein1 (cIAP1) and cIAP 2, both of which also belong to the E3 ligase family. Those two proteins then trigger lys-48 polyubiquitination in TRAF3, and finally enhance NF-κB and MAPK activation. However, when TLR4 is translocated to the endosome, cIAP1 and cIAP 2 cannot be recruited to TRAF6 anymore. Then TRAF3 is directly modified on lys63 for polyubiquitination, and further more triggers TBK1 activation and induces type I IFN production [162] (See Figure1.22).

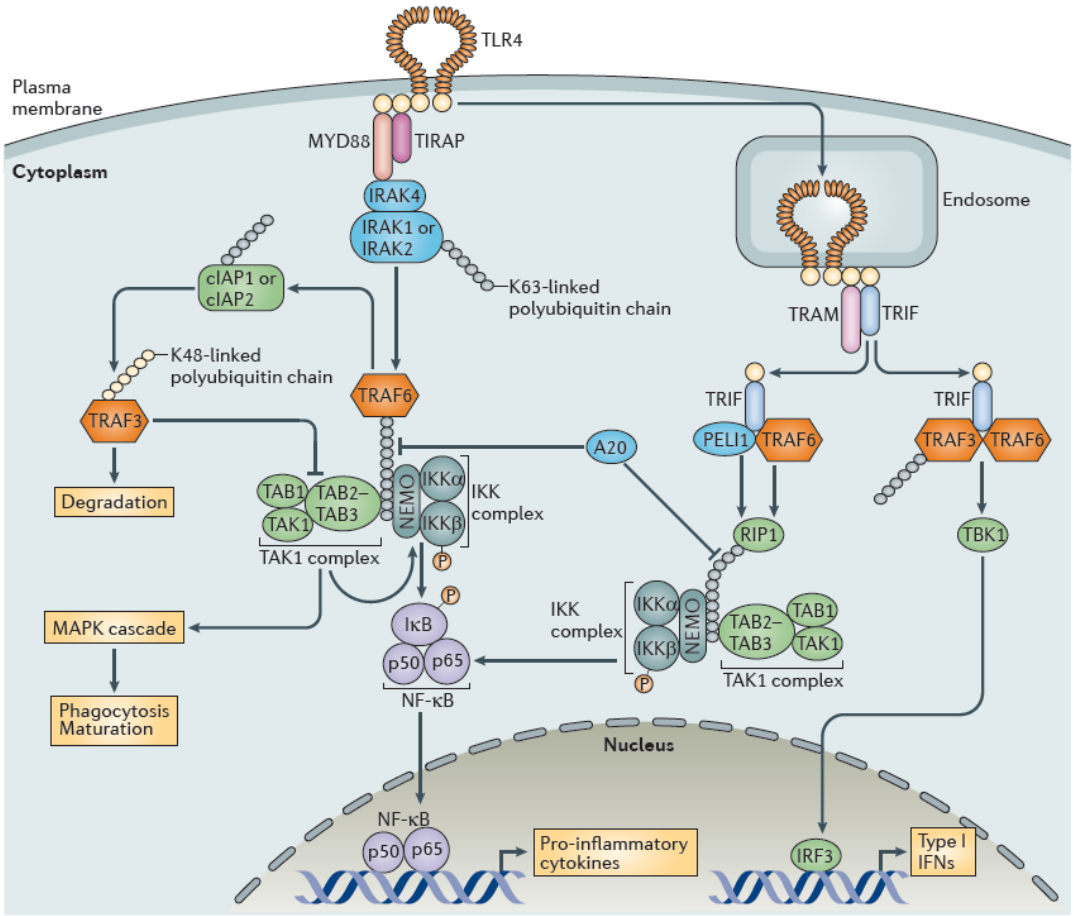

Figure1.22 The ubiquitination communication in TLR signalling pathway (Jiang and Chen 2011)

As a counter of ubiquitination, deubiquitination exists in cells as well. A20 and CYLD are two of the best known deubiquitination enzymes inhibiting NF-κB activation. The ubiquitination is not only involved in innate immunity, but also adaptive immunity. There are still a lots of unknowns factors in this field and future research is needed to investigate on it.

1.7 The relationship between TLR signalling pathway genetic variants and diseases.

Although plenty of research has been done on immunity, most of the immunological knowledge we have gained is based on mice or cell line experiments. How accurate and reliable is these information and can we apply it to human immunity? Human genetic studies are an effective approach to precisely define the role of molecules in nature [163]. The crucial element of the innate defence are the germline encoded receptors named Toll-like receptors which are composed of conserved motifs that can detect

various pathogen-associated molecular patterns and activate the production of inflammatory cytokines. More than 10 years effort in this field have identified that two classical TLR/IL-1R signalling pathways, a MyD88 dependent signalling pathway, and a the MyD88 independent signalling pathway, which is employed by TLR3 and partial TLR4 signalling pathways. Meanwhile, deficiencies in those two signalling pathways in humans being have been described. MyD88-IRAK4 deficiency leads to greater susceptibility for pyogenic bacteria [164], and TLR3-Unc93b-TRAF3 deficiency leads to higher susceptibility for herpes simplex encephalitis (HSE) [35].

1.7.1 The MyD88-IRAK4 deficiency

The knowledge on primary immunodeficiencies (PID) was considerably expanded ever since Bruton worked on the X-linked agammaglobulinemia in 1952 [165]. In 2001, single genetic hypomorphic mutations in NEMO (IKKγ) were found to be related to X-linked recessive anhidrotic ectodermal dysplasia with immunodeficiency (EDA-ID) [166]. Subsequently, a hypermorphic mutation in IκBα was discovered to be related to autosomal dominant EDA-ID [167]. NF-κB activation was impaired in both mutations and those patients were susceptible to invasive pneumococcal disease which paved the way for studying the inborn errors of IRAK4 and MyD88. IRAK4 deficiency was discovered in 2003 in three unrelated children who were susceptible to pyogenic bacteria infection. Until now, 28 IRAK4 (homozygous or heterozygous) deficient patients were found to harbour a variety of mutations, which all abolished the IRAK4 protein expression as being proved by western blot. Mostly, the kinase domain of IRAK4 was affected [153]. These patients presented with a life-threatening without treatment of antibiotics or intensive care but narrow and transient predisposition to infection during the first 10 years of life, which was mostly restricted to pyogenic bacterial diseases, particularly invasive pneumococcal disease IPD [168]. Consistent with IRAK4 deficiencies, MyD88 deficiencies were discovered in 2008. Nine children presented with invasive pyogenic bacterial diseases but did not have any IRAK4 deficiency. Instead, they had three different autosomal recessive mutations of MyD88, including one deletion (Glu52) and two missense mutations (L93P and R98C) [169]. These three mutations all impaired the interaction of MyD88 with IRAK4 in the context of the Myddosome formation [155, 169]. Similar to IRAK4-deficient patients, MyD88-deficient children are only threatened by pyogenic bacterial infection in early

infancy, although one needs to be caution to extrapolate from 9 subjects. However, they have normal resistance to other microbes and display an improving clinical status with age. This may indicate that the shaped adaptive immunity which develops throughout childhood compensates at later age for the defects in the innate immunity. It is interesting to notice that the mortality rate of MyD88 or IRAK4 deficient patients is 30-40% in children. This calculation is already taking into account the prophylaxis treatment, including intensive care and antibiotic up-taken. The natural course of such mutations is most likely to be fully lethal.

Recently, a somatic mutation in MyD88 (L256P) was shown to relate to chronic lymphocytic leukemia (2.9% occurrence) and diffuse large B cell lypmphoma (29% occurence). It was assumed that this TIR domain mutation constitutively activates the production of various pro-inflammatory cytokines, which is pivotal for the tumour cells to survive [170, 171]. Meanwhile, it provides an opportunity of treatment for those patients or hyperinfection related diseases with IRAK4 inhibitors to block the constitutively activated signalling in malignant cells.

1.7.2 The TLR3-UNC93B1-TRIF-TRAF3 deficiency

TLR3 7, 8, and TLR9 are jointly defined as nucleic acid sensing PRRs, which are important to produce type I IFN to fight against viruses. Except for TLR3, 7, 8 and 9 are all dependent on MyD88 signalling pathway. Both TLR3 and the RIG-I like receptor (RLR) families can detect dsRNA. However, till now, no genetic deficiency in the RLR family has been discovered. A deficiency of the TLR3-IFN signalling pathway in response to viruses is cause by autosomal recessive mutation in UNC93B1, which was first described in 2006 [172]. UNC93B1 is an endoplasmic protein with 12 membrane-spanning domains, and which is involved in TLR3, TLR7 and the TLR9 signalling. It functions as a transporting protein for the nucleotide sensing TLRs, to transport them from the ER to endolysosomes, where they localize and recognize their ligands. In addition, UNC93B1 assists TLRs in identifying pathogens and inducing signal transduction. The clinical syndrome of those patients presents recurrent herpes simplex encephalitis (HSE). Following that, two French children from non-consanguineous families with recurrent HSE were detected with autosomal dominant TLR3 deficiency in 2007 [35]. Continually, autosomal dominant mutations in TRAF3 [173] and autosomal recessive or dominant mutations of TRIF [174] were

recently found by two groups. All of those patients displayed a similar clinical syndrome with UNC93B1 deficient patients. The HSE also mainly occurred in early childhood, in patients under the age of 6 years, following a first infection by herpes simplex virus type1. Strikingly, the TLR3-UNC93B1-TRIF-TRAF3 deficient patients are only susceptible to HSE without susceptibility by other viruses. Furthermore research is required to elucidate the mechanism of TLR3-UNC93B1-TRIF-TRAF3 deficiency.

1.7.3 TLR signalling pathway polymorphisms.

Soon after the discovery of TLRs, a body of research has shed light on the genetic variations of TLRs. The most popular genetic variation characterized in research is the non-synonymous single nucleotide polymorphism. This means one base change alters the genetic triplet code, which further induces changes in the amino acid residue of the encoded protein. Finally, the change in the amino acid sequence might have some impact on the function of the protein due to potential changes in the electric charge and structure of the protein. The first genetic variation discovered in TLRs were the polymorphisms in TLR4 (D299G and T399I). It was reported that those two polymorphisms decrease the interaction of TLR4 with LPS, and to thus increase the susceptibility to sepsis [175, 176]. Then, the polymorphism R753Q in TLR2 was found to impair TLR2 dependent signalling and was shown to be associated with the susceptibility to tuberculosis [177], and to protect from the development of late-stage lyme disease [178]. R392X, one interesting polymorphism in TLR5, results in a stop codon in position 392, and thus generates a total defect of TLR5 to recognize flagellin. However, the frequency of this mutation is approximately 10% in the European population and 23% in other populations. The epidemiological studies imply that this mutation increases the susceptibility of Legionnaire's disease [179], but has no relation with typhoid fever caused by *Salmonella typhimurium* [180]. Strikingly, this mutation can reduce the susceptibility of systemic lupus erythematosus [181] and Crohn's disease [182]. Regarding the TIR domain containing adaptor MAL, one non-synonymous polymorphism was presented as S180L. Initially, it was shown to be associated with decreasing the susceptibility of tuberculosis. However, meta-analysis did not provide any evidence that MAL S180L is involved in protecting patients from tuberculosis [101, 102]. D96N was another one polymorphism which was found in

lymphoma patients. However, case control study indicates that no relationship is linked between lymphoma and the D96N genetic variants [183]. In contrast to the complete deficiency in TLR signalling pathway, those polymorphisms in the TLR family lack replications and functional studies. Moreover, the epidemiological studies have limitations in size and location. Therefore, the results must be interpreted with caution. Now, it is possible to conduct genome-wide association studies or whole genome/whole exome sequencing, and many more mutations and polymorphisms are expected to be identified in association studies, as exemplified for the somatic MyD88 in B cell malignancies (L256P). Simililary, TLR7 and TLR8 were recently identified to be associated with celiac disease which involved an abnormal intestinal immune response to dietary gluten [184].

Because IRAK1 was the first member described in the IRAK family, many SNP studies were carried out on IRAK1. The variants F196S and S532L were in complete linkage disequilibrium that carries the 196F/532S genetic variation with low radical bone mineral density [185]. Later on, IRAK1 was shown to be associated with C-reactive protein in a diabetes heart disease study [186] and sepsis [187]. Interestingly, IRAK1 was also involved in the pathogenesis of rheumatoid arthritis [188] and systemic lupus erythenatisus(SLE) [135] . Meanwhile, genetic variants in IRAK3 were also reported to be associated with asthma [189]. However, those studies are also limited in size and population, the OR value is not significant enough and solid functional studies are lacking. It is worthwhile to apply new sequencing methods and to perform functional studies to present more convincing results of valuable genetic variance in the IRAK family.

1.8 Aim of Ph.D. project

The aim of this study was to functionally and epidemiologically characterize the causal relationship between non-synonymous single nucleotide polymorphisms of IRAK2 and certain kinds of diseases. The function of IRAK2 in the TLR/IL-1R signalling pathway was so far investigated by many researchers, indicating that within the IRAK protein family, IRAK2 fulfils similar functions like IRAK1, but more in response to activation of NF-κB at late time points. Furthermore, in the published research IRAK2 was mainly studied in mouse cell lines or mouse models, not taking into account of different splice variants of IRAK2 that exist in humans and mice. The precise role of IRAK2 in humans therefore remains enigmatic. Moreover, no reports are published that address the relationship between genetic variants of IRAK2 and the susceptibility to certain kind of diseases. Therefore, this work focused on the in-depth molecular studies on IRAK2 SNPs and their clinical epidemiological relevance. Furthermore, dysfunctional SNPs of IRAK2 served as a probe to decipher the signalling properties of IRAK2 in human system.

First, experimental studies of IRAK2 were established by comparing the signalling properties of IRAK2 with IRAK1 and 3 in an *in vitro* assay. Meanwhile, the SNPs of IRAK1 and 3 were chosen as well. Then functionally interesting SNPs of IRAK1, 2 and 3 were screened for interesting phenotype by *in vitro* assays in a human cell system. Plasmids encoding for polymorphisms of IRAK2 were overexpressed into the human cell system and their impact on the activation of the transcription factor NF-κB and the production of pro-inflammation cytokines were measured. Based on this information, the SNPs of interest were selected and the mechanistic molecular biology studies were conducted to understand how these variants alter the signalling functions of IRAK2 WT. Thus, these variants served as probes to gain further insight into the IRAK2-NF-κB signalling pathway. The research included studies for protein-protein interaction, downstream partner protein activation and post-translational modifications. Moreover, the impact of IRAK2 variants on the TLR signalling pathway was further investigated in reconstituted IRAK2 knockout murine macrophages.

Meanwhile, the SNPs of interest were analysed in epidemiological studies to discover the relationship between these IRAK2 SNPs and the progression and prognosis of certain kinds of diseases.

Chapter 2: Methods and Materials

2.1 Molecular Biological Methods

2.1.1 Generation of ds-oligonucleotide sequences.

Oligonucleotides sequences were designed using the vector NTI, Geneious software (Biomatters) or online primer design systems provided Agilent Technologies. The synthesis was done by MWG Biotech or Biomers Biotech. Double stranded oligonucleotides were generated by first mixing equimolar amount of two complementary single-stranded molecules in distiled H_2O and denaturing the mixture for 5min at 95 ℃. Then the sample was slowly cooled down by 0.3 ℃ per second to 30 ℃. The hybridized double-stranded oligonucleotides were checked via running 3% agarose gel. For ligation purposes, 20nmol of double-stranded oligonucleotides were phosphorylated by 14U T4-polybnucleotide kinase (PNK, NEB), the reaction contained additionally 50mM of adenosine triphosphate (ATP) with an adequate amount of 10×PNK buffer (NEB). The mixture was incubated at 37 ℃ for 1hour. The PNK activity was stopped by adding 50mM EDTA and incubating the reaction at 68 ℃ for 10min.

2.1.2 Polymerase chain reaction (PCR)

PCR methods were majorly used for site-directed mutagenesis and for cloning gene constructs into plasmids; for each purpose different protocols were used (see table 2.1 and 2.2). All PCR reactions were prepared with 4-100ng of DNA template, 0.2pmol of the forward and 0.2pmol of the reverse primers, 0.2mM deoxyribonucleotide triphosphates (dNTPs), 2mM $MgSO_4$ and 2U of the thermostable *Pfu or Vent* polymerase in a reaction volume of 20-50µl containing the appropriate amount of the reaction buffer. The cloning enzymes were purchased from NEB, the enzymes for mutagenesis reactions were provided with the QuickChange site-directed Mutagenesis kit from Agilent Techologies. The PCR reactions were run on a MJ Research Thermo Cycler or a PEQ lab cycler, which were programmed according to the parameters listed below (Table2.1 and Table 2.2)

Table 2.1 PCR cloning program

Program Steps	Cycles	Temperature(℃)	Time	Application
Initial Denaturation	1	95 95	1min 1min	
Pre-amplification (optional)	5	50-60 72 95	45s 1min/1000bp 1min	-annealing a short tag -cloning a new constructs with restriction sites
Amplification	30	50-65 72	45s 1min/1000bp	
Extension	1	72	10min	
Storage	1	4	Infiniti	

Table 2.2 Site-directed mutagenesis

Program step	Cycles	Temperature(℃)	Time
Initial denaturation	1	95 95	1min 1min
Amplification	18	60 68 68	45s 1min/1000bp 10min
Storage	1	4	Infiniti

2.1.3 Quantitative real-time polymerase chain reaction

The quantitative Real-time Polymerase Chain Reaction (qPCR) is an improvement of a standard PCR. The difference between a standard PCR and qPCR is that the amplified DNA is measured according to the reaction in progresses in real time. This method was applied to quantify the mRNA expression of certain genes when stimulating cells with TLR ligands. In order to compare the gene expression levels, total RNA was extracted from cells. In the case of macrophages, 1-1.5×10^5 per well cells were seeded into 24-well plates, and treated with specific ligands. The RNA was then extracted by using the RNeasy mini kit (Qiagen). Each well was treated with 350µl of the provided RLT buffer, which was supplemented with 1% of bete-mercaptoethnaol. The subsequent steps for RNA isolation were conducted according to the protocol of the manufacture. In order to avoid DNA contamninations, the isolated RNA was digested using the Ambion DNA-free kit (Life Techonologies). The genomic DNA was eliminated by adding 1µl of *rDNase I* to 1400ng of RNA mixed in the provided buffer conditions. The

reaction was incubated at 37 ℃ in a thermocycler block for 30min. The DNase enzyme was subsequently removed by adding 2.5µl of the DNase inactivation reagent followed by incubation at room temperature for 2 min, meanwhile flipping the reaction every other second. The microtube was centrifuged for 1mintue at maximum speed in order to precipitate the genomic DNA. Then 20µl of the supernatant, the contained the RNA was transferred to a new microtube. The purified mRNA with this reaction was transcribed to cDNA using the Hight Capacity RNA to cDNA kit (Life Technologies). 1µl of the reverse transcriptase (RT) was added to 9µl of the purified RNA diluted in the appropriate amount of the provided transcription buffer. The reaction was heated at a thermocycler at 95 ℃ for 1min, and then incubated at 37 ℃ for 1hour, followed by a final inactivation period of 5 minutes at 95 ℃. A potential contamination of the purified RNA with genomic DNA was assessed by a 'RT-minus' control in which the transcriptase and the transcription buffer were replaced with distilled H_2O.

The mRNA of interest was quantified by applying a Tagman probe-based real time PCR. The qPCR experiments were done at a Applied Biosystem 7500 faster real time PCR system (Life Technologies). Gene-specific primers were purchased from Life Technologies (see appendix), and the qPCR reactions were conducted according to the protocol provided by the company. The quantified mRNA level of the TATA-binding protein (TBP) served as a reference and was used for normalization purpose.

2.1.4 Plasmids and DNA purification

Plasmids which were bought from companies were first transformed and then propagated in the type of bacteria that is suitable for the respective plasmid construct. After an overnight growth on the agar plates, several colonies were picked up and inoculated into 3-5ml LB medium (mini prep) or into 50ml-200ml LB medium (medi prep) that was supplemented with the required antibiotics. The cultures were maintained for 16 hours culture at 37 ℃. Then the DNA was extracted from the bacteria using the Promega high yield kits for mini and medi prep.

A PCR-clean up kit or Gel- extraction kit (Qiagen) was used to purify DNA fragments of PCR products

2.1.5 Agarose gel electrophorsis

Agarose gels were prepared with agarose (Roth) at 0.7-3% solutions, dissolved in sodium borate buffer (Brody and Kern 2004) containing 0.004% ethidium bromide (AppliChem), which intercalates into the double-stranded DNA helix. The agarose solution was heated and then cast into a chamber with a comb (PEQ Lab), which created the loading pocket. When cooling down, the solution polymerized to a gel. The DNA samples were diluted in 10×loading dye (NEB) and loaded into the gel. The DNA fragments were horizontally separated insodium borate buffer at 100-150V in sodium borate buffer. The 2-log DNA ladder (NEB) was used as a DNA marker. The DNA fragments agarose gels were visualized and documented with a UV-transilluminator (Pharmacia Biotech).

2.1.6 Restriction digestion

Restriction digests were either done to generat complementary sticky ends of DNA products for DNA ligation (cloning) or to checking the correct insertion of a gene in a plasmid. 2-5 µg of the vector was digested with 5-10U of the repective restriction enzyme(Fermentas Fast digest enzymes) in a 10×FastDigest buffer (Fermentas) by incubating the reaction at 37℃ for 1hour. The digest was further analysed by agarose gel electrophoresis. In cases where the cleaved DNA was needed for cloning, the fragment of interest was purified by a gel extraction kit (Qiagen). In selected case, restriction enzymes were purchased from NEB; the reaction was set up according to the directions of the manufactures.

2.1.7 Ligation

DNA fragments were ligated into a plasmid backbone by applying choosing a molecular ratio of backbone plasmid and gene of insertion of either 1:3, 1:4 or 1:1, depending on the length of the insert. The total ligation volume was kept at as 20µl, containing 1µl T4-ligase (Roche), and the required amount of gene insert and plasmid backbone, in buffer conditions provided by Roche. The reaction was performed at 16℃ overnight or at room temperature for 2-4 hours. In certain cases, the backbone needed be dephosphorylated to avoid self-recirculation. For this aim, 1µg of the digested plasmid backbone was incubated with 2.5µl of the Antarctic phosphatise (NEB) in the buffer recommended by the manufacturer. 10µl of the ligation reaction was transformed

to required competent cells (DH5α or DB3.1). The new cloning constructs were further analysed by restriction enzyme digestion and correct insertion of the gene was confirmed by Sanger sequencing (GATC Biotech).

2.1.8 Plasmids transformation

Plasmids transformations were performed with 100ng of DNA and 20-100µl of competent bacteria (E.coli DH5α, DB3.1 (containing *CcdB* resistant gene) or XL-blue/Gold). Usually, DH5α were used for plasmid transformations. DB 3.1 bacterial cells were used for propagating plasmids that encoded for the *CcdB* gene. *CcdB* is a lethal gene that targets the DNA gyrase and thus inhibits the bacteria growth. DB3.1 competent bacteria have a specific mutation in the gyrase, which make them resistant to *CcdB*. In the case where the plasmids were generated by mutagenesis, 1µl of the PCR product was transformed to XL-Gold bacteria to obtain higher transformation efficiencies. The transformed bacteria were incubated on ice for 30min in 14ml polypropylene round-bottom tubes (BD) before applying a heat-shock in a water bath at 42℃ for 45s. The tubes were placed back on ice for 2min and 200µl of pre-warmed S.O.C or NZY+ medium was added to cultivate the transformed bacteria for 1 hour at 37℃. 200µl of the bacterial suspension was plated on agar plates containing the required selective antibiotics.

2.1.9 Gateway® cloning: LR cloning

Gateway recombination cloning technology (Life technology) is a system with which allows the shuffling of genes from one plasmid to another by making use of specific recombination sites. The gene of interest was cloned to the pENTR1A entry clone (Life Technologies) which has attL1 and attL2 recombination sites. The gene of insert was shuttled into a destination clone which has attR1 and attR2 sites and additionally encoded for protein tags, see figure 2.1. In general, the reaction was prepared with 25ng of the entry clone, 75ng of the destination vector, 1µl of the LR clonase II Enzyme Mix (Invitrogen), and adjusted to a total volume of 5µl with TE buffer (pH=8.0). The reaction was incubated at room temperature (25℃) for 1hour, and then stopped by adding 0.5µl of proteinase K at 37℃ for 10min, 1µl of the reaction was transformed to DH5a bacteria. The colonies, which grew in the presence of the respective antibiotic, were picked and further cultivated for plasmid isolations. In order to confirm that the gene of interest was inserted into the destination vector, the plasmids were digested

with BsrGI (Fermentas with Tango buffer), which cuts at the att recombination sites. The correct size of the insertion was confirmed by agarose gel electrophoresis.

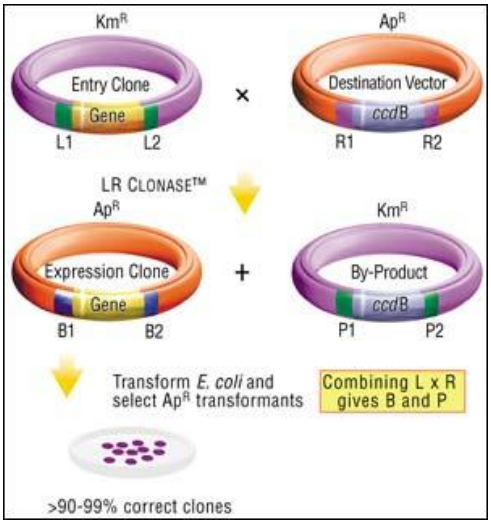

Figure 2.1 The Schematic diagram for LR reactions (Life Technologies)

2.1.10 Plasmid constructs and cloning stragtegies

2.1.10.1 Generation of Gateway compatible full length of human IRAK2

The IRAK2-encoding plasmid (NCBI accession No. AAC50954) was bought from Imagenes (IRCMP5012D0935D); the vector backbone was P4-Topo backbone. Due to the lack of proper antibodies that specifically recognize IRAK2 proteins, the IRAK2 IRAK2 gene was cloned to a pENTR1A (Life Technologies), which facilitates the transfer of the IRAK2 gene to Gateway compatible destination vectors encoding in-frame for an N- or C-terminal Strep-HA or Flag. For this purpose, forward and reverse primers were designed to generate a Gateway entry clone of IRAK2: the forward primer contained a BamHI restriction site; the Reverse Primer 1 contained a NotI restriction site and did not encode for a stop codon to allow for the adding of C-terminal tag. Alternatively, the reverse primer 2 also contained a NotI restriction site as well and encoded for a stop codon in order to generate plasmids with N-terminal tag. Certain mutations were generated on the IRAK2 pENTR1A construct by site-directed mutagenesis. All primers are listed in the Appendix.

2.1.10.2 Generation of Gateway compatible human IRAK2 death domain constructs

An IRAK2 death domain (IRAK2DD) construct was generated according to the amino acid sequence that was elucidated in the Myddosome structure (Lin et el. 2010) which includes the first 122 amino acids of IRAK2. The forward primer and reverse primers used are listed in the appendix. The Subsequent steps were the same as the ones applied to generate the IRAK2 for full length entry plasimds. Additionally, IRAK1DD and IRAK3DD constructs were generated according to the same procedures (see the appendix). The sequence of all the Gateway compatible plasmids encoding for the death domain encoding was confirmed by DNA sequencing.

2.1.10.3 Generation of IRAK2 strep-HA pcDNA^{TM}5/FRT construct

The Strep-HA pcDNA^{TM}5/FRT construct is a Gateway compatible destination vector and allows for the introduction of a N- or C- terminal comprising Strep and HA double tags. The plasmids were obtained from Dr. Andreas Pichlmair (CeMM, Vienna, Austria). In general, overexpression of a gene of interested based on this expression vector can be detected via the HA tag and purified via Strep tag. Additionally, the vector possesses two more special characteristic which are the Flp recognition target (FRT) site fused with a hygromycin resistant gene and a tetracycline-regulated, hybrid human cytomegalovirus (CMV)/TetO2 promoter cloned upstream to the gene of interest. The FRT site allows for the stable integration of the gene of interest, when co-transfecting the respective plasmid and the pOG44 plasmid (encoding a Flp recombinase) into Flp-In HEK293T-Rex cell line is a host cell line allowing for the stable intergration of the gene of interest into its genome via the FRT recombination site. The host cell line is equipped with a FRT site due to the stable integration of the pFRT/lac-zeo plasmid which has a single FRT site under the control of the SV40 early promoter. Mover, this plasmid encodes for a lacZ-Zeocin gene which makes the cells resistant to zeocin. Furthermore, the Flp-In HEK293T-Rex cells constitutively express the Tet repressor which is under control of the CMV promoter and fused to the blasticidin resistant gene. Usually, the Tet-repressor gene is independent from FRT sites. The Tet repressor normally binds to the TetO2 promoter and thus represses the transcription of the gene of interest. However, tetracycline can counteract the funcitions of the Tet repressor and avctivates the TetO2 promoter to induce the transcription of the gene of interest (see figure 2.2)

The IRAK2 gene that was cloned to the pENTR1A plasmid can be easily shuttled into the Strep-HA pcDNA^{TM}5/FRT destination vector. The correct insertion was confirmed by BsrGI digestion and the protein expression was analysed by immunoblotting for the HA tag detection. The same vector was also used to when cloning all IRAK2 mutants, the IRAK1 and IRAK3 genes, and when constructing all the IRAKDD constructs.

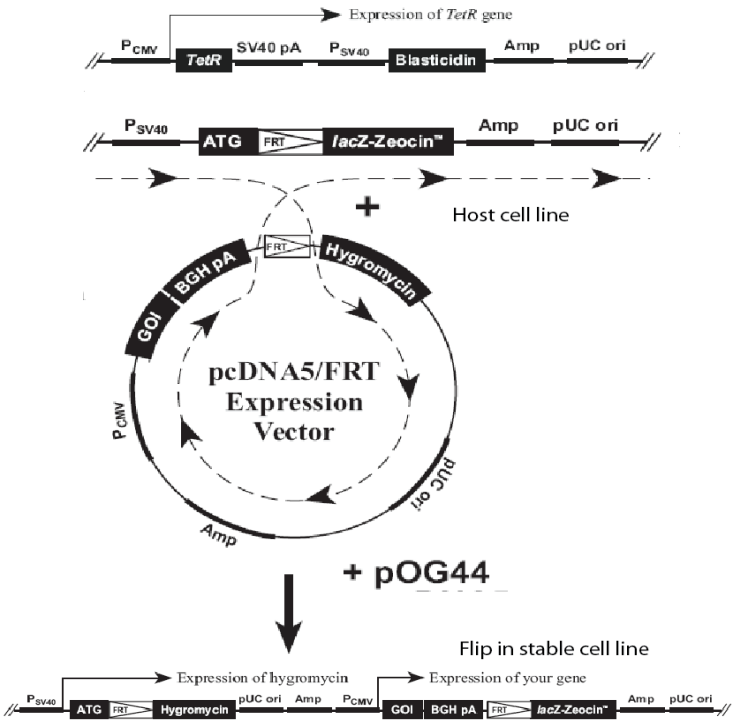

Figure 2.2 The diagram of generation of Flp-In stable cell line (Life Technology)

2.1.10.4 Generation of the IRAK and TRAF6 constructs for LUMIER assay

In order to perform high throughput protein-protein interaction screening, the LUMIER method was applied [190]. The one protein was tagged with Protein-A (Gateway destination vector, pT-Rex-DEST30 encoding for proteinA), the other protein interaction partner was tagged with the Renilla luciferase (Gateway destination vector pcDNA3nt-renilla or pT-Rex-DEST30 ct-Renilla). The destination vectors were obtained from the Core facility of Genomics and Proteomics, German Cancer Research Center(Dr. Manfred Kögl, DKFZ). Gateway LR reactions were done to generate IRAK and TRAF6 constructs for LUMIER assays. See Appendix.

2.1.10.5 Generation of Flag-tagged TRAF6 gene constructs

Gateway compatible plasmids encoding for human TRAF6 were bought from the Core facility of Genomics and Proteomics, German Cancer Research Centre (Dr. Manfred

Kögl, DKFZ). In order to conduct the co-immunoprecipitations, TRAF6 was introduced into a N-terminal or C-terminal Flag-tagged Gateway-compatible expression vectors (from Dr. Stefan Pusch, Department of Pathology, University of Heidelberg, Germany). The expression of the protein fused to the tags was confirmed by immunoblot analysis.

2.1.10.6 Generation of IRAK2 wild-type and mutants constructs for retroviral transduction

A retroviral vector is an infectious virus used to introduce a non-viral gene into mitotic cells *in vivo* or *in vitro*. The advantage of this vector is that it has higher transduction efficiencies than lipofectamine or calcium phosphate and can allow for the stable integration the gene of interest into the genome of the cell. pMXs-IP-puro vector (received from Dr. Kevin Michael Dennehy, Department of Virology, University of Tübingen) is a retroviral transduction vectors. The gene of interest flanked at the 5' and 3' end by long term repeat (LTR). The vector was transfected in to a packaging cell line (Phoenix ampho(provided by Dr. Kevin Michael Dennehy) or Phoenix eco(provided by Dr. Markus Feuerer).Since the vector contains the packaging sequence ψ, the RNA is recognized by capsid proteins encoded by the packaging cell line and packed into viral particles that are released into supernatant. The cultured supernatant is harvested after 48hours post-transfection, and applied to the cell-line of interest to generate stable cell lines. Cells that were successfully infected and integrated the genes of interest were selected by adding 10µg/ml puromycin. This is due to the fact that the pMXs-IP-puro vector has an internal ribosomal entry site (IRES) that allows for the expression the puromycin resistance gene, which makes stably transfected cell lines resistant to puromycin selection. Figure 2.3 shows schematic structure of the pMXs-IP-IRES-puro vector containing a N-terminal HA tagged human IRAK2.

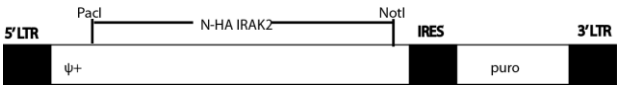

Figure 2.3 The schematic structure of pMXs-IP retroviral vector

2.1.11 Cultivation and cryo-preservation of transformed bacteria cells

Transformed bacteria were cultured in LB medium, which contained the required concentration of the antibiotics, and incubated at a shaker at 200rpm for 16 hours, 37 ℃. Glycerol stocks were prepared by using 500µl bacteria of the baterial suspension and

adding 150µl 100% glycerol. The bacterial glycerol stocks were shock-frozen in liquid nitrogen and stored at -80 ℃.

2.2 Biochemical Methods

2.2.1 Protein quantification

Protein concentrations of cell lysate were determined with the bicinchoninic acid assay (BCA) (Thermo Fisher Scientific). The assay is based on a colormertric technique, in which the total protein concentration is quantified by a color change of the sample solution from green to purple. Bicinchoninic acid, sodium salt, is a stable, water-soluble compound capable of forming an intense purple complex with cuprous ion (Cu^{1+}) in an alkaline environment. This reagent forms the basis of an analytical method capable of monitoring cuprous ion produced in the reaction of protein with alkaline Cu^{2+} (biuret reaction). The colour produced from this reaction is stable and increases in a proportional fashion over a broad range of increasing protein concentrations [191]. Bovine serum albumin (BSA) served as a standard protein solution that was diluted with the required lysis buffer to concentrations ranging from 0.125mg/ml to 2mg/ml. The protein concentrations were determined in a 96 flat-bottom microplate, in which 200µl working reagent was mixed with 25µl of the protein sample, followed by an incubating at 37 ℃ for 30min. The working reagent was made from solution A and solution B, mixed in a 50:1 ratio. In cases where the protein lysate exceeded the absorption range, samples were diluted in a 1:2 ratio with lysis buffer or H_2O. Each sample was measured in duplicates. The concentration was determined at a wavelength of 562nm with a 96 well plate reader (BMG labtech)

2.2.2 SDS-polyacrylamid electrophoresis

The Sodium–Dodecyl-Sulfate-PolyAcrylamide Gel Electrophoresis (SDS-PAGE) was performed with the Invitrogen X cell Surelock Mini Cell chamber system. Protein samples were diluted with the 4×NuPAGE LDS (Invitrogen) and 10×Sample reducing buffer (Invitrogen) and denatured at 90 ℃ for 10min.

The protein separation was carried out with pre-casted gels. Proteins with a molecular weight ranging from 10kDa to 140kDa were separated on Bis-Tris 4-12% gradient gels with MES or MOPS running buffer. . The gel was run for 70 mins at175V. Proteins with larger molecular weight were run on Tris-Acetate 3-8% gradient gels with Tris-Acetate

running buffer. Similarly, the separation was carried out for 70 mins at 150V. 4µl of a prestained protein marker (PageRuler, Fermentas) was loaded on each gel and served as a reference for the molecular weight.

2.2.3 Immunoblot analysis

The immunoblot analysis was carried out after SDS-PAGE. It was performed within an X-cell Surelock Mini chamber (Invitrogen). The transfer buffer(Invitrogen) was prepared with 20% methanol (Roth), Whatman filter papers and the nitocellular membrane were preincubated in the transfer buffer to enhance the transfer efficiency. The proteins were transfered to a nitrocellulose membrane with either 0.45µm or 0.25µm pore size; depending on the protein size. The transfer was conducted at 30V, for 1-2 hours (depending on the protein size). The transfer efficiency was confirmed by the transfer of the pre-stained protein marker. Then, the nitrocellulose membrane was blocked for 30-60 min in a 3% skimmed milk or 5% BSA diluted in PBS with 0.5%Tween or in TBS with 0.1%Tween buffer. The membrane was incubated overnight at 4℃ with respective primary antibody, which was diluted in the desired blocking buffer. The membranes were washed 3×5min with the respective washing buffer (PBS-0.5% Tween orTBS-0.1% Tween) before adding the secondary antibody diluted in the respective blocking buffer. The membranes were incubated for 1.5-2 hours at room temperature with secondary antibody that is conjugated to the horseradish peroxidise (HRP). The membranes were again washed 3×5min with the required buffer. Meanwhile, the enhanced chemical luminescence (ECL, Thermo fisher scientific) solution was prepared. The membranes were incubated with the ECL solution for at least 2 min, and then exposed to photographic films (GE health care). When dectecing another protein on the same membrane, the membrane was incubated with stripping buffer (Thermo Fisher Scientific) for 15min at room temperature. In order to confirm secondary antibody was stripped off, the membrane were incubated with ECL solution for 2min, and exposed for 3min to X-ray film. If no signal was detected after developing, the membranes were re-incubated with the blocking buffer, followed by the incubation with the respective primary and secondary antibodies. The stripping and re-incubation of the membranes with other antibodies was only done in cases, whether the respective secondary antibodies were produced from different species; this helped in controlling cross-reactivity of the antibodies.

2.2.4 Two-dimensional gel electrophoresis

The two-dimensional gel electrophoresis can be used to detect post-translational modifications of a protein. All experiments were carried out with a GE IPGphore Electrophoresis machine. Immunoprecipitated protein samples were resuspended in 13μl lysis buffer (7M urea, 2M thiourea, 4% CHAPS, IPG buffer 3-10 2%, + protease inhibitor cocktail) and incubated for 30min at room temperature shaking at 400 rpm. Then 117 μl of rehydration buffer (7M urea, 2M thiourea, 2% CHAPS, IPG buffer 3-10 0.5%, 40mM DTT) was added, and the samples were evenly distributed on 7cm strip ceramic holders (GE Healthcare). The IPG strips covered the pH range from 3 to 10 (GE Healthcare). The strips were covered with 600 μl pure oil (GE Healthcare) and closed with a plastic lid. The protein samples were absorbed overnight to the agarose strip at 30V. Before conducting the iso-electrophoretic focusing, small rectangular whatman paper pieces (3mm×10mm) were moisturized and placed between the agarose strip and the anode or cathode to increase the conductivity.The samples were separated and focused by first maintaining 300V for 1 hour (step-n-hold), then applying a gradient increase to 1000V with 30min, followed by another increase to 5000V within 1.5 hours, and keeping the voltage constant at 5000V for 36min (step-n-hold). Each strip acquired in total 7000-8000 Vhs. The agarose strips were taken out from the strip holders and washed briefly with distilled H_2O. The proteins were loaded on the strips in 2.5ml of 1% DTT which was diluted in 1×LDS buffer (Invitrogen). Then the strips were incubated for 15min with 2.5ml of 2.5% iodoacetamide which were diluted in LDS buffer. This step helped alkylating thiol groups and thus preventing reoxidation during electrophoresis, which may create artefacts in the saparation. The strips were adjusted to fit in the pocket of the IPG zoom precast Bis-Tris 4-12% gel (Invitrogen). and the position was fixed with 0.5% 1×MES agarose buffer. The separation was carried out with the MES buffer, was first applying 100V for 5min, and then increasing the voltage to 200V for 45min. The separated spots were identified by immunoblot analysis as described in section 2.2.3

2.3 Cell Biological Assay

2.3.1 Cell lines and cultivation

The following cell lines were used as in this thesis: HEK293T cells (obtained from Dr. Alexander Dalpke, Department of Medical Microbiology and Hygiene, University of Heidelberg, Germany), HEK293 Flp-In T-Rex cell line(from Dr. Andreas Pichlmair, CeMM,Vienna, Austria), IRAK2 knock out macrophage cells(from Dr. Katherine A. Fitzgerald, Division of Infection Disease and Immunology, Department of Medicine, University of Massachusetts Medical School, Worcester, MA, USA), Phoenix ampho cells (from Dr. Kevin Dennehy, Institute of Medical Virology, University of Tübingen, Germany) .

HEK293T, Phoenix ampho and Flp-In HEK293 T-Rex cell lines were cultured in Dulbecco's Modified Eagles Medium (DMEM Sigma), and supplemented with 10% FCS (Biowestern), 100u penicillin/streptomycin (Invitrogen), and 100u glutamine (Invitrogen). The Flp-In HEK293T-Rex cell line needed additionally the antibiotics, blasticidin (15 µg/ml, Invitrogen) and zeocin (100 µg/ml, Invitrogen) to maintain the Tetracycline repressor and FRT site. In cases when the Flp-In HEK293T-Rex cell line was used for stable transfections, zeocin was replaced with hygromycin (100 µg/ml, Invitrogen) to select the interested stable cell line.

IRAK2 knock out macrophage cells were cultured in DMEM, supplemented with 10% FCS, 10 µg/ml ciprofloxacin, and 100u glutamine. IRAK2 reconstituetions were conducted in these cells via retrovial transductions (see 2.3.9). Throughout the infection period cells were maintained under security level 2 conditions (S2 lab). 10 µg/ml of puromycin was added when selecting for cells that stably intergrated the gene of interest.

All cell lines were cultivated at 37 ℃ in an incubator adjusted to 5% CO_2.

2.3.2 Transfection of plasmids to mammalian cell lines

2.3.2.1 Calcium phosphate transfection

Calcium phosphate was taken as a transient transfection reagent for HEK293T cells, and generally applied for signalling and gene expression assays in HEK293T cells. 2×HBS (50mM HEPES pH 7.05±0.05, 10 mM KCl, 12 mM Dextrose, 280 mM NaCl,

1.5 mM Na_2HPO_4) and 2M $CaCl_2$ were prepared for transfection. According to the set-up of the experiment, different transfection mixes were required, as shown in Table2.3.

Table2.3 The calcium phosphate transfection method

Format	24 wells plates/each well	6cm dishes	10cm dishes
Cell number	7.5×10^4	7.0×10^5	1.5×10^6
Aim	Dual Luciferase Assay	WB blot	Co-IP
Plasmids for gene of interest (100ng/μl)	1μl	25μl	40μl
EGFP (100ng/μl)	1μl	5μl	10μl
NF-κB firefly reporter (100ng/μl)	1μl	0	0
Renilla luciferase (100ng/μl)	0.1μl	0	0
$CaCl_2$ (2M)	1.2μl	22μl	61μl
H_2O	5.7μl	308μl	389μl
2xHBS	10μl	360μl	500μl
Total volume	20μl	720μl	1000μl

The transfection mixture was added drop-wise into the wells. Then the plates were shaken slowly side to side or forward and backward to evenly distribute the transfection mixture. In general, the efficiency of transfection was over 90%.

2.3.2.2 Lipofectamine 2000 (Invitrogen) transfection

Lipofectamine 2000 (Invitrogen) was taken as a transient transfection method for LUMIER assays as described below. The efficiency of transfection was around 70-80%.

Table 2.4 Lipofectamine 2000 (Invitrogen) transfection method

Format	96 wells plates/each well
Aim	LUMIER assay
Gene of interest 1(10ng/μl)	2μl
Gene of interest 2(10ng/μl)	2μl
Optimem	6μl
Lipofectamine mix	6μl
Incubating for 20min at room temperature before adding to cells	
Lipofectamine mix:	12.6μl lipofectamine 2000 + 1200μl optimem / plate
Incubating 5min before adding to DNA mixture	

2.3.2.4 X-treme GENE HP transfection

The X-treme GENE HP transfection method was used to perform retroviral

transductions. 2µg retroviral plasmid encoding the gene of interest was mixed with OptiMEM (Life Technologies) to reach a total volume of 100µl. Then 6µl of the X-treme gene transfection solution (Roche Applied Science) was added into the OptiMEM-DNA mixture: the ratio of gene and X-treme gene transfection solution was 1:3. The transfection mixture was mixed by pipetting up and down for several times and incubating the solution at room temperature for 20min. The DNA-transfection mixture was added to the cells and the plates were shaken side to side to ensure an even distribution of the transfection mixture.

2.3.3 Stable transfections of Flp-In™ 293T-REx™ cell lines

Flp-In™ 293T-Rex cells were used to generate a cell line stably expressing IRAK2-HA, 700000 Flp-In™ 293T-Rex cells were seeded into a 6cm dish in 5ml DMEM medium that did not contain any selective antibiotics. 0.2µg of the pcDNA5TM/FRT plasmid encoding for IRAK2-HA and 1.8µg pOG44 (ratio: 1:9) were co-transfected into Flp-In™ 293T-Rex cells by calcium phosphate method. The transfection mix was added to the Flp-In^{TM} HEK293T-Rex cells; additionally, GFP encoding plasmids were transfected to a separate dish to assess the transfection efficiency. After two days, the cells were trypsinized and transferred from the 6cm dish to a 10cm dish, keeping the cells in 10ml of DMEM. Blasticidin (15µg/ml) and hygromycin (100µg/ml) were added two days later (Invitrogen) and the selection medium was replenished every 3-4 days. After two weeks, the cellular foci were formed, indicating a successful stable integration of the gene of interest into the Flp-In™ 293T-Rex cells. Due to the fact that this cell line only contained one FRT site for recombination, the cellular colonies all shared the exact same site for the integration of the gene (this was analysed beforehand in the lab). In order to confirm that IRAK2-HA is expressed cells were treated with 1µg/ml of tetracycline for at least 2 hours. Subsequently, an immunoblot analysis of the cell lysate was conducted to probe the expression of IRAK2-HA.

2.3.4 Gene expression analysis

All the expression plasmids generated in this thesis were analysed for the correct expression of respective cloned genes. HEK293T cells were seeded into 24 well plates with 75000 cells per well. 100ng of the gene encoding plasmids were transfected and after 48 hours the cells were lysed with 60µl RIPA lysis buffer (pH=6.9) freshly supplemented with protease and phosphatise inhibitors (Roche). In some cases,

HEK293T cells were seeded into 6 well plates, with 700000 cells per well. 2.5 μg of gene encoding plasmids and 0.5 μg EGFP encoding plasmids were co-transfected into each well. After 48 hours, the medium was removed and 250μl of the lysis buffer was added.

The cell lysis was conducted for 15min, keeping the cell culture dishes/plates on ice. The cellular lysates were then collected in 1.5ml tubes and centrifuged at 13000rpm for 10min at 4 ℃ to pellet the cellular debris. The supernatant with the lysed proteins was transferred to a new 1.5ml tube. In order to compare the protein expression levels, the BCA assay was carried out (see 2.2.1). The protein concentrations were adjusted to similar values with the lysis buffer. The samples were separated by SDS-PAGE to then probe for the protein of interest in a subsequent immunoblt assay (see 2.2.3)

2.3.5 Dual luciferase assay

In order to analyse if certain proteins can induce signalling pathways, Dual Luciferase Assays (Promega) was performed to check for the activation of transcription factors. This work focused on the activation of NF-κB, IRF3 and AP-1 transcription factors using firefly luciferase reporter plasmids. The plasmid constructs contained the promoter binding motifs of the respective transcription factors that were cloned upstream to the firefly luciferase gene. Therefore, signalling activities were analysed by detecting the luminescence of firefly. Different transcription factor encoding plasmids were tagged with firefly (*Photinus pyralis* (Strategene)) luciferase reporter. Additionally, a Renilla (*Renilla reniformi or sea pansy*) luciferase reporter vector with constitutive expression served as a transfection control were used for Dual Luciferase Assa.. The firefly luciferase reporter gene was measured by adding luciferase Assay Reagent II to generate a luminescent signal lasting at least one minute. After quantifying the firefly luminescence, this reaction is quenched, and the Renilla luciferase reaction is initiated simultaneously by adding Stop & Go reagent to the same sample. Both reporters yield linear assays with attomole ($<10^{-18}$) sensitivities and no endogenous activity in the experimental host cells.

Usually, Dual Luciferase Assay was conducted in HEK293T cells. 75000 HEK293T cells per well were seeded in 24 well plates. Transfection was conducted after 2-4 hours of seeding. The transfection mixture is listed in table 2.3. DNA plasmids (including

EGFP, NF-κB firefly luciferase reporter, and Renilla luciferase reporter) concentrations were adjusted to 100ng/μl. EGFP was taken as a control of transfection efficiency; Renilla luicferase reporter plasmid was taken as a relative expression control. Cells were lysed with passive lysis buffer (Promega) after 48 hours' transfection. 60μl passive lysis buffer was added into each well, and plates were shaken at 1000rpm for 15min at the room temperature. Then samples were frozen at -80℃ for 15min and thawed at the room temperature in order to extract all proteins from the cells into the lysate. To separate debris, lysed samples were centrifuged at 2500rpm for 10min. Luminometric measurements were carried out in 96 well white plates (Nunc) by analyzing 10μl of the cell lysate. The measurements were performed with a luminometer (Fluostar (BMG Labtech)). 50μl of the firefly luciferase substrate (beetle luciferin, promega) and 50μl of the Renilla luciferase substrate (coelenterazine, Promega) were sequentially injected to the sample. The luminescence signals were captured at every 0.5 seconds during a time window of 10s, and expressed as relative light units. The relative activity of firefly luciferase reporter was normalized to the signals of the renilla luciferase reporter. The measurements were conducted in triplicates, and presented as mean value ± standard deviations.

2.3.6 LUMIER

Luminescence-based mammalian interactome is an automated high throughput technology designed for the systematic mapping of dynamic protein-protein interaction networks in mammalian cells [190]. It can display the relative interaction intensity of interacted proteins. In this method one protein of interest is fused to a Protein-A tag, which is then co-transfected with the other protein of interest that has a Renilla luciferase tag. The protein complex is purified from the cellular lysates by immunoprecipiation with IgG Dynabeads M-280 (Invitrogen) which detects the Protein-A tagged protein. The interaction intensity is then detected by conducting a Renilla luciferase enzymatic assay. The method described here was optimized by Dr. Manfred Kögl (DKFZ). 10000 HEK293T cells were seeded per well into 96 well plates and cultivated in 100μl growth medium. 2-4 hours after seeding, 20ng of the plasmids encoding for the Renilla fused protein (one protein of intereste) and 20ng of expression plasmids for the Protein A-tagged protein partner were co-transfected by Lipofectamine 2000 (Invitrogen). Fos (Renilla-tagged) and Jun (Protein A-tagged)

were set up as a positive interaction control for each experiment [190]. Meanwhile, a negative control was set up by co-transfecting the empty vector plasmids which only encoded for the Renilla luciferase and the Protein A-tag. Each condition was done in triplicates. The cells were lysed 48 hours after transfection with 10µl lysis buffer 2 which was supplemented with fresh Proteinase inhibitor cocktail (Roche), Phos-stop (Roche), DTT (1M), Benzonase 0.0125 U/µl and 1% of IgG Dynabeads M-280 (Invitrogen). The samples were lysed for 15 minutes on ice. Triton-X100 may interfere with the luciferase measurement. Therefore, 100µl of PBS was added to the lysate, and 10µl of the diluted suspension were again diluted in 90µl PBS. These diluted samples were used to measure for the raw Renilla luciferase activity within the cellular lysate. The remaining amount of the cellular lysate was subjected to a magnetic plate washer (Tecan) to perform the immunoprecipitation of the Protein A -tagged protein and to remove unbound Renilla-tagged proteins. The immunoprecipiates were then analysed for their Renilla activity to quantify the amount of interaction between the Protein A and Renilla-tagged proteins. The substrate for the Renilla luciferase was prepared by adding 18µl of co-elenterazine (P.J.K) into 15 ml of Renilla assay buffer (see appendix). The final concentration of coelenterazine was kept at 2.5µM. The renilla activity was detected at a platereader (Infinity 200, Tecan) which automatically added 70µl of the renilla luciferase substrate to the well and measured the enzymatic luciferase activity in a time window of one second (see figure 2.4). The protein interaction intensity was calculated according to the following ratio [190], which was modified by Dr. Manfred Kögl .

$$Interaction\ Intensity = \frac{\dfrac{\text{sample(binding renilla activity)}}{\text{sample(raw renilla activity)}}}{\dfrac{\text{negative control(binding renilla activity)}}{\text{negative control(raw renilla activity)}}}$$

The whole experimental procedures see the figure below:

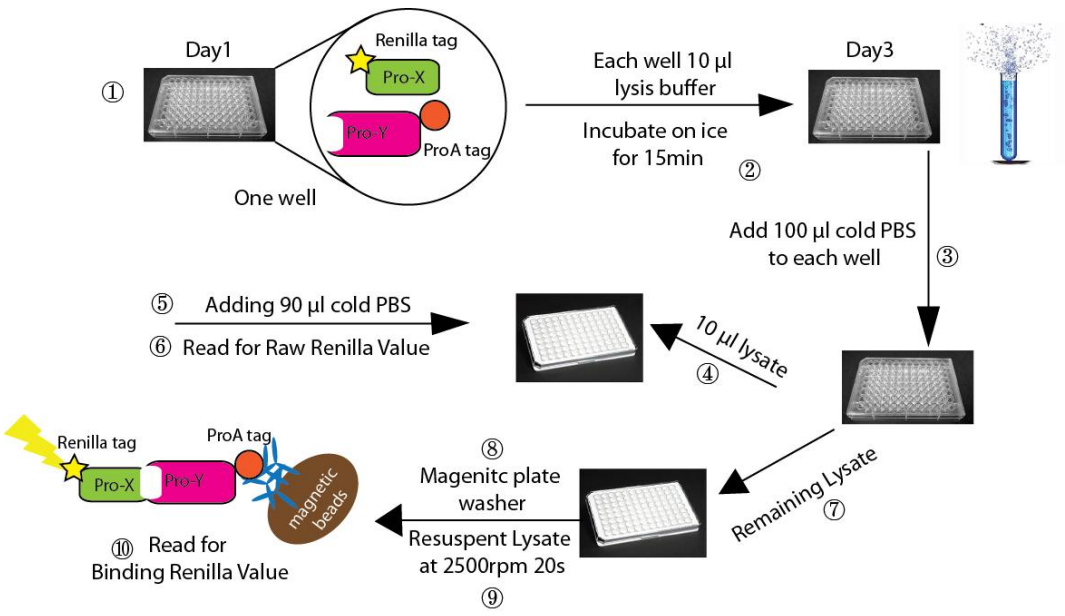

Figure 2.4 The schematic diagram of the LUMIER procedure

2.3.7 ELISA

Enzyme-Linked Immunosorbent Assay was used to detect for the induction of pro-inflammatory cytokines on a protein level. In order to confirm that different SNPs can alter the NF-κB activation on a protein level, IL-8 production in HEK293T cells and TNF-α production in macrophages were measured by ELISA. In the cellular system of HEK293T, human IL-8 was taken as readout. Supernatants were collected 48 hours after transfecting certain expression plasmids into HEK293T cells and the concentration of IL-8 was detected (Biolegend). For the reconstituted IRAK2 knockout macrophages, mouse TNF-α (Biolegend) was taken as readout for NF-κB activation when stimulating the cells with different TLR ligands. In both conditions, 96 well plates were pre-coated either with IL-8 or TNF-α monoclonal antibodies overnight at 4 ℃. According to the protocol which was provided by the company, the plates was blocked with 1× assay buffer for 1 hour, then 100µl of the cell culture supernatant (according to the different sensitivity and ability of various kit, dilutions of the samples were required) and 100µl of a standard human recombinant IL-8 dilution series (ranging from 15.6 to 1000pg/ml) or of mouse recombinant TNF-α (concentrations from 7.8 to 500 pg/ml) were added into each well of a 96 well plate, respectively. Each sample was analysed in triplicates or at least duplicates and the samples were incubated at room temperature for 2 hours. Then 100µl of biotinylated anti-human IL-8 or anti-mouse TNF-α detection antibody were added into each well and the samples were

again incubated at room temperature for 1 hour. Finally, 100µl of avidin-HRP was added to each well and incubated at room temperature for another 30 minutes. Sequentially, TMB substrate was added and the colorimetric reaction was stopped by adding the provided stop solution. The concentrations of IL-8 or TNF-α were measured at the wave length of 450 nm on a 96 well plate-reader (Fluostar, BMG). In order to substract any background noise of the plates, the plates were again measured at 570nm and the respective values were substracted from the readings at 450nm.

2.3.8 Immunoprecipitation

Immunoprecipitation is a method in which a protein of interest is precipitated by using a specific antibody. The advantage of this method is that the protein of interest can be isolated from the whole cell lysate and be concentrated on modified agarose beads. It was applied in this thesis to detect protein-protein interactions. In the case of IRAK2 and TRAF6 interactions, 1.5 million HEK293T cells were seeded into 10 cm dishes, and 4 µg of each gene encoding plasmids and 1µg of EGFP encoding plasmids were co-transfected into HEK293T cells with the calcium phosphate transfection method. The efficiency of transfection was assessed with the fluorescent microscope after 48 hours of transfection. Usually, the transfection efficiency reached up to 90%. The culture medium was then removed and the cells were washed with 3 ml of cold PBS. The cells were lysed with 850µl of the respective lysis buffer by incubating the dishes on ice for 15min. The celluare lysates were transferred into a 1.5ml tube and incubated for additional 30min on ice to thoroughly lyse the cells. Meanwhile centrifuge was pre-cooled to 4℃, and the cell debris was then separated from the lysate by centrifuging the samples at 13000g for 10 minutes. The supernatant was transferred to a new 1.5ml tube. In cases where the expression levels of each sample were needed to be compared, a BCA assay was conducted as well (see 2.2.1). 800µl of the lysate was applied for immunoprecitations. When precipitated HA-tagged proteins, 1.5µl of an α-HA mouse antibody was added to the lysate. In the case of TRAF6 ubiquitination assays, 4µl of a TRAF6 monoclonal antibody (Santa Cruz) was added to the lysate. The samples were rotated end-to-end for one hour at 4℃. Then 30µl of an A/G agarose bead slurry (Thermo Fisher Scientific) was added to the samples and rotated end-to-end for additional two hours at 4℃. In order to get rid of unbound proteins, agarose beads were washed three times with cold lysis buffer. In the case of TRAF6 ubiquitiantion assays,

IAA and proteinase inhibitor and phos-stop were freshly added. The samples were centrifuged at 6000 g for 2 minutes, which precipitated the agarose beads bound to the protein interaction complex. The washing buffer was carefully removed from the pellet, and the samples were again washed for another 2 times. If no further studies were performed on the same day, the samples were kept at -20 ℃. For SDS PAGE analysis, the samples were treated with 14µl of 4×LDS buffer (Invitrogen, NuPAGE) with 3µl of a sample reducing agent (Invitrogen NuPAGE) and heated at 90 ℃ for 10 minutes. This procedure helped in releasing the protein complex from the agarose beads, Then SDS-PAGE was carried out and the proteins of interest were detected by immunoblot analysis.

2.3.9 Retroviral transduction

Retroviral transduction was used to introduce N-terminal HA tagged human IRAK2 into murine IRAK2 KO macrophages. N-terminal HA tagged IRAK2 was introduced into the pMXs-IP retroviral vector which is based on the Moloney Murine Leukemia Virus (MMLV), whose LTR is the most commonly used for retroviral vectors, and is expressed in almost all cell types (see 2.1.9.6) The viral stocks were generated by transfecting pMXs-IP-puro plasmids which contained the N-terminal HA tagged IRAK2 into the Phoenix ampho cells, which is a packaging cell line.

On the first day, 5×10^5 Phoenix ampho cells per well were seeded into a 6 well plate with 3 ml growth medium; two wells of Phoenix ampho cells were prepared for each transduction condition.

On the second day, 2µg of the plasmid carrying the gene of interest was transfected into each well with the X-treme gene HP transfection reagent. The ratio of the plasmid and the transfection reagent was 1: 3 (1µg plamid and 3µl X-treme gene HP).

On the third day, 3×10^5 of the mouse IRAK2 knockout macrophages were seeded per well into a separate 6-well plate and were maintained in 2ml growth medium; one well was prepared for each transduction condition.

On the fourth day, virues were harvested from the Phoenix ampho cells. The viruses were released into the supernatant and contained the gene of interest. Since two wells were prepared for one transduction condition, the supernatant (containing the viruses)

of both wells were pooled and passed through a 0.45 micro-m filter to remove cellular debris. The volume of viral stock was approximately 5ml. Polybrene (Sigma, hexadimethrine bromide) was added into the viral stock to reach a final concentration of 8μg/ml. Polybrene is used to enhance the efficiency of transduction by neutralizing the charge repulsion between virions and sialic acid on the cell surface. The culture medium of the macrophages was removed from the IRAK2 knock out macrophages and replaced by the viral stock medium. The centrifuge was pre-warmed to 32 ℃ and the plates containing the IRAK2 knockout macrophages with the viral medium were centrifuged down at 2000 rpm for 2 hours. Then the plates were placed back into the incubator.

In order to avoid that polybrene may inhibit the growth of the cells; the viral supernatant was replaced with growth medium after 6 hours of infection. In the case that the infected cells are in suspension, they can be counted on the same day of infection and directly be resuspended into the viral supernatant.

2.4 Infection of reconstituted macrophages with Influenza A

The Influenza A strain WT PR8 and △ NS1 were obtained from Prof. Dr. Oliver Plantz (Interfaculty of Cell biology Department of Immunology, University of Tübingen, Germany). The following protocol was applied to infect macrophages with the Influenza A strain.

Day 1: Seeding of 1.5×10^5 macrophages per well into 24 well plates with 500μl culture medium.

Day 2: The growth medium was removed and the cells were washed with 1 ml PBS, since FCS affects the infection efficiency. Meanwhile, “infection PBS” (PBS with trypsin) and “infection medium” (DMEM without FCS, supplemented with trypsin and BSA) were prepared. Viruses were diluted in the ‘infection PBS’ solution to the required concentrations (MOI of 1, 10 or 100), added to the cells and incubated at 37 ℃ for 30 min in the S2 incubator. Then the “infection PBS” solution containing viral media was replaced with 500μl of the “infection medium” and then incubated at the 37 ℃ in the incubator. After required amount of time, RNA was harvested according to the protocol (RNeasy kit, Qiagen) (see 2.1.3).

2.5 Infection of reconstituted macrophages with *Salmonella typhimurium*

Salmonella typhimurium (strain LT2) was a gift from Dr. Samuel Wager (Department of Medical Microbiology and Hygiene, University hospital of Tübingen). The following protocol was applied to infect macrophages with *Salmonella typhimurium.*

On the first day, *Salmonella typhimurium* was inoculated in 5ml LB medium and kept at 37℃ for overnight (at least 16 hours). Meanwhile, 1.5×10^5 of the reconstituted macrophages were seeded into each well of a 24 well plate with 500 µl of culture medium.

On the second day, *Salmonella typhimurium* were cultured again by inoculating overnight culture into 5ml of fresh LB medium at 1:10 dilution, and cultivating the suspension for another 2-3 hours at 37℃. Then the OD value of *Salmonella typhimurium* was measured at 600 nm. An OD value of 0.9 corresponds to approximately 1.0×10^9 *Salmonella typhimurium* in 1ml LB medium. Then *Salmonella typhimurium* were diluted with in HBSS in a 1:10 ratio (see Appendix) which inhibited the growth of *Salmonella typhimurium.* The cultural medium of the reconstituted macrophages was removed and washed once with 500µl HBSS. In the case of macrophage infections, a MOI of 1 or 10 was chosen. HBSS containing the required amount of *Salmonella typhimurium* were added into each well and incubated at 37℃ for 30 min in the S2 incubator. At the same time, the infection medium (DMEM supplemented with FCS and spectinomycin 50ng/ml-100ng/ml) was prepared. The HBSS containing *Salmonella typhimurium* was replaced by 500µl of the infection medium which kills all of the extracellular *Salmonella typhimurium*. RNA was harvested according to the required experimental conditions (see 2.1.3).

2.6 Computational methods.

2.6.1 Homology modelling of IRAK2 kinase domain.

The structural homology model of the IRAK2 kinase domain was done by Dr. Andriy Kubarenko to gain further insights into the three dimensional location of the amino acid residues of interest. The structure of the kinase domain of IRAK2 was generated according to IRAK4 KD structure which is available at the PDB databank (PDB code 2NRU). Protein structure images were generated with the PyMOL software.

2.6.2 Software tools and web-based browsers

The DNA sequences were aligned and checked by vector NTI Advanced (Invitrogen) or Geneious software (www.geneious.com). Additionally, the Geneious software was used to generate plasmid maps for the expression plasmids and to design the cloning primers. Furthermore, Geneious was used to analyse protein sequences and to perfom protein sequence alignments. Site-directed mutagenesis primers were designed by the website which is provided by Agilent. The qPCR primers were directly designed and purchased from Life Technology. Figures were done with Prism or Adobe Illustrator.

2.6.3 Statistic analysis

Statistical analysises were mainly done in Excel using the student *t*-test; two-way ANOVA was done in Stata. The epidemiological data analysis was done with SPSS 20.0 (SPSS, Chicago, Illinois, USA) or SAS (SAS Institute Inc., Cary, NC, USA).

Chapter 3: Results and Discussion

3.1 Part I: IRAK2 played a central role in the TLR signalling pathway.

3.1.1 Introduction

The aim of part I was to decipher the role of IRAK2 in the TLR signalling pathway. The IRAK family consists of four members: IRAK1, IRAK2, IRAK3 and IRAK4. IRAK4 is essential for TLR/IL-1R-mediated signal transduction [192]. IRAK4 deficient mice are shown to be resistant to LPS- induced shock [146]. In humans, IRAK4 deficiency leads to recurrent infections with pyogenic bacteria, especially *Streptococcus pneumonia* [164]. In contrast, IRAK3 is shown to inhibit the production of pro-inflammatory cytokines and block the formation of the IRAK1-TRAF6 complex [87]. Furthermore, IRAK1-deficient mice are resistant to LPS inoculation. Moreover, IRAK1 is essential for the production of TLR7/9-induced type I interferons [94]. However, IRAK1-deficient cells are still able to produce cytokines after TLR or IL-1R stimulation [130]. It was therefore assumed that other IRAK family members should be able to participate the production of pro-inflammatory cytokines. Macrophages derived from IRAK2 deficient mice showed reduced TNF-α production upon stimulation with multiple TLR ligands, with the exception of TLR3 [137]. Particularly, IRAK2 appears to be essential for sustaining TLR-mediated expression of pro-inflammatory cytokines at late time points [137]. However, siRNA silenced IRAK2 human PBMC severely reduced the TNF-α production when stimulating with TLR4 or TLR7 ligands within 30 minutes [193]. Moreover, another study showed that IRAK2 has no impact on early or late TLR4-induced NF-κB activation [140]. Based on these controversial arguments, we would like to clarify the role of IRAK2 in TLR signalling pathway.

3.1.2 IRAK2 can only induce NF-κB activation in HEK293 cells

It was shown that overexpression of human IRAK2 in HEK293T cells induced NF-κB activation. Moreover, IRAK2 is essential for the activation of IRF3 in stably transfected TLR3-HEK293T cells [88]. However, overexpression human IRAK2 in HEK293T cells cannot drive the activation of IRF3 [88]. In order to confirm the IRAK2 construct and further elucidate the role of IRAK2 in pro-inflammatory signalling pathways, dual luciferase assays were carried out with a NF-κB luciferase reporter, a ISG56 luciferase reporter (IRF3 activation indicator), and an AP-1 luciferase reporter (MAP kinase signalling pathway) See figure3.1.

HA-tagged human IRAK2 plasmids were introduced into pcDNA5/FRT/TO based expression plasmid and transfected to HEK293 cells to first analyse for the induction of NF-κB. Fig. 3.1 A shows that overexpression of IRAK2 strongly induced NF-κB activation, which confirmed that the IRAK2 construct is correct and the transfection was efficient.

Additionally, either HA-tagged IRAK1 or IRAK2 or IRAK3 was transfected to the cells to check and compare for the IRF3 activation. The transfection of TRIF expression plasmids served as a positive control for IRF3 activation (figure 3.1 B). Whereas TRIF induced high level of ISG promoter activation, neither IRAK2 nor IRAK1 nor IRAK3 overexpression resulted in any IRF3 activation in HEK293T cells. This observation is consistent with the results obtained in another lab [88]

Subsequently, the induction of the MAPK pathway was investigated for which transfections of MyD88 expression plasmids served as positive control for AP-1 activation. However, neither IRAK2 nor MyD88 could induce AP-1 activation (Figure 3.1 C). This might due to defects in the AP-1 reporter construct or this system cannot work out in HEK293T cells.

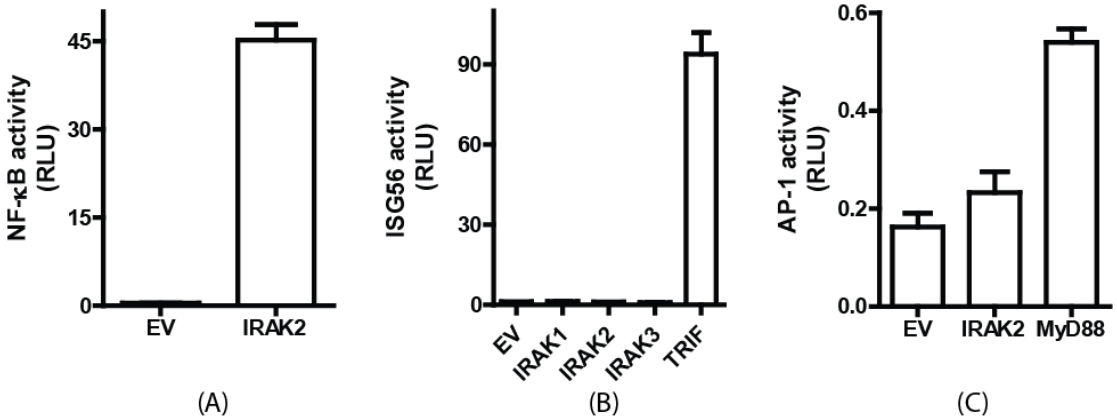

Figure 3.1 IRAK2 overexpression results in NF-κB activation, but not MAPK or IRF3 signaling in HEK293T cells. (A) Transfection of 100ng of IRAK2-HA encoding plasmids and 100ng of NF-κ B luciferase reporter plasmids into HEK293T cells, (B) Co-transfection of 100ng IRAK encoding plasmids with ISG56 luciferase reporter plasmids. (C): Transfection of 100ng of IRAK2-HA encoding plasmids and 100ng of AP-1 luciferase reporter plasmids. The measurements were conducted 48 hours post-transfection in Fluro star (BMG Labtech). Experiments were repeated three times.

Based on the results shown above, the NF-κB reporter assay was used for further experiments to serve as a read-out for functionally characterizing IRAK2 and genetic variants of IRAK2 proteins in HEK293T cells. However, in order to decipher the

complex role of IRAK2 in the TLR/IL-1R signalling pathway, subsequent experiments focused on the reconstitution of IRAK2 knockout macrophages.

3.1.3 IRAK2 rescued the pro-inflammatory cytokines production in macrophages

IRAK2 has been shown to be involved in TLR2, TLR3, TLR4, TLR7/8, and TLR9 signalling to sustain NF-κB activation at late time points [137]. Thus, the following experiments focused on investigating the role of IRAK2 upon stimulation with different TLR ligands.

Mouse *Irak*2 knockout macrophage cells were kindly provided by Dr. Katherine A. Fitzgerald (Division of Infectious Diseases and Immunology, University of Massachusetts Medical School, Worcester, USA). The advantage of murine macrophages is that they can directly test the TLR ligand activation. However, these macrophage cells are not easily transfected by calcium phosphate and lipofectamine. Retroviral transduction is a method which can easily introduce a gene of interest into mitotic cells. Human IRAK2 has around 65% identity with murine *Irak*2. Moreover, the death domain (for oligomerization) and kinase domain of murine and human IRAK2 are well conserved. We assumed that human IRAK2 possibly can rescue the signalling properties in TLRs signalling pathways. This method is also conducted by Dr. Nagpal who investigated defected mutants in MyD88 [194] and Mal [195].

The retroviral transduction vector pMXs-IP-puro was kindly provided by Dr. Kevin Micheal Dennehy. The schematic structure was described in section 2.1.9.6. The human N-terminal-HA tagged IRAK2 WT was introduced into pMXs-IP-puro via pacI and NotI restriction enzyme respectively and the successful retroviral transduction was selected by 10μg puromycin and confirmed by immunoblot assay (as described in section 2.1.9.6 and 2.3.9). Figure 3.2 A shows that HA-tagged human IRAK2 was expressed in the KO macrophages.

TNF-α is one of several pro-inflammatory cytokines which is produced and secreted when NF-κB is activated. Therefore, mock treated and IRAK2-HA reconstituted KO cells were stimulated with different TLRs ligands, and the amount of TNF-α production was measured by ELISA (see Figure 3.2). Stimulations of TLR2 (Pam_2CSK_4), TLR4 (LPS) and TLR7 (R848) resulted in moderate levels of TNF-α secretion in mock treated cells, which was strongly enhanced in IRAK2 reconstituted cells (Figure 3.2 B).

This observation is consistent with the data generated by Sinead Flannery in human PBMCs (Trinity College, University of Dublin, Ireland). However, TLR3 (Poly I: C), TLR5 (Flagellin) and TLR9 (CpG) ligands only slightly increased TNF-*α* secretion (Figure 3.2 C). Additionally, PMA and ionomycin was added to the cells; it is known that this treatment results in the activation of the protein kinase C (PKC) and in the subsequent production of pro-inflammatory cytokines. This condition therefore served as a positive control for TNF-*α* secretion. Interestingly, upon stimulation with PMA and ionomycin, reconstituted macrophages resulted in a 3-fold higher production of TNF-*α* in comparison to mock treated cells; this may, indicate that IRAK2 is also involved in PKC activation.

Conclusively, IRAK2 is demonstrated be important for TLR2, TLR4 and TLR7 induced TNF-α production in macrophages.

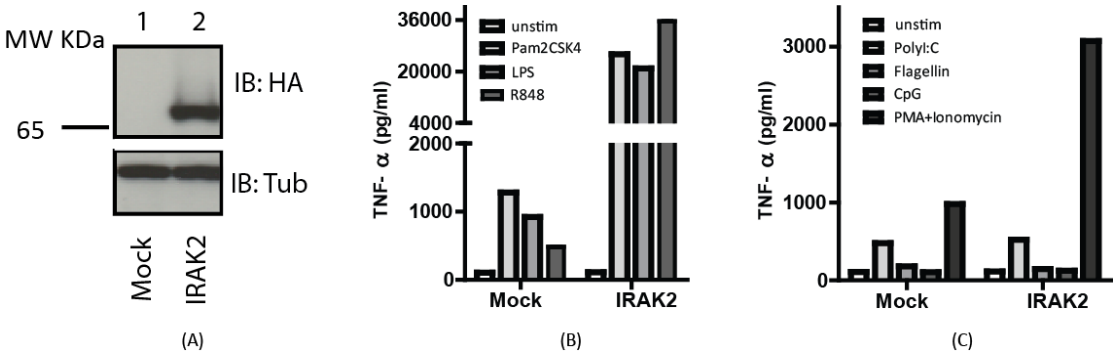

Figure 3.2 IRAK2 rescues TNF-α production in IRAK2 KO macrophages stimulated with TLR2, TLR4 and TLR7 ligands. (A) Cell lysates of human N-HA IRAK2 reconstituted macrophages or mock reconstituted macrophages were harvested and probed with anti-HA (rabbit) monoclonal antibody. (B) and (C): The 25000 cells were seeded stimulated overnight with the indicated TLR ligands. The amount of TNF-α in the culture supernatants was analyzed by ELISA. Stimulations with Pams2CSK4 (1µg/ml), PolyI:C (10µg/ml), LPS (0.05µg/ml), Flagellin (50µg/ml), R848 (1µg/ml) CpG (2.5mM) and PAM (10µg/ml)+ Ionomycin (1mM) The results are reported as a mean of triplicates ± S.D. The graph is a representative of three independent experiments.

In order to investigate the role of IRAK2 in the context of pathogenic infections, mock treated and IRAK2 reconstituted macrophages were treated with influenza A (PR8 strain) and *Salmonella typhimurium* (strain LT2). The cellular response to these infectious agents was quantified by the mRNA levels for *Tnf-a*, *Il-6*, *Il-1β*, *Ifn-β* and *Ccl5*. The infection with influenza A did not induce any changes in the induction of pro-inflammatory cytokines and type I interferons (data was not shown). However, reconstituted macrophages resulted in enhanced mRNA levels for *Il-1β* and *Il-6* upon

stimulation by *Salmonella typhimurium* (Figure 3.3) The significant induction of *Tnf-a*, *Ccl5* or *Ifn-β* was not observed in this experimental set up.

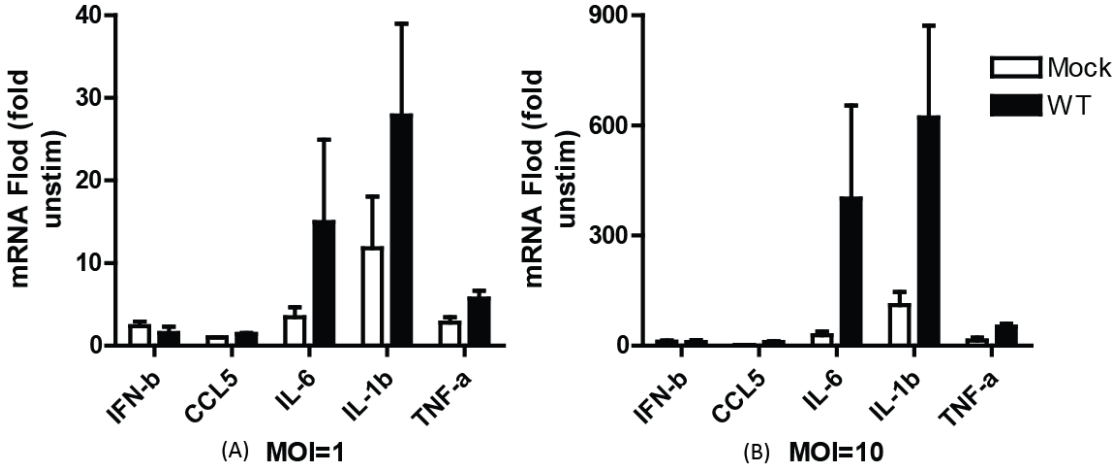

Figure 3.3 IRAK2 is critical for the pro-inflammatory response against *Salmonella typhimurium*. 1.5×10^6 cells of mock treated and IRAK2-HA reconstituted macrophages were challenged for 3 hours with (A) 1 MOI and (B) 10 MOI of *Salmonella typhimurium*. The mRNA levels of *Ifn-β*, *Ccl-5*, *Il-6*, *Il-1β* and *Tnf-α* were determined and normalized to the unstimulated conditions. Mean+SEM. of three independent experiments is shown.

3.1.4 IRAK2 enhanced the phosphorylation of p38, p65, ERK and Akt

Previous experiments showed that the reconstitution of human IRAK2 into murine IRAK2 knockout macrophages can rescue the production of several pro-inflammatory cytokines. In order to confirm that this also involved the activation of the respective signalling pathways, further experiments analysed the phosphorylation of p38, p65 and Akt, which is a preliminary test.

Akt, also known as protein kinase B (PKB), is a serine/threonine-specific protein kinase that plays a key role in multiple cellular processes such as metabolism, apoptosis, cell proliferation, transcription and cell migration. IRAK1 was required for IL-1β induced phosphorylation of the PKB signalling pathway [196]. Recently, unpublished data of Isabelle Bekeredjian-Ding (Institute of Microbiology, Immunology and Parasitology, University of Bonn, Germany) showed that IRAK4 interacted with Akt to crosslink the TLR with the PKB signalling pathway. Additionally, it is well known that pathogenic infections have an impact on the cellular metabolism. Therefore, Akt was included into our preliminary investigation as well.

The stimulation of reconstituted macrophages with Pam_2CSK_4, LPS and R848 demonstrated that p38 and p65 were phosphorylated even in the absence of IRAK2 at low level (mock treated control). However, the phosphorylation intensity was enhanced in macrophages which were reconstituted with IRAK2. Interestingly, phosphorylation of Akt only occurred in macrophages which were reconstituted with human IRAK2. This might indicate that IRAK2 possibly interact with IRAK4 and then involved in the PKB signalling pathway (Figure 3.4).

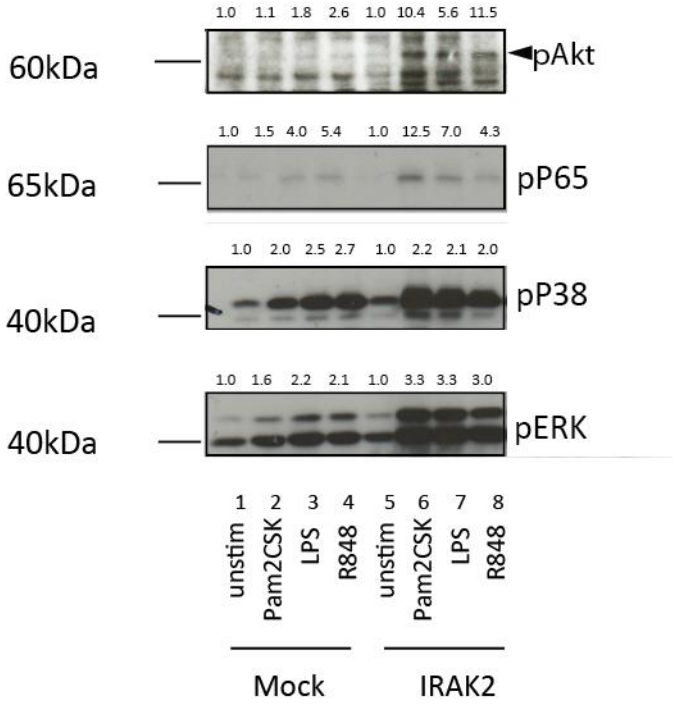

Figure 3.4 IRAK2 enhanced the activation of NF-κ B and MAP kinases signalling pathways and triggered the phosphorylation of Akt upon TLR stimulation. Mock and WT cells were treated with the indicated ligands for 30 min. Cell lysate were analysed on SDS-PAGE and by immunoblot assay to probe for phosphor-Akt, -p65, -p38 and –ERK, respectively. Phospho Akt experiment was repeated twice. The densitometry was analysed with Image J.

If the total amount of Akt, p65, p38 and ERK are kept at same level, then we can assume that IRAK2 plays an important role to boost the induction of the NF-κB and MAP kinase signalling pathways. Furthermore, IRAK2 appears to play a unique and critical role in the activation of Akt. Therefore, as kinases are involved in various signalling pathways, further experiments focused on understanding the post-translation modifications in IRAK2.

3.1.5 Post-translational modifications in IRAK2

Post-translational modifications are essential for proteins undergoing signal transduction and protein-protein interaction. Previous research demonstrated that IRAK1 undergoes several post-translation mofications, including phosphorylation, polyubiquitiantiaon and sumoylation[124]. Phosphorylated IRAK1 disassociates from MyD88, and induces TRAF6 activation. The polyubiquitination results in the degradation of IRAK1 through the 26S proteasome. Sumoylated IRAK1 translocates into the nucleus and induces Stat3 activation [124]. Regarding IRAK2, which is a serine and threonine kinase and has the similar functional structure with IRAK1, we assume that IRAK2 might undergo certain kinds of post-translation modifications as well. IRAK2 may undergo auto-phosphorylation or become phosphorylated by other kinases like IRAK4; these events would both cause phosphorylations on serine or threonine residues in IRAK2. However, this was not well characterized within current research. Therefore the subsequent experiments aimed to discover the pattern of post-translational modifications of IRAK2.

Two-dimensional (2D) gel electrophoresis is a method which is generally applied for separating the whole cellular proteome according to two properties of proteins: the isoelectric point (IP) and the molecular weight. The first separation was conducted according to the different IPs .Then the second separation was performed by another property (molecular weight) in a direction 90 degree based on the first separation. Additionally, 2D gel electrophoresis also detects the post-translation modifications within one protein if conducted with immunoblot. 2D gel electrophoresis was chosen as a substantial and cost-effective method to get an overview of post-translation modifications in IRAK2. Phosphorylations would usually shift the isoelectric point of the protein to a more acidic pH range. Moreover, ubiquitination would usually increase the protein weight. Thus different spots will be observed in the blot if the protein undergoes phosphorylation or ubiquitination.

In order to enhance the detection of post-translational modifications in IRAK2, HA-tagged IRAK2 WT was over-expressed into HEK293T cells. The HA-tagged IRAK2 were isolated and enriched by HA-immuno-precipitation. Then the enriched protein samples were used for 2D separation pH (3-10), followed by immunoblot

analysis. Additionally, the cells were transfected with an empty vector control to probe for unspecific spots (Figure 3.5 C).

HA-tagged IRAK2 is predicted to have an isoelectric point of around 5.4. According to the literature, phosphorylation would usually shift the isoelectric point of the protein to a more acidic pH value. The 2D gel showed that IRAK2 mainly had isoelectric species in the range from pH 3 to 7 (Figure 3.5 A and D Box1). A few spots were even found to be beyond this range, but appear to be unspecific, since these are also detected in the empty vector control. Some studies indicate that IRAK family members are special serine/threonine kinase with additional tyrosine phosphorylation activity [121]. In order to analyse if IRAK2 has phosphorylations on tyrosine residues, the immunoblots were probed with a α-phospho-tyrosine antibody. However, no specific spots were detected (data not shown).

In order to further elucidate if IRAK2 modifications in the pH range of 3-7 are due to auto-phosphorylation, 2D separations were conducted with the HA-tagged IRAK2 mutant K237A. It is well known that the K237A mutation abolishes IRAK2 kinase functions[137]. In comparison to WT IRAK2, K237A resulted in marginal but not strong differences in the modification profile (Figure 3.5 A, B and D Box1). However, the high amount of acidic isoelectric species complicates a decent separation of the individual spots. The isoelectric focusing was conducted for the pH range of 3-10. Alternatively, separations of overexpressed HA tagged IRAK2 on a pH range from 4-7 would help in further distinguishing the profile of mutant K273A from WT IRAK2. Based on the results shown here, one may conclude that the large amount of IRAK2 WT modifications in the pH range 3-7 are not due to auto-phosphorylation events, and may rather imply that IRAK2 becomes modified by upstream kinases like IRAK4.

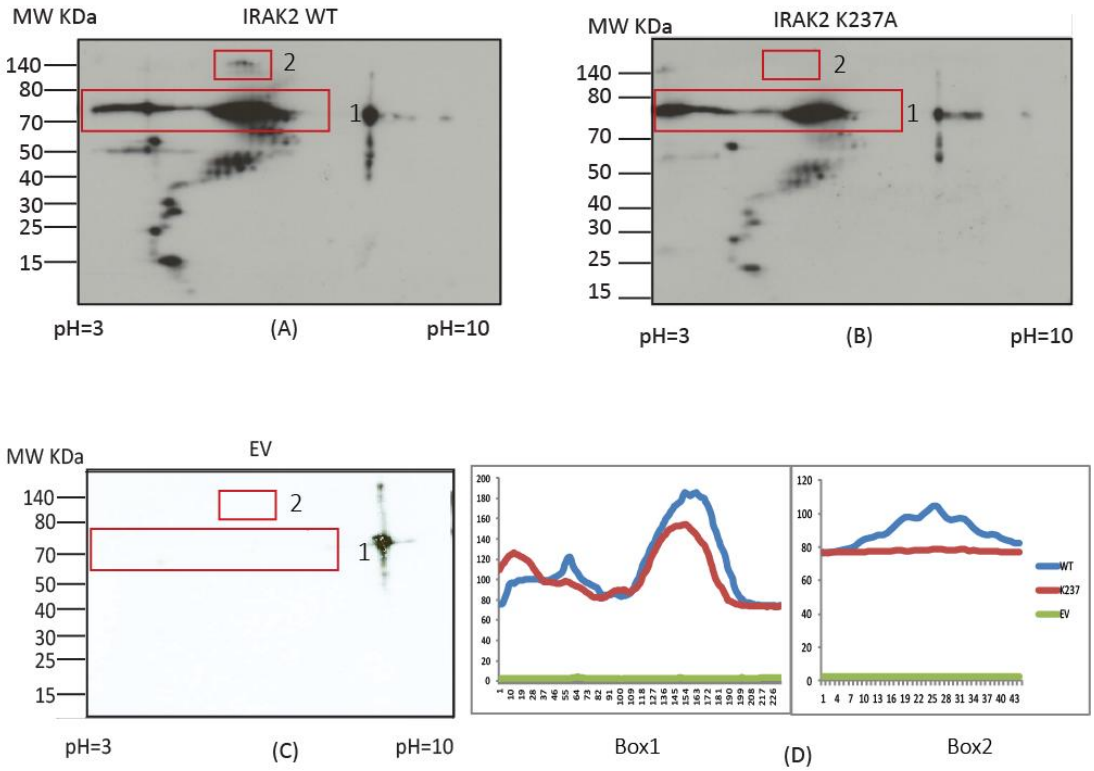

Figure 3.5 Profile of post-translational modifications in IRAK2. 4 µg of expression plasmids encoding for HA-tagged IRAK2 WT, K237A or EV were transfected into HEK293T cells. After 48 hours, immunoprecipitations were done with an α-HA mouse monoclonal antibody. The samples were subjected to IEF, followed by SDS-PAGE on a 4-12% Bis-Tris gel. The immunoblot analysis was then done with a α-HA rabbit monoclonal antibody showing the profile for (A) IRAK2-HA WT, (B) IRAK2-HA K273A and (C) the EV control. (D) Comparison of the profile of EV (green), WT IRAK2 HA (blue) and mutant K237A (red) quantified by Image J and the figure D was generated by Microsoft excel. Box1 shows the shift of phostphorylation sites. Box2 shows the shift of MW.

The calculated molecular weight of IRAK2 HA is 70 kDa. Several separated spots were identified for IRAK2 WT, ranging from 15 kDa to 140 kDa. It seems as if IRAK2 undergoes a certain amount of degradation. The experiments were repeated at least 3 times, showing the same result. Of note, the immunoblot analysis probed for an HA-tag that was fused to the C-terminal part of IRAK2. Any sort of degradation may therefore first occur at the N-terminal end of IRAK2. In order to further investigate this notion, the same experiment was performed for N-terminal HA-tagged IRAK2. In turn, the degraded spots disappeared (data not shown). This may be indicative for a mechanism in which IRAK2 degradation is starting at the N-terminal end of the protein.

Moreover, as one of the most well-known post-translational modifications, ubiquitination shifts the molecular weight of a protein to higher positions. IRAK2 WT does show several separated spots in the higher molecular weight range of approximately 140kDa (Figure 3.5 A and D Box2). Compared to IRAK2 WT, the

mutant K237A showed a similar pattern of separation. However, IRAK2 K237A did not show any higher molecular weight modifications, implicating an absence of poly-ubiquitination (Figure 3.5 B and D Box2).

Having noticed that IRAK2 is likely to be phosphorylated, to further elucidate post-translational modifications and identity precise phosphorylation sites in IRAK2, a HEK293 cell line stably expressing strep-HA-tagged IRAK2 was generated. The expression of IRAK2 was induced by adding tetracycline. IRAK2 was purified by strep tag, followed by phospho enrichment (Done by Daniel Backes, a master student supervised by me). Then the enriched samples were used for mass spectrometry analysis which was conducted at the proteomics centre of Tübingen University, Germany. Most of IRAK2-specific peptide fragments were identified. Only one phosphorylation site was found in IRAK2 and the position is determined at serine 144 which locates in the proline, serine and threonine rich region in IRAK2. (Figure 3.6) Possibly due to the low yield, some additionally phosphorylation sites were not detected. Higher amount purification of IRAK2 was performed which confirmed that the phosphorylation site is S144.

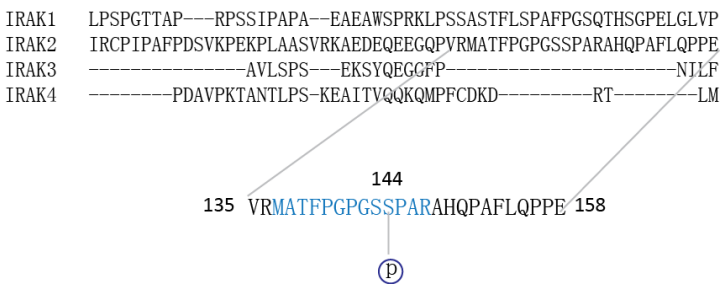

Figure 3.6 The novel phosphorylation site in IRAK2

In conclusion, in agreement with 2D gel analysis, one novel phosphorylation site was found in IRAK2. However, there might be additional phosphorylation sites and other post-translational modifications in IRAK2. To address those questions, higher quantities of purified IRAK2 are required. Future studies will also have to investigate the properties of S144 phosphorylation in signal transduction.

3.1.6 Discussion

3.1.6.1 IRAK2 plays a central role in the TLR signalling pathway

First, it is known that IRAK2 plays a role in the production of pro-inflammatory cytokines up on multiple TLR ligands stimulations [137]. So far, IRAK2 functions were mainly elucidated by applying TLR-ligands as stimuli on IRAK2 deficient macrophages or reconstituted macrophages. Similarly, this thesis investigated the functional properties of IRAK2 in a murine cell system of reconstituted IRAK2 macrophages. It revealed that the agonists of TLR2, TLR4 and TLR7 induced a high amount of TNF-α production in a IRAK2 dependent manner. This is consistent with the fact that IRAK2 deficient macrophages had decreased TNF-α production which was observed in primary IRAK2 deficient macrophages upon stimulation with MALP-2, LPS and R848[137, 140]. Moreover, reduced TNF-α production was detected in human PBMCs which were knocked down IRAK2 and were stimulated with TLR4 and TLR7 agonists [193].

However, in this thesis the reconstituted IRAK2 macrophages did not elevate TNF-α production upon activation of TLR9 agonist. This result stands in contrast to the published data in which IRAK2 deficient mice are displayed to be resistant to TLR9-mediated septic shock[137]. Moreover, in the same study, the IRAK2 deficient peritoneal macrophages demonstrated decreased IL-6 and TNF-α production upon CpG stimulation. Therefore, it rules out that the discrepancy may be caused by differences in different cell types, but may rather human IRAK2 have different specificity.

Although IRAK2 did not impact on TLR3-induced production of pro-inflammatory cytokines in murine macrophages, it is shown to be critical for polyI:C induced NF-κB activation in a HEK293T cell system that stably expressed TLR3[88]. Furthermore, in the same study co-immunoprecipitation assays showed that over-expression TLR3 in HEK293T cells results in an interaction with IRAK2 even in the absence of polyI:C stimulation [88]. Moreover, the poxvirus protein A52 specifically targets IRAK2 to inhibit NF-κB activation in all TLRs signalling pathways, which was functionally characterized in both to human and mouse cells [88, 197]. Altogether, these results therefore endorse the fact that IRAK2 is involved in TLR3 induced NF-κB activation. The discrepancy of IRAK2 function in TLR3 might be causes by different cell type and different species.

Conclusively, the data in this work and the current literature emphasize IRAK2 as a central component in the TLR signalling pathway. The functional studies reveal differences with regard to their response to various TLR ligands. This may be affected by the cell type, which was used for experiments (see Table 3.1). IRAK2 is expressed universally and may therefore play distinct roles in different cell types. When considering all the experimental set ups, IRAK2 is found to be involved in the signalling pathways elicited by all the receptors of the TLR family, to integrate the signal in response to various pathogenic compounds. The impact on the respective pathway may alter between different cell types.

Table 3.1 reported the dependency of IRAK2 in various TLRs

Cell Type	Receptors	Readout	IRAK2 dependency
IRAK2 deficient macrophages	TLR2,4,7,8,9	TNF-α	partially decreased [137, 140]
	TLR2,	IL-6	absolutely diminished [137]
	TLR4,7,8, 9	IL-6	partially decreased [137, 140]
	TLR4, TLR7	chemokines	partially decreased [140]
Human PBMC	TLR4, TLR7	IL-8	decreased to basal level[193]
silenced IRAK2	TLR4, TLR7	TNF-α	decreased to basal level[193]
HEK293T silenced IRAK2	TLR3, 4, 7	NF-κB activation	partially decreased [88]
Human IRAK2 reconstituted mouse *Irak*2 KO macrophages (our experiments)	TLR2,4,7	TNF-α (protein level)	Strongly enhanced
	TLR2,4,7	IL-6,IL-1β (mRNA level)	Strongly enhanced

Second, another controversial point is the functional involvement of IRAK2 at late time of NF-κB/MAP kinase activation as proposed by Kawagoe et al, 2008. IRAK2 deficient macrophages were generated and challenged with the TLR2 ligand MALP-2. In comparison to WT macrophages, experiments on IRAK2 deficient cells revealed that the activation of the NF-κB and MAP kinase signalling pathway was only impacted at later time points. This led to the notion that IRAK1 may be involved at early time points of the signalling pathway, whereas IRAK2 is essential in sustaining the response at late time points [137].

However, the IRAK2 deficient macrophages were generated by Xiaoxia Li (Department of Immunology, Lerner Research Institute, Cleveland clinic, USA), 30 minutes of LPS stimulation showed an impaired activation of MAP kinases-mediated

signalling [140]. Moreover, silencing the expression of IRAK2 in human PBMCs reduced the phosphorylation of p38 upon already after 20minutes of stimulation with TLR4/TLR7 agonists [193]. Also this thesis showed IRAK2 reconstituted macrophages enhanced the Pam2CSK4, LPS and R848-mediated NF-κB and MAP kinases activation within 30minutes. Interestingly, macrophages derived from the wild-derived mouse strain MOLF/Ei presented a quicker and higher production of IL-6 and phosphorylation of p105 and p38 in comparison to the classical inbred strain C57BL/6J [198]. The reason for these differences is a deletion in the promoter of the inhibitor *Irak*2c splice isoform found in MOLF/Ei mice, which leads to an increased ratio of pro to anti-inflammatory IRAK2 isoforms. Conclusively, the hypothesis that IRAK2 may only be involved in later time points requires further investigation. The initial observation of Kawagoe stands in contrast to the subsequent findings published in the literature (See Table 3.2). The current work rather agrees with the view that IRAK2 mediates an immediate response to TLR agonists

Table 3.2 The dependency of IRAK2 at early or later time point of NF-κB activation

Cell Type	Signalling Pathway	Early time Point	Later Time Point/ after 4hours
Macrophages	NF-κB	Yes[140]	Yes[137]
	MAP kinase	Yes[140]	Yes[137]
	IRF3	N.D.	No[137]
Human PBMC	NF-κB	Yes[193]	N.D.
	MAP kinase	Yes[193]	N.D.
HEK293T	NF-κB	N.D.	Yes[88]
	MAP kinase	N.D.	Yes[88]
	IRF3	N.D.	Yes[88]
IRAK2 reconstituted macrophages (our experiments)	NF-κB	Yes	Yes
	MAP kinase	Yes	N.D.
	IRF3	N.D.	N.D.

3.1.6.2 What are the functions of human IRAK2 vs mouse IRAK2

As known, only one splice variant of IRAK2 exist in humans while four splice variants of IRAK2 are in mice, namely *Irak*2a, *Irak*2b, *Irak*2c and *Irak*2d. Moreover, IRAK2 function in mice appears to be more complicated: *Irak*2a and *Irak*2b are positive regulators of the NF-κB activation, while *Irak*2c and *Irak*2d are negative regulators

[139]. Additionally, *Irak*2a, b and d share the same start codon in exon 1, whereas the negative regulator *Irak*2c encompasses its own start codon in exon 4(see section 1.4.2). Therefore, caution is required when using the IRAK2 deficient mice as a research model to draw experimental conclusion on the functions of human IRAK2. Furthermore, the genetic background of the knock mice is needed to be considered in detail. For instance, Kawagoe (Osaka University) generated the *Irak*2 deficient mice by replacing exon 4, 5, and 6 of *Irak*2 with a neomycin-resistance cassette in the embryonic stem cells. This method might abrogate all of the four isoforms of IRAK2. However, the IRAK2 deficient mice that generated by Xiaoxia Li (Department of Immunology, Lerner Research Institute, Cleveland clinic, USA), have replaced 5' regulatory region, exon1, and 2.1kb of intron 1 replaced with a neomycin resistance gene. In this approach, *Irak2*c may still be expressed. It is unclear if endogenous murine *Irack2*c could inhibit human IRAK2 when reconstituting into IRAK2 deficient cells. See figure3.7

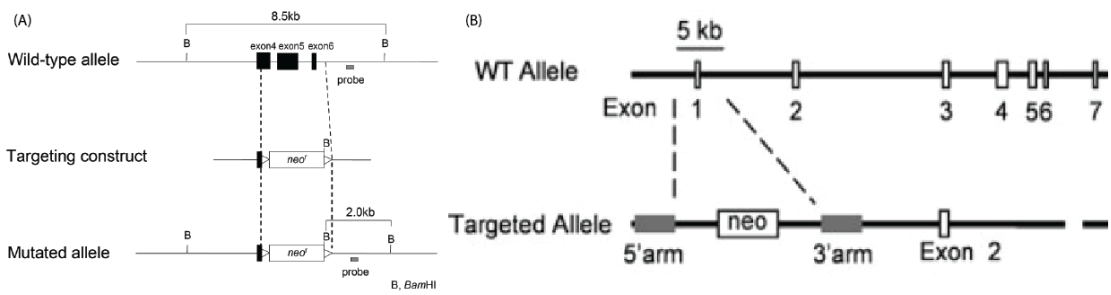

Figure 3.7 Structure of generating IRAK2 deficient mice. (A): the generating way from Kawagoe, replaced exon 4, 5, 6 with a neomycin-resistance cassette (adoptred from Kawagoe *et al.* 2008). (B): the way of Li generated IRAK2 deficient mice, replaced 5' regulatory region, exon1, and 2.1kb of intron 1 with a neomycin resistance gene (adopted from Wan *et al*. 2009).

Moreover, the protein sequence identity of human and mouse IRAK2 is only around 65%. The degree of conservation is high in the known functional domains, such as the DD and the KD (see the section 1.4.2). However, a lot of differences exist in the non-coding region and in the ProST domain of IRAK2. These regions are poorly characterized in IRAK2 and they might cause some differences in the response to pathogens. In order to better understand the functions of human IRAK2, a human cell system may be more adequate for this research purpose, albeit it is more difficult to manipulate. Using siRNA or shRNA techniques may help us to down-regulate IRAK2 protein expression in different cell types and this may help to characterize IRAK2

functions in detail. Alternatively, all from carries with hypo or hyperfunctional IRAK2 alleles could serve as probe to study human IRAK2. See part III.

3.1.6.3 IRAK2 plays an important role in the anti-infection response to *Salmonella typhimurium*

Aforementioned, most IRAK2 functions were elucidated by applying TLR-ligands as stimuli on IRAK2 deficient macrophages or reconstituted macrophages. However, in our living world, many pathogens express agonists of more than one PRR, and the immune system must integrate signalling through multiple PRRs to specify the correct cytokine response [199]. What is the role of IRAK2 when the organism encounters the invasion of a pathogen? No pathogenic infection on reconstituted IRAK KO macrophages was conducted before to analyse for the production of pro-inflammatory cytokines and interferons.

Our experiments showed that the mRNA expression levels of *Il-6* and *Il-1β* were obviously enhanced upon infection with *Salmonella typhimurium*. The mRNA level of *Tnf-α* was enhanced as well but not significantly. As known, *Salmonella typhimurium* is an intracellular parasite of macrophages [200] and has several PAMPs, such as LPS, lipoproteins and flagellin, which are recognized by TLR4, TLR2 and TLR5 respectively [201]. The infection with this pathogen is known to trigger the production of pro-inflammatory cytokines such as IL-1β and IL-6 [201]. Hence, upon infection of *Salmonella*, mRNA expression of *Il-1β* and *Il-6* was observed, which indicated IRAK2 plays a role in regulating *Il-6* and *Il-1β* production in mRNA level at even early time points. This experiment emphasizes the role of IRAK2 as a central regulator downstream of the TLR signalling pathway. Especially when encountering a pathogen like *Salmonella typhimurium*, that express a variety of pathogenic patterns, IRAK2 seems to be indispensable for induction of a pro-inflammatory response, which needs to be verified in infection models.

However, no significant mRNA level of pro-inflammatory cytokines were observed when treating the macrophages with Influenza A. This may be due to the fact that different strains of Influenza A are known to have different specificities in infecting murine macrophages. The strain used in this thesis was the Influenza A PR8. It was shown that strain A/PR/8/34(PR8: H1N1) infects macrophages poorly, while the strain BJ×109 infects macrophages very efficiently [202]. However, PR8 has much stronger

abilities to infect epithelial cells [202], and which may therefore be suitable for investigating the role of IRAK2 in epithelial cells.

This thesis emphasizes future experiments on the involvement of IRAK2 in certain disease models with careful consideration of the species and the cell type that is investigate, as well as the type of pathogen that is used for the study. Regarding the preliminary observation from *Salmonella typhimurium* infections in macrophages, it is worthwhile to further decipher the role of IRAK2 in *Salmonella* infected disease.

3.1.6.4 The role of IRAK2 in addition to the conventional TLR pathway

Surprisingly, reconstituted IRAK2 macrophages recovered for the phosphorylation of Akt (also called Protein kinase B (PKB)) when stimulating with Pam_2CSK_4, LPS and R848. The Akt signalling pathway is mainly involved in cell proliferation, metabolism, migration and metastasis. Akt becomes activated by sequential phosphorylating at T308 and S473 which were accomplished by PDK1 (Phosphoinositide-dependent kinase 1) and mTORC2 respectively [203].

Studies on PI3-K knockout mice support the idea that PI-3K negatively regulates TLR activation [204]. Moreover, primary macrophages derived from mice with conditional knockout of PDK1 in myeloid lineages have elevated levels of TNF-α and IL-6 mRNA. While immediate TLR4 activation is intact, these PDK1 deficient macrophages revealed prolonged ubiquitination of TRAF6 upon LPS stimulation. This indicated that PDK-1 may have a negative feedback on NF-κB activation in macrophages [205]. Interestingly, alignment of TIR domains of TLR2, 3, and 5 reveals that they all endowed a conserved YXXM which presents a potential PI3-K binding site [206]. Furthermore, it has been discovered that the TIR containing adaptor protein Mal directly interacts with PI3-K subunit p85α which drives phosphorylation of Akt [207]. Moreover, it was shown that Mal could further interact with IRAK2 upon TLR4 stimulation [208], which might indicate IRAK2 also involved into the Akt signalling pathway. Strikingly, it was shown that PI3-K directly bound to the cytoplasmic domain of IL-1R (Try-E-X-Met) upon phosphorylation of Try479 in IRAK1 [209]. However, A similar experiment was done in IRAK1 deficient cells which revealed that IRAK1 is required for PI-3K/Akt signalling [196]. Intriguingly, co-immunoprecipitation assay demonstrated that IRAK2 interacts with Akt, which depends on the phosphorylation status of Akt. The activation of Akt decreases the binding of IRAK2 quickly. Moreover,

a kinase defective mutant of Akt impairs IRAK2 and MyD88 dependent NF-κB activation which indicates that Akt may facilitate IRAK2 induced NF-κB activation [210]. It therefore seems as if activated PI3-K regulates TLR signalling in both positive and negative ways. PI3-K is believed to be a gate-keeper to control excessive innate immune responses and is proposed as an early event in TLR signalling[206].

Furthermore, a global, quantitative and kinetic analysis of the phophoproteome of primary macrophages was conducted to investigate kinase cascades triggered by the TLR4 ligand LPS on system level. The macrophages were cultured in stable isotope labelled amino acids (SILAC) to conduct a phosphopeptide enrichment and high-resolution mass spectrometry analysis. Surprisingly, the mTOR, ATM/ATR and Akt kinases were highlighted as hotspots in other signalling modules. In order to confirm that the activation of Akt is related to TLR4 activation, the pharmacological inhibitor of Akt was used which led to the elevated of pro-inflammatory cytokines. The inhibition of Akt for 15mins strongly enhanced the production of *Tnf* and CD69 [211].

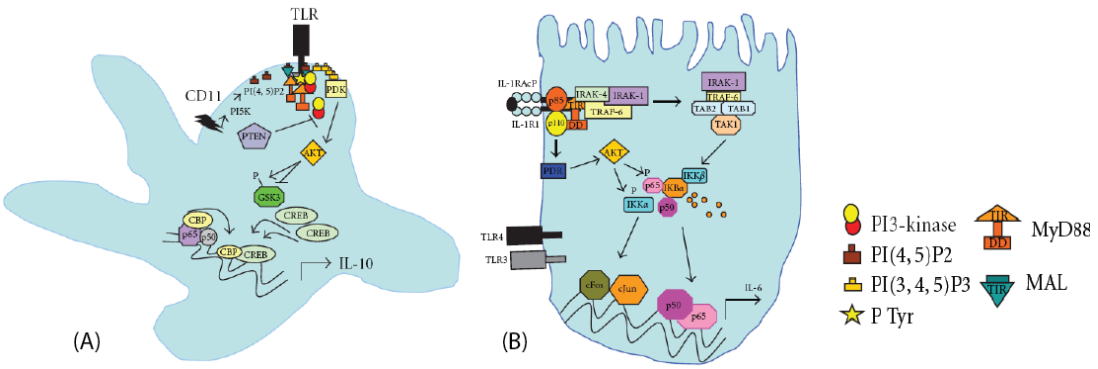

Figure3.8 Akt pathway control of pro and anti-inflammatory cytokines production. (a) The negative feedback of pro-inflammatory cytokines production. (b) the positive feedback of pro-inflammatory cytokines production (modificated from Cahill, Rogers et al. 2011).

Although our experiment only showed that reconstituted IRAK2 macrophages activated the phosphorylation of Akt which need to be further investigate on different cell type, especially in certain kind of cancer primary cells. Collectively, the data in this thesis and the recent literature described here strongly implicate a crosstalk between the TLR and the PI3-K signalling pathway.

It is conceivable that when the organism faces inflammation, it should concordantly rhythm of the whole body. It is known that chronic inflammation might be a factor of

cancer. Meanwhile, the Akt signalling pathway determines cell proliferation, survival and growth. Interestingly, the deregulation of the Akt pathway is associated with a variety of human cancers, and several mouse models with activated Akt pathway support the role of Akt in cancer development. However, the precise relationship between the kinase of the IRAK family in TLRs signalling pathway and Akt is not clear yet. Further investigations are required to precisely determine the physiological setting and the molecular components that link these two pathways.

3.1.6.5 What kind of post-translation modifications occur in IRAK2?

It had been established that IRAK1 and IRAK4 were the only active kinases from the IRAK family; this was assumed because they both share an enzymatically important an aspartate residue in the kinase domain. IRAK4 was thought to undergo autophosphorylation upon the activation of TLRs. Then IRAK4 phosphorylates the residues T209 and T387 in IRAK1, which leads to full enzymatic acticity. Subsequently, several autophosphorylations occur in ProST domain of IRAK1. In comparison to IRAK1, IRAK2 has an asparagine residue instead of an aspartate residue. Nonetheless, IRAK2 has been shown to possess a kinase activity which is dependent on the residue K237 and found to be essential for the activation of TLR-NF-κB pathway [137, 212]. Whether IRAK2 is autophosphorylated or phosphorylated by other IRAKs had not been known yet.

Our 2D-PAGE displayed several isoelectric species with a molecular weight of around 70 kDa and additionally, some high molecular weight species were identified. These observations imply that phosphorylations and ubiquitinations occur in IRAK2.

It was assumed that phosphorylation on IRAK2 are accomplished by IRAK1[141]. However, the phosphorylation of IRAK2 even occurred in IRAK1$^{-/Y}$ macrophages upon MALP-2 stimulation. On the other hand, IRAK4 deficiency was shown abrogated the phosphorylation of IRAK2, which suggested that activated IRAK4 phosphorylated IRAK2, thereby inducing its enzymatic activity[137]. These results support the view that a certain amount of modifications in IRAK2 are accomplished by upstream kinases.

However, the kinase activity of IRAK2 is essential for activation of NF-κB. It was shown that co-expression of IRAK1 and IRAK2 leads to the phosphorylation of IRAK2,

whereas co-expression of IRAK1 with an IRAK2 construct that carries the KK237AA mutation in the ATP-binding pocket failed to induce IRAK2 phosphorylation [141]. Additionally, reconstitution of IRAK2-/- macrophages with wild type IRAK2 restored the phosphorylation of IRAK2 in response to MALP-2, albeit reconstitution with K237A IRAK2 did not, which indicates that the kinase activity of IRAK2 is required for IRAK2 phorsphorylation[137]. These studies therefore indicated the possibility that the kinase activity of IRAK2 is required for inducing autophosphorylation in IRAK2. The results of the 2D-PAGE analysis showed a few, but not pronounced changes in the acidic range of the gel, when comparing the IRAK2 WT and kinase-deficient mutant. This may therefore suggest that the modifications observed here are not induced by auto-catalytic activities, but by IRAK4 or other, so far unknown.

So far, no evidence existed that described any specific phosphorylation sites in IRAK2. One novel phosphorylation site S144 was found via mass spectrometry. This is the first study revealing a phosphorylation site in IRAK2. This phosphorylation site is located in the ProST domain of IRAK2, which is the linker region between DD and KD and is a domain rich in proline, serine and threonine residues. However, the precise functions of ProST domain are not clear yet. It was shown that the proline/serine/threonine rich region in the class II transactivator (CIITA) is very important for transcriptional activities by mediating protein-protein interactions [213, 214]. Interestingly, it was revealed that phosphorylation in ProST domain of IRAK1 is very important to induce IRAK1 conformation change and disassociate from Myddosome complex and further inducing the downstream activation [215]. Similarly, IRAK2 needs to disassociate from the Myddosome complex as well, whether the phosphorylation of S144 encompasses the same function which needs to be further delineate.

3.2 Part II: IRAK2 plays a central role in the Myddosome formation

3.2.1 Introduction

The aim of part II was to elucidate the extent role of IRAK2 in the Myddsome structure. The crystal structure of Myddosome was proposed by Lin *et al* in 2010. The multimeric macrocomplex consists of death domains of 6×Myd88-4×IRAK4-4×IRAK2 death domain complex. The stable crystal structure of Myddosome was generated by recombinant expression and purification of the proteins in *Escherichia coli*. Therefore, three questions arise: (1) Can the Myddosome be formed in the mammalian cells? (2) Can the FL protein also form multimers? (3) Can IRAK2 further interact with IRAK1 or IRAK3 (the two remaining members in the IRAK family, whose positions in the Myddosome are unclear). This part will address these three questions and will focus on the central role of IRAK2 in mediating the interaction between MyD88 and IRAK family members

3.2.2 Results

3.2.2.1 Gene expression and signalling properties of IRAK2 construct.

As described in section 2.1.9.3, the human IRAK2 (Imagenes: IRCMP5012D0935D) gene encode plasmid was inserted into pENTRI1A backbone. Furthermore, IRAK2 (full length) FL or DD was introduced into pcDNA5/FRT/TO-based expression plasmid to add an N- or C-terminal Strep-HA-tag (T. Bürckstümmer, CeMM, Vienna). Additionally, to compare with IRAK1or IRAK3, the FL or DD version of IRAK1 and IRAK3 were introduced into pcDNA5/FRT/TO-based expression plasmid as well.

The gene expression of IRAK1, 2 and 3 FL and DD HA-tagged proteins was detected by overexpressing each construct in the mammalian cell line HEK293T. After 48 hours of transfection, cell lysates were applied for SDS-PAGE and immunoblot analysis. . Figure3.1 confirmed that all of the genes, which are encoded by the plasmids, are expressed. The FL IRAK1, 2 and 3 proteins have a similar molecular weight of around 80kDa, 70 kDa and 70 kDa, respectively, while the DD of IRAK1, 2 and 3 have a molecular weight of around 12 kDa.

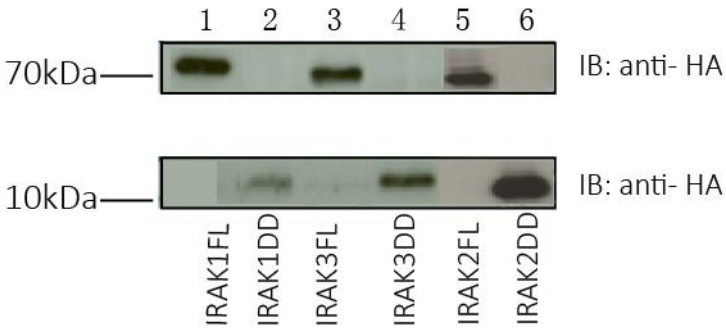

Figure 3.9 IRAK1,2,3 FL and DD genes expression. Cell lysate from overexpressed IRAK1FL (lane 1), IRAK1DD (lane2), IRAK3FL (lane 3), IRAK3DD (lane4), IRAK2FL (lane5), IRAK2DD (lane6) are shown in the immunoblot. Proteins were separated on a 10% Tris-Glycine gel and immunobloted with an anti-HA antibody (rabbit). IRAK2FL and DD expression assays were done separately.

Results showed that the expression level of the IRAK1DD was relatively low. In order to confirm the expression of IRAK1DD, SDS-PAGE was conducted for cell debris of the lysate as well. It demonstrated that the protein is expressed and mostly retained in the cellular debris after lysing the cells under the buffer conditions described in buffer1 (Data was not shown). Thus, several different lysis buffers (lysis buffer2 and passive lysis buffer from Promega) were applied to improve the extraction of the IRAK1DD. However, the applied lysis buffers were still not efficient enough to extract all of the IRAK1DD proteins. Nonetheless, the IRAK1DD protein expression level was comparable to IRAK1FL.

Since the gene expression level of all proteins constructs seemed to comparable, subsequent studies on the signaling properties of each constructs were conducted in HEK293T as well. Although HEK293T cells do not express all TLRs, all necessary proteins downstream of the receptor are expressed, which facilitates the over-expression analysis of IRAKs in terms of NF-κB activation[141]. In order to analyze the signaling features of each construct, three different doses for each plasmid were transfected into the HEK293T cell line. Additionally, 100ng of NF-κB reporter and 10ng of the Renilla-luciferase encoding plasmids were transfected into each condition to perform a dual luciferase assay (Figure 3.10 A, B, C.) The measurement showed that IRAK1, 2, 3 FL encoding plasmids all induced NF-κB activation in a dose-dependent manner. The IRAK1 and IRAK3 DD induced NF-κB activation as well, IRAK1DD induced NF-κB activation at the same extent as FL IRAK1. On the other hand, IRAK3DD only slightly reduced the activation of NF-κB in comparison to its FL protein. Interestingly, IRAK2 DD could not trigger any NF-κB activation.

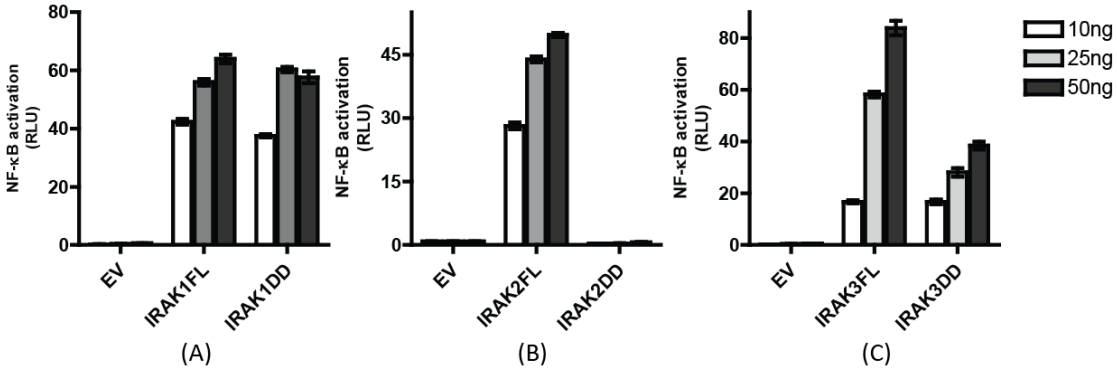

Figure 3.10 NF-κB signaling assay of IRAK1, 2, 3 FL and DD constructs. HEK293TT cells were transfected with 100ng NF-κB-luciferase reporter plasmids and 10ng renilla Renilla luciferase expressing control plasmids and the indicated amounts of the IRAK encoding plasmids,. (a) IRAK1 FL and DD; (b) IRAK2 FL and DD; (c) IRAK3 FL and DD.

Thus, it indicates that the kinase activity of IRAK2 plays an essential role of NF-κB activation.The Myddosome structure suggests that IRAK2 can stably interact with IRAK4. Therefore, LUMIER experiments were carried out to test whether the Myddosome structure exists in mammalian cell lines.

3.2.2.2 IRAK2DD strongly interacts with IRAKs DD

IRAK1, 2, 3 and 4 FLs and DDs were introduced individually into a pT-Rex-Dest30-based expression plasmid containing N- or C-terminal Renilla or Protein A tags via LR reaction (see section 2.1.10.4). The genes expression levels were confirmed as well (Data was not shown). Since Renilla- and ProteinA-tags are relatively high molecular weight fusion tags, the protein function may be affected by these fusion constructs. Therefore those constructs were transfected into HEK293T cells to perform an NF-κB dual lucifease assay as well. The measurement revealed that these fusion proteins were able to induce signaling which was similar to the results obtained from HA tagged proteins (Data was not shown).

Given the fact that the IRAK2DD directly forms the third layer of the Myddosome by interacting with the IRAK4DD, the position of IRAK1 and IRAK3 are not known yest. Then the LUMIER method was applied to test for the interaction of the IRAK2DD with the other IRAKs DDs (IRAK1 and IRAK3) in mammalian cells. The advantage of the LUMIER is that it can provide relative interaction intensities for proteins of interest in a high throughput assay, which co-immunoprecipitation assay hardly can quantify the relative interaction intensity. In order to get an overview of IRAK2 DD interactions with MyD88DD and other IRAKs DDs, 20ng of Renilla-tagged IRAK2DD encoding

plasmids were co-transfected with 20ng of Protein-A tagged MyD88DD or other IRAK DD encoding plasmids into HEK293T cells. The transcription factor subunits Jun and Fos are known to strongly interact with each other [190]. Additionally, generally a luminescence intensity ratio above 3 is considered a significant interaction [190].

Thus, Protein-A tagged Jun and Renilla-tagged Fos were co-transfected and served as a positive control for a protein interaction. In order to confirm that the LUMIER system can assess the interaction properties of the IRAK2DD, IRAK4DD interactions with MyD88DD and IRAK2DD were carried out (Figure 3.11A). Figure 3.11.A shows that IRAK4DD strongly interacted with MyD88DD and IRAK2DD, implying that a Myddosome structure can be formed in HEK293T cells, and that the LUMIER method is reliable at capturing Myddosome interactions. It is described that IRAK4DD possesses very specific affinities. Regarding the possibility that IRAK2 may associate with MyD88 or Mal, IRAKsDDs interactions with MyD88DD were performed as well. Figure 3.11 B shows that only MyD88 has a stronger interaction with IRAK4DD. These results therefore demonstrate that the formation of the Myddosome structure is of highly sequential and specific nature.

Subsequently, the interaction between IRAK4DD and IRAK1DD/IRAK3DD was analysed. However, the interaction intensity between IRK4DD and IRAK1DD or IRAK3DD is very weak. Since IRAK2DD forms the third layer of Myddosome, subsequent analyses addressed the questions if it can recruit other IRAKs as well. The results reveal that IRAK2DD strongly interacted with IRAK4DD. Figure 3.11 C Additionally, IRAK2DD interacted with IRAK1DD, IRAK3 DD and its own DD. Clearly, IRAK2DD can mediate interaction between Myddosome and IRAK1DDs or IRAK3DDs. This means that IRAK1 and IRAK3 were no be directly recruited to IRAK4 but via IRAK2 (see section 3.2.2.4). However, the DD of IRAKs naturally does not solely exist in the cytosol. Furthermore, experiments on the full-length proteins were conducted since kinase domains of IRAKs affect signalling (see figure 3.10 and [155]) and may interfere with the interactions of IRAK2 and the other IRAKs.

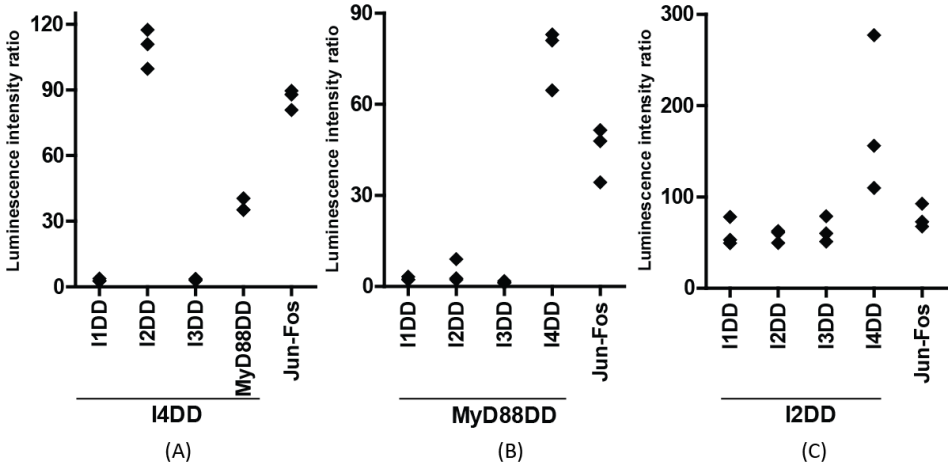

Figure 3.11 IRAK2DD interacts with all IRAKs DDs. (a) IRAK4D(I4DD) interactions with rest IRAKs DDs; Renilla tagged IRAK4DD co-transfected with protein A tagged IRAK1DD(I1DD) or IRAK2DD(I2DD) or IRAK3DD(I3DD) or MyD88DD into HEK293T cells; (b) MyD88DD interactions with IRAKs DDs; protein tagged MyD88 co-transfected with Renilla-tagged I1DD or I2DD or I3DD or I4DD into HEK293TT cells; (c) I2DD interactions with IRAKs DDs. Renilla tagged I2DD co-transfected with protein-A tagged I1DD or I2DD or I3DD or I4DD into HEK293TT cells. ILUMIER luciferase readout was performed at the TECAN infinity200 48 hours post-transfection. Jun-proteinA and Fos-renilla served as positive controls.

3.2.2.3 Full length IRAK2 interacts with Full length IRAKs.

According to the procedure described above, 20ng of Renilla-tagged FL IRAK2 and Protein-A-tagged FL IRAK1, 2, 3, 4 encoding plasmids were individually co-transfected into HEK293T cells. The analysis confirmed that DDs interactions do occur. As shown in Figure 3.12, FL IRAK2 still maintained interaction with FL IRAK1, IRAK2, IRAK3 and IRAK4(Figure 3.12C). IRAK2 had a high affinity to IRAK4. Consistent with the IRAK4 DD interactions, IRAK4 FL preferred to recruit IRAK2 FL and MyD88 FL as well. Figure 3.12 A.

Direct interactions between IRAK2DD and MyD88DD were not detectable when overexpressing the respective protein constructs. In order to investigate if the kinase domain of IRAK2 may be important for associations with MyD88FL, MyD88FL interactions with FL IRAKs were carried out. As expected, MyD88FL interacted with IRAK4FL. However, no interactions between IRAK2FL and MyD88FL were detected. Figure3.12 B.

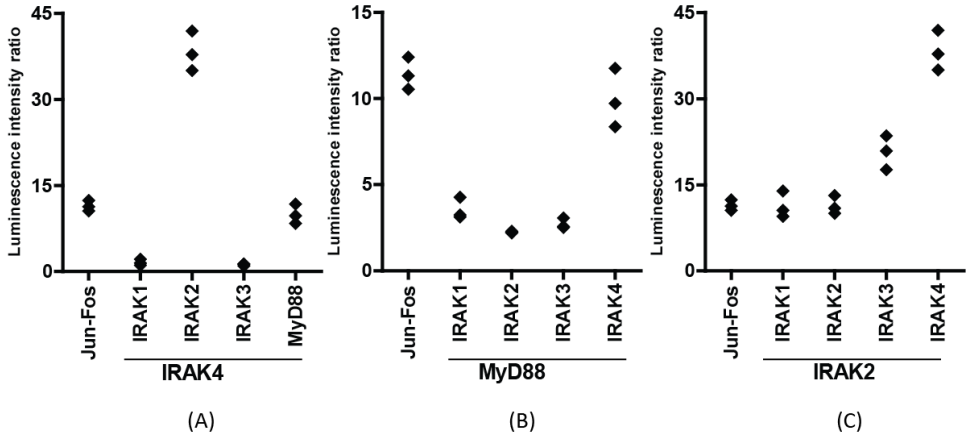

Figure3.12 IRAK2FL interacts with all FL of IRAKs. (a) HEK293T cells were transfected with Renilla tagged IRAK4 either with protein A tagged IRAK1, 2, 3, or MyD88 respectively. (b) HEK293T cells were transfected with each Renilla tagged IRAKs together with Protein A tagged MyD88. (c) HEK293T cells were transfected with Renilla tagged IRAK2 with protein A tagged each IRAKs individually. The luminescence was measured in fluro star.

All in all, compared with the DDs interaction, the interaction affinities of the full-length proteins were lower. Interestingly, IRAK2 interaction with MAL was reported before (1997). However, no interaction was found in this experiment. (Data was not shown.).

3.2.2.4 IRAK2 bridges the interaction between IRAK4 and IRAK1/3.

It was shown that IRAK4 is the first kinase that is recruited to MyD88 upon activation of TLRs. IRAK4 subsequently undergoes autophosphorylation and phosphorylates IRAK1. It was assumed that IRAK4 interacts with IRAK1. However, Lin et al. failed to generate the crystal structure of MyD88-IRAK4-IRAK1 DDs complex[86] and the measurement of LUMIER did not show any interaction between IRAK4 and IRAK1 or IRAK3. Due to the fact that IRAK2 interacts with each IRAK, it is conceivable that IRAK2 may bridge the interaction between IRAK4 and IRAK1 or IRAK3. Therefore, 20ng of HA-tagged IRAK2 (or HA-tagged IRAK3 served as a control, HA tag cannot be purified by the IgG Dynabeads M-280 (Invitrogen) with either 20ng of Protein-A tagged IRAK1 or IRAK3, and 20ng of Renilla-tagged IRAK4 were co-transfected into HEK293T cells. After 48hours, the relative interaction intensity was measured and the results revealed that IRAK2 increases the interaction between IRAK4 and IRAK1 or IRAK3 (Figure 3.13). In order to investigate whether the kinase domain of IRAK2 is crucial to mediate the interactions between IRAK4 and IRAK1/IRAK3, FL and DD constructs of IRAK2 (control IRAK3) were tested separately. Figure 3.13 A shows that the presence of the IRAK2 DD helped in enhancing the interaction between IRAK4DD and IRAK1DD and IRAK3DD; the increase of interaction efficiency is 2-3 fold higher

than in the empty vector control. This was similarly observed when adding FL IRAK2 instead of IRAK2DD (see Figure 3.13 B). However, when analysing the situation for the FL IRAK proteins, IRAK2FL only induced a marginal increase of an interaction between FL IRAK4 and IRAK1/IRAK3 (Fig 3.13 C). The effects were specifically observed when co-transfecting IRAK2, but were not detectable when applying IRAK3 DD or FL constructs. In conclusion, the assays support the notion that IRAK2 plays a central role in mediating the interaction between IRAKs

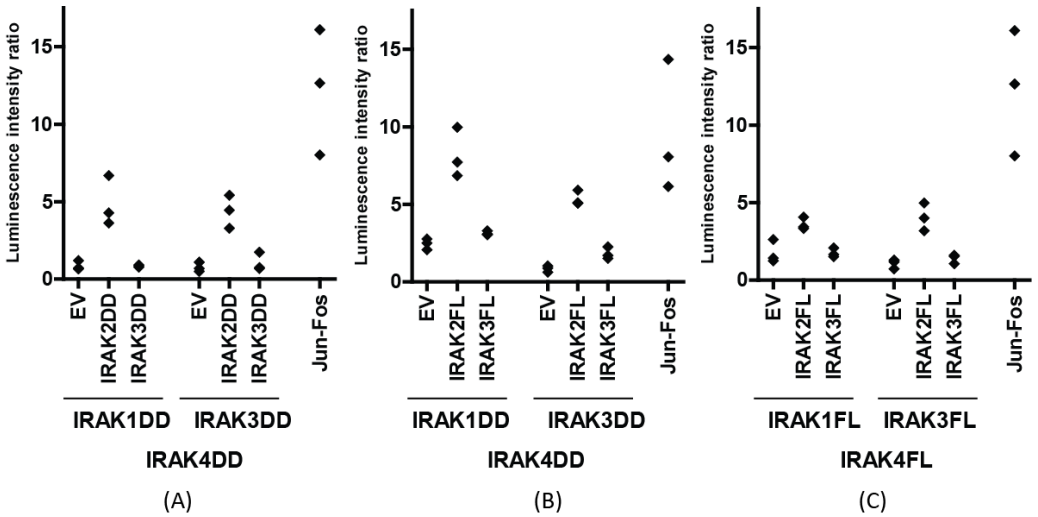

Figure3.13: IRAK2 bridges the interaction between IRAK4 and IRAK1/IRAK3. (a,b)Renilla-tagged IRAK4DD and ProteinA tagged IRAK1DD or IRAK3DD were transfected into HEK293T cells. (a)Additionally, HA-tagged IRAK2DD or IRAK3DD or empty vector was co-transfected for each condition. (b)HA-tagged IRAKFL or IRAK3FL or empty vector was co-transfected for each condition. (c) Renilla-tagged IRAK4FL and ProteinA tagged IRAK1FL or IRAK3FL were transfected into HEK293T cells. Additionally, HA-tagged IRAKFL or IRAK3FL or empty vector was co-transfected for each condition.

3.2.3 Discussion

3.2.3.1 IRAK2 plays a central role in the Myddosome formation.

The crystal structure of the Myddosome consists of six MyD88, four IRAK4 and four IRAK2DDs which form a left-handed helix. It revealed that the assembly of this complex follows a hierarchical and sequential process, in which the sequential recruitment of each DD increases the stability of the complex [154, 216]. Complementarity in charge and shape between the bottom and top surfaces of the DDs are involved in the formation of this multimeric assembly. For example, the bottom surface of IRAK4 matches well with the top surface of MyD88 both in charge and shape complementarity. IRAK2 is only recruited to the complex when IRAK4 is present because the bottom surface of IRAK2 matches well with the top surface of IRAK4 both in charge and shape complementarity[86]. See figure 3.14.

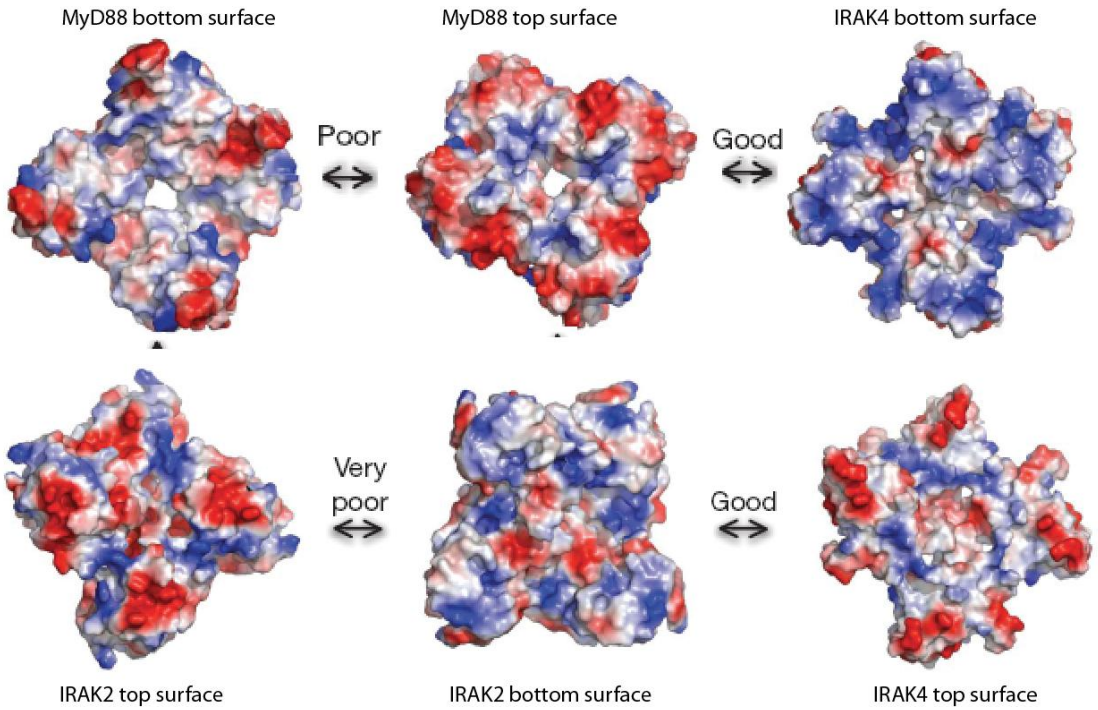

Figure 3.14 The charge and shape complementarity in MyD88-IRAK4-IRAK2 interaction.
(Modified from Lin, Lo *et al*. 2010)

The results of this thesis show that MyD88 preferentially interacted with IRAK4, and that within the IRAK family, IRAK2 preferentially interacted with IRAK4. In comparison to all the other DD containing proteins involved in the TLR pathway, IRAK4 preferentially interacted with IRAK2 and MyD88. This phenomenon was observed for the DD proteins alone, but also in the context of the FL proteins.These

results are consistent with the formation of Myddosome structure and endorse the view that upon signal activation MyD88 first recruits IRAK4, which then interacts with IRAK2.

According to the current literature, IRAK2 and IRAK1 are described to fulfil redundant roles. It is believed that IRAK1 would similarly function downstream of IRAK4 and that it may be incorporated into the Myddosome in a way as it has been demonstrated for IRAK2 (see figure introduction). This notion is emphasized by finding in which IRAK1 lost its phosphorylation in the IRAK4 deficient macrophages [137]. Furthermore, IRAK1 was shown to be phosphorylated in the absence of IRAK2 [137]. However, in our LUMIER experiments no interaction was observed between IRAK4 and IRAK1. Opposed to the current view, this data implies that the formation of the Myddosome is of a different nature in the case of IRAK1. Co-immunoprecipitatetion assays showed that IRAK1 interacted with IRAK4 in macrophages upon stimulation of MALP-2 for 1.5 hours but this could be indirect. In the same study, IRAK2 is demonstrated to maintain the interaction with IRAK4 for 8 hours[137]. Furthermore, it is known that IRAK1 associated with Pin1 which is a prolyl isomerise and catalyses the conversion of specific phosphorylated motifs. The activity of Pin1 leads to a conformation change in the phosphorylated form of IRAK1, which might be an important step for IRAK1 to disassociate from the Myddosome complex [215]. However, any association between IRAK2 and Pin1 was not found which might explain why IRAK2 keeps its association within the Myddosome complex [215]. All of these data indicated that the interaction between IRAK1 and IRAK4 is of transient nature, while the interaction between IRAK2 and IRAK4 is stable.

The functional impact of IRAK3 on the signalling and the formation of the Myddosome remain also controversial. IRAK3 was initially described to be a negative regulator in TLR-NF-κB signalling pathway [87]. It was shown that IL-12 and IL-8 production were increased in the IRAK3 deficient macrophages upon stimulation of multiple TLR ligands. However, the overexpression study in HEK293 cells showed that IRAK3 is capable of inducing a NF-κB dependent response. This was observed for the FL protein but also in the context of the IRAK3DD proteins. The functions discrepancy of IRAK3 might due to cell type and different species.

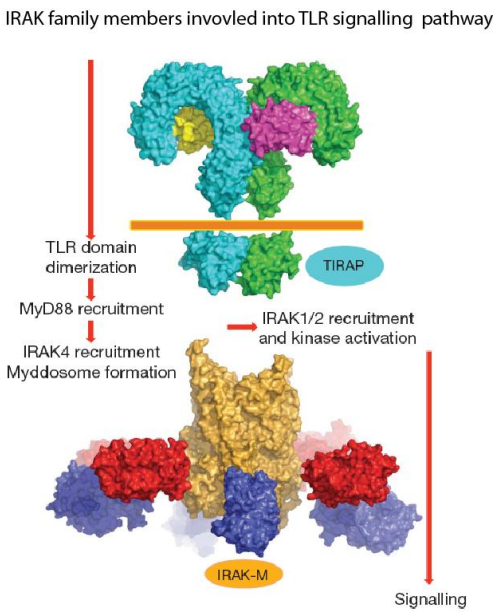

Figure 3.15 IRAK family involved in the TLR signalling pathway.(modified from Lin, Lo *et al*. 2010) A model of the TLR signalling complex that recruits the MyD88–IRAK4–IRAK2 complex with proteins drawn to scale. TLRs, cyan and green (PDB code 3FXI for the extracellular domain of TLR4 and PDB code 2J67 for the TIR domain of TLR10). MD2, yellow and magenta (PDB code 3FXI incomplex TLR4). Orange, MyD88–IRAK4–IRAK2complex. Red, IRAK4 kinase domain (PDB code2NRU). Blue, IRAK2 kinase domain using that of IRAK4.

Regarding the Myddosome formation, it is assumed that IRAK3 prevented IRAK2 or IRAK1 from dissociating from the Myddosome complex by interacting with IRAK2[86]. In fact, interactions between IRAK4 and IRAK3 were not detected in the LUMIER experiment, whereas IRAK3 strongly interacted with IRAK2. Interestingly, the over-expression of IRAK2 enhanced the interaction between IRAK4 and IRAK1/IRAK3. This data supports the view that the whole signalling multimeric complex of Myddosome is stabilized and strongly dependent on IRAK2. It is conceivable that the observed signalling functions of IRAK3 are an artefact of the overexpression of IRAK3, and may be severely reduced when having the other IRAK members expressed at similar levels. Unfortunately, the NF-κB activation was not measured for conditions in which IRAKs were co-expressed with IRAK3. This kind of study might provide us more information about the functions of IRAK3 and may further clarify the supposedly negative regulation of IRAK3. Additionally, it is conceivable that using siRNA of IRAK3 knockdown endogenous IRAK3 of different cell type might help us understand the role of IRAK3.

In conclusion, these studies imply that the Myddosome formation is subjected to highly regulatory mechanisms that determine assembly and disassembly of the complex.

Further experimental studies on the cellular formation of the Myddosome are required to identify the molecular factors and physiological conditions that determine the IRAK1 or IRAK2 dependent Myddosome formation and the involvement of IRAK3.

3.2.3.2 The IRAK FL proteins adjust for the proper interaction intensity within the Myddosome.

The study on the DD and FL interactions showed that DD interactions are generally stronger than FL interactions. However, in comparison to the DD proteins, the FL proteins are capable of inducing stronger transduction of the signalling pathway [155]. For example, the relative interaction intensity of the MyD88DD-MyD88DD homodimer is shown to be 10 fold higher than for MyD88FL proteins. However, the same amount of MyD88FL induced stronger activation of NF-κB than MyD88DD alone [155].This tendency was similarly observed in the experiments of this thesis. Interactions of IRAK4DD with IRAK2DD reached a value of up to 150, whereas IRAK4FL and IRAK2 FL interactions only reached a value of 40. Similarly, IRAK2 interactions with IRAK3 were strongly increased for the DD proteins alone. However, the highest induction of the signalling pathway was only observed for IRAK2 FL and IRAK3 FL, respectively. The Myddosome structure should represent a flexible multimer formation, which allows for the quick assembly and disassembly of the complex. The DD domains alone can hold up a strong association of the complex, whereas the respective kinase domains disrupt this rigid assembly to thus allow for the engagement of activated IRAKs with further downstream signalling components. The downstream actions involve for instance the interaction of IRAK2 with TRAF6. Additionally, Myddosome interactions are shown to bring the kinase domains and the ProST domains of IRAKs into proximity for phosphorylation and activation of IRAKs [86, 119]. The phosphorylation in the ProST domain of IRAK1 then facilitates its dissociation from MyD88 to further induce IRF7 activation [215].

In agreement with the study of Lin et al (2010), these data support the model in which Myddosome is a sequential assembly of DD containing proteins. In an unstimulated case MyD88 and IRAK proteins may be randomly found in the cell (Figure 3.16 A). As soon as stimulations occur, MyD88 first activates IRAK4 (Figure 3.16 B), this in turn leads to strong complex formation with IRAK2. Then IRAK2 recruited IRAK1 and mediated the interaction between IRAK1 and IRAK4, which results in the phosphorylation of IRAK1 (Figure3.16 C). Finally, modified IRAK1disassociates from

the Myddosome complex and induces the subsequent activation. However, the modified IRAK2 still keeps the interaction with IRAK4 to recruit TRAF6 and further induce the ubiquitination of TRAF6 (Figure3.16 D). Ultimately, the ubiquitinationed TRAF6 further interacted with downstream partner and induce NF-κB activation. When IRAK2 cannot be full modified, although it can still interact with TRAF6, the ubiquitination level of TRAF6 will be impaired (See section 3.3.2.5).

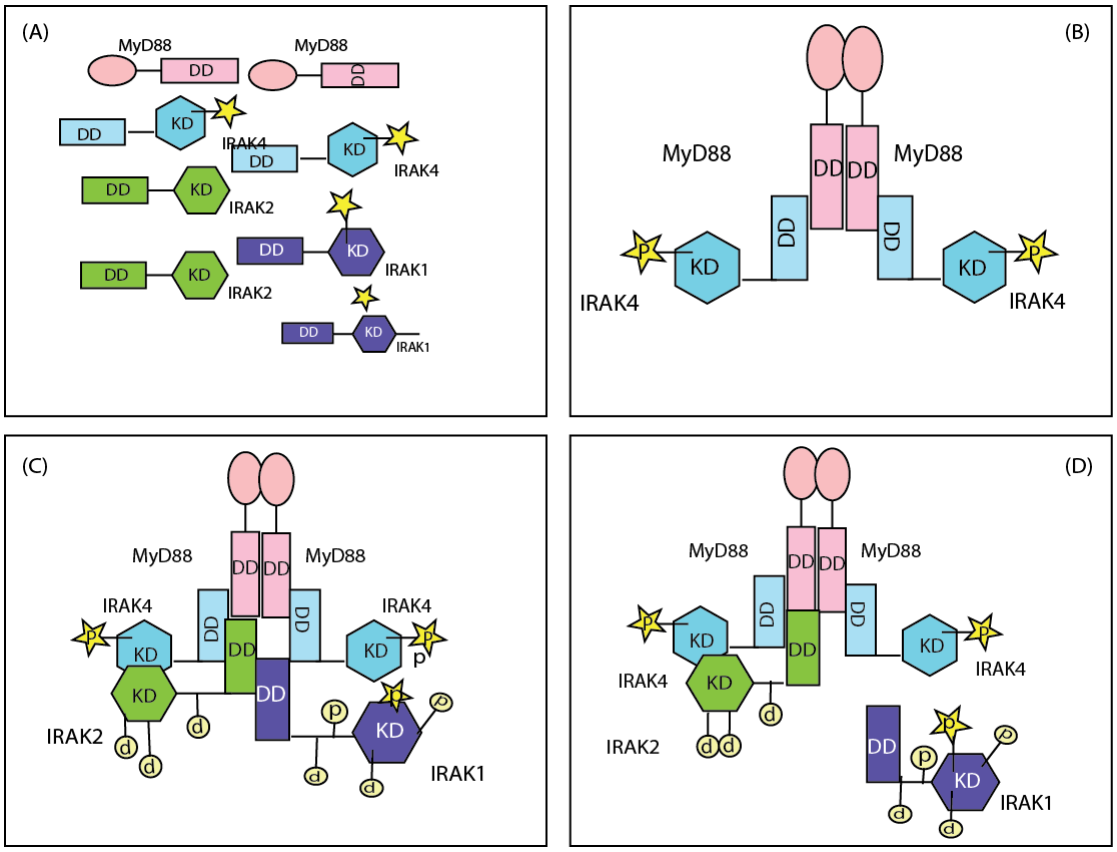

Figure 3.16 The schematic diagram of sequential assembly and disassembly in Myddosome structure. (A) The situation in the absence of any stimulation (B) the homo/oligomerisation of MyD88 recruits IRAK4 to the assembly by homotypic DD interaction. This induces IRAK4 autophosporylation. (C) Autophosphorylated IRAK4 recruits IRAK2 by homotypic DD interactions to induce phosphorylation of IRAK2. Then phosphorylated IRAK2 recruited IRAK1 and bridge the interaction between IRAK4 and IRAK1. Finally, IRAK1 was fully activated by IRAK4. (D) Activated IRAK1 dissociate from the complex to transduce further downstream signaling. However, IRAK2 still keeps the interaction with IRAK4 and further recruited TRAF6 and induce the ubiquitination level of TRAF6. Yellow star indicates the autophosphorylation site. P indicates phosphorylation.

3.3 Part III: IRAK2 genetic variants R214G and L392V reduced TLR dependent signalling

3.3.1 Introduction

The aim of this part was to identify functionally interesting the non-synonymous single nucleotide polymorphisms (SNPs) of IRAK1, 2, and 3, by using a HEK based NF-κB screening assay. The mechanistic differences between WT and SNPs were investigated by biochemical and molecular biological methods. Meanwhile, the functionally interesting SNPs were genotyped in clinically relevant epidemiological studies to discover the causal relationship between the SNP and certain kinds of diseases. According to at least one of the following three criteria, SNPs were chosen for further epidemiological and functional studies: 1) The SNP should occur in the human population with a verified frequency of at least>0.0005; 2) The SNP should be non-synonymous (i.e. affected amino acid) and occur within a functional domain of IRAK. 3) The affected amino acid should have a certain degree of conservation within the IRAK family. Thus, 3, 12 and 5 SNPs were selected for the research on IRAK1, IRAK2 and IRAK3 respectively. The information on the IRAK SNPs was acquired from the NCBI SNP database in the year 2009 (See figure 3.17 and Table 3.3). Two SNPs of IRAK2 need to be further specified: R498G (rs7513222) was initially listed with a frequency of 0.08 in the NCBI SNP database, but it was recently removed for an unknown reason; no frequency is reported for L78M (rs11709928), but the degree of conservation is very high among the IRAKs family members. Thus, both SNPs were still chosen for the study. See figure 3.17

Additionally, IRAK4 was well investigated and the structure of IRAK4 was published. Hence, the SNPs of IRAK4 were not included into our study.

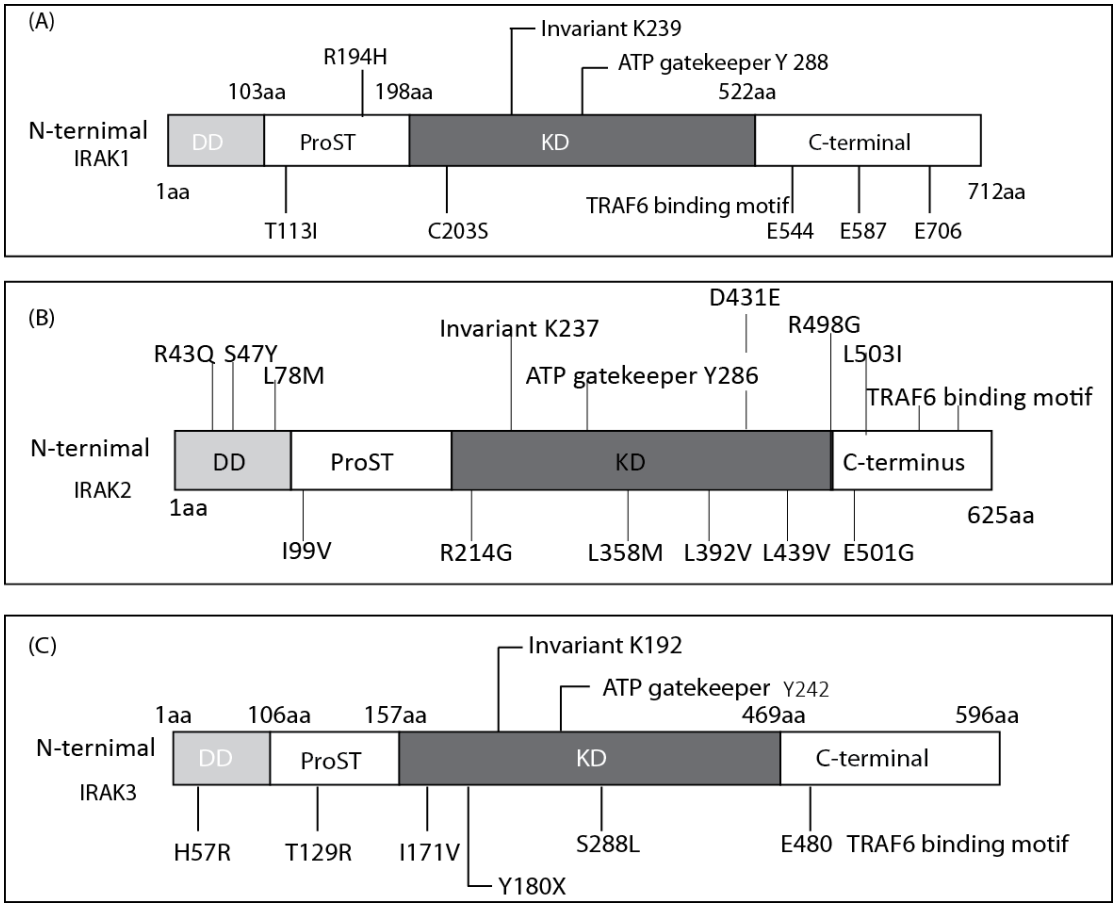

Figure 3.17 SNPs in human IRAK1, IRAK2 and IRAK3. (a) Three SNPs of IRAK1 were studied, T113I and R194H are located in the ProST domain (*white box*) and C203S is located in the kinase domain (*black box*). (b) Twelve SNPs of IRAK2 were analysed: R43Q, S47Y and L78M are located in the death domain (*gray box*); I99V is located in the ProST domain (*white box*); R214G, L358M, L392V, D431E and L439V are located in the kinase domain (*black box*); R498G, E501G and L503I are located in the C-terminal TRAF6 binding domain (*white box*).(c) Five SNPs of IRAK3 were analysed, H57R is located in the death domain(*gray box*); T129R is located in the ProST domain (*white box*), I171V and Y180X are located in the kinase domain(*black box*). Additionally, the invariant lysine, the ATP gatekeeper tyrosine and the TRAF6 binding motif are indicated in each IRAK protein.

To date, no comprehensive studies were conducted to elucidate how the mechanism of genetic variants in IRAK1, 2 and 3 affects the human health. Therefore, molecular studies were first performed for selected SNPs in IRAK1, 2 and 3. Furthermore, an epidemiological analysis was carried out for the functionally relevant SNPs to then identify the causal relationship between genetic variants and certain diseases.

Table 3.3 Frequency information of selected non-synonymous SNPs in humanIRAK2. The SNPs information was derived from the NCBI SNP database. The SNPs were discovered in the Halotype Map (HapMap) project which focused on an Asian and European population and in an Exome sequencing project (ESP) cohort study which focused on the American population.

Amino acid change	rs Number	Exon position	Codon change	Location in protein structure	3D	MAF	Source	Population	Evidence
T113I	rs11465829	3	A**C**C ⇒ A**T**C	ProST	No	0.0012	IIPGA-WEISS-MARTINEZ	African American/European	n/a
R194H	rs11465830	5	CGC ⇒ CAC	ProST	No	0.0115	ESP_cohort populations	American	n/a
C203S	rs10127175	6	TGT ⇒ **A**GT	ProST	No	0.0157	HapMap/ESP_cohort populations	European/ Asian/American	Yes
R43Q	rs34945585	2	C**G**G ⇒ C**A**G	DD	Yes	0.0005	ESP_cohort populations	American	n/a
S47Y	rs11465864	2	T**C**C ⇒ T**A**C	DD	Yes	0.0101	HapMap/ESP_cohort populations	European/ Asian/American	n/a
L78M	rs11709928	2	**C**TG ⇒ **A**TG	DD	Yes		n/a	n/a	n/a
I99V	rs55898544	3	**A**TC ⇒ **G**TC	ProST	Yes	0.011	ESP_cohort populations	American	n/a
R214G	rs35060588	5	**C**GC ⇒ **G**GC	KD	No	0.0408	ESP_cohort populations	American	n/a
L358M	rs77590560	9	**C**TG ⇒ **A**TG	KD	No	0.0118	ESP_cohort populations	American	n/a
L392V	rs3844283	9	**C**TG ⇒ **G**TG	KD	No	0.3036	HapMap/ESP_cohort populations	European/ Asian/American	n/a
D431E	rs708035	11	GA**T** ⇒ GA**A**	KD	No	0.2115	HapMap	Asian	n/a
L439V	rs11465927	11	**C**TC ⇒ **G**TC	KD	No	0.0156	HapMap/ESP_cohort populations	European/ Asian/American	n/a
R498G	rs75132222	12	G**C**T ⇒G**G**T	C-terminus	No	0.08	ESP_cohort populations	American	n/a
E501G	rs12486661	12	G**A**G ⇒ G**G**G	C-terminus	No	0.0014	ESP_cohort populations	American	n/a
L503I	rs9854688	12	**C**TC ⇒ **A**TC	C-terminus	No	0.0334	HapMap/ESP_cohort populations	European/ Asian/American	n/a
H57R	rs35239505	2	C**A**T ⇒C**G**T	DD	No	0.009	HapMap	Asian/European	n/a
T129R	rs76652915	4	A**C**A ⇒A**G**A	DD	No	0.255	HapMap	Asian/European	n/a
I171V	rs34682166	5	**A**TT ⇒**G**TT	ProST	No	0.191	HapMap	Asian/European	n/a
Y180X	rs76408141	5	TA**C** ⇒TA**A**	KD	No	0.022	HapMap	East Asian CHB+JPT	n/a
S288L	rs35574245	8	T**C**G ⇒T**T**G	KD	No	0.087	HapMap	Asian/European	n/a

3.3.2 Results

3.3.2.1 Functional studies of genetic variants in IRAKs in a HEK293T cell system

As presented in section 2.1.2 and 2.1.10, the selected SNPs of human IRAK1, 2 and 3 were introduced into Gateway-compatible plasmid constructs of IRAK1, 2 and 3 as mutants by site-directed mutagenesis. Therefore, the non-synonymous variants of IRAK proteins are referred to as mutants in this part of results. The IRAK mutants were shuttled into a pcDNA5/FRT/TO-based expression plasmid to add an N- or C-terminal Strep-HA-tag**.**

The gene expression of the IRAK1, 2 and 3 mutants was determined by transfecting the respective plasmid into HEK293T cells. 48 hours post-transfection, cell lysates were applied to SDS-PAGE and immunoblot analysis. In order to control for loading errors, β-tubulin served as a loading control. Additionally, the transfection of the pcDNA5/FRT/TO empty vector served as a negative control. See figure 3.18.

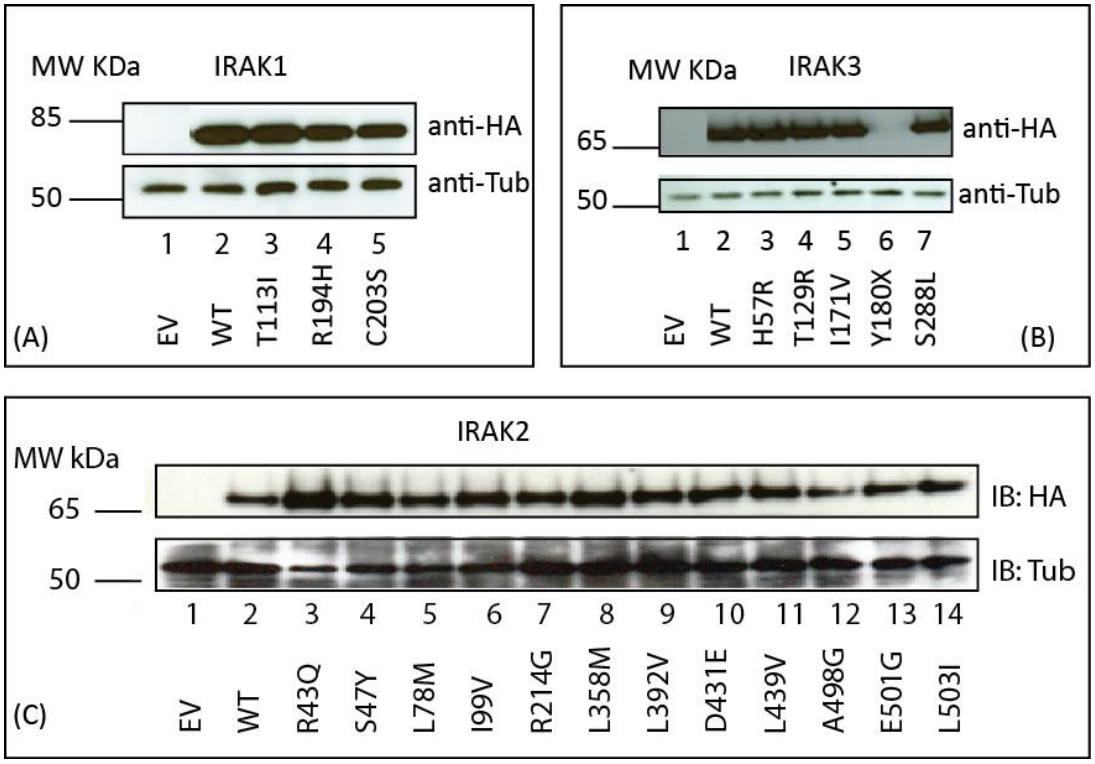

Figure 3.18 Gene expression of IRAK mutants. 100ng of IRAK-encoding plasmids were transfected into HEK293T cells, cell lysates were harvest after 48 hours of transfection and (A) separated on a 4-12% Bis-Tris gradient gel for IRAK1 proteins, or (B) and (C) analysed on a 3-8% Tris-Acetate gel for IRAK3(B), 2(C) mutants, respectively. An immunoblot analysis was performed probing for the HA tag with an anti-HA (rabbit, upper panel) or an anti-tubulin (mouse, lower panel) antibody. The expression analysis was repeated at least twice for each IRAK mutant.

The molecular weight of IRAK1, 2 and 3 is around 80kDa, 70kDa, 70kDa, respectively. The analysis confirmed that the expression of all IRAK mutants is at a similar level with the respective WT protein. One special case of mutant Y180X of IRAK3, no HA tag was observed in immunoblot which indicated the expression of Y180X is correct, because the HA tag is added in the C-terminal of this protein and the mutation X generated a stop codon at Y180 residue. Thus, the C-terminal HA tag cannot be expressed. Then, the subsequent studies then focused on analysing the signalling functions of these mutants in terms of NF-κB activation**.**

3.3.2.2 Seven SNPs in IRAK2 alter NF-κB activation in HEK293T cells

As described in section 3.10, over-expression of IRAK1, 2 and 3 proteins in HEK293T cells can induce NF-κB activation. Hence, an NF-κB dual luciferase assay was carried out to compare the signalling ability of the IRAK mutants with the respective WT protein. Figure 3.3.2 displays a dose-dependent induction of NF-κB activation when transfecting increasing amounts of the IRAK WT plasmids.

In Comparison to IRAK1 WT, T113I, R194H and C203S did not show any significant differences. Therefore, no further studies were carried to analyse the impact of these SNPs in IRAK1 (Figure 3.19 A).

Similarly, most of the IRAK3 mutants did not show any significant differences in comparison to WT protein. However, the nonsense mutants Y180X reduced NF-κB activation dramatically (Figure 3.19 B). Since the stop mutation (X) in Y180 residue generated a truncated version of IRAK3 which lacked the kinase domain and C-terminal TRAF6 binding domain. The putative invariant lysine residue is located at 192. Overexpression the mutation K192A cannot induce any NF-κB activation which indicates the K192 is critical for the kinase activity of IRAK3 (see in Appendix). Thus, the truncated version Y180X is deficient of the invariant lysine which cannot induce NF-κB activation consequently. However, the frequency of Y180X is very low in the human population, and has only been reported in an Asian cohort study. Hence, no further study was performed to investigate on IRAK3 SNPs

Interestingly, compared to IRAK2 WT, R43Q, R214G, L392V, A498G and L503I showed reduced NF-κB activation while S47Y and L78M significantly enhanced NF-κB activation. The remaining SNPs maintained approximately the same amount of

signalling as quantified for IRAK2 WT. Additionally, K237A and E528A mutants were generated and analysed in parallel, as these mutants are known to completely abolished NF-κB activation as observed by Sinead Keating in 2007 (Data was shown in the Appendix). In conclusion, seven out of twelve SNPs in IRAK2 alter NF-κB activation. Hence, further studies focused on these seven SNPs in IRAK2 (see figure 3.19 C).

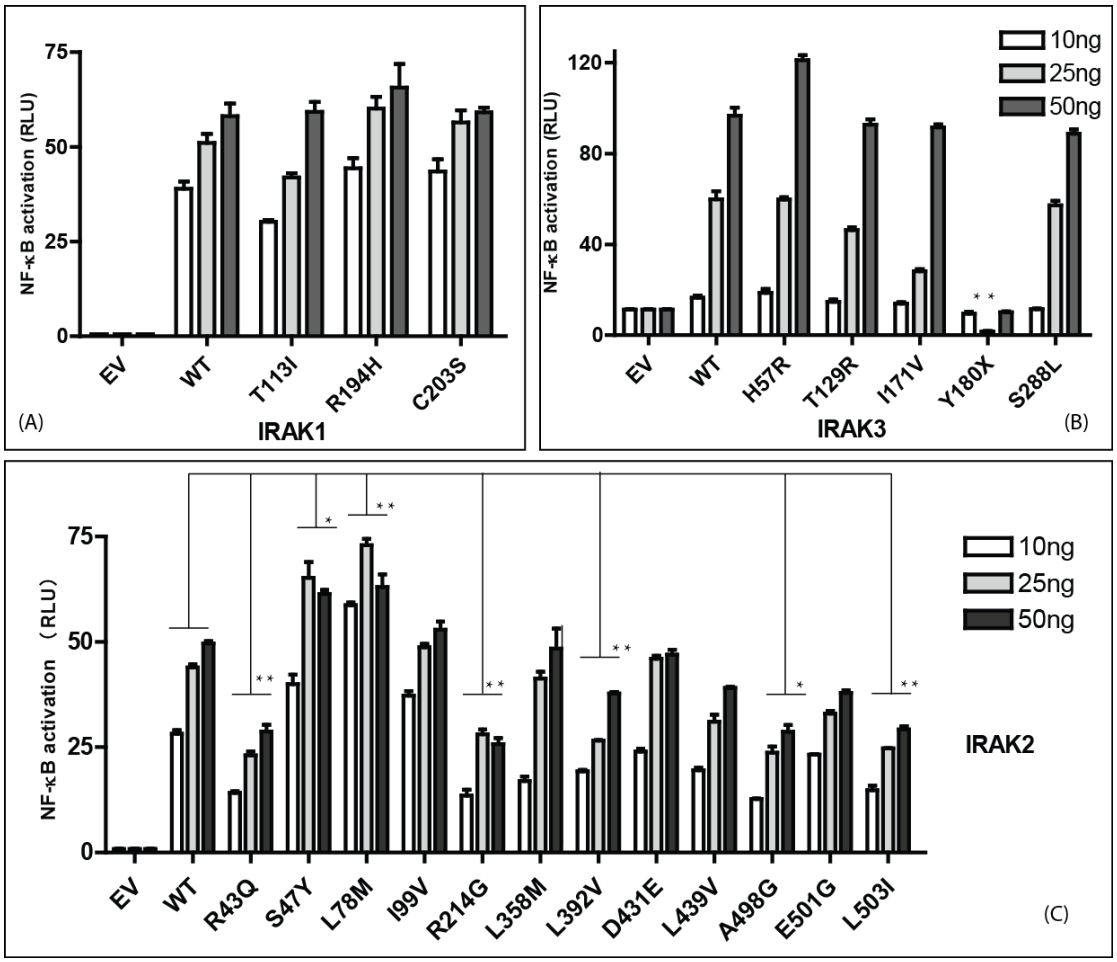

Figure 3.19 NF-κB activation analysis of SNPs in IRAK1, 2 and 3. Different doses of HA-tagged IRAK encoding plasmids, 100ng of theNF-κB firefly reporter plasmids and 10ng of the Renilla reporter plasmids were transfected into HEK293T cells. The total DNA amount was kept constant and by titrating the required amount of the empty vector into the transfection mixture. The NF-κB reporter activity was measured after 48 hours post-transfection. This experiment was repeated at least 3 times. The statistical analysis was performed by a Two-Way ANOVA.

The activation of NF-κB is known to produce several kinds of pro-inflammatory cytokines and chemokines such as TNF-α, IL-6 and IL-8. In turn, the production of the pro-inflammatory cytokine IL-8 was analysed by ELISA (see figure 3.3.3) The results verified that IL-8 was produced in a dose-dependent pattern; based on the increasing amounts of IRAK2 encoding plasmids that were transfected into HEK293T cells, increasing levels of IL-8 were detected in the cell culture supernatant. Meanwhile, IL-8

secretion was reduced for the R43Q, R214G, L392V, R498G and L503I variants, whereas two SNPs, S43Y and L78M, enhanced the IL-8 production compared to WT IRAK2. All together, the relative levels of IL-8 production were consistent with the quantified amount of NF-κB activation. The analysis showed that the R214G and L392V mutants reduced the production IL-8 by 30% and 20% respectively. The R43Q significantly decreased IL-8 production as well. However, due to the low frequency in the population this SNP was not further considered in epidemiological and functional studies. On the one hand, it is interesting to understand the molecular mechanisms that determine a reduced NF-κB activation; on the other hand regarding the frequency distribution of these SNPs, this study also focused on finding carriers of these SNPs for further epidemiological research. R214G an L392V occur frequently in the European population. Therefore, the following molecular and epidemiological studies focused on IRAK2 R214G and L392V. See figure 3.20

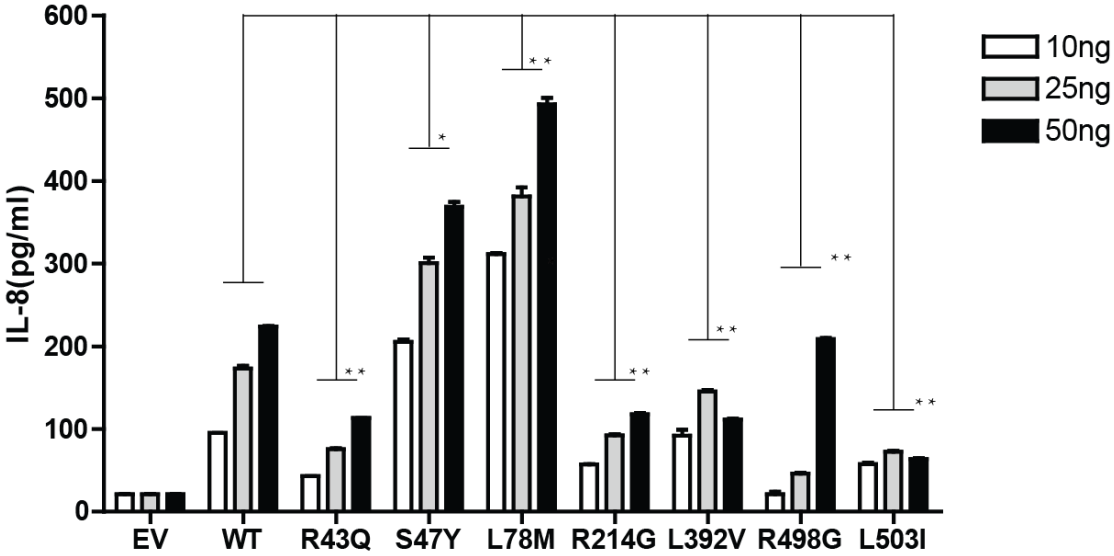

Figure 3.20 R214G and L392V reduced IL-8 production. Different amounts of IRAK2 WT and mutants encoding plasmids were transfected into HEK293T cell respectively. The cell culture supernatant was harvested 48 hours post-transfection and analysed by IL-8 ELISA. The statistical analysis was done by the Two-Way ANOVA.

3.3.2.3 Homology modelling of the IRAK2 kinase domain

R214G and L392V are located in the kinase domain of IRAK2. As aforementioned, the crystal structure of the FL IRAK2 protein is yet unknown. So far, only the crystal structure of the IRAK2 death domain was elucidated by X-ray diffraction [86]. Any structural information on the IRAK2 kinase domain is not provided. However, the crystal structure of the FL IRAK4 was characterized [121]. Thus, adopting the IRAK4

kinase domain structure as a template, Dr. Andriy V. Kubarenko in our lab generated a homology model of the IRAK2 kinase domain structure to gain further insight on the structural properties of the two mutants R214G and L392V (Figure 3.21 A). In this model residue R214 is exposed on the surface and faces the ATP loop region, where the invariant lysine K237 and the gatekeeper Y286 are located. K237 is assumed to act as a critical enzymatic residue in the IRAK2 kinase. R214 coordinates the ATP loop region via hydrogen bonds. The change of arginine to glycine at this position might destroy the stability of this structure (Figure 3.21 B). In contrast to R214, L392 is buried in the proximity of the putative activation loop of IRAK2 (Figure 3.21 C).

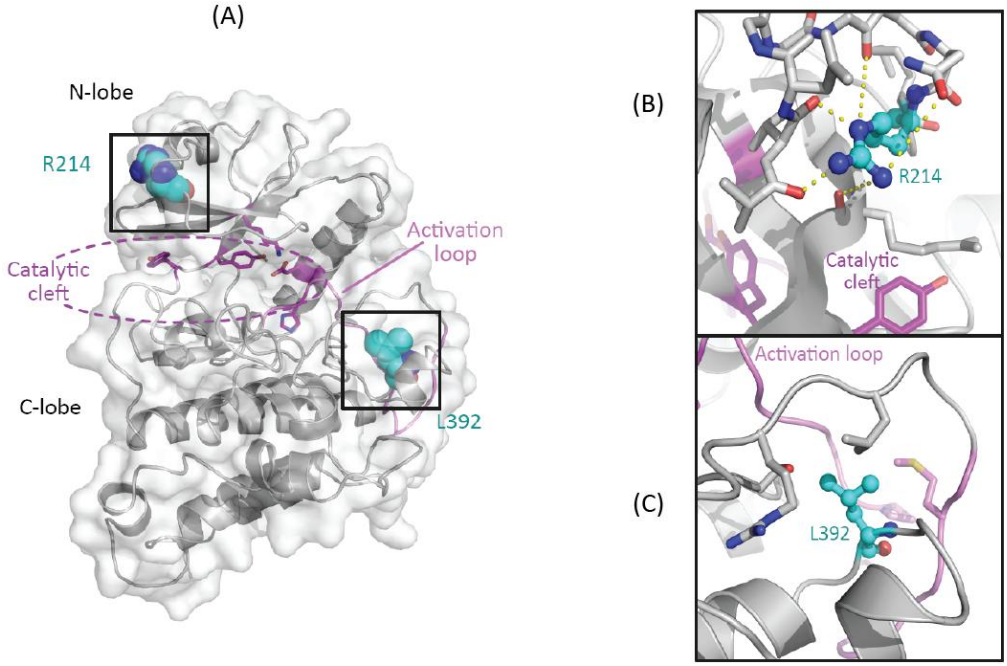

Figure 3.21 3D homology model of the IRAK2 kinase domain. Important areas for the kinase activity are highlighted: the catalytic residues are in magenta, putative activation loop in pink. R214G and L392V are shown in cyan. (B): R214 (G) is exposed on the surface of the catalytic cleft ;(C) L392V is buried in the C-loop adjacent to the putative activation loop. Predicted hydrogen bonds are shown as yellow dashes.

Furthermore, to analysis for the conservation degree of R214 and L392 among different species, protein sequence alignments were performed with IRAK2 from humans, porcine, Macaca mulatta, Bos Taurus, Mus musculus and Rattus norvegicus. Interestingly, the alignment reveals that R214 only exits in human IRAK2, while other species carry a conserved histidine at this position. In contrast to R214, L392 is highly conserved throughout all species, which suggests an important function for this residue in signal transduction. See figure 3.22 (A)

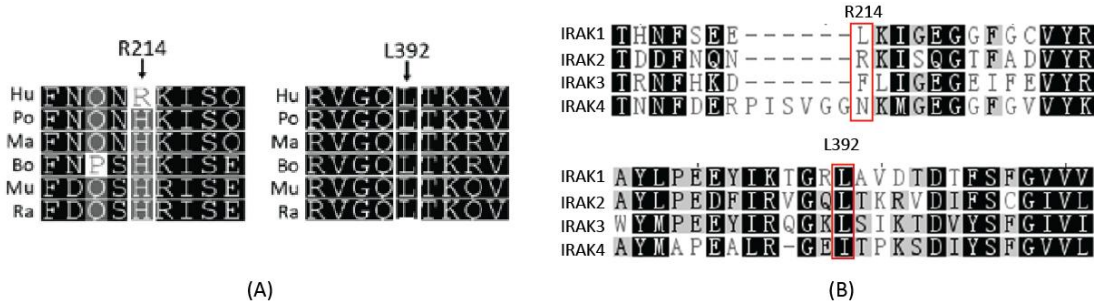

Figure 3.22 Sequence conservation of R214 and L392. (A)Multiple sequences alignments of IRAK2 homologus from different species. Hu(human), Po(porcine), Ma(Macaca Mulatta), Bo(Bos Taurus), Mu(Mus musculus), Ra(Rattus norvegicus.) sequence alignments were conducted by using Clustal W. (B) The protein sequences alignment of IRAK family.

Alignments of IRAK2 with other members (IRAK1, 3 and 4) of the IRAKs family were conducted as well. However, the conservation degree of R214 is very low while L392V keeps the high conservation degree (See figure 3.22B). Conclusively, it is shown that the L392 is highly conserved among IRAKs and species, which indicates that L392V may impact the process of certain kind of diseases which were proven in the part IV.

3.3.2.4 R214G and L392V maintain the interaction with TRAF6

In order to further investigate the reason for the dysfunctional behaviour of the two mutants in IRAK2, R214G and L392V, following experiments concentrated on protein-protein interactions in terms of the NF-κB signalling pathway. The Myddosome structure displayed that IRAK2 builds up the fourth layer by hetero-oligomerization with IRAK4 and homo-oligomerization with itself [86]. According to part II, the LUMIER results revealed that WT IRAK2 can interact with IRAK4 and with itself. Additionally, TRAF6 was proposed as downstream protein of IRAK2 to induce NF-κB activation. Regarding the impaired signalling activity which was most likely caused by changing the interaction intensity with its partner, we applied LUMIER to test the interaction between IRAK2 and itself, IRAK4 or TRAF6 (Figure 3.23) As described before, IRAK2 R214G and L392V were introduced into a pT-Rex-Dest30-based expression plasmid containing N- or C-terminal Renilla or Protein A tags via LR reaction respectively. The expression and signaling ability of these constructs was confirmed by immunoblot and dual luciferase assay.

In the context of Renilla or Protein A fusion constructs, both SNPs remain to be hypofunctional in terms of NF-κB activation (data not shown). However, the LUMIER results revealed that R214G increased the interaction with IRAK2 and IRAK4, while

L392V reduced the interaction with IRAK2 and IRAK4. Figure 3.23 B and C

LUMIER was then applied to assess the interaction of IRAK2 proteins with the downstream signaling partner TRAF6. The quantified interaction intensities were not as strong as the interactions of IRAK2 with IRAK4. However, in repeated experiments R214G showed a decreased the interaction with TRAF6, whereas L392V slightly increased the interaction with TRAF6. In comparision to the interaction intensity between WT IRAK2 and TRAF6, these differences between R214G and L392V were not significant (figure 3.23 D). The LUMIER results therefore indicate that the two mutants, R214G and L392V, keep the interaction with TRAF6. In order to confirm the assumption that the two SNPs still interacted with TRAF6, co-immunoprecipitation were then performed.

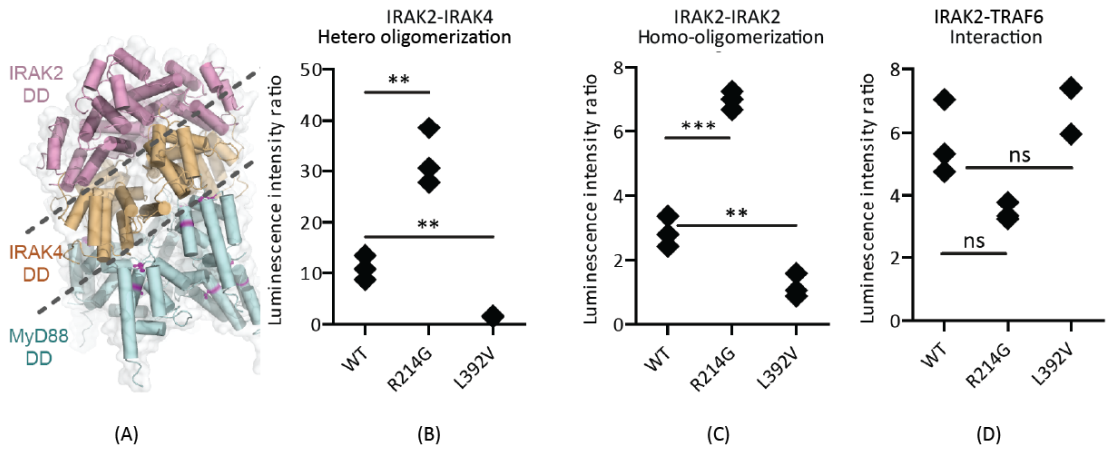

Figure 3.23 LUMIER interaction assay for IRAK2 R214G and L392V. (a) Myddosome structure demonstrates the interactions between IRAK2 and IRAK4 DDs (Adopted from George, Motshwene et al, 2011). (b)-(d): LUMIER experiments: Over-expression of Renilla-tagged IRAK2 WT, R214G or L392V IRAK2 and Protein A tagged IRAK4 WT in HEK293T cells. R214G increased the interaction intensity with IRAK4 whereas L392V reduces the interaction intensity with IRAK4. (c) Over-expression of Renilla-tagged IRAK2WT, R214G or L392V and ProteinA tagged IRAK2 WT into HEK293T cells. R214G increased the interaction intensity whereas L392V reduces the interaction intensity with IRAK2 (d). Over-expression of Renilla-tagged IRAK2 WT, R214G or L392V and ProteinA- tagged TRAF6 WT into HEK293T cells. R214G decreased the interaction intensity whereas L392V slightly increased the interaction intensity with TRAF6. Jun-ProteinA and Fos-Renilla served as positive control as described before. The experiments were repeated at least three times. The statistical analysis was done with a student's t-test.

The interaction between IRAK2 and TRAF6 is considered as an essential step to induce NF-κB activation [88]. To confirm the results obtained from LUMIER, co-immunoprecipitation assays were carried out. Thus, expression constructs encoding for Flag-tagged TRAF6 and HA-tagged IRAK2 were co-transfected into HEK293T cells. Additionally, HA-tagged IRAK2 K237A and IRAK2DD constructs were applied

as controls, because both constructs are known to completely abolish the activation of NF-κB, Moreover, a R214G and L392V double mutants was generated to enhance the individual effect seen by the mutants.

Figure 3.24 shows a strong interaction between IRAK2 WT and TRAF6 (lane7) which implies that over-expression results into the assembly of these proteins in the absence of TLRs stimulation as shown before. However, IRAK2 R214G and L392V were able to maintain the interaction with TRAF6; this was similarly observed for the IRAK2 double mutants (R214G+L392V). These results are therefore consistent with the LUMIER results. Interestingly, the kinase dead IRAK2 muatant K237A still retained the interaction with TRAF6 (lane 11). IRAK2 DD proteins on the other hand did not keep any interaction with TRAF6 (lane 12), indicating that the DD of IRAK2 is not sufficient for the interaction with TRAF6.

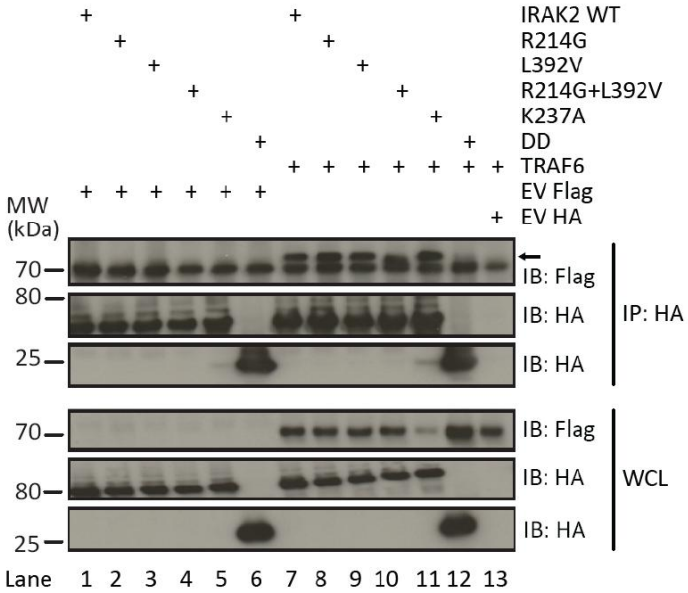

Figure 3.24 R214G and L392V maintain the interaction with TRAF6. Co-transfection of expression plasmids for HA-tagged IRAK2 WT or mutants and Flagged-tagged TRAF6 into HEK293T cells. HA-tagged IRAK2 was precipitated by applying a mouse monoclonal α-HA antibody. Cell lysates and immunoprecipitated samples were separated on a 4-12% Bis-Tris gradient gel and analysed by immunoblot with α-HA and α-Flag rabbit monoclonal antibodies. The experiments were repeated twice.

3.3.2.5 R214G and L392V reduced the ubiquitination level of TRAF6

TRAF6 is an E3 ligase and its ubiquitination was the precondition to induce NF-κB activation. Previous studies revealed that the overexpression of IRAK2 can induce TRAF6 ubiquitination which finally triggers NF-κB activation [88]. As previously

described, IRAK2 possesses two TRAF6 binding motifs [123]. Particularly, the glutamate residue E528 in the first TRAF6 binding motif of IRAK2 is essential to trigger TRAF6 ubiquitination [88]. However, the mutation E528A still maintains interaction with TRAF6 without inducing TRAF6 ubiquitination [88]. Additionally, overexpressing E528A abolished the NF-κB activation in dual luciferase assays [88]. Based on that information, the ubiquitination of endougenous TRAF6 was analysed by over-expressing HA-tagged IRAK2 WT and mutants in HEK293T cells. Additionally, HA-tagged ubiquitin was co-transfected to probe ubiquitination with an anti-HA antibody. The IRAK2 E528A protein served as a positive control (See figure 3.25A). Strikingly, IRAK2 WT strongly induced TRAF6 ubiquitination whareas R214G and L392V both reduced the ubiquitination level of TRAF6. Meanwhile, the positive control E528A almost completely abolished the ubiquitination of TRAF6. The results may be confounded by the fact that the IRAK2 constructs and ubiquitin both have the same HA-tag. Therefore, endogenous ubiquitination assay was analysed when overexpressing HA- tagged IRAK2 proteins in HEK293T cells. this experiments was perfomed in collaboration by Sinead M. Flannery (School of Biochemistry and Immunology, Trinity Biomedical Sciences Institute, Trinity College, Ireland) see figure 3.25 (B). Overexpression of WT IRAK2 strongly triggered TRAF6 ubiquitination (lane 1). Compared to WT IRAK2, R214G and L392V reduced the amount of ubiquitination on TRAF6; especially L392V almost completely abrogated the ubiquitination of TRAF6.

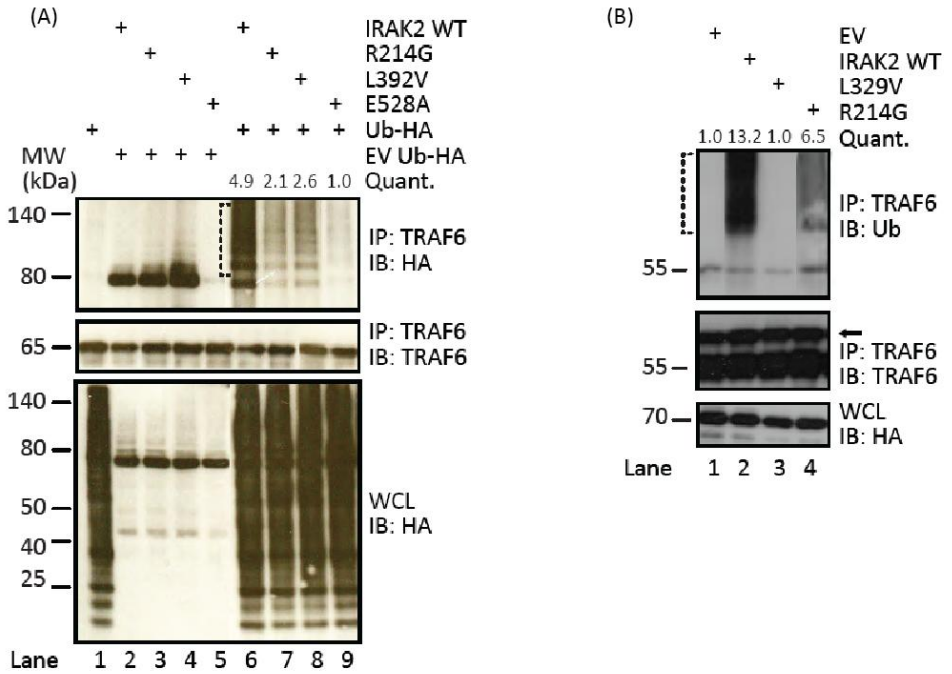

Figure 3.25 R214G and L392V reduce the ubiquitination of TRAF6. 4μg of expression plasmids encoding for HA-tagged IRAK2 WT or mutants were transfected into HEK293T cells (A) Co-transfection with 4μg of plasmids encoding for HA-tagged ubiquitin into HEK293T cells (a). 48 hours post-transfection, endogenous TRAF6 was immunoprecipitated by applying a rabbit polyclonal α-TRAF6 antibody. Cell lysate and immunoprecipitated samples were separated on 4-12% Bis-Tris gradient gels and analysed by immunoblot with α-HA rabbit monoclonal antibody to probe for ubiquitine or α-TRAF6 mouse monoclonal antibody was used to precipitate TRAF6. (B)Endogenous ubiquitination of TRAF6 was detected by applying α-ubiquitine mouse monoclonal antibody. The densitometry was analysed by Image J, the relative value is presented according to each leane. The experiment was repeated twice**.**

3.3.2.6 R214G and L392V change the post-translation modifications pattern of IRK2

According to the results of part I, it is believed that IRAK2 may undergo phosphorylation and ubiquitination. The two hypofunctinal mutants, R214G and L392V reduced the ubiquitination level of TRAF6. It is conceivable that both mutants may alter the post-translational modifications on IRAK2 (e.g. phosphorylation or ubiquitination). Hence, 2D gel electrophoresis was performed to analyze the differences between mutants and WT IRAK2. In comparison to IRAK2 WT, the two mutants maintained the large amount of modifications (See figure3.26)

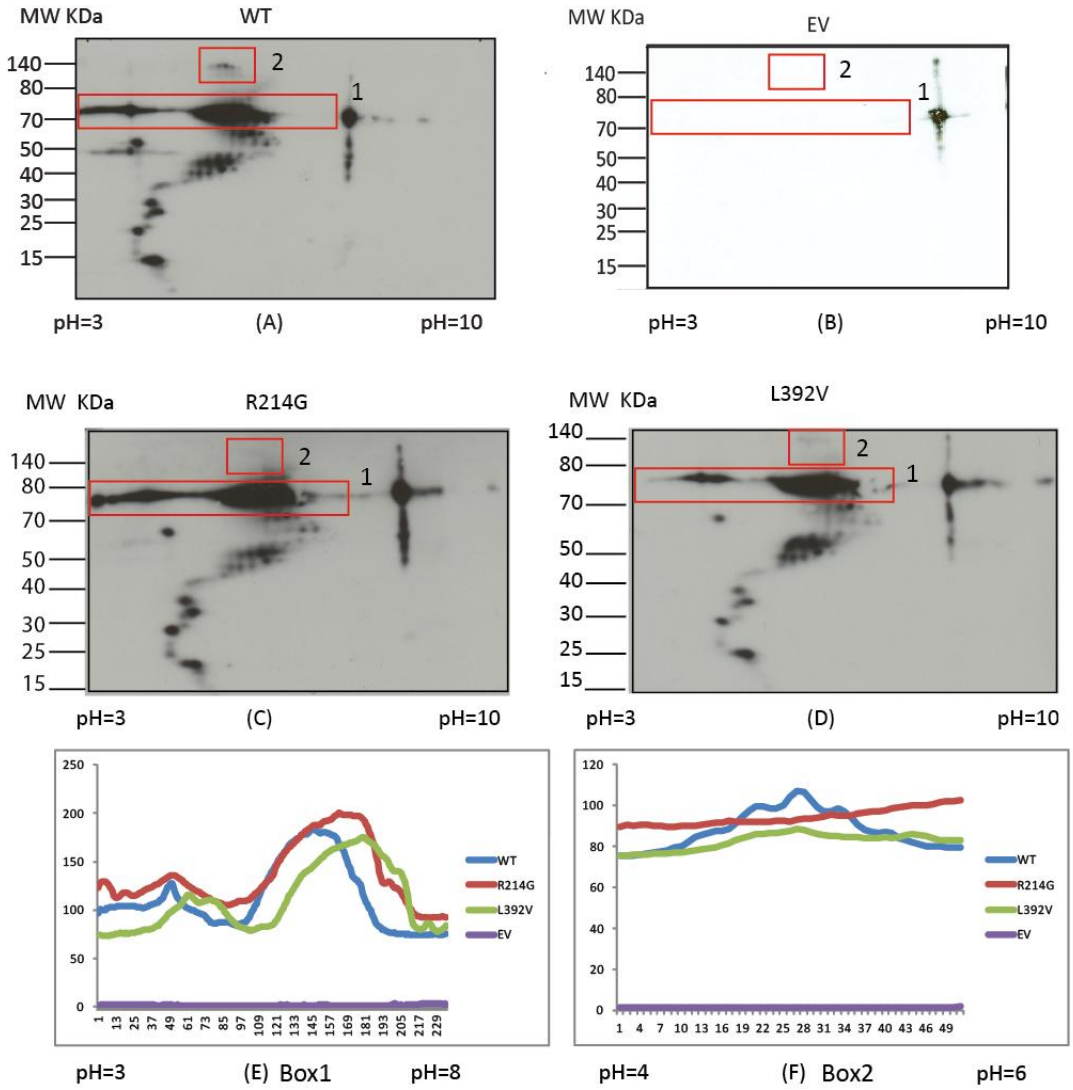

Figure 3.26 Post-translational modifications profiles of IRAK2 WT, R214G and L392V. 4µg of expression plasmid encoding for HA-tagged IRAK2WT, R214G, L392V or EV were transfected into HEK293T cells. After 48 hours, IRAK2s were immunoprecipitated by applying α-HA mouse monoclonal antibody and the samples were subjected to IEF overnight and separated by SDS-PAGE via a 4-12% pre-cast Bis-Tirs gel, then continued with immunoblot with α-HA rabbit monoclonal antibod. Experiments were repeated twice.

However, R214G and L392V slightly shift the acidic modifications found for IRAK2 in the range of 80kDa (see figure 3.26 A, C, D, E). Additionally, the pattern at high molecular weight are absent in IRAK2 R214G and L392V, which has been similarly observed for the kinase dead IRAK2 K237A with K237A which abolished NF-κB activation (Figure 3.5 D and 3.26 F). Although L392V showed very vagure pattern at that position, they are not as strong as WT. these results may imply the higher molecular weight species are essential for IRAK2 to induce NF-κB activation. As discussed before (see sections 3.2.3), the higher molecular weight range of IRAK2 may implicate polyubiquitiantion event. In order to precisely characterize these modifications, mass

spectrometry analysis is needed.

Until now, the functions of IRAK2 WT and mutants were investigated thoroughly in HEK293T cells. However, HEK293T cells are not immune cells and the functional impact of these mutants may be different in immune cells. Moreover, HEK293T cells have endogenous IRAK2 which might interfere with the functional analysis on the overexpressed IRAK2 proteins. It is worthwhile to understand the functional properties of IRAK2 SNPs in immune cells without the interference of endogenous IRAK2.

3.3.2.7 Gene expression of reconstituted IRAK2 WT and SNPs stable cell line

As mentioned before, the retroviral vectors encoding for the IRAK2 mutants were generated by site-directed mutagenesis based on the pMXs-IP-puro vactor encoding for IRAK2 WT (section 3.1.3). Additionally, the empty vector pMXs-IP-puro was introduced into IRAK2 knockout macrophages to serve as a negative control.

The stable cell lines of IRAK2 WT and mutants were generated as described in section 2.3.9 The gene expression of IRAK2WT and mutants proteins were confirmed by immunoblot analysis with cell lysates (Figure 3.27). The expression levels of HA-tagged IRAK2 WT and mutants is comparable in those stable cell lines. No unspecific bands are detected in the empty vector control.

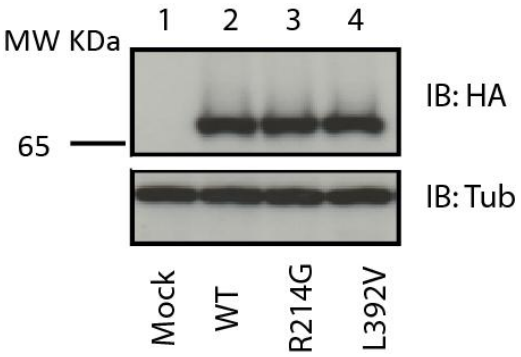

Figure 3.27 Expressions of IRAK2 WT and mutants in reconstituted macrophages. IRAK2 deficient macropahges were infected with an IRES-Puromycin expressing retrovirus MSCV carrying HA tagged versions of either wild type IRAK2 or mutant R214G or mutant L392V. The positive cells were selected based on puromycin resistance at 10μg/ml. The expression levels of the proteins were analysed with an anti-HA monoclonal antibody. Tubulin served as a loading control.

3.3.2.8 R214G and L392V maintained the production of TNF-α

In order to investigate whether the mutants impact on TNF-α production in response to TLR stimulation, an ELISA was conducted. Since TLR2, TLR4 and TLR7 ligands are

the strongest agonists that induce TNF-α production (see the results of Part I), only these three ligands were applied to analyse for TNF-α production (Figure 3.28) In comparison to the mock control, reconstituted macrophages enhanced the production of the TNF-α. However, no significant differences were observed between IRAK2 WT and mutants after stimulation with Pam_2CSK_4 (TLR2 ligands), LPS (TLR4) and R848 (TLR7). This experiment was repeated three times, where the readout indicated certain differences between WT and mutants. These small variations may also be due to differences in cell counting and seeding, or the status of the cells such as passage number and growth situation. In order to avoid those technical problems, quantitative PCR was carried out to screen for the activation of TNF-α and other pro-inflammatory cytokines.

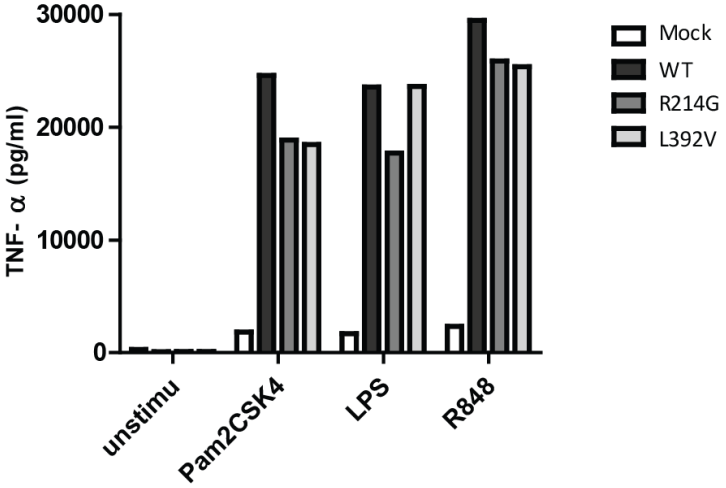

Figure 3.28 R214G and L392V do not alter TNF-α production. IRAK2 WT, R214G and L392V protein expression was reconstituted in IRAK2 knockout macrophages. 25000 cells were seeded and stimulated with Pams2CSK4 (1μg/ml), LPS (0.05μg/ml) and R848 (1μg/ml) for 16 hours and the amount of TNF-α was measured by ELISA. The data is presented for one experiment mean ± STD. The experiments were repeated three times**.**

3.3.2.9 R214G and L392V reduced mRNA expression levels of IL-1β and IL-6 in reconstituted macrophages

It was demonstrated that the recruitment of NF-κB to the *Il-6* promoter within 8 hours was impaired in *Irak*2 deficient macrophages when stimulating with the TLR2 for 8 hours[137]. Thus, it suggested that IRAK2 is involved in *Il-6* promoter activation. In order to further explore the functional properties of IRAK2, the quantitative PCR was carried out to screen for the induced transcription of *Tnf-a, Il-1β, Il-6* and *Ccl5*. TLR2, TLR4 and TLR7 stimulations were performed for 3 hours and the mRNA levels of these cytokines was quantified by Taqman-probed qPCR (Figure 3.29)

After reconstitution, IRAK2 WT and mutants all strongly induced the transcription of *Tnf-α*, *Ccl5*, *Il-1β* and *Il-6* activation upon TLRs stimulation. In general, LPS stimulation preferentially induced *Il-6*, while Pam_2CSK_4 induced the same amount of *Il-1β* and *Il-6*. R848 induced the highest amount of *Tnf-a* and *Il-1β*. When analysing the IRAK2 mutants, no significant difference between WT and mutant IRAK2 proteins was observed for the induction of *Tnf-α* and *Ccl5*. This result is in agreement with the fact, which no differences were observed for the production of TNF-α in the ELISA experiment. However, IRAK2 R214G and L392V cells showed reduced mRNA levels of *Il-1β* and *Il-6* when stimulating the cells with the selected TLR ligands. However, the transcriptional induction was not completely abrogated in these two cases, as the quantified levels were still thousand fold higher in comparison to the mock treated IRAK2 deficient cells. Although strong reduction of *Il-1β* and *Il-6* mRNA levels are observed, statistical significance was not reached in these experiments.

In order to investigate whether the mutants also impact on the production of pro-inflammatory cytokines when challenged with by pathogens, experiments with *Salmonella typhimurium* infections were carried out. However, no difference were observed (Data was not shown) due to several reasons. Since it is only a preliminary test, further detail investigation are still required.

Conclusively, IRAK2 R214G and L392V are variants of IRAK2 which reduce the production of *Il-1β* and *Il-6* in macrophages upon stimulation wih TLR2, 4 and 7.

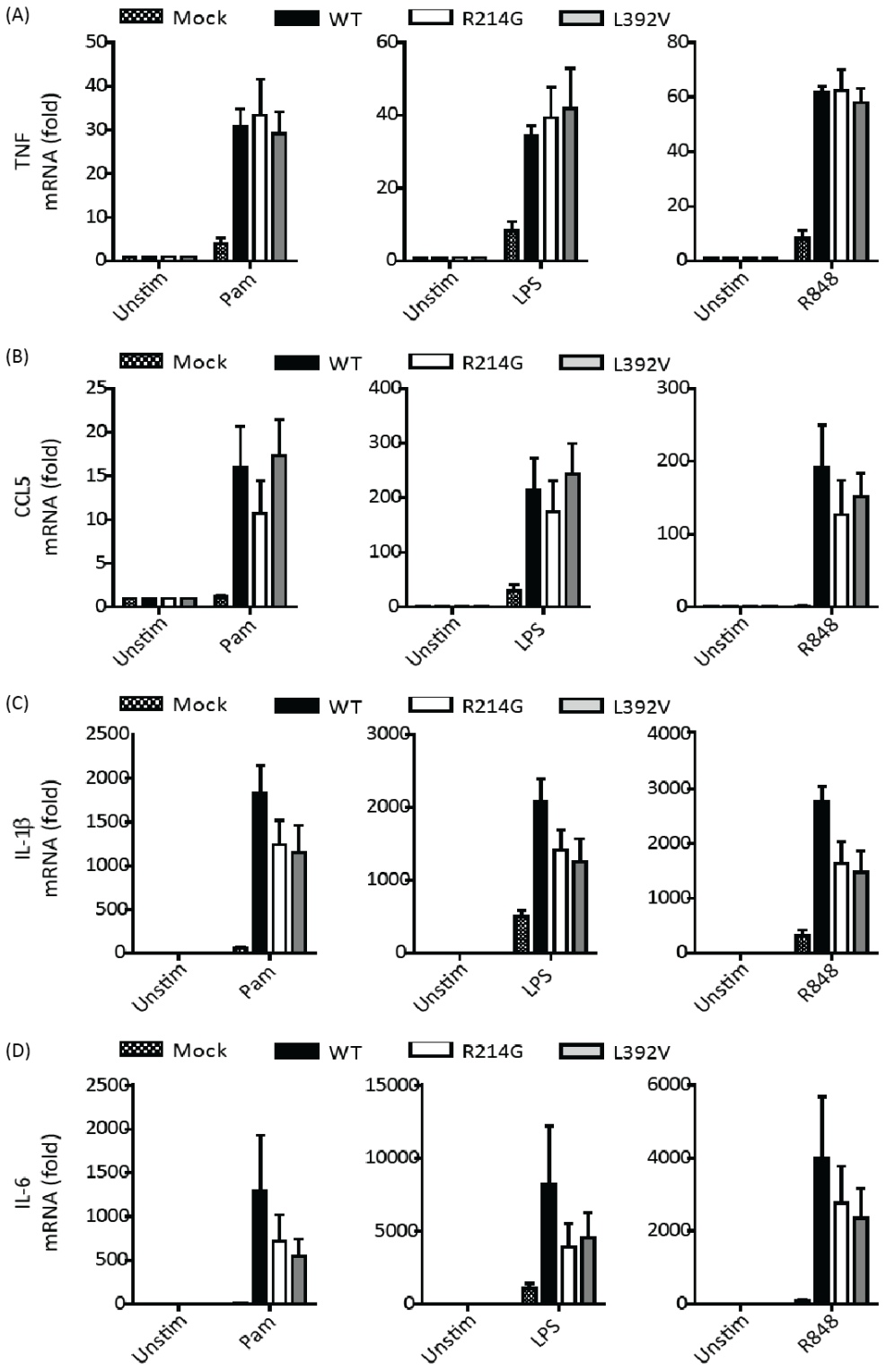

Figure 3.29 IRAK2 R214G and L392V reduced the transcriptional induction of *Il-1β* and *Il-6*. The relative mRNA levels in reference to the unstimulated mock induction (cehquered), WT human IRAK2 (black), R214G(white) or L392V(grey) reconstituted macrophages. Upon stimulation with Pam2CSK4, LPS or R848 for 3 hours, mRNA levels of *Tnf-α* (A), *Ccl5*(B), *Il-1β*(C) and *Il-6* (D) were determined. Mean+SEM. of combined data of four independent experiments are shown

3.3.3 Discussion

3.3.3.1 R214G and L392V impaired the ubiquitionation of TRAF6

The results obtained from part III indicated that R214G and L392V are hypofunctional SNPs of IRAK2. The reduced NF-κB activation is caused by decreased TRAF6 ubiquitination.

First, the LUMIER data particularly revealed that the IRAK2 mutants R214G and L392V interfere with the Myddosome assembly. Residue R214G strongly increased the interaction with IRAK4 and itself. In contrast to the R214G mutation, IRAK2 L392V severely decreased the interaction with IRAK4 and itself. The residues R214 and L392 are both located in the kinase domain of IRAK2. The data implies that the kinase domain appears to participate in the formation of Myddosome. It was proposed that the DD of IRAK4 is important to recruit IRAK2 via homotypic interactions, which brings the kinase domain of IRAK4 close to the kinase domain of the IRAK2 kinase domain[86]. Thus, IRAK2 becomes fully activated by IRAK4 and further recruit and interact with TRAF6 and induce the ubiquitination of TRAF6 [13](see figure 3.16).

How do the two IRAK2 mutants reduce NF-κB activation? R214G appears to have an increased affinity with IRAK4 and itself, which means that it was captured in the Myddosome and cannot be released from the Myddosome. TRAF6 still can be recruited to IRAK2 but it cannot be fully ubiquitinationed due to the less modification in IRAK2, which is shown in the 2D gel analysis. Moreover, the co-immunoprecipitation assay and LUMIER experiments confirmed that IRAK2 R214G kept the same interaction with TRAF6 comparing to IRAK2 WT. Although IRAK2 L392V showed a decreased the interaction with IRAK4 which means IRAK2 may not be fully activated and cannot further induce TRAF6 ubiquitination. However, the co-immunoprecipitation and LUMIER assay showed that IRAK2 L392V kept the same interaction intensity with TRAF6 in comparison to WT, which implies that the interaction between IRAK2 and TRAF6 could occur by overexpression, but the fully activated IRAK2 is essential for the ubiquitination of TRAF6.

Moreover, the assembly intensity of Myddosome is critical for the activation of IRAK2, which might affect the ubiquitination of TRAF6. . This is consistent with the overexpression of IRAK2 mutants E528A and K237A in HEK293T cells which

abolished the NF-κB activation, but maintained the interaction with TRAF6. E528 is a key residue in the first TRAF6 binding motif of IRAK2. The mutation of this residue completely abolishes the ubiquitination of TRAF6, while the interaction with TRAF6 is retained [88]. The residue K237 is assumed to control the intrinsic kinase activity. Also our experiments showed that the overexpression of the IRAK2 K237A mutant in HEK293 cells resulted in abrogated NF-κB activation, whereas the interaction with TRAF6 was maintained.

In conclusion, the ubiquitination level of TRAF6 is a key step to induce NF-κB activation, which is dependent on the enzymatic activity of IRAK2. In turn, the integrity and activation of IRAK2 is very important for the signal transduction of NF-κB.

Additionally, 2D gel analysis showed that the IRAK2 mutants R214G and L392V lost modifications in the higher molecular weight range. IRAK4 was thought to act as upstream signalling partner of IRAK2, which means that the proper interaction with IRAK4 is a critical step to fully activate IRAK2. Although R214G increased the interaction with IRAK4 and the mutant L392V rather reduced the interaction; nonetheless both of these two SNPs lost the higher molecular weight modifications. Additionally, the kinase dead K237A of IRAK2 lost these modifications as well. It is conceivable that this modification is pivotal for IRAK2 to induce TRAF6 ubiquitination. It is therefore necessary to perform the mass spectrometry to analysis on these higher molecular weight shifts, which can be done by enrichment of these higher molecular weight protein by staining the 2D gel with coomassie and isolate them from gel. It may provide hints about post-translation modifications on IRAK2, and further *in vitro* assays might help to understant its impact on the signal transduction. Moreover, a crystal structure of FL IRAK2 and the FL Myddosome individually can further explain the opposed behaviour of IRAK2 R214G and L392V in terms of IRAK4 interaction.

Till now, it is not clear whether TRAF6 was first recruited to the complex, ubiquitinationed and then released [217] or if fully activated IRAKs dissociate from the Myddosome complex to then interact with TRAF6 [218]. Unfortunately, our experimental results cannot confirm of these scenarios which one may hold true. It is always very complicated to elucidate the precise mechanism underlying cellular signalling. Recently, the ubiquitination events in the RIG-signalling pathway were

clarified by using biochemical reconstitution experiments combined with biophysical techniques. Thus, applying the same method would help us to understand the mechanism of Myddosome assembly and how associations with TRAF6 lead to its ubiquitination. Additionally, these two hypofunctional mutants can serve as useful functional probes for such studies to help us understand the signalling events following the Myddosome assembly.

3.3.3.2 IRAK2 R214G and L392V impaire the transcription of IL-1β and IL-6

The qPCR results revealed that *Tnf-α*, *Ccl-5*, *Il-6* and *Il-1β* were dramatically enhanced in human IRAK2 reconstituted macrophages when they were stimulated with the ligands of TLR2, 4 and 7. This result is consistent with data obtained from the infection of macrophages with *Salmonella typhimurium*; which resulted in transcriptional activation of *Tnf-α*, *Ccl-5*, *Il-6* and *Il-1β*, particularly with *Il-6* and *Il-1β*.

It was shown that the transcription of *Il-6* was impaired in IRAK2 deficient macrophages upon MALP-2 stimulation [137]. Consistent with this observation, the transcriptional activation of *Il-6* was massively enhanced when stimulating human IRAK2 reconstituted macrophages with TLR2, 4 and 7 ligands. Similarly, the infection with *Salmonella typhimurium* also triggered the transcriptional activation of *Il-6* in human IRAK2 reconstituted macrophages (see part I). Moreover, in comparison to mock reconstituted macrophages, no transcriptional activation of *Il-6* was observed. All together, these data indicate that IRAK2 is essential for the transcriptional activation of *Il-6*.

Interestingly, the two hypofunctional mutants of IRAK2, R214G and L392V reduced the transcriptional activation of *Il-6*. However, no significant differences of IL-6 transcription were shown between IRAK2 WT and mutants, which be explained by the large standard deviations of the different measurements. In order to confirm that this phenomenon is of statistical significance, an *Il-6* RNA blot assay can aid in understanding if the two mutants impact on the transcription of *Il-6*. Alternatively, IL-6 ELISA assays may further delineate the impact of IRAK2 WT and the two mutants on the production of IL-6. Furthermore, it would also be informative to analyse if the colorectal cancer patients who carry the IRAK2 SNP alleles, also show impaired levels of IL-6, and if this may correlate with a decreased in survival time of these patients.

Similar to the transcription of *Il-6*, the transcriptional activation of *Il-1β* was massively enhanced in the human IRAK2 reconstituted macrophages comparing to the mock control. However, only little research was performed to elucidate the role of IRAK2 in inducing the transcriptional activation of *Il-1β*. The research of Wan et al. (2009), describes a reduced IL-1β production in IRAK2 deficient macrophages, which were stimulated with LPS for 1.5 hours. However, the amount of IL-1β was recovered after 3hours of stimulation. In this thesis the R214G and L392V reduced the transcriptional activation of *Il-1β* which is similar to the effect on the transcriptional activation of *Il-6*. It is conceivable that IRAK2 may play a critical role in the transcriptional activation of *Il-1β*. However, further research is required to confirm the relation between IRAK2 and IL-1β. The mechanism for IL-1β production involve two steps: first, the precursor of IL-1β needs to be produced intracellularly by activation of NF-κB, and mature IL-1β is generated through proteolytic cleavage by caspase-1; then mature IL-1β is released to the supernatant. Second, the extracellular mature IL-1β activates the IL-1R signalling pathway to produce more IL-1β. IRAK2 is a kinase of the TLR and IL-1R signalling pathways (see figure introduction 1.2.1.2 and figure 1.4), whether it will balance the production of IL-1β is unknown. In order to confirm the role of IRAK2 in the transcriptional activation *IL-1β*, the *IL-1β* RNA blot could help us understand the dependency between IL-1β and IRAK2. Additionally, the WB of intracellular precursor IL-1β and extracellular mature IL-1β can help us to understand the role of IRAK2 in regulating the production of IL-1β on a protein level.

In contrast to the transcriptional activation of *Il-1β* and *Il-6*, the two hypofuncational mutants, R214G and L392V did not shown any discernable differences from IRAK2 WT in terms of transcriptional activation of *Tnf-α* and *Ccl-5*, these results is consistent with previous research[140]. On the other hand, these data also indicate that IRAK2 is not essential for the transcriptional activation of *Tnf-α*, but it is required to stabilize the mRNA level of *Tnf-α* [140, 193]. In the case of *Ccl-5*, the transcription activation was slightly impaired in those two mutants upon the R848 stimulation which might indicate a special role of IRAK2 in TLR7 activation. Furthermore, this result might supported the hypothesis that the IRAK2 variants L392V has a reduced HCV auto clearance (See part IV 3.4.2.2 and 3.4.3).

Conclusively, IRAK2 plays an essential role in the production of multiple

pro-inflammatory cytokines, particularly for IL-1β and IL-6. IRAK2 might be important for the TLR7 induced the production of pro-inflammatory cytokines and Ccl-5. IRAK2 appears to play a special of role of regulating IL-1β and IL-6; but how would the two genetic variants of IRAK2 impact on the progress or the prognosis of diseases? Therefore, further investigations are required to decipher the role of IRAK2 in epidemiological studies.

3.4 Part IV: Genetic variants in IRAK2 impact on the progress and prognosis of infection-related diseases.

3.4.1 Introduction

Epidemiological studies can provide us with the information if certain genetic variants are related to the susceptibility to certain kind disease. For instance, TLR3 deficiency is related with herpes virus encephalitis [35]. IRAK2 also plays a role in protection the mice against pathogens [137]. However, little is known about the associations between the SNPs of IRAK2 and diseases generally, particularly these two hypofunctional SNPs of IRAK2, R214G (rs35060588) and L392V (rs3844283). The two hypofunctional genetic variants in IRAK2 occur relatively frequently in the human population: rs35060588 (R214G) occurs with 3 and 9 % in Americans and Europeans, respectively, but not in Asians or Africans; rs3844283 (L392V) is found with frequencies between 15 and 44 % in Americans, Europeans, Asians and Africans. Are these carriers potentially susceptibile to any infection-related diseases? In order to address this question, three epidemiological studies were carried out in collabration to analyse if the two hypofuntional genetic variants are related to the following diseases: (1) the survival analysis of colorectal cancer patients, (2) HCV clearance, and (3)the development of gastritis.

3.4.2 Results

3.4.2.1 R214G reduced the survival time of colorectal cancer patients

The association of the two IRAK2 alleles (R214G and L392V) with colorectal cancer (CRC) survival was analyzed in a German progression cohort of colorectal cancer (CRC (n=613)). This study was done in collaboration with Dr. Asta Försti (Division of Molecular Genetic Epidemiology, German Cancer Research Center (DKFZ), Germany). No association was observed for rs3844283 (L392V) with the progress of CRC, whereas heterozygous carriage of the rs35060588 (R214G) G allele reduced the survival time of CRC (HR 1.60 [1.01-2.52], p=0.04, Table 3.4). However, only four persons were homozygous for the G allele and none of them died during the study period. Therefore, no firm conclusions can be drawn. Nonetheless, heterozygous carriage of R214G in CRC patients was associated with an exacerbate progress of CRC.

Table 3.4 Frequencies of IRAK2 rs 3844283 and 35060588 with CRC-specific survival.

rs number	Genotype	CRC-specific survival			
		No. at risk	No. died (%)	HR (95% CI)	p value
rs35060588	CC	524	124 (23.66)	1	
(R214G)	CG	69	22 (31.88)	**1.60 (1.01-2.52)**	**0.04**
	GG	4	0 (0.00)	-	
	CG+GG	73	22 (30.14)	**1.52 (0.96-2.40)**	**0.07**
rs3844283	CC	196	51 (26.02)	1	
(L392V)	CG	297	71 (23.91)	0.92 (0.63-1.32)	0.64
	GG	111	25 (22.52)	0.80 (0.49-1.32)	0.39
	CG+GG	408	96 (23.53)	0.89 (0.63-1.26)	0.49

3.4.2.2 L392V reduced the HCV clearance

The epidemiological study of the relation between IRAK2 variants and HCV clearance was conducted in collaboration with Dr. Janett Fischer (University Hospital Leipzig, Division of Gastroenteroly and Hepatology, Leipzig, Germany). The overall distribution of these two hypofunctional IRAK2 alleles in a German HCV cohort is presented in Table 3.5. No significant difference of genotype frequency was observed which was tested with the Hardy-Weinberg equilibrium. For the rs35060588 (R214G) variant, the frequency of homozygous genotype GG was below 1%. Therefore, no further analysis was conducted. In the German cohort study, 264 (29.5%) patients had spontaneous viral clearance. Significant distribution differences in the genotype of the IRAK2 rs3844283 (L392V) was observed between spontaneous clearance and chronic infection patients. Meanwhile, the known polymorphisms in IL28B rs12979860 and rs8099917 were also displayed the significant differences in genotype distribution between spontaneous clearance and chronic infection patients (see table 3.5). When analyze the relationship between each polymorphism (rs3844283 (OR=0.66, p=0.005), rs129798609 (OR=0.23, $p=2.9\times10^{-21}$) and rs8099917 (OR=0.25, $p=1.4\times10^{-15}$)) with chronic infection by univariate analysis method, it shows each polymorphism is a risk factor for the progress of a chronic HCV infection (see table 3.6). Additionally, in order to rule out the cross-talk between these polymorphisms, multuivariate analysis still confirmed that the G allele of IRAK2 rs3844283 is a independent risk factor for chronic HCV infection, since carriage of the IRAK2 rs3844283 G allele reduced the possibility to spontaneously clear HCV to 0.68 [0.49-0.93], p=0.015. As reported before, the polymorphism of IL28B rs12979860 and rs8099917, were associated with a

treatment failure, respectively (Table 3.6). However, no association was observed between L392V and the failure of SVR treatment. This cause relationship between L392V and chronic HCV infection was confirmed in an independent SWISS HCV cohort study as well [219].

Table 3.5 Frequencies of IRAK2 rs3844283 and rs35060588 and IL-28B rs1297860 and rs8099917

Polymorphism		Overall	spontaneous clearance	chronic infection	SVR	non-response
rs35060588	**CC**	86.2%	-	-	-	-
	CG	13.5%	-	-	-	-
	GG	0.3%	-	-	-	-
rs3844283	**CC**	34.4%	41.3%	31.5%	29.6%	32.6%
	CG	50.4%	46.2%	52.1%	52.8%	52.3%
	GG	15.2%	12.5%	16.3%	17.6%	15.1%
rs12979860	**CC**	37.7%	62.1%	27.4%	36.5%	22.8%
	CT	48.2%	29.6%	55.9%	49.8%	58.7%
	TT	14.1%	8.3%	16.7%	13.7%	18.5%
rs8099917	**TT**	59.2%	80.3%	50.4%	59.7%	45.0%
	TG	34.0%	17.4%	40.9%	32.6%	44.6%
	GG	6.8%	2.3%	8.7%	7.7%	10.4%

Table 3.6 Association of IRAK2 rs3844283 and Il28B rs12979860 and rs8099917 with the natural course of HCV infection and spontaneous virologic response

Parameter	Spontaneous clearance				Sustained virologic response (SVR)			
	Univariate analysis		Multivariate analysis		Univariate analysis		Multivariate analysis	
	OR [95% CI]	p-value	OR [95% CI]	p-value	OR [95% CI]	p-value	OR [95% CI]	p-value
rs3844283	**0.66 [0.49-0.88]**	**0.005**	**0.68 [0.49-0.93]**	**0.015**		0.469		0.555
rs12979860	**0.23 [0.17-0.31]**	**$2.9x10^{-21}$**	**0.35 [0.24-0.51]**	**$5.2x10^{-8}$**	0.52 [0.35-0.75]	0.001	0.30 [0.19-0.49]	$7.5x10^{-7}$
rs8099917	**0.25 [0.18-0.35]**	**$1.4x10^{-15}$**	**0.50 [0.32-0.76]**	**0.001**	0.55 [0.39-0.78]	0.001	0.39 80.25-0.60]	$2.6x10^{-5}$
sex		0.824		0.216		0.102		0.824
age		0.625		0.549	0.97 [0.95-0.98]	0.0003	0.95 [0.93-0.97]	$2.2x10^{-6}$
HCV RNA log_{10} concentration		-		-	0.62 [0.47-0.82]	0.001	0.60 [0.45-0.81]	0.001

3.4.2.3 L392V increase the susceptibility of gastritis progressing to gastric cancer

The analysis of progression of gastritis to gastric cancer, another malignancy in which the innate immune system has been investigated in collaboration with Institute for Microbiology and Hygiene CCM, Charité-University Medical Center, Germany. This progression from gastritis to gastric cancer case control study revealed a significant association between IRAK2 rs3855283 (L392V) and gastric cancer. The analysis indicated that carriage of rs3855283 G allele and rs3855283GG allele doubled the risk of the progression from gastritis to gastric cancer (OR 2.04 [1.25-3.42], p=0.003). Concurrent infection of *Helicobacter pylori* slightly increased the OR value (OR 2.25 [1.28-4.00], p=0.002). However, the major affect source is the rs3855283. Collectively, this suggests that the carriage of rs3855283 G allele will increase the susceptibility of gastritis to gastric cancer. The rs3855283GG genotype may therefore be an independent prognostic marker for the progression of gastritis to gastric cancer.

Table 3.7 Frequencies of IRAK2 rs3844283 in gastritis and gastric cancer patients

Polymorphism	Gastric Cancer	High Risk Gastritis(HRG)	OR value 95% CI	P value
CC	36(27%)	58(43%)	**2.04**	**0.003**
CG	71(53%)	55(40%)	**(1.225-3.421)**	
GG	28(21%)	23(17%)	CC/CG+GG	
Only H.pylori positive	Gastric Cancer	High Risk Gastritis(HRG)	OR value 95% CI	P value
CC	28(27%)	54(46%)	**2.25**	
CG	59(57%)	44(37%)	**(1.282-4.000)**	**0.002**
GG	16(16%)	20(17%)	CC/CG+GG	

3.4.3 Discussion

3.4.3.1 Genetic variants in IRAK2 effect on the progress and prognosis of infection related diseases

It is known that IRAK4 or MyD88 deficiency is correlated with recurrent pyogenic bacterial infections in early childhood [220]. Recently, it was found that the somatic L265P mutation in MyD88 is also highly related with diffuse large B-cell lymphoma [171]. However, in comparison to IRAK2, germ-line encoded mutations are relatively rare in MyD88 and IRAK4. Here, the hypothesis of a "Common disease, rare variant" (CDRV) may apply, in which rare DNA sequence variations, seem to have a high penetrance, and therefore seem to dramatically determine the genetic susceptibility to common diseases [221]. IRAK4 and MyD88 are highly conserved and polymorphisms hardly occur with frequencies of over 1 %. Patients which carry deficiencies of IRAK4 or MyD88, are highly susceptible to bacterial infections, and early diagnosis, clinical care and the prophylactic treatment with antibiotics is important to prevent from early childhood death[220]. In times, when clinical facilities and care were less developed and when antibiotics were not available, patients with MyD88 and IRAK4 deficiencies must have faced a huge selective pressure; this may explain their rare occurrence in the population.

Meanwhile, the hypothesis of "common disease, common variant" (CDCV) points out that genetic variations in multiple genes with appreciable frequencies in the population, but potentially low penetrance, are the major contributors to genetic susceptibility to a common disease [221]. With regard to this view, R214G (rs35060588) and L392V (rs3844283) could more likely be classified as "common disease, common variants".

Infection-related CRC patients with IRAK2 rs35060588 showed a decreased survival time. This was especially found for heterozygous carriers of the rs35060588 allele. However, only 4 homozygous patients were followed who did not succumb to disease-related death.

It was shown that increased IL-6 expression exacerbates the prognosis of colorectal cancer [222]. Interestingly, the experiments in this thesis and previous studies [137] showed that the transcription of IL-6 was controlled by IRAK2. However, the rs35060588 reduced the mRNA levels of IL-6 when stimulating macrophages with TLR2/4/7. How exactly rs35060588 influences the progress of CRC in the organism

remains to be understood and requires further investigation. Of note, IRAK2 in-vitro studies were mainly conducted in immune cells; since IRAK2 is ubiquitously expressed, it worthwhile to analyse the impact of IRAK2 and the IRAK2 variants in colorectal cancer cells.

The HCV case control study showed that carriage of rs3844283 (L392V) correlated with a decreased ability for HCV auto clearance, which results in the fact that these patients are susceptible to chronic HCV infection. Furthermore, IL-28B rs12979860 and rs8099917 are known factors for high susceptibility to HCV infection. Even when using a multivariate analysis to exclude the impact of IL-28B rs12979860 and rs8099917, rs3844283 still shows up as an independent risk factor for HCV infected patients to progress to chronic inflammation. The clearance of the HCV virus mainly depends on the production of type I and type III interferons [223], and on the activation of the adaptive immune response [224] .

In our experiments IRAK2 was defined as a major inducer for pro-inflammatory cytokines. Reconstituted macrophages produced a certain amount of IFN-β upon R848 stimulation. Moreover, it also shown that reconstituted macrophages produce an appreciable amount of Ccl-5 when stimulated with TLR2, TLR4 and TLR7 agonists. Ccl-5 is thought to facilitate induction of chemotaxis in immune cells and activation of hepatic stellate cells at sites of liver inflammation during chronic hepatitis C virus infection [225]. Importantly, Ccl-5 participates in the establishment of T-helper 1 responses which is crucial in controlling HCV infection outcome [225]. Moreover, HCV also can be cleared by RIG-I like receptors in hepatocytes [226]. Recently, it was shown that IRAK2 was involved in the RIG-I signalling pathway undirectly [227]. Conclusively, IRAK2 is involved in the TLR7 activation, Ccl-5 production and RIG-I like receptors signalling pathways. It is therefore conceivable that defects in IRAK2 may impair the response to HCV, and may explain why rs3844283 carriers are susceptible to chronic HCV infection and show reduced abilities for the viral clearance.

The last case control study on high-risk gastritis showed that in comparison to the IRAK2 WT allele, rs3844283 almost doubled the patient's risk for progression to gastric cancer. Gastric cancer is the third most common cause for cancer-related death [228]. Interestingly, IL-1β was demonstrated to be another risk factor for gastric cancer; in particular, IL-1β is shown to inhibit the acid production and low amounts of gastric

acid are related with gastritis and gastric cancer [229].The experiments here show that IRAK2 affects the transcription of IL-1β. However, IRAK2 L392V (rs3844283) reduced the IL-1β production by in the in-vitro assay which is controversial to the observation that IL-1β induces gastritis and gastric cancer. How exactly rs3822283 impacts on the progression of gastritis still needs to be studied. In this context it may be worthwhile to analyse in in-vitro studies the functional effects of IRAK2 in parietal cells response to IL-1β. In theory, the similar method also can be applied for the study of the response to HCV in hepatocytes.

It is first time to discover the association between SNPs of IRAK2 and diseases in human. Overall, these three diseases are all infection-related diseases. It is known that IRAK2 plays a central role in regulating the production of pro-inflammatory cytokines. However, the precise role of IRAK2 in the progress of those diseases is not clear. Does IRAK2 and the TLR signalling pathway cooperate with other PRR signalling pathway? How does IRAK2 particularly functions in the response to pathogen? The mechanism underlying this epidemiological association are yet unknown and require further studies in these disease-related in-vitro or in-vivo models. In this work causal relationships were investigated in gastritis, HCV auto clearance and colorectal cancer case control studies. In addition to these, it is conceivable that IRAK2, as a central regulator of innate immune signalling pathways, is also having an impact on many other infection-related diseases. Referring to the CDCV hypothesis, IRAK2 may be emphasized as a common variant that does not show immediate impact (“penetrance”) in the population and in response to disease. However, in combination with certain environmental cues and physiological conditions, IRAK2 may represent a risk factor, that contributes to disease. At this point it is noteworthy, that IRAK2 SNPs are occurring with different frequencies in different ethnic groups, the studies here mainly focused on Caucasian populations. The analysis in different cohorts may further provide insights if IRAK2 may differently impact disease in certain ethnicities.

Chapter 4: Conclusion

Conclusion

This chapter concludes the research in this thesis by summarizing contributions and proposing some thoughts for future work.

Although IRAK2 has been studied in numerous molecular studies, this is the first time using SNPs as probes to investigate the integrity importance of IRAK2 in human system and in reconstituted mouse *Irak2* knock out macrophages. Meanwhile, this is also the first time to investigate the causal relationship between hypofunctional polymorphisms of IRAK2 and human diseases. Based on the in-depth research in this dissertation, several contributions have been achieved, which also provides some implication for future research.

4.1 IRAK2 generally plays a central role in TLR-NF-κB signalling pathway

First, from the molecular point, LUMIER results first indicate that the full-length MyD88, IRAK4 and IRAK2 also generate the multimeric complex in mammalian cells as well, and this full-length complex also formed highly in order. It is consistent with published the Myddosome structure which consists of only DDs of MyD88, IRAK4 and IRAK2 in bacterial system[86]. However, the stoichiometry of these full-length molecular still needs further investigation. Interestingly, only IRAK2 further interacts with IRAK1 and IRAK3, which so far has not been investigated. It implies that IRAK2 plays a vital role in mediating or adjusting the TLR-NF-κB signal transduction.

Moreover, our research displayed that the kinase domain of IRAK2 also has impact on the assembly of the Myddosome by adopting the genetic variants R214G and L392V. IRAK2 R214G increased the interaction with IRAK4 and itself whereas the redisue L392V decreased the interaction with IRAK4 and itself in comparison with IRAK WT. However, these two variants still kept the interaction with TRAF6. Moreover, the adopted 3D model of IRAK2 kinase domain further displayed that residue R214 is exposed on the surface and faces the ATP loop region, in where the invariant lysine K237 and the gatekeeper Y286 is located. In contrast to R214, residue L392 is buried in the proximity of the putative activation loop of IRAK2. These two variants provided further information on the structure of IRAK2, which still need to be verified by using X-ray to reveal the crystal structure of IRAK2.

To further investigate the reason of defect activation of two IRAK2 variants, TRAF6 ubiquitination experiment was performed. IRAK2 was thought as a trigger of the ubiquitination of TRAF6 which is a critical step to induce the activation of NF-κB. Our results revealed that the two hypofunctional genetic variants R214G and L392V reduced the NF-κB activation by reducing the ubiquitiantion level of TRAF6 but maintained the same interaction intensity with TRAF6 in comparison to IRAK2 WT, which is consistent with the behaviour of mutation IRAK2 E528A[88]. To further address the mechanism of the reduced ubiquitination of TRAF6, 2D gel electrophoresis was carried out to seek differences between IRAK2 WT and genetic variants in post-translational modifications, which has so far not been delineated in detail. Our experiments indicate that these modifications are critical for signal transduction. However, the precise nature of these modifications is not known yet and further studies in this field are required. For instance, elucidation of the crystal structure of IRAK2 or the phosphorylation/ubiquitination mass spectrometry analysis of IRAK2 would be profound studies on the molecular mechanism of IRAK2 signalling properties.

To further investigate the role of IRAK2 in innate immunity, human IRAK2 reconstituted mouse IRAK2 knockout macrophages were generated. The TNF-a production was significantly enhanced in the reconstituted IRAK2 WT macrophages upon stimulation with TLR2, 4 and 7 ligands. This finding denoted that IRAK2 is specific for the production of pro-inflammatory cytokines upon TLR2, 4 and 7 activations. Although previous research indicated that the production of TNF-α and IL-8 was impaired in the IRAK2 silenced human PBMCs by stimulating with TLR4 and TLR7 ligands[193]. Whether IRAK2 has specificity for certain kinds of TLR ligands still needs further investigation. Due to the difference between mouse macrophages and human PBMC, the function of IRAK2 might be redefined according to different cell types, since IRAK2 is expressed universally.

Previous experiments indicate that IRAK2 plays an essential role in sustaining NF-κB activation in later time points[137]. In this thesis, it confirmed that IRAK2 does have an essential role both in the early time points of NF-κB activation. Stimulating the human IRAK2 reconstituted mouse macrophages with TLR ligands, phosphor p38, p65 and ERK were detected within 30mins. Additionally, our studies first revealed that IRAK2 is unique and essential for the phosphorylation of Akt upon the stimulation of TLR

ligands. Akt is mainly responsible for the cell proliferation and apoptosis. Importantly, the deregulated Akt pathway is associated with variety of human cancers, and several small molecular inhibitors targeting Akt have been developed and already tested in the clinical trial [230]. The fact that IRAK2 regulates Akt implies that IRAK2 may be involved in the progression of chronic inflammation to cancer.

Although it is known that the deficiency of IRAK2 impaired the transcriptional activation of *Il-6* [137]. Here, the experiments emphasize that the transcriptional activation of *Il-1β* is highly dependent on IRAK2 as well. Additionally, the transcriptional activation of *Il-1β* and *Il-6* was impaired when reconstituting the KO macrophages with IRAK2 R214G and L392V. Thus, it further confirmed that IRAK2 has a unique role in regulating transcriptional activation of *Il-1β* and *Il-6*. Intriguingly, the precursor IL-1β can be produced by activating TLR-induced transcription factor NF-κB and the bioactive IL-1β was processed by cleavage of the activation of caspase-1 which is the key component in the large complex inflammasome. Then the bioactive IL-1β was released into the extracellular space and bound to IL-1R to activate the pro-inflammatory cytokines production (see figure 1.9). IRAK2 is the downstream kinase of TLR and IL-1R, which might indicate that IRAK2 is involved into the IL-1β production. Since deregulation of IL-1β production is related with several auto-inflammatory conditions, such as Mukle-Wells syndrome, Type-1 diabetes and gout [68, 231, 232], it is worth to investigate the role of IRAK2 in these diseases.

4.2 IRAK2 genetic variants are related with the progression or prognosis of certain kinds of diseases.

Meanwhile, the impaired transcriptional activation in *Il-1β* and *Il-6* implies that these genetic variants of IRAK2 may have an impact on the progression and prognosis of certain kinds of infection-related diseases. It is known that genetic variants in IRAK1 are highly related with the pathogenesis of SLE [135] and the deficiency of IRAK4 is correlated with recurrent pyogenic bacterial infection in childhood[164].The minor allele frequencies of IRAK2 R214G (rs35060588) and L392V (rs3844283) in the human population are relatively high which might affect diseases susceptibility in a large number of individuals. Epidemiological studies reveal that the carriage of R214G decreased the survival time in the infection related colorectal cancer patients. Interestingly, high level IL-6 is tightly related with the unfavorite prognosis of CRC.

Moreover, two independent HCV cohort studies found that IRAK2 L392V carriers could reduced HCV clearance ability, and were therefore more susceptible to chronic HCV infection. It is known that HCV was eliminated by type I and type III IFN, which are mainly produced by RIG-I like receptor and TLR3 activation. So far, the IRAK2 function in TLR3 and RIG-I like receptor has not been addressed in detail. Interestingly, the Ccl5 is another key factor to facilitate the adaptive immunity, which is crucial in controlling the outcome of HCV infection. In our studies, Ccl5 production was also impaired in the two genetic variants, which may imply that IRAK2 plays a special role in TLR7 activation. Due to the universal expression of IRAK2 in organism, the IRAK2 function in hepatocytes needs to be further investigated. Additionally, the case control study on the progression from high risk gastritis to gastric cancer patients revealed that IRAK2 L392V doubled the risk for high risk gastritis patients to progress to a gastric cancer. Additionally, high amount of IL-1β is a risk factor for gastric cancer and it was impaired in our L392V reconstituted macrophages. However, the results are controversial which need in-depth research of IRAK2 in the gastritis environment.

How the genetic variants contribution to individual susceptibility to common complex diseases such as diabetes, osteoporosis, and cancer, there are two major hypotheses. One is the 'Common Disease, Common Variant (CDCV)' hypothesis argues that genetic variations with appreciable frequency in the population at large, but relatively low 'penetrance' (or the probability that a carrier of the relevant variants will express the disease), are the major contributors to genetic susceptibility to common diseases, such as hypertension. Another one is the 'Common Disease, Rare Variant (CDRV)' hypothesis, on the contrary, argues that multiple rare DNA sequence variations, each with relatively high penetrance, are the major contributors to genetic susceptibility to common diseases, such as familial breast cancer induced by BRCA1 and BRCA2 mutations[221]. Regarding the 'common disease, common variants' hypothesis, IRAK2 R214G and L392V might be considered as common variants that do not response to diseases immediately. However, in co-incidence with certain environmental cues and physiological conditions, IRAK2 may serve as a risk factor and contributed to the pathogenesis of diseases. Furthermore, only two hypofunctional variants were analyzed in this dissertation, it is worthwhile to perform adequate hyperfunctional variants functional and epidemiological studies to prove our results from another angel.

4.3 Could IRAK2 be a therapeutic target?

Collectively, our research highlights the need for further research on IRAK2, especially the relationship between genetic variants and susceptibility to certain kinds of diseases. Taking genetic variants as probes can help us to understand the complex interplay of signalling transduction and the relationship with certain kinds of diseases. IRAK2 may represent a suitable target in the treatment of disease, especially in those cases where genetic variants of IRAK2 may contribute to progression of the disease. As more and more researches have been conducted, the IRAK family members exhibit their specific functions in certain immune response branch. For instance, IRAK1 is specific for the production of type I IFN upon activation of TLR7 and TLR9; IRAK2 are mainly responsible for the production of pro-inflammatory cytokines. Regarding the fact that IRAK4 is the initiating kinase in the NF-κB activation, inhibition of the kinase activity of IRAK4 might interfere the activation of IRAK1 or IRAK3. The inhibitor of IRAK2 would be more specific for controlling over produced pro-inflammatory cytokines. Moreover, high levels of IL-1β and IL-6 are related with some autoimmunity diseases and genetic variants of IRAK2 altered the production of IL-1β and IL-6, which indicates that IRAK2 might be involved into the pathogenesis of autoimmunity diseases.

As an approach for personalized therapy, the design of specific IRAK2 kinase antagonists/agonists may help patients to conquer the chronic inflammation related diseases (HCV) or autoimmune diseases (rheumatoid arthritis).

Reference

1. Beck, G. and G.S. Habicht, *Immunity and the invertebrates.* Sci Am, 1996. **275**(5): p. 60-3, 66.
2. Charles A Janeway, J., Paul Travers, Mark Walport, and Mark J Shlomchik., *The Immune system in Health and Disease*2001, New York and London: Garland science.
3. Alberts, B.A.J., Julian Lewis, Martin Raff, Keith Roberts, and Peter Walters, in *Molecular Biology of the Cell*2002, Garland Science: New York and London.
4. Stvrtinová, V.J.J.a.I.H., *Inflammation and Fever from Pathophysiology: Principles of Disease*, 1995, Slovak Academy of Sciences:Academic Electronic Press.: Computing Centre.
5. Alt, F.W., et al., *VDJ recombination.* Immunol Today, 1992. **13**(8): p. 306-14.
6. Janeway Jr, C., *Approaching the asymptote? Evolution and revolution in immunolog.* Cold Spring Harb Symposia on Quantitative Biology. , 1989. **54**(1): p. 1-13.
7. Gutcher, I. and B. Becher, *APC-derived cytokines and T cell polarization in autoimmune inflammation.* J Clin Invest, 2007. **117**(5): p. 1119-27.
8. Watanabe, N., et al., *Hassall's corpuscles instruct dendritic cells to induce CD4+CD25+ regulatory T cells in human thymus.* Nature, 2005. **436**(7054): p. 1181-5.
9. Mauri, C. and A. Bosma, *Immune regulatory function of B cells.* Annu Rev Immunol, 2012. **30**: p. 221-41.
10. Medzhitov, R. and C.A. Janeway, Jr., *Innate immunity: the virtues of a nonclonal system of recognition.* Cell, 1997. **91**(3): p. 295-8.
11. Piccinini, A.M. and K.S. Midwood, *DAMPening inflammation by modulating TLR signalling.* Mediators Inflamm, 2010. **2010**.
12. Palm, N.W. and R. Medzhitov, *Pattern recognition receptors and control of adaptive immunity.* Immunol Rev, 2009. **227**(1): p. 221-33.
13. Takeuchi, O. and S. Akira, *Pattern recognition receptors and inflammation.* Cell, 2010. **140**(6): p. 805-20.
14. Meylan, E., J. Tschopp, and M. Karin, *Intracellular pattern recognition receptors in the host response.* Nature, 2006. **442**(7098): p. 39-44.
15. Anderson, K.V., G. Jurgens, and C. Nusslein-Volhard, *Establishment of dorsal-ventral polarity in the Drosophila embryo: genetic studies on the role of the Toll gene product.* Cell, 1985. **42**(3): p. 779-89.
16. Lemaitre, B., et al., *The dorsoventral regulatory gene cassette spatzle/Toll/cactus controls the potent antifungal response in Drosophila adults.* Cell, 1996. **86**(6): p. 973-83.
17. Nomura, N., et al., *Prediction of the coding sequences of unidentified human genes. I. The coding sequences of 40 new genes (KIAA0001-KIAA0040) deduced by analysis of randomly sampled cDNA clones from human immature myeloid cell line KG-1.* DNA Res, 1994. **1**(1): p. 27-35.
18. Taguchi, T., et al., *Chromosomal localization of TIL, a gene encoding a protein related to the Drosophila transmembrane receptor Toll, to human chromosome 4p14.* Genomics, 1996. **32**(3): p. 486-8.
19. Poltorak, A., et al., *Defective LPS signaling in C3H/HeJ and C57BL/10ScCr mice: mutations in Tlr4 gene.* Science, 1998. **282**(5396): p. 2085-8.
20. Medzhitov, R., P. Preston-Hurlburt, and C.A. Janeway, Jr., *A human homologue of the Drosophila Toll protein signals activation of adaptive immunity.* Nature, 1997. **388**(6640): p. 394-7.
21. Bowie, A. and L.A. O'Neill, *The interleukin-1 receptor/Toll-like receptor superfamily: signal generators for pro-inflammatory interleukins and microbial products.* J Leukoc Biol, 2000. **67**(4): p. 508-14.
22. Hashimoto, C., K.L. Hudson, and K.V. Anderson, *The Toll gene of Drosophila, required for dorsal-ventral embryonic polarity, appears to encode a transmembrane protein.* Cell, 1988. **52**(2): p. 269-79.

23. Akira, S., S. Uematsu, and O. Takeuchi, *Pathogen recognition and innate immunity.* Cell, 2006. **124**(4): p. 783-801.
24. Jin, M.S., et al., *Crystal structure of the TLR1-TLR2 heterodimer induced by binding of a tri-acylated lipopeptide.* Cell, 2007. **130**(6): p. 1071-82.
25. Barbalat, R., et al., *Toll-like receptor 2 on inflammatory monocytes induces type I interferon in response to viral but not bacterial ligands.* Nat Immunol, 2009. **10**(11): p. 1200-7.
26. Qureshi, S.T., et al., *Endotoxin-tolerant mice have mutations in Toll-like receptor 4 (Tlr4).* J Exp Med, 1999. **189**(4): p. 615-25.
27. Shimazu, R., et al., *MD-2, a molecule that confers lipopolysaccharide responsiveness on Toll-like receptor 4.* J Exp Med, 1999. **189**(11): p. 1777-82.
28. Kim, H.M., et al., *Crystal structure of the TLR4-MD-2 complex with bound endotoxin antagonist Eritoran.* Cell, 2007. **130**(5): p. 906-17.
29. Park, B.S., et al., *The structural basis of lipopolysaccharide recognition by the TLR4-MD-2 complex.* Nature, 2009. **458**(7242): p. 1191-5.
30. Kaisho, T., et al., *Endotoxin-induced maturation of MyD88-deficient dendritic cells.* J Immunol, 2001. **166**(9): p. 5688-94.
31. Hayashi, F., et al., *The innate immune response to bacterial flagellin is mediated by Toll-like receptor 5.* Nature, 2001. **410**(6832): p. 1099-103.
32. Yonekura, K., S. Maki-Yonekura, and K. Namba, *Complete atomic model of the bacterial flagellar filament by electron cryomicroscopy.* Nature, 2003. **424**(6949): p. 643-50.
33. Alexopoulou, L., et al., *Recognition of double-stranded RNA and activation of NF-kappaB by Toll-like receptor 3.* Nature, 2001. **413**(6857): p. 732-8.
34. Kato, H., et al., *Differential roles of MDA5 and RIG-I helicases in the recognition of RNA viruses.* Nature, 2006. **441**(7089): p. 101-5.
35. Zhang, S.Y., et al., *TLR3 deficiency in patients with herpes simplex encephalitis.* Science, 2007. **317**(5844): p. 1522-7.
36. Mancuso, G., et al., *Bacterial recognition by TLR7 in the lysosomes of conventional dendritic cells.* Nat Immunol, 2009. **10**(6): p. 587-94.
37. Schlaepfer, E. and R.F. Speck, *TLR8 activates HIV from latently infected cells of myeloid-monocytic origin directly via the MAPK pathway and from latently infected CD4+ T cells indirectly via TNF-alpha.* J Immunol, 2011. **186**(7): p. 4314-24.
38. Rasmussen, S.B., et al., *Type I interferon production during herpes simplex virus infection is controlled by cell-type-specific viral recognition through Toll-like receptor 9, the mitochondrial antiviral signaling protein pathway, and novel recognition systems.* J Virol, 2007. **81**(24): p. 13315-24.
39. Krug, A., et al., *Herpes simplex virus type 1 activates murine natural interferon-producing cells through toll-like receptor 9.* Blood, 2004. **103**(4): p. 1433-7.
40. Krug, A., et al., *TLR9-dependent recognition of MCMV by IPC and DC generates coordinated cytokine responses that activate antiviral NK cell function.* Immunity, 2004. **21**(1): p. 107-19.
41. Parroche, P., et al., *Malaria hemozoin is immunologically inert but radically enhances innate responses by presenting malaria DNA to Toll-like receptor 9.* Proc Natl Acad Sci U S A, 2007. **104**(6): p. 1919-24.
42. Coban, C., et al., *Toll-like receptor 9 mediates innate immune activation by the malaria pigment hemozoin.* J Exp Med, 2005. **201**(1): p. 19-25.
43. Barton, G.M. and J.C. Kagan, *A cell biological view of Toll-like receptor function: regulation through compartmentalization.* Nat Rev Immunol, 2009. **9**(8): p. 535-42.
44. Sims, J.E., et al., *cDNA expression cloning of the IL-1 receptor, a member of the immunoglobulin superfamily.* Science, 1988. **241**(4865): p. 585-9.
45. Gay, N.J. and F.J. Keith, *Drosophila Toll and IL-1 receptor.* Nature, 1991. **351**(6325): p. 355-6.
46. O'Neill, L.A., *The interleukin-1 receptor/Toll-like receptor superfamily: 10 years of progress.* Immunol Rev, 2008. **226**: p. 10-8.
47. Greenfeder, S.A., et al., *Molecular cloning and characterization of a second subunit of the interleukin 1 receptor complex.* J Biol Chem, 1995. **270**(23): p. 13757-65.
48. Huang, J., et al., *Recruitment of IRAK to the interleukin 1 receptor complex requires interleukin 1 receptor accessory protein.* Proc Natl Acad Sci U S A, 1997. **94**(24): p. 12829-32.

49. Christian korherr, R.H., Werner Falk, *IL-1 receptor internalisation requires the cytoplasmic part of the IL-1 receptor accessory protein.* Cytokine, 1997. **9**: p. 946.
50. Robinson, D., et al., *IGIF does not drive Th1 development but synergizes with IL-12 for interferon-gamma production and activates IRAK and NFkappaB.* Immunity, 1997. **7**(4): p. 571-81.
51. Schmitz, J., et al., *IL-33, an interleukin-1-like cytokine that signals via the IL-1 receptor-related protein ST2 and induces T helper type 2-associated cytokines.* Immunity, 2005. **23**(5): p. 479-90.
52. Sutton, C., et al., *A crucial role for interleukin (IL)-1 in the induction of IL-17-producing T cells that mediate autoimmune encephalomyelitis.* J Exp Med, 2006. **203**(7): p. 1685-91.
53. Yoneyama, M. and T. Fujita, *Structural mechanism of RNA recognition by the RIG-I-like receptors.* Immunity, 2008. **29**(2): p. 178-81.
54. Yoneyama, M., et al., *The RNA helicase RIG-I has an essential function in double-stranded RNA-induced innate antiviral responses.* Nat Immunol, 2004. **5**(7): p. 730-7.
55. Kato, H., et al., *Cell type-specific involvement of RIG-I in antiviral response.* Immunity, 2005. **23**(1): p. 19-28.
56. Yoneyama, M., et al., *Shared and unique functions of the DExD/H-box helicases RIG-I, MDA5, and LGP2 in antiviral innate immunity.* J Immunol, 2005. **175**(5): p. 2851-8.
57. Saito, T., et al., *Regulation of innate antiviral defenses through a shared repressor domain in RIG-I and LGP2.* Proc Natl Acad Sci U S A, 2007. **104**(2): p. 582-7.
58. Kato, H., et al., *Length-dependent recognition of double-stranded ribonucleic acids by retinoic acid-inducible gene-I and melanoma differentiation-associated gene 5.* J Exp Med, 2008. **205**(7): p. 1601-10.
59. Cui, S., et al., *The C-terminal regulatory domain is the RNA 5'-triphosphate sensor of RIG-I.* Mol Cell, 2008. **29**(2): p. 169-79.
60. Takahasi, K., et al., *Solution structures of cytosolic RNA sensor MDA5 and LGP2 C-terminal domains: identification of the RNA recognition loop in RIG-I-like receptors.* J Biol Chem, 2009. **284**(26): p. 17465-74.
61. Kawai, T., et al., *IPS-1, an adaptor triggering RIG-I- and Mda5-mediated type I interferon induction.* Nat Immunol, 2005. **6**(10): p. 981-8.
62. Meylan, E., et al., *Cardif is an adaptor protein in the RIG-I antiviral pathway and is targeted by hepatitis C virus.* Nature, 2005. **437**(7062): p. 1167-72.
63. Seth, R.B., et al., *Identification and characterization of MAVS, a mitochondrial antiviral signaling protein that activates NF-kappaB and IRF 3.* Cell, 2005. **122**(5): p. 669-82.
64. Xu, L.G., et al., *VISA is an adapter protein required for virus-triggered IFN-beta signaling.* Mol Cell, 2005. **19**(6): p. 727-40.
65. Philpott, D.J. and S.E. Girardin, *Nod-like receptors: sentinels at host membranes.* Curr Opin Immunol, 2010. **22**(4): p. 428-34.
66. Kim, D.H. and F.M. Ausubel, *Evolutionary perspectives on innate immunity from the study of Caenorhabditis elegans.* Curr Opin Immunol, 2005. **17**(1): p. 4-10.
67. Tschopp, J., F. Martinon, and K. Burns, *NALPs: a novel protein family involved in inflammation.* Nat Rev Mol Cell Biol, 2003. **4**(2): p. 95-104.
68. Davis, B.K., H. Wen, and J.P. Ting, *The inflammasome NLRs in immunity, inflammation, and associated diseases.* Annu Rev Immunol, 2011. **29**: p. 707-35.
69. Martinon, F. and J. Tschopp, *NLRs join TLRs as innate sensors of pathogens.* Trends Immunol, 2005. **26**(8): p. 447-54.
70. Creagh, E.M. and L.A. O'Neill, *TLRs, NLRs and RLRs: a trinity of pathogen sensors that co-operate in innate immunity.* Trends Immunol, 2006. **27**(8): p. 352-7.
71. Ogura, Y., et al., *Nod2, a Nod1/Apaf-1 family member that is restricted to monocytes and activates NF-kappaB.* J Biol Chem, 2001. **276**(7): p. 4812-8.
72. Bertin, J., et al., *Human CARD4 protein is a novel CED-4/Apaf-1 cell death family member that activates NF-kappaB.* J Biol Chem, 1999. **274**(19): p. 12955-8.
73. Martinon, F. and J. Tschopp, *Inflammatory caspases: linking an intracellular innate immune system to autoinflammatory diseases.* Cell, 2004. **117**(5): p. 561-74.

74. Martinon, F., K. Burns, and J. Tschopp, *The inflammasome: a molecular platform triggering activation of inflammatory caspases and processing of proIL-beta.* Mol Cell, 2002. **10**(2): p. 417-26.
75. Mariathasan, S., et al., *Cryopyrin activates the inflammasome in response to toxins and ATP.* Nature, 2006. **440**(7081): p. 228-32.
76. Kanneganti, T.D., et al., *Bacterial RNA and small antiviral compounds activate caspase-1 through cryopyrin/Nalp3.* Nature, 2006. **440**(7081): p. 233-6.
77. O'Neill, L.A., K.A. Fitzgerald, and A.G. Bowie, *The Toll-IL-1 receptor adaptor family grows to five members.* Trends Immunol, 2003. **24**(6): p. 286-90.
78. Xu, Y., et al., *Structural basis for signal transduction by the Toll/interleukin-1 receptor domains.* Nature, 2000. **408**(6808): p. 111-5.
79. O'Neill, L.A. and A.G. Bowie, *The family of five: TIR-domain-containing adaptors in Toll-like receptor signalling.* Nat Rev Immunol, 2007. **7**(5): p. 353-64.
80. Lord, K.A., B. Hoffman-Liebermann, and D.A. Liebermann, *Nucleotide sequence and expression of a cDNA encoding MyD88, a novel myeloid differentiation primary response gene induced by IL6.* Oncogene, 1990. **5**(7): p. 1095-7.
81. Wesche, H., et al., *MyD88: an adapter that recruits IRAK to the IL-1 receptor complex.* Immunity, 1997. **7**(6): p. 837-47.
82. Medzhitov, R., et al., *MyD88 is an adaptor protein in the hToll/IL-1 receptor family signaling pathways.* Mol Cell, 1998. **2**(2): p. 253-8.
83. Kawai, T., et al., *Unresponsiveness of MyD88-deficient mice to endotoxin.* Immunity, 1999. **11**(1): p. 115-22.
84. Li, S., et al., *IRAK-4: a novel member of the IRAK family with the properties of an IRAK-kinase.* Proc Natl Acad Sci U S A, 2002. **99**(8): p. 5567-72.
85. Motshwene, P.G., et al., *An oligomeric signaling platform formed by the Toll-like receptor signal transducers MyD88 and IRAK-4.* J Biol Chem, 2009. **284**(37): p. 25404-11.
86. Lin, S.C., Y.C. Lo, and H. Wu, *Helical assembly in the MyD88-IRAK4-IRAK2 complex in TLR/IL-1R signalling.* Nature, 2010. **465**(7300): p. 885-90.
87. Kobayashi, K., et al., *IRAK-M is a negative regulator of Toll-like receptor signaling.* Cell, 2002. **110**(2): p. 191-202.
88. Keating, S.E., et al., *IRAK-2 participates in multiple toll-like receptor signaling pathways to NFkappaB via activation of TRAF6 ubiquitination.* J Biol Chem, 2007. **282**(46): p. 33435-43.
89. Wang, C., et al., *TAK1 is a ubiquitin-dependent kinase of MKK and IKK.* Nature, 2001. **412**(6844): p. 346-51.
90. Yi, A.K. and A.M. Krieg, *CpG DNA rescue from anti-IgM-induced WEHI-231 B lymphoma apoptosis via modulation of I kappa B alpha and I kappa B beta and sustained activation of nuclear factor-kappa B/c-Rel.* J Immunol, 1998. **160**(3): p. 1240-5.
91. Beinke, S., et al., *Lipopolysaccharide activation of the TPL-2/MEK/extracellular signal-regulated kinase mitogen-activated protein kinase cascade is regulated by IkappaB kinase-induced proteolysis of NF-kappaB1 p105.* Mol Cell Biol, 2004. **24**(21): p. 9658-67.
92. Zhong, J. and J.M. Kyriakis, *Dissection of a signaling pathway by which pathogen-associated molecular patterns recruit the JNK and p38 MAPKs and trigger cytokine release.* J Biol Chem, 2007. **282**(33): p. 24246-54.
93. Kawai, T., et al., *Interferon-alpha induction through Toll-like receptors involves a direct interaction of IRF7 with MyD88 and TRAF6.* Nat Immunol, 2004. **5**(10): p. 1061-8.
94. Uematsu, S., et al., *Interleukin-1 receptor-associated kinase-1 plays an essential role for Toll-like receptor (TLR)7- and TLR9-mediated interferon-{alpha} induction.* J Exp Med, 2005. **201**(6): p. 915-23.
95. Takaoka, A., et al., *Integral role of IRF-5 in the gene induction programme activated by Toll-like receptors.* Nature, 2005. **434**(7030): p. 243-9.
96. Yamamoto, M., et al., *Essential role for TIRAP in activation of the signalling cascade shared by TLR2 and TLR4.* Nature, 2002. **420**(6913): p. 324-9.
97. Kagan, J.C. and R. Medzhitov, *Phosphoinositide-mediated adaptor recruitment controls Toll-like receptor signaling.* Cell, 2006. **125**(5): p. 943-55.

98. Dunne, A., et al., *Structural complementarity of Toll/interleukin-1 receptor domains in Toll-like receptors and the adaptors Mal and MyD88.* J Biol Chem, 2003. **278**(42): p. 41443-51.
99. Mansell, A., et al., *Mal interacts with tumor necrosis factor receptor-associated factor (TRAF)-6 to mediate NF-kappaB activation by toll-like receptor (TLR)-2 and TLR4.* J Biol Chem, 2004. **279**(36): p. 37227-30.
100. Gray, P., et al., *MyD88 adapter-like (Mal) is phosphorylated by Bruton's tyrosine kinase during TLR2 and TLR4 signal transduction.* J Biol Chem, 2006. **281**(15): p. 10489-95.
101. Khor, C.C., et al., *A Mal functional variant is associated with protection against invasive pneumococcal disease, bacteremia, malaria and tuberculosis.* Nat Genet, 2007. **39**(4): p. 523-8.
102. Hawn, T.R., et al., *A polymorphism in Toll-interleukin 1 receptor domain containing adaptor protein is associated with susceptibility to meningeal tuberculosis.* J Infect Dis, 2006. **194**(8): p. 1127-34.
103. Miggin, S.M., et al., *NF-kappaB activation by the Toll-IL-1 receptor domain protein MyD88 adapter-like is regulated by caspase-1.* Proc Natl Acad Sci U S A, 2007. **104**(9): p. 3372-7.
104. Yamamoto, M., et al., *Cutting edge: a novel Toll/IL-1 receptor domain-containing adapter that preferentially activates the IFN-beta promoter in the Toll-like receptor signaling.* J Immunol, 2002. **169**(12): p. 6668-72.
105. Oshiumi, H., et al., *TICAM-1, an adaptor molecule that participates in Toll-like receptor 3-mediated interferon-beta induction.* Nat Immunol, 2003. **4**(2): p. 161-7.
106. Yamamoto, M., et al., *Role of adaptor TRIF in the MyD88-independent toll-like receptor signaling pathway.* Science, 2003. **301**(5633): p. 640-3.
107. Hirotani, T., et al., *Regulation of lipopolysaccharide-inducible genes by MyD88 and Toll/IL-1 domain containing adaptor inducing IFN-beta.* Biochem Biophys Res Commun, 2005. **328**(2): p. 383-92.
108. Sato, S., et al., *Toll/IL-1 receptor domain-containing adaptor inducing IFN-beta (TRIF) associates with TNF receptor-associated factor 6 and TANK-binding kinase 1, and activates two distinct transcription factors, NF-kappa B and IFN-regulatory factor-3, in the Toll-like receptor signaling.* J Immunol, 2003. **171**(8): p. 4304-10.
109. Jiang, Z., et al., *Toll-like receptor 3-mediated activation of NF-kappaB and IRF3 diverges at Toll-IL-1 receptor domain-containing adapter inducing IFN-beta.* Proc Natl Acad Sci U S A, 2004. **101**(10): p. 3533-8.
110. Meylan, E., et al., *RIP1 is an essential mediator of Toll-like receptor 3-induced NF-kappa B activation.* Nat Immunol, 2004. **5**(5): p. 503-7.
111. Rowe, D.C., et al., *The myristoylation of TRIF-related adaptor molecule is essential for Toll-like receptor 4 signal transduction.* Proc Natl Acad Sci U S A, 2006. **103**(16): p. 6299-304.
112. McGettrick, A.F., et al., *Trif-related adapter molecule is phosphorylated by PKC{epsilon} during Toll-like receptor 4 signaling.* Proc Natl Acad Sci U S A, 2006. **103**(24): p. 9196-201.
113. Carty, M., et al., *The human adaptor SARM negatively regulates adaptor protein TRIF-dependent Toll-like receptor signaling.* Nat Immunol, 2006. **7**(10): p. 1074-81.
114. Martin, M., et al., *Interleukin-1-induced activation of a protein kinase co-precipitating with the type I interleukin-1 receptor in T cells.* Eur J Immunol, 1994. **24**(7): p. 1566-71.
115. Cao, Z., W.J. Henzel, and X. Gao, *IRAK: a kinase associated with the interleukin-1 receptor.* Science, 1996. **271**(5252): p. 1128-31.
116. Rosati, O. and M.U. Martin, *Identification and characterization of murine IRAK-M.* Biochem Biophys Res Commun, 2002. **293**(5): p. 1472-7.
117. Flannery, S. and A.G. Bowie, *The interleukin-1 receptor-associated kinases: critical regulators of innate immune signalling.* Biochem Pharmacol, 2010. **80**(12): p. 1981-91.
118. Neumann, D., et al., *Threonine 66 in the death domain of IRAK-1 is critical for interaction with signaling molecules but is not a target site for autophosphorylation.* J Leukoc Biol, 2008. **84**(3): p. 807-13.
119. Kollewe, C., et al., *Sequential autophosphorylation steps in the interleukin-1 receptor-associated kinase-1 regulate its availability as an adapter in interleukin-1 signaling.* J Biol Chem, 2004. **279**(7): p. 5227-36.

120. Michael U. Martin, C.k., *Interleukin-1 receptor-associated kinase-1 (IRAK-1): A self-regulatory adapter molecule in the signaling cascade of the Toll/IL-1 receptor family.* Signal Transduction, 2001. **1**(1-2): p. 37-50.
121. Wang, Z., et al., *Crystal structures of IRAK-4 kinase in complex with inhibitors: a serine/threonine kinase with tyrosine as a gatekeeper.* Structure, 2006. **14**(12): p. 1835-44.
122. Kuglstatter, A., et al., *Cutting Edge: IL-1 receptor-associated kinase 4 structures reveal novel features and multiple conformations.* J Immunol, 2007. **178**(5): p. 2641-5.
123. Ye, H., et al., *Distinct molecular mechanism for initiating TRAF6 signalling.* Nature, 2002. **418**(6896): p. 443-7.
124. Ringwood, L. and L. Li, *The involvement of the interleukin-1 receptor-associated kinases (IRAKs) in cellular signaling networks controlling inflammation.* Cytokine, 2008. **42**(1): p. 1-7.
125. Liu, G., Y.J. Park, and E. Abraham, *Interleukin-1 receptor-associated kinase (IRAK) -1-mediated NF-kappaB activation requires cytosolic and nuclear activity.* FASEB J, 2008. **22**(7): p. 2285-96.
126. Su, J., et al., *Differential regulation of interleukin-1 receptor associated kinase 1 (IRAK1) splice variants.* Mol Immunol, 2007. **44**(5): p. 900-5.
127. Yamin, T.T. and D.K. Miller, *The interleukin-1 receptor-associated kinase is degraded by proteasomes following its phosphorylation.* J Biol Chem, 1997. **272**(34): p. 21540-7.
128. Windheim, M., et al., *Interleukin-1 (IL-1) induces the Lys63-linked polyubiquitination of IL-1 receptor-associated kinase 1 to facilitate NEMO binding and the activation of IkappaBalpha kinase.* Mol Cell Biol, 2008. **28**(5): p. 1783-91.
129. Huang, Y., et al., *IRAK1 serves as a novel regulator essential for lipopolysaccharide-induced interleukin-10 gene expression.* J Biol Chem, 2004. **279**(49): p. 51697-703.
130. Thomas, J.A., et al., *Impaired cytokine signaling in mice lacking the IL-1 receptor-associated kinase.* J Immunol, 1999. **163**(2): p. 978-84.
131. Kanakaraj, P., et al., *Interleukin (IL)-1 receptor-associated kinase (IRAK) requirement for optimal induction of multiple IL-1 signaling pathways and IL-6 production.* J Exp Med, 1998. **187**(12): p. 2073-9.
132. Schoenemeyer, A., et al., *The interferon regulatory factor, IRF5, is a central mediator of toll-like receptor 7 signaling.* J Biol Chem, 2005. **280**(17): p. 17005-12.
133. Balkhi, M.Y., K.A. Fitzgerald, and P.M. Pitha, *Functional regulation of MyD88-activated interferon regulatory factor 5 by K63-linked polyubiquitination.* Mol Cell Biol, 2008. **28**(24): p. 7296-308.
134. Oganesyan, G., et al., *Critical role of TRAF3 in the Toll-like receptor-dependent and -independent antiviral response.* Nature, 2006. **439**(7073): p. 208-11.
135. Jacob, C.O., et al., *Identification of IRAK1 as a risk gene with critical role in the pathogenesis of systemic lupus erythematosus.* Proc Natl Acad Sci U S A, 2009. **106**(15): p. 6256-61.
136. Muzio, M., et al., *IRAK (Pelle) family member IRAK-2 and MyD88 as proximal mediators of IL-1 signaling.* Science, 1997. **278**(5343): p. 1612-5.
137. Kawagoe, T., et al., *Sequential control of Toll-like receptor-dependent responses by IRAK1 and IRAK2.* Nat Immunol, 2008. **9**(6): p. 684-91.
138. Maloney, G., M. Schroder, and A.G. Bowie, *Vaccinia virus protein A52R activates p38 mitogen-activated protein kinase and potentiates lipopolysaccharide-induced interleukin-10.* J Biol Chem, 2005. **280**(35): p. 30838-44.
139. Hardy, M.P. and L.A. O'Neill, *The murine IRAK2 gene encodes four alternatively spliced isoforms, two of which are inhibitory.* J Biol Chem, 2004. **279**(26): p. 27699-708.
140. Wan, Y., et al., *Interleukin-1 receptor-associated kinase 2 is critical for lipopolysaccharide-mediated post-transcriptional control.* J Biol Chem, 2009. **284**(16): p. 10367-75.
141. Wesche, H., et al., *IRAK-M is a novel member of the Pelle/interleukin-1 receptor-associated kinase (IRAK) family.* J Biol Chem, 1999. **274**(27): p. 19403-10.
142. Li, H., et al., *IL-1 receptor-associated kinase M is a central regulator of osteoclast differentiation and activation.* J Exp Med, 2005. **201**(7): p. 1169-77.
143. Su, J., et al., *The interleukin-1 receptor-associated kinase M selectively inhibits the alternative, instead of the classical NFkappaB pathway.* J Innate Immun, 2009. **1**(2): p. 164-74.
144. del Fresno, C., et al., *Tumor cells deactivate human monocytes by up-regulating IL-1 receptor associated kinase-M expression via CD44 and TLR4.* J Immunol, 2005. **174**(5): p. 3032-40.

145. Zhou, H., et al., *IRAK-M mediates Toll-like receptor/IL-1R-induced NFkappaB activation and cytokine production.* EMBO J, 2013. **32**(4): p. 583-96.
146. Suzuki, N., et al., *Severe impairment of interleukin-1 and Toll-like receptor signalling in mice lacking IRAK-4.* Nature, 2002. **416**(6882): p. 750-6.
147. Burns, K., et al., *Inhibition of interleukin 1 receptor/Toll-like receptor signaling through the alternatively spliced, short form of MyD88 is due to its failure to recruit IRAK-4.* J Exp Med, 2003. **197**(2): p. 263-8.
148. Koziczak-Holbro, M., et al., *IRAK-4 kinase activity is required for interleukin-1 (IL-1) receptor- and toll-like receptor 7-mediated signaling and gene expression.* J Biol Chem, 2007. **282**(18): p. 13552-60.
149. Koziczak-Holbro, M., et al., *IRAK-4 kinase activity-dependent and -independent regulation of lipopolysaccharide-inducible genes.* Eur J Immunol, 2008. **38**(3): p. 788-96.
150. Kawagoe, T., et al., *Essential role of IRAK-4 protein and its kinase activity in Toll-like receptor-mediated immune responses but not in TCR signaling.* J Exp Med, 2007. **204**(5): p. 1013-24.
151. Kim, T.W., et al., *A critical role for IRAK4 kinase activity in Toll-like receptor-mediated innate immunity.* J Exp Med, 2007. **204**(5): p. 1025-36.
152. Qin, J., et al., *IRAK4 kinase activity is redundant for interleukin-1 (IL-1) receptor-associated kinase phosphorylation and IL-1 responsiveness.* J Biol Chem, 2004. **279**(25): p. 26748-53.
153. Picard, C., et al., *Inherited human IRAK-4 deficiency: an update.* Immunol Res, 2007. **38**(1-3): p. 347-52.
154. Kersse, K., et al., *The death-fold superfamily of homotypic interaction motifs.* Trends Biochem Sci, 2011. **36**(10): p. 541-52.
155. George, J., et al., *Two human MYD88 variants, S34Y and R98C, interfere with MyD88-IRAK4-myddosome assembly.* J Biol Chem, 2011. **286**(2): p. 1341-53.
156. Pickart, C.M. and D. Fushman, *Polyubiquitin chains: polymeric protein signals.* Curr Opin Chem Biol, 2004. **8**(6): p. 610-6.
157. Keating, S.E. and A.G. Bowie, *Role of non-degradative ubiquitination in interleukin-1 and toll-like receptor signaling.* J Biol Chem, 2009. **284**(13): p. 8211-5.
158. Conze, D.B., et al., *Lys63-linked polyubiquitination of IRAK-1 is required for interleukin-1 receptor- and toll-like receptor-mediated NF-kappaB activation.* Mol Cell Biol, 2008. **28**(10): p. 3538-47.
159. Butler, M.P., J.A. Hanly, and P.N. Moynagh, *Kinase-active interleukin-1 receptor-associated kinases promote polyubiquitination and degradation of the Pellino family: direct evidence for PELLINO proteins being ubiquitin-protein isopeptide ligases.* J Biol Chem, 2007. **282**(41): p. 29729-37.
160. Jiang, X. and Z.J. Chen, *The role of ubiquitylation in immune defence and pathogen evasion.* Nat Rev Immunol, 2012. **12**(1): p. 35-48.
161. Chang, M., W. Jin, and S.C. Sun, *Peli1 facilitates TRIF-dependent Toll-like receptor signaling and proinflammatory cytokine production.* Nat Immunol, 2009. **10**(10): p. 1089-95.
162. Tseng, P.H., et al., *Different modes of ubiquitination of the adaptor TRAF3 selectively activate the expression of type I interferons and proinflammatory cytokines.* Nat Immunol, 2010. **11**(1): p. 70-5.
163. Casanova, J.L. and L. Abel, *The human model: a genetic dissection of immunity to infection in natural conditions.* Nat Rev Immunol, 2004. **4**(1): p. 55-66.
164. Picard, C., et al., *Pyogenic bacterial infections in humans with IRAK-4 deficiency.* Science, 2003. **299**(5615): p. 2076-9.
165. Casanova, J.L. and L. Abel, *Primary immunodeficiencies: a field in its infancy.* Science, 2007. **317**(5838): p. 617-9.
166. Doffinger, R., et al., *X-linked anhidrotic ectodermal dysplasia with immunodeficiency is caused by impaired NF-kappaB signaling.* Nat Genet, 2001. **27**(3): p. 277-85.
167. Courtois, G., et al., *A hypermorphic IkappaBalpha mutation is associated with autosomal dominant anhidrotic ectodermal dysplasia and T cell immunodeficiency.* J Clin Invest, 2003. **112**(7): p. 1108-15.

168. Ku, C.L., et al., *Selective predisposition to bacterial infections in IRAK-4-deficient children: IRAK-4-dependent TLRs are otherwise redundant in protective immunity.* J Exp Med, 2007. **204**(10): p. 2407-22.
169. Netea, M.G., C. Wijmenga, and L.A. O'Neill, *Genetic variation in Toll-like receptors and disease susceptibility.* Nat Immunol, 2012. **13**(6): p. 535-42.
170. Puente, X.S., et al., *Whole-genome sequencing identifies recurrent mutations in chronic lymphocytic leukaemia.* Nature, 2011. **475**(7354): p. 101-5.
171. Ngo, V.N., et al., *Oncogenically active MYD88 mutations in human lymphoma.* Nature, 2011. **470**(7332): p. 115-9.
172. Casrouge, A., et al., *Herpes simplex virus encephalitis in human UNC-93B deficiency.* Science, 2006. **314**(5797): p. 308-12.
173. Perez de Diego, R., et al., *Human TRAF3 adaptor molecule deficiency leads to impaired Toll-like receptor 3 response and susceptibility to herpes simplex encephalitis.* Immunity, 2010. **33**(3): p. 400-11.
174. Sancho-Shimizu, V., et al., *Herpes simplex encephalitis in children with autosomal recessive and dominant TRIF deficiency.* J Clin Invest, 2011. **121**(12): p. 4889-902.
175. Arbour, N.C., et al., *TLR4 mutations are associated with endotoxin hyporesponsiveness in humans.* Nat Genet, 2000. **25**(2): p. 187-91.
176. Lorenz, E., et al., *Relevance of mutations in the TLR4 receptor in patients with gram-negative septic shock.* Arch Intern Med, 2002. **162**(9): p. 1028-32.
177. Ogus, A.C., et al., *The Arg753GLn polymorphism of the human toll-like receptor 2 gene in tuberculosis disease.* Eur Respir J, 2004. **23**(2): p. 219-23.
178. Schroder, N.W., et al., *Heterozygous Arg753Gln polymorphism of human TLR-2 impairs immune activation by Borrelia burgdorferi and protects from late stage Lyme disease.* J Immunol, 2005. **175**(4): p. 2534-40.
179. Hawn, T.R., et al., *A common dominant TLR5 stop codon polymorphism abolishes flagellin signaling and is associated with susceptibility to legionnaires' disease.* J Exp Med, 2003. **198**(10): p. 1563-72.
180. Dunstan, S.J., et al., *Host susceptibility and clinical outcomes in toll-like receptor 5-deficient patients with typhoid fever in Vietnam.* J Infect Dis, 2005. **191**(7): p. 1068-71.
181. Hawn, T.R., et al., *A stop codon polymorphism of Toll-like receptor 5 is associated with resistance to systemic lupus erythematosus.* Proc Natl Acad Sci U S A, 2005. **102**(30): p. 10593-7.
182. Gewirtz, A.T., et al., *Dominant-negative TLR5 polymorphism reduces adaptive immune response to flagellin and negatively associates with Crohn's disease.* Am J Physiol Gastrointest Liver Physiol, 2006. **290**(6): p. G1157-63.
183. George, J., et al., *MyD88 adaptor-like D96N is a naturally occurring loss-of-function variant of TIRAP.* J Immunol, 2010. **184**(6): p. 3025-32.
184. Dubois, P.C., et al., *Multiple common variants for celiac disease influencing immune gene expression.* Nat Genet, 2010. **42**(4): p. 295-302.
185. Ishida, R., et al., *Association of a haplotype (196Phe/532Ser) in the interleukin-1-receptor-associated kinase (IRAK1) gene with low radial bone mineral density in two independent populations.* J Bone Miner Res, 2003. **18**(3): p. 419-23.
186. Lakoski, S.G., et al., *The association between innate immunity gene (IRAK1) and C-reactive protein in the Diabetes Heart Study.* Exp Mol Pathol, 2007. **82**(3): p. 280-3.
187. Arcaroli, J., et al., *Variant IRAK-1 haplotype is associated with increased nuclear factor-kappaB activation and worse outcomes in sepsis.* Am J Respir Crit Care Med, 2006. **173**(12): p. 1335-41.
188. Zhang, H., et al., *IRAK1 rs3027898 C/A polymorphism is associated with risk of rheumatoid arthritis.* Rheumatol Int, 2012.
189. Balaci, L., et al., *IRAK-M is involved in the pathogenesis of early-onset persistent asthma.* Am J Hum Genet, 2007. **80**(6): p. 1103-14.
190. Barrios-Rodiles, M., et al., *High-throughput mapping of a dynamic signaling network in mammalian cells.* Science, 2005. **307**(5715): p. 1621-5.
191. Smith, P.K., et al., *Measurement of protein using bicinchoninic acid.* Anal Biochem, 1985. **150**(1): p. 76-85.

192. Janssens, S. and R. Beyaert, *Functional diversity and regulation of different interleukin-1 receptor-associated kinase (IRAK) family members.* Mol Cell, 2003. **11**(2): p. 293-302.
193. Flannery, S.M., et al., *Human interleukin-1 receptor-associated kinase-2 is essential for Toll-like receptor-mediated transcriptional and post-transcriptional regulation of tumor necrosis factor alpha.* J Biol Chem, 2011. **286**(27): p. 23688-97.
194. Nagpal, K., et al., *Natural loss-of-function mutation of myeloid differentiation protein 88 disrupts its ability to form Myddosomes.* J Biol Chem, 2011. **286**(13): p. 11875-82.
195. Nagpal, K., et al., *A TIR domain variant of MyD88 adapter-like (Mal)/TIRAP results in loss of MyD88 binding and reduced TLR2/TLR4 signaling.* J Biol Chem, 2009. **284**(38): p. 25742-8.
196. Neumann, D., et al., *IL-1beta-induced phosphorylation of PKB/Akt depends on the presence of IRAK-1.* Eur J Immunol, 2002. **32**(12): p. 3689-98.
197. Harte, M.T., et al., *The poxvirus protein A52R targets Toll-like receptor signaling complexes to suppress host defense.* J Exp Med, 2003. **197**(3): p. 343-51.
198. Conner, J.R., Smirnova, II, and A. Poltorak, *A mutation in Irak2c identifies IRAK-2 as a central component of the TLR regulatory network of wild-derived mice.* J Exp Med, 2009. **206**(7): p. 1615-31.
199. Liu, Y.C., et al., *TLR2 signaling depletes IRAK1 and inhibits induction of type I IFN by TLR7/9.* J Immunol, 2012. **188**(3): p. 1019-26.
200. Gog, J.R., et al., *Dynamics of Salmonella infection of macrophages at the single cell level.* J R Soc Interface, 2012. **9**(75): p. 2696-707.
201. Cook, P., et al., *Salmonella-induced SipB-independent cell death requires Toll-like receptor-4 signalling via the adapter proteins Tram and Trif.* Immunology, 2007. **122**(2): p. 222-9.
202. Reading, P.C., et al., *Influenza viruses differ in ability to infect macrophages and to induce a local inflammatory response following intraperitoneal injection of mice.* Immunol Cell Biol, 2010. **88**(6): p. 641-50.
203. Yang, W.L., et al., *Regulation of Akt signaling activation by ubiquitination.* Cell Cycle, 2010. **9**(3): p. 487-97.
204. Tsukamoto, K., et al., *Critical roles of the p110 beta subtype of phosphoinositide 3-kinase in lipopolysaccharide-induced Akt activation and negative regulation of nitrite production in RAW 264.7 cells.* J Immunol, 2008. **180**(4): p. 2054-61.
205. Chaurasia, B., et al., *Phosphoinositide-dependent kinase 1 provides negative feedback inhibition to Toll-like receptor-mediated NF-kappaB activation in macrophages.* Mol Cell Biol, 2010. **30**(17): p. 4354-66.
206. Cahill, C.M., J.T. Rogers, and W.A. Walker, *The role of phosphoinositide 3-kinase signaling in intestinal inflammation.* J Signal Transduct, 2012. **2012**: p. 358476.
207. Santos-Sierra, S., et al., *Mal connects TLR2 to PI3Kinase activation and phagocyte polarization.* EMBO J, 2009. **28**(14): p. 2018-27.
208. Fitzgerald, K.A., et al., *Mal (MyD88-adapter-like) is required for Toll-like receptor-4 signal transduction.* Nature, 2001. **413**(6851): p. 78-83.
209. Marmiroli, S., et al., *Phosphatidylinositol 3-kinase is recruited to a specific site in the activated IL-1 receptor I.* FEBS Lett, 1998. **438**(1-2): p. 49-54.
210. Cenni, V., et al., *Interleukin-1-receptor-associated kinase 2 (IRAK2)-mediated interleukin-1-dependent nuclear factor kappaB transactivation in Saos2 cells requires the Akt/protein kinase B kinase.* Biochem J, 2003. **376**(Pt 1): p. 303-11.
211. Weintz, G., et al., *The phosphoproteome of toll-like receptor-activated macrophages.* Mol Syst Biol, 2010. **6**: p. 371.
212. Yin, W., et al., *The kinase activity of interleukin-1 receptor-associated kinase 2 is essential for lipopolysaccharide-mediated cytokine and chemokine mRNA stability and translation.* J Interferon Cytokine Res, 2011. **31**(5): p. 415-22.
213. Chin, K.C., G.G. Li, and J.P. Ting, *Importance of acidic, proline/serine/threonine-rich, and GTP-binding regions in the major histocompatibility complex class II transactivator: generation of transdominant-negative mutants.* Proc Natl Acad Sci U S A, 1997. **94**(6): p. 2501-6.
214. Rao, S., et al., *SPI-B activates transcription via a unique proline, serine, and threonine domain and exhibits DNA binding affinity differences from PU.1.* J Biol Chem, 1999. **274**(16): p. 11115-24.

215. Tun-Kyi, A., et al., *Essential role for the prolyl isomerase Pin1 in Toll-like receptor signaling and type I interferon-mediated immunity.* Nat Immunol, 2011. **12**(8): p. 733-41.
216. Gay, N.J., M. Gangloff, and L.A. O'Neill, *What the Myddosome structure tells us about the initiation of innate immunity.* Trends Immunol, 2011. **32**(3): p. 104-9.
217. Akira, S. and K. Takeda, *Toll-like receptor signalling.* Nat Rev Immunol, 2004. **4**(7): p. 499-511.
218. Brikos, C., et al., *Mass spectrometric analysis of the endogenous type I interleukin-1 (IL-1) receptor signaling complex formed after IL-1 binding identifies IL-1RAcP, MyD88, and IRAK-4 as the stable components.* Mol Cell Proteomics, 2007. **6**(9): p. 1551-9.
219. Prasad, L., et al., *Cohort Profile: the Swiss Hepatitis C Cohort Study (SCCS).* Int J Epidemiol, 2007. **36**(4): p. 731-7.
220. Picard, C., et al., *Clinical features and outcome of patients with IRAK-4 and MyD88 deficiency.* Medicine (Baltimore), 2010. **89**(6): p. 403-25.
221. Schork, N.J., et al., *Common vs. rare allele hypotheses for complex diseases.* Curr Opin Genet Dev, 2009. **19**(3): p. 212-9.
222. Waldner, M.J., S. Foersch, and M.F. Neurath, *Interleukin-6--a key regulator of colorectal cancer development.* Int J Biol Sci, 2012. **8**(9): p. 1248-53.
223. Thomas, E., et al., *HCV infection induces a unique hepatic innate immune response associated with robust production of type III interferons.* Gastroenterology, 2012. **142**(4): p. 978-88.
224. Rehermann, B., *Hepatitis C virus versus innate and adaptive immune responses: a tale of coevolution and coexistence.* J Clin Invest, 2009. **119**(7): p. 1745-54.
225. Katsounas, A., J.F. Schlaak, and R.A. Lempicki, *CCL5: a double-edged sword in host defense against the hepatitis C virus.* Int Rev Immunol, 2011. **30**(5-6): p. 366-78.
226. Eksioglu, E.A., et al., *Characterization of HCV interactions with Toll-like receptors and RIG-I in liver cells.* PLoS One, 2011. **6**(6): p. e21186.
227. Hou, J., et al., *MicroRNA-146a feedback inhibits RIG-I-dependent Type I IFN production in macrophages by targeting TRAF6, IRAK1, and IRAK2.* J Immunol, 2009. **183**(3): p. 2150-8.
228. Jemal, A., et al., *Global cancer statistics.* CA Cancer J Clin, 2011. **61**(2): p. 69-90.
229. Shanks, A.M. and E.M. El-Omar, *Helicobacter pylori infection, host genetics and gastric cancer.* J Dig Dis, 2009. **10**(3): p. 157-64.
230. Liu, P., et al., *Targeting the phosphoinositide 3-kinase pathway in cancer.* Nat Rev Drug Discov, 2009. **8**(8): p. 627-44.
231. Dunne, A., *Inflammasome activation: from inflammatory disease to infection.* Biochem Soc Trans, 2011. **39**(2): p. 669-73.
232. Mitroulis, I., K. Kambas, and K. Ritis, *Neutrophils, IL-1beta, and gout: is there a link?* Semin Immunopathol, 2013.

Appendix

Appendix A: Reagent and buffers

A1: Cloning primers

Primer pair	Name		Sequence	Properties
1	pENTR1A based FL hIRAK2	F	ATATAG GATCC CA ATGGCCTGCTACATCTACCAG	Overhang+ BamHI +Start codon+IRAK2
		R1	ATATC GCGGCCGC CTA GGGGCCAAAGAGCTCAATGCT	Overhang+ NotI + Stop codon +end part of IRAK2
		R2	ATATC GCGGCCGC GA GGGGCCAAAGAGCTCAATGCT	Overhang+ NotI +open+end part of IRAK2
2	pENTR1A based DD hIRAK2 (1-112 aa)	F	ATATA GGATCC CA ATGGCCTGCTACATCTACCAG	Overhang+ BamHI +Start codon+IRAK2
		R1	ATATC GCGGCCGC CTA TGGCTTCACAGAGTCAGGGAA	Overhang+ NotI + Stop codon +DD IRAK2
		R2	ATATC GCGGCCGC CT TGGCTTCACAGAGTCAGGGAA	Overhang+ NotI +open+DDIRAK2
3	pENTR1A based DD hIRAK(1-109aa)	F	ATATA GGATCC CA ATGGCCGGGGGGCCGGGCCCG	Overhang+ BamHI +Start codon+IRAK1
		R1	ATATC GCGGCCGC CTA CGGAAGCGGGGCGGGAGGGTG	Overhang+ NotI + Stop codon +DD IRAK1
		R2	ATATC GCGGCCGC CT CGGAAGCGGGGCGGGAGGGTG	Overhang+ NotI +open+DDIRAK1
4	pENTR1A based DD hIRAK3(1-109aa)	F	TATATA GGTACC AC ATGGCGGGGAACTGTGGGGCC	Overhang+ KpnI +Start codon+IRAK1
		R1	TATATA GCGGCCGC TCA TCCATAGTTTGTAATTAAATG	Overhang+ NotI + Stop codon +DD IRAK3
		R2	TATATA GCGGCCGC CA TCCATAGTTTGTAATTAAATG	Overhang+ NotI +open+DDIRAK3
5	N-HA tagged IRAK2	F	TCGACTTAATTAAGCCGCCACCATGTA CCCATACGACGTCCCAGACTACGCTGG	Insertion an in-frame Met-HA tag at the N-terminus of IRAK2 following the att site
		R1	GATCCCAGCGTAGTCTGGGACGTCGTA TGGGTACATGGTGGCGGCTTAATTAAG	
6	C-HA tagged IRAK2	F	GGCCGCACTACCCATACGACGTCCCAG ACTACGCTTAGC	Insertion an HA tag at the C-terminus of IRAK2 prior to the att site
		R1	TCGAGCTAAGCGTAGTCTGGGACGTCG TATGGGTAGTGC	

A2: Mutagenesis primers

Primer Pair	Name	Sequence	Properties
1	IRAK2 R43Q	F_catggacttgatcttctgcagctgggtcaggtc R_gacctgacccagctgcagaagatcaagtccatg	SNP
2	IRAK2 S47Y	F_gcacccgctccatgtacttgatcttccgc R_gcggaagatcaagtacatggagcgggtgc	SNP
3	IRAK2 L78M	F_ctccaggcggcacatgaggtccacaagtt R_aacttgtggacctcatgtgccgcctggag	SNP
4	IRAK2 I99V	F_ggaatgggacacctgacttcaggagccggtttc R_gaaaccggctcctgaagtcaggtgtcccattcc	SNP
5	IRAK2 R214G	F_cccctggctgattttgccgttttgattgaagtcat R_atgacttcaatcaaaacggcaaaatcagccagggg	SNP
6	IRAK2 L358M	F_tttgttgacaggacacatatgagccattgggtgag R_ctcacccaatggctcatatgtgtcctgtcaacaaa	SNP
7	IRAK2 L392V	F_actcgctttgtcacctgccccacccg R_cgggtggggcaggtgacaaagcgagt	SNP
8	IRAK2 D431E	F_cgaggcggtgctgcttggaatttcactgaggag R_ctcctcagtgaaattccaagcagcaccgcctcg	SNP
9	IRAK2 L439V	F_cgtcttcctggagcagaccgaggcggt R_accgcctcggtctgctccaggaagacg	SNP
10	IRAK2 A498G	F_ccgctcttccacaccagccacagagcc R_ggctctgtggctggtgtggaagagcgg	SNP
11	IRAK2 E501G	F_cctcggagccgcccttccacagcag R_ctgctgtggaagggcggctccgagg	SNP
12	IRAK2 L503I	F_gtctcccgacctcggatccgctcttc R_gaagagcggatccgaggtcgggagac	SNP
13	IRAK2 K237A	F_gggaagccattcgtcttcgcgaagctcagagagacag c R_gctgtctctctgagcttcgcgaagacgaatggcttccc	Mutation
14	IRAK2 E528A	F_ccaacaccccagaggcaacagacgacgttga R_tcaacgtcgtctgttgcctctggggtgttgg	Mutation

A3: qPCR primers

qPCR primers	Catalog Number (Life Technology)
TNFa	Mm00443260_g1
IL-6	Mm00446190_m1
IL-1B	Mm00434228_m1
CCL5	Mm01302427_m1
Tbp	Mm00446971_m1

A4: Overview of purchased and gifted plasmids

Gene	Properties	Source
EGFP	Enhanced green fluorescent protein (EGFP) encoding plasmids (pC1-EGFP vector)	BD Clontech.
NF-κB Firefly reporter	Firefly luciferase reporter gene under the control of a synthetic NF-κB promoter	Stratagene
Renilla Luciferase	Renilla luciferase repoter gene constitutively expressed under the control of TK promoter	Promega
IRAK1 stop Entry clone	pENTR221 based entry clone containing isoform A,712aa	imaGenes; OCAAo5051C0298D
IRAK1 open Entry clone	pENTR221 based entry clone containing isoform A,712aa	imaGenes; OCAAo5051C0299D
IRAK2 TOPO plasmid	Human IRAK2 containg 625aa	imaGENES, IRCMp5012D0935D
IRAK3 Entry clone open	pDONR223 based entry clone containing isoformA,596aa	DKFZ Core Facility, Germany
pENTR1A	Gateway compatible entry clone	Invitrogen
Jun Protein A	pT-REx-DEST30 based vector backbone encoding N terminal tagged Jun-Protein A	DKFZ Core Facility, Germany
Fos Renilla	pcDNA3 based vector encoding C-terminally tagged Fos-Renilla	DKFZ Core Facility, Germany
Flip recombinase	pOG44 vector encoding for the Flp recombinase	Dr. Andreas Pichlmair,CeMM, Vienna, Austria
Strep-HA pcDNATM5/FRT	Destination gateway clone for N-terminal Strep-HA tagging; gene is under the control of a tetracyclineregulated, hybrid CMV/TetO2 promoter; the plasmid contains FRT site for stable transfection	
Renilla pcDNA3 nt Renilla	Destination gateway vector for N-terminal Renilla tags	DKFZ Core Facility, Germany
Protein A Pt-Rex-DEST30	Destination gateway vector for N-terminal Protein-A tags	DKFZ Core Facility, Germany
TRAF6	pDONR223 based entry clone	DKFZ Core Facility, Germany
Flag destination clone	pDONR223 based entry clone	Dr.Stefan Push, Uni-HD, Germany
pMXs-IP-puro	MMLV based retroviral tranduction vector	Dr. Kevin-Michael Dennehy, University of Tübingen, Germany

A5: Overview of antibodies list

Name	Species	Dilution ratio	Working buffer	Company	Catalog number
Anti-HA	mouse	1:5000	TBS-Tween 0.5%+ 3% skimed milk	Sigma	H9658
Anti-HA	rabbit	1:5000	TBS-Tween 0.5%+ 3% skimed milk	CST	C2954
Anti-Flag	rabbit	1:2500	TBS-Tween 0.5%+ 3% skimed milk	Sigma	F7425
Anti-TRAF6	mouse	1:1000	TBS-Tween 0.5%+ 3% skimed milk	Santa cruz	sc-8409
Anti-TRAF6	rabbit	1:1000	TBS-Tween 0.5%+ 3% skimed milk	Santa cruz	sc-7221
Anti-rabbit HRP	goat	1:5000	TBS-Tween 0.5%+ 3% skimed milk	Vector	PI-1000
Anti-mouse HRP	goat	1:5000	TBS-Tween 0.5%+ 3% skimed milk	Promega	W4023
Anti-Renilla	mouse	1:2500	TBS-Tween 0.5%+ 3% skimed milk	Millipore	MAB4400
Anti-ProteinA	rabbit	1:60000	TBS-Tween 0.5%+ 3% skimed milk		
Anti-Tubulin	mouse	1:2500	TBS-Tween 0.5%+ 3% skimed milk	Sigma	T4026
Anti-Ubiquitin	mouse	1:1000	TBS-Tween 0.5%+ 3% skimed milk	Santa cruz	

A6: TLR ligands

Ligands name	Working concentration	Company
Pam2CSK4	1μg/ml	Invivogen
Poly I:C	10μg/ml	Axxora
LPS	0.05μg/ml	Invivogen
Flagellin	50ng.ml	Imgenex
R848	1μg/ml	Invivogen
CpG 2006	0.5μg/ml	Tip Biomol

A7: Recipes of buffers

Buffer name	Recipe
Lysis buffer 1	20 mM Tris, pH 7.5, 250 mM NaCl, 1 % Triton-X100, 10 mM EDTA, 10 mM DTT,protease and phosphatase inhibitors
Lysis buffer 2	50 mM HEPES, 150 mM NaCl, 1 % NP-40, 20 mM β-glycerophosphate, 2 mM DTT, 1mM sodium orthovanadate and protease inhibitors (Roche)
Lysis buffer 3	7 M urea, 2 M thiourea, 2 % CHAPS, 40 mM DTT, protease inhibitors (Roche) and 0.5 %of immobilized pH gradient buffer 3-10 NL (GE Healthcare)
Lysis buffer 4	50 mM HEPES, pH7.5, 200 mM NaCl, 1 mM EDTA, 10% (v/v) glycerol, 1% (v/v) NP40, freshly added Complete proteinase inhibitors (Roche), Phos-Stop phosphatase inhibitor (Roche) and 10 uM Iodoactetamide
Rehydration buffer	7 M urea, 2 M thiourea, 2 % CHAPS, 40 mM DTT, protease inhibitors (Roche) and 0.5 % of immobilized pH gradient buffer 3-10 NL (GE Healthcare)
PBS	8 g NaCl, 0.2 g KCl, 1.44 g Na2HPO4, add with dH2O to 1 l, pH 7.4
TBS	50 mM Tris HCl, pH 7.4 and 150 mM NaCl
TBS-Tween 0.1%	TBS+0.1% Tween
Renilla substrate buffer	220 mM potassium phosphate buffer (1 M K2HPO4, 1 M KH2PO4, pH 5.1), 1.1 M NaCl, 2.2 mM EDTA and 0.44 mg/ml BSA
Sodium Borate buffer	5 mM di-sodium borate
stop solution	2N H2SO4
HBS	50 mM HEPES pH 7.05,10 mM KCl,12 mM Dextrose,280 mM NaCl,1.5 mM Na2HPO4
Polybrene	4mg/ml stock
HBSS	0.137mM NaCl, 5.4mM KCl, 0.25mM Na_2HPO_4, 0.44mMKH_2PO_4, 1.3Mm $CaCl_2$, 1.0m M, 4.2Mm $NaHCO_3$

A8: Recipes of medium

Medium	Recipe
LB media	5 g Bacto-Tryptone, 5 g Bacto-Yeast, and 10 g NaCl, add with dH2O to 1 l
NZY+ broth	5 g NaCl, 2 g MgSO4*7H2O, 5 g Bacto-Yeast Extract, 10 g NZ amine, add with dH2O to 1 l
SOC	20 g Bacto-Tryptone, 5 g Bacto-Yeast extract, 0.5 g NaCl, 2.5 ml of 1 M KCl, 20 ml of 1M glucose, add with dH2O to 1 l

Appendix B1: The signalling properties of defect mutants of IRAK2

In order to confirm the signalling properties of selected negative controls such as double mutants R214G +L392V, K237A and E528A, NF-κB reporter dual luciferase assay and IL-8 ELISA assay were performed. See figure 5.1.

Overexpression IRAK2 K237A and E528A in HEK293T cells, these two mutants almost completely abrogated the activation of NF-κB and the production of IL-8. The double mutant has slightly stronger defect than the single mutations.

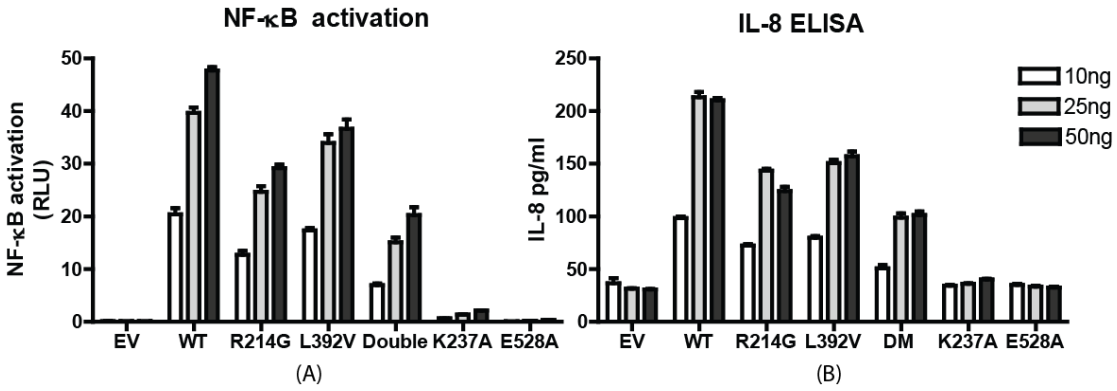

Figure B1: The signalling properties of defect mutants of IRAK2. Overexpression each plasmid into HEK293T cells as indicate doses. (a): Cell were lysed 48 hours post-transfection with passive lysis buffer and the NF-κB luminescence were measured with flurostar (Biotech).(b): Supernatant were harvest 48 hours post-transfection and the amount of IL-8 were measured by ELISA.

Appendix B2: The signalling properties of defect mutants of IRAK3

Overexpression IRAK3 WT, DD, Y180X, K192A and empty vector in HEK293T cells. K192A dimished the NF-κB activation completely.

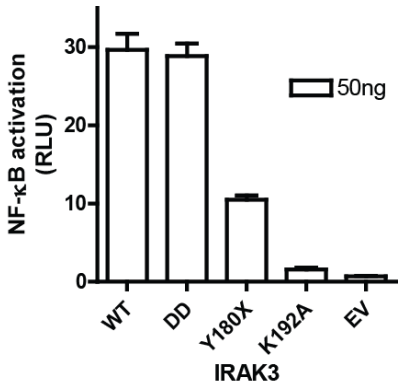

Figure B2: The signalling properties of defect mutants of IRAK3. Overexpression each plasmid into HEK293T cells as indicate doses. Cell were lysed 48 hours post-transfection with passive lysis buffer and the NF-κB luminescence were measured with flurostar (Biotech).